

**DETERMINATION OF DOSE FROM LIGHT CHARGED IONS RELEVANT
TO HADRON THERAPY USING THE PARTICLE AND HEAVY ION
TRANSPORT SYSTEM (PHITS)**

A Thesis

by

MICHAEL PATRICK BUTKUS

Submitted to the Office of Graduate Studies of
Texas A&M University
in partial fulfillment of the requirements for the degree of

MASTER OF SCIENCE

August 2011

Major Subject: Health Physics

Determination of Dose from Light Charged Ions Relevant to Hadron Therapy Using the
Particle and Heavy Ion Transport System (PHITS)

Copyright 2011 Michael Patrick Butkus

**DETERMINATION OF DOSE FROM LIGHT CHARGED IONS RELEVANT
TO HADRON THERAPY USING THE PARTICLE AND HEAVY ION
TRANSPORT SYSTEM (PHITS)**

A Thesis

by

MICHAEL PATRICK BUTKUS

Submitted to the Office of Graduate Studies of
Texas A&M University
in partial fulfillment of the requirements for the degree of

MASTER OF SCIENCE

Approved by:

Chair of Committee,	Stephen Guetersloh
Committee Members,	John Ford
	Joseph Natowitz
Head of Department,	Raymond Juzaitis

August 2011

Major Subject: Health Physics

ABSTRACT

Determination of Dose From Light Charged Ions Relevant to Hadron Therapy Using the Particle and Heavy Ion Transport System (PHITS).

(August 2011)

Michael Patrick Butkus, B.Eng., New Mexico Tech University

Chair of Advisory Committee: Dr. Stephen Guetersloh

In conventional radiotherapy for tumor treatment, photons are used to impart an energetic dose inside a tumor with the goal of killing the cancerous cells. This process is intrinsically inefficient due to the fact that photons lose their energy exponentially with depth causing the highest dose to occur in overlying healthy tissue. However, charged particles with a mass of 1 amu or greater lose their energy in a manner that allows for a high dose to be localized at significant depth. The area of high dose localization is known as the Bragg Peak. Exploitation of the Bragg Peak could lead to more efficient non-invasive treatment plans by reducing the dose in healthy tissues.

Using the Particle and Heavy Ion Transport System (PHITS), the dose and fragmentation particles from ions of ^1H , ^4He , ^7Li , ^{12}C , ^{16}O , and ^{20}Ne were found at varying depths in a water phantom. A water filled cylindrical phantom with a radius of 10 cm was used to mimic a human body. The energy of each ion was selected so that the Bragg Peak would occur approximately 10 cm into the depth of the water phantom where a 1 cm radius water sphere was placed to simulate a solid tumor.

Dose equivalent localization rates within the tumor were found to be 14.5, 36.5, 45.7, 49.5, 41.3, and 34.1% for ^1H , ^4He , ^7Li , ^{12}C , ^{16}O , and ^{20}Ne , respectively. The percentage of dose within the tumor increased with increasing atomic number up to ^{12}C , decreasing thereafter. The total dose distal from the tumor ranged from 0.1, 0.9, 2.8, 0.9, 0.5, and 0.6% for the ions ordered by their masses. Complementing its high dose in the tumor, carbon was seen to experience the lowest amount of dose escaping due to fragmentation and scattering, on a dose normalized basis.

ACKNOWLEDGMENTS

I would like to extend a tremendous amount of gratitude to my committee chair, Dr. Stephen Guetersloh, as well as my committee, Dr. John Ford and Dr. Raymond Natowitz, for their help with this thesis and the knowledge I have gained in my graduate career.

To my parents and family, thanks for your continued support and encouragement throughout my higher education. Love you guys.

And to all my great friends I have met here thanks for the great times. Chambers, Dolen, Duncan, Prater, Roberts, Talamantes party on. Cox, congratulations on being the first to 100, it was luck. Timmy, sorry for your scar. Martin, thanks for betting me I would never write this paper; you know that's the real reason I finished.

TABLE OF CONTENTS

		Page
	ABSTRACT	iii
	ACKNOWLEDGMENTS	v
	TABLE OF CONTENTS	vi
	LIST OF FIGURES	viii
	LIST OF TABLES	xi
CHAPTER		
I	INTRODUCTION	1
II	BACKGROUND	4
	History of Charged Particle Therapy	4
	Charged Particle Interactions and the Bragg Peak	6
	Charged Particle Tracks	10
	Quality Factor for Charged Particles	13
	Effects of Dose Fractionation	15
	Fragmentation and Scattering	18
III	METHODS AND MATERIALS	20
	Particle Heavy Ion Transport System (PHITS)	20
	Phantom Geometry and Particle Beams	20
	Dose Calculations	22
	Fragmentation and Scattering Analysis	24
IV	RESULTS AND DISCUSSION	25
	LET and Dose Analysis	25
	Dose Equivalence	39
	Fragmentation and Scattering	47

CHAPTER	Page
V CONCLUSIONS	62
REFERENCES	64
APPENDIX A.....	66
APPENDIX B.....	73
APPENDIX C.....	94
APPENDIX D.....	117
APPENDIX E.....	140
VITA.....	154

LIST OF FIGURES

FIGURE	Page
1	Relative Dose Distributions from Beams of Charged and Uncharged Radiation Types..... 7
2	Contrast of Radiation Therapy with ^{12}C Ions to that of IMRT for the Same Dose Delivered to a Tumor Volume 8
3	Chatterjee Energy Density for a Radius of 0.3 μm Surrounding the Particle Track of a 296 MeV $\text{u}^{-1} {}^{20}\text{Ne}$ Ion as it Enters a Water Volume..... 12
4	Survival Curves for Irradiation of SCC25, H184B5-1M/10 V79, SQ20B, and HF19 Cell Lines Using ^{12}C Beams of Different LET and ^{60}Co Photons 16
5	Comparison of AG1522B Cell Survival when Irradiated with 250 keV X-rays and 16.6 keV $\mu\text{m}^{-1} {}^{12}\text{C}$ Ion in Different Fractions 17
6	Geometry of Water Phantom Used to Simulate a Human Body and Tumor for Heavy Ion Transports 21
7	LET Depth Profiles for Various Ion Beams, of Concern in Charged Particle Therapy, Passing Through a Water Phantom..... 26
8	LET Depth Profile of ^1H 116.5 MeV u^{-1} Traversing Through 1 g cm^{-3} Water 27
9	LET Depth Profile of ^4He 116.5 MeV u^{-1} Traversing Through 1 g cm^{-3} Water 28
10	LET Depth Profile of ^7Li 134.5 MeV u^{-1} Traversing Through 1 g cm^{-3} Water 29
11	LET Depth Profile of ^{12}C 219 MeV u^{-1} Traversing Through 1 g cm^{-3} Water 30
12	LET Depth Profile of ^{16}O 259 MeV u^{-1} Traversing Through 1 g cm^{-3} Water 31

FIGURE	Page
13 LET Depth Profile of ^{20}Ne 296 MeV u^{-1} Traversing Through 1 g cm^{-3} Water.....	32
14 Percent of Measured LET from Non-Primary Particles in a Water Phantom for Various Ion Beams.....	33
15 Dose Percentage Rates for Various Ion Beams in a Tumor and in Different Regions of a Body Relative to the Tumor	36
16 Quality Factors (Q) for Various Ion Beams as They Approach Their Bragg Peaks Traversing Through Water.....	40
17 Dose Equivalence Normalized to Entrance Dose for Various Ion Beams as They Traverse Water	42
18 Percentage Increases in Dose Equivalence, Normalized to Entrance Dose Equivalence as Various Ions Pass Through a Tumor Volume.....	43
19 Dose Equivalence Percentage Rates for Various Ion Beams in a Tumor and in Different Regions of a Body Relative to the Tumor.....	45
20 Percentage of Primary Particles Remaining Within the Original Beam Width (0.1 cm) as They Approach Their Bragg Peak at 10 cm and Continue Until All Stop	49
21 Total Energy Escaping a 0.1 cm Radius in the Form of Neutrons for Various Ion Beams Having a Depth of 10 cm, on a Per Particle Basis.....	51
22 Total Energy Escaping a 0.1 cm Radius for Various Ion Beams Having a Depth of 10 cm, Normalized to Maximum Dose Equivalence.....	52
23 Total Energy Escaping a 1 cm Radius for Various Ions Having a Depth of 10 cm, Normalized to Maximum Dose Equivalence.....	53
24 Total Energy Escaping a 1 cm Radius from Different Particles for a Beam of $116.5 \text{ MeV u}^{-1} \text{ } ^1\text{H}$ Particles Delivering a Maximum Dose of 10 Sv	55
25 Total Energy Escaping a 1 cm Radius from Different Fragmentation and Scattering Isobars for a Beam of $116.5 \text{ MeV u}^{-1} \text{ } ^4\text{He}$ Particles Delivering a Maximum Dose of 10 Sv	56

FIGURE		Page
26	Total Energy Escaping a 1 cm Radius from Different Fragmentation and Scattering Isobars for a Beam of $134.5 \text{ MeV u}^{-1} \text{ } ^7\text{Li}$ Particles Delivering a Maximum Dose of 10 Sv	57
27	Total Energy Escaping a 1 cm Radius from Different Fragmentation and Scattering Isobars for a Beam of $219 \text{ MeV u}^{-1} \text{ } ^{12}\text{C}$ Particles Delivering a Maximum Dose of 10 Sv	58
28	Total Energy Escaping a 1 cm Radius from Different Fragmentation and Scattering Isobars for a Beam of $259 \text{ MeV u}^{-1} \text{ } ^{16}\text{O}$ Particles Delivering a Maximum Dose of 10 Sv	59
29	Total Energy Escaping a 1 cm Radius from Different Fragmentation and Scattering Isobars for a Beam of $296 \text{ MeV u}^{-1} \text{ } ^{20}\text{Ne}$ Particles Delivering a Maximum Dose of 10 Sv	60

LIST OF TABLES

TABLE		Page
1	List of Ions and Energies Used for Transport Simulations	22
2	Depths in cm Where LET Was Scored in μm Bins for Dose Simulations	23
3	Percentage Differences Between PHITS Simulated LETs and Bethe Approximated LETs for Charged Particles.....	34
4	Average Dose in nGy Per Input Particle at Different Depths for All Ions Used in PHITS Analysis.....	38
5	Required Particle Fluencies to Cause a Maximum Dose of 10 Gy and 10 Sv from Various Ions	46
6	Percentage of Primary Particles Passing Into the Tumor at Different Radii Centered Around the Tumor	48

CHAPTER I

INTRODUCTION

The foremost goal of radiotherapy is to maximize the radiation dose to a tumor while minimizing the dose to the surrounding healthy tissues. The greater the dose that can be imparted in the tumor the greater the probability of controlling it, while minimizing the dose to healthy tissues will decrease the probability of causing undesirable side effects. In conventional radiotherapy, photons are used as the energy carriers to impart a dose in the tumor. Because of the exponential attenuation of photons higher doses are incurred in areas proximal to the tumor. However, charged particles, with an inverse depth-dose relationship allow for the region of highest dose to occur within the tumor so that a greater therapeutic benefit may be derived from the use of these particles in tumor treatment.

In addition to a favorable depth-dose profile, the dense ionizing tracks that arise from interactions of massive charged particles result in high linear energy transfer (LET) rates, defined as the energy lost by an ion as it travels through a unit depth of material. As a charged particle loses its energy and slows down its LET gradually increases and then experiences a large jump at the end of its track, this sudden increase is known as the Bragg Peak and is the reason for localized dose in depth for charged particles.

This thesis follows the style of Health Physics.

The damaging effect that charged particles have on cells has been seen to be different than those of other radiations. For equal amounts of dose absorbed by a cell, charge particles produce more cellular apoptosis than x-rays and photons. To account for these differences a weighing factor called the relative biological effectiveness (RBE) was introduced that compares the doses of different radiation types and energies to that of 250 keV x-rays to produce an equivalent effect. (Attix 2004) With consideration of the RBE, a quality factor (Q) can then be applied which estimates the relative hazard of dissimilar radiations for humans. The product of the dose and Q is known as the dose equivalence (H) and allows for biological comparison between radiation types. As the LET of a charged particle increases, its dose equivalence increases, leading to further increases in the therapeutic ratio of therapy with charged particle, defined as the ratio of dose in a tumor to the dose in healthy tissues.

When using charged particles for therapy, spurious doses from fragmentation and scattering must be considered. Fragmentation occurs when an ion breaks apart, forming two or more less massive ions. These lighter ions will have the same kinetic energy as the incident particle and due to their lighter mass and lower atomic number they will have a longer range and could travel beyond the boundary of the tumor to deposit a dose in healthy tissues distal of the tumor. Scattering of ions will also occur, causing doses away from the intended straight line path of the ion beam. Fragmentation and scattering are some of the largest potential drawbacks to therapy with charged particles.

The focus of this thesis is that of therapy simulations using the Particle and Heavy Ion Transport Code System (PHITS) to determine the LET and dose distributions

at different depths in a water phantom for a variety of ion beams that all have the same projected range. Furthermore, the fragmentation fluences at several points within the phantom were investigated for the different beam types.

Due to the different physical and biological effects from varying particles, some terminology should be briefly explained to help separate the types of therapy.

Radiotherapy (RT) will be used as an umbrella term for all therapies in which ionizing radiation is used as an energy carrier. Intensity-modulated radiotherapy (IMRT) will be used to describe therapies that use photons as energy carrier. Charged particle therapy (CPT), commonly called hadron therapy, will be used to describe therapies that use stripped nuclei to deliver dose. Furthermore, CPT can be broken down into proton therapy (PT) and heavy-charged particle therapy (HCPT), the former consisting of only protons and the latter of any ion with an atomic number greater than one. Particles used in HCPT are considered high LET radiations, while those used in PT and IMRT are considered low LET. Although charged particles, electrons, muons, and other non-nuclei are not considered part of CPT for the purposes of this paper unless specifically noted.

CHAPTER II

BACKGROUND

History of Charged Particle Therapy

Since the discovery of radioactivity, its potential for use in the treatment of cancers has been investigated. The basic premise for RT is to impart a great enough energetic dose in a tumor to fatally injure the cancerous cells. Initially, photons and x-rays were the only particles that could be produced with sufficient energy to reach a depth relevant for tumor therapy. As such, radiotherapy with photons became the standard procedure and the usage of photon therapies has far surpassed those of any other particles. (Raju 1996)

However, as early as 1946, Robert Wilson proposed protons as a cancer treatment modality. (Wilson 1946). By 1954 pituitary suppression treatments using protons began on humans at the Berkley Lab in California. Pituitary treatments were initially undertaken in lieu of cancer treatments because the boundaries of the pituitary gland are well defined and imaging techniques were not yet evolved enough to take full advantage of the use of proton beams. (Raju 1996) By 1974 techniques had greatly improved in PT and can be highlighted in the successful clinical results of the Harvard Cyclotron Laboratory regarding bony and cartilaginous tumors of the skull base and cervical spine. (Suit 1992)

In 1990, due to the success of proton treatments, Loma Linda Medical Center became the first site to complete the building of a proton beam in a dedicated medical facility. The number of proton treatments facilities has since been expanded, and as of 2011 there are over 32 working proton facilities with over 62,000 patients having been treated with protons. (PTCOG 2011) Several more facilities are currently being planned for operational use in the near future.

The history of HCPT is even more concise than that of protons. The potential uses of heavy ions were also speculated about as early as 1946, however, the first patient was not treated with them until 1975. The earliest beginnings of HCPT can be traced back to Cornelius Tobias who created a steady high energy carbon beam at Berkeley in 1942. However, it took until the early 1970s at the Princeton-Penn accelerator to be able to create heavy ion beams with enough energy to be applicable for cancer therapy. Finally, in 1974, Lawrence Berkeley Labs combined their low energy heavy ion linear accelerator to their Bevatron to create an accelerator that could bring heavy ions to relativistic energies. This combination was named the BEVALAC and was the location of the first heavy-ion radiotherapy group. (Raju 1996)

Initial emphasis was placed on neon and Joseph Castro carried out 239 phase I-II clinical tests with neon at the BEVALAC. Encouraging results were seen for advanced macroscopic salivary gland carcinomas, paranasal sinus tumors, advanced soft tissue sarcomas, macroscopic sarcomas of bone, locally advanced prostate carcinomas, and biliary tract carcinomas (Linstadt et al., 1991). Tumors in the skull base were found to exhibit the greatest benefit from HCPT. Five year local control rates of 85, 78, 63, and

58 % were seen for meningioma, chondrosarcoma, chordoma, and other sarcomas, respectively. (Castro et al., 1994) The BEVALAC was shut down before phase III trials could be completed to fully analyze the differences between HCPT and PT. Current research in CPT continues at the HIMAC facility in China, Japan and the GSI facility in Darmstadt, Germany. Approximately 7,000 patients have been treated at these facilities. Initial results are promising, but more time must pass to fully understand the long term effects of heavy ion irradiation on secondary cancer induction. Currently there are six facilities worldwide capable of HCPT with another six being planned in Germany, China, Austria, and Italy. (PTCOG 2011) The new facilities are designed to be able to deliver both PT and HCPT in the form of ^{12}C ions (Amaldi and Kraft 2007).

Charged Particle Interactions and the Bragg Peak

While traversing matter, charged and uncharged ionizing radiations undergo fundamentally different interactions which lead to dissimilar manners in which they dissipate their energy. Uncharged particles lose the majority of their energy in either a single or a few head on collisions with the atoms of the medium they are crossing. In a homogenous medium, a photon has an equal probability of interaction at every depth interval, assuming constant energy. Charged particles are not as heavily affected by head on collisions and also lose their energy through numerous columbic interactions as they transverse matter (Attix 2004). As a charged particle loses energy it slows down and as a result interacts with more electrons in the medium. At the end of the charged

particle track, maximum interactions occur which directly relates to maximum energy transferred and maximum dose. This region of maximum dose is known as the Bragg peak and is shown in Fig. 1 which compares relative doses between PT, HCPT, and therapy with uncharged radiations at different depths.

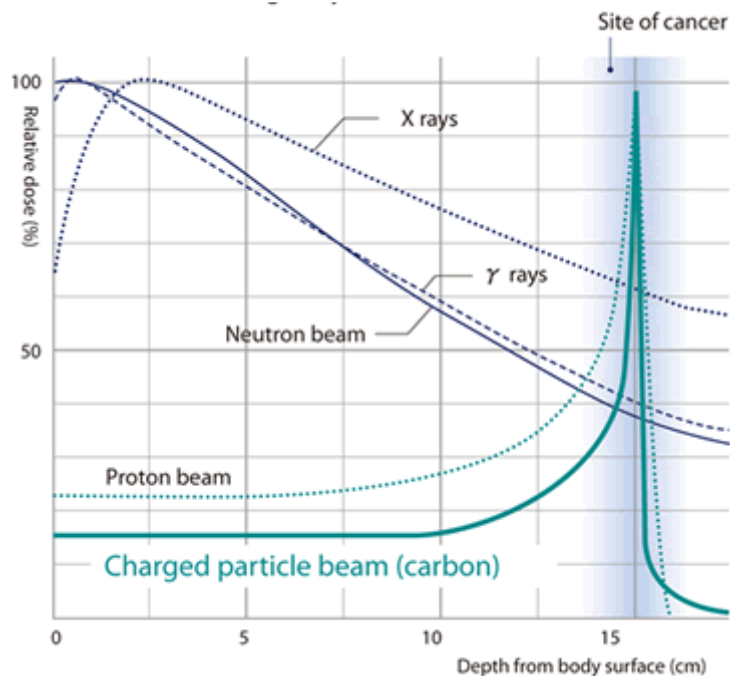


Fig 1. Relative dose distributions from beams of charged and uncharged radiation types. For charged radiations the maximum dose occurs in significant depth, while for uncharged radiations the maximum occurs near the entrance of the particle. The dose in depth allows for the potential use of charged particles to greatly spare healthy tissue in tumor therapies. (Courtesy NIRS)

As shown in Fig.1, provided by the Japanese National Institute of Radiological Sciences (NIRS), some general observations can be made about the advantages of HCPT. Most obvious is the inverse dose-depth profile of charged particles showing that maximum dose will occur at a tumor site instead of in the superficial regions of the body. With the maximum dose existing in the tumor the therapeutic ratio of CPT will be

greater than that of IMRT. The increase in the therapeutic ration can be seen in Fig. 2, which shows a comparison of the dose mapping between therapies involving ^{12}C ions and photons for the equal doses delivered to a brain tumor. In addition to a maximum dose in depth, the sharp drop off of the Bragg Peak shows that the dose distal to the tumor rapidly approaches zero as a particle near the end of its range.

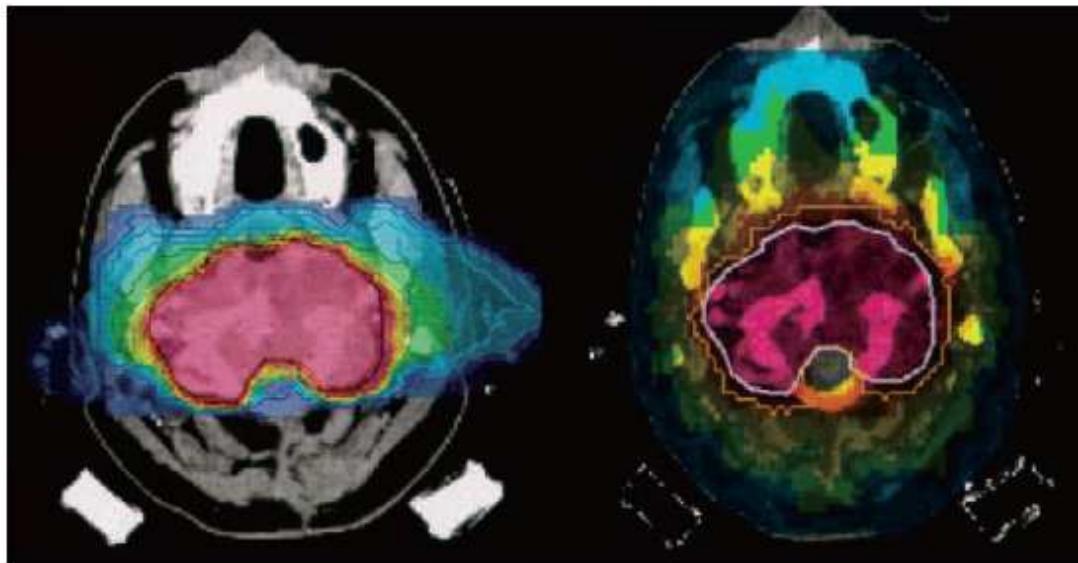


Fig 2. Contrast of radiation therapy with ^{12}C ions (left) to that of IMRT (right) for the same dose delivered to a tumor volume. Red=90% isodose, yellow=70% isodose, green=50% isodose, blue=20% isodose. The tumor boundary is the black line in the left image and the white line in the left image. In the carbon therapy doses to the healthy tissues outside the tumor are seen to be much smaller than in IMRT and the radiation field more confined near the tumor. (Amaldi and Kraft 2007)

The Bragg Peak can be understood by first assuming that an ion will undergo one of two types of interactions. The first interactions are “soft collisions” that occur when the charged particle passes far away from an atomic nucleus and transfers a small amount of energy by exciting the energy level of the medium. The second interactions are “hard collisions” and occur when the charged particles passes very close to the atom

of the medium and a physical interaction with an electron occurs, causing the ejection of a delta ray. This delta ray, with its own kinetic energy will then dissipate its energy by engaging in columbic force interactions.

The rate of energy lost by the particle (stopping power) will be the sum of the energy lost from hard and soft collisions. To make the stopping power independent of a medium's density, the density is commonly divided out resulting in the mass stopping power, shown in eqn (1) and known as the Bethe approximation. (Attix 2004)

$$-\left(\frac{dE}{\rho dx}\right) = \frac{\pi r_0^2 N_A Z}{A} \cdot \frac{4m_0 c^2 z^2}{\beta^2} \cdot \left[\ln\left(\frac{2m_0 c^2 \beta^2}{(1-\beta^2)I}\right) - \beta^2 \right] \quad (1)$$

where $m_0 c^2$ = rest mass of an electron

Z = atomic number of medium

A = mass number of medium

N_A = Avogadro constant

r_0 = classical electron radius

z = charge of particle

β = velocity of particle relative to the speed of light $\left(\frac{v}{c}\right)$

I = mean excitation potential of medium

ρ = density of medium

Substitution of constants into eqn (1) yields a simplified Bethe approximation, shown by eqn (2).

$$-\left(\frac{dE}{\rho dx}\right) = 0.3071 \frac{Zz^2}{A\beta^2} \left[13.8373 + \ln\left(\frac{\beta^2}{1-\beta^2}\right) - \beta^2 - \ln I \right] \quad (2)$$

The inverse β^2 term outside of the bracket helps to illustrate how the stopping power quickly increases as particle velocity is reduced. Also, the z^2 term shows that the stopping power of ions are proportional to the square of their charge. With this taken into consideration, an alpha particle accelerated to the same energy as a proton would have 4 times greater the stopping power.

The range (R) of the charged particle can then be determined as the inverse integral of the mass stopping power:

$$R = \int_0^{E_0} \left(\frac{dE}{\rho dx} \right)^{-1} dE \quad (3)$$

The range calculation assumes that the particle is constantly slowing down and does not experience discrete and sporadic energy losses. (Attix 2004)

Charged Particle Tracks

A heavy charged particle will lose approximately half of its energy in the form of excitation events and electron plasma oscillations (soft collisions) and the other half in ionization events (hard collisions), which liberate electrons and eject them as delta rays. (Chatterjee and Schaefer 1976) The energy deposition events from excitations occur very close to the actual particle, while the delta rays create energetic spurs projecting radially from the particle. The region in which excitation events predominate is known as the core and its radius was described by Chatterjee and Schaefer as:

$$r_{core} = 0.0116 \beta \quad (4)$$

where r_{core} is in microns of water. This region surrounding the core, where ionization events predominate, is known as the penumbra, and its maximum radius is described by Chatterjee and Schaefer as:

$$r_{penumbra} = 0.768E - 1.925 \sqrt{E} + 1.257 \quad (5)$$

where $r_{penumbra}$ is in microns of water and E is in MeV u^{-1} . The radius of the penumbra will decrease as particle energy is decreased. From eqns (4) and (5) the energy densities of the core and penumbra can be described by eqns (6) and (7):

$$\rho_{core} = \frac{0.5LET}{\pi r_{core}^2} + \frac{0.5LET}{2\pi r_{core}^2 \ln \sqrt{e} \frac{r_{penumbra}}{r_{core}}} \quad (6)$$

$$\rho_{penumbra} = \frac{0.5LET}{2\pi r^2 \ln \sqrt{e} \frac{r_{penumbra}}{r_{core}}} \quad (7)$$

where r is the distance away from the center of the core and LET is in $\text{keV } \mu\text{m}^{-1}$. The energy density is assumed constant throughout the core region and then decreases radially as a function of r^2 throughout the penumbra. The density of the core region is much higher than that of the penumbra and the total fraction of energy dissipated in micron distances away from the center of a particle track can be described by eqn (8).

$$F = 0.5 + \frac{1+2 \ln \frac{r}{r_{core}}}{4 \ln \sqrt{e} \frac{r_{penumbra}}{r_{core}}} \quad (8)$$

Eqn (8) is only applicable for distances greater than that of the core radius. Because 50% of the energy deposition occurs in the core and a high percentage of the penumbra's energy deposition occurs very close to the core boundary, a very high concentration of energy density is seen around the particle track. Fig. 3 give an example of this high energy density, which only expands 0.155% of the total penumbra radius, yet the energy density drop off is almost 6 orders of magnitude. The given figure is for that of a ^{20}Ne 296 MeV u^{-1} ion used in this experiment, at the entrance of the phantom. Because of this high energy concentration around the track, LET is a more appropriate measurement to use than absorbed dose when studying HCPs. Absorbed dose ($\frac{d\epsilon}{dm}$), averages imparted

energy over an entire mass, while LET measures the energy transferred over a unit distance. When using LET in lieu of absorbed dose, the compactness of energy deposition is appreciated because its value is not being averaged from a small area with a high energy density to a large area with a low or nonexistent energy density.

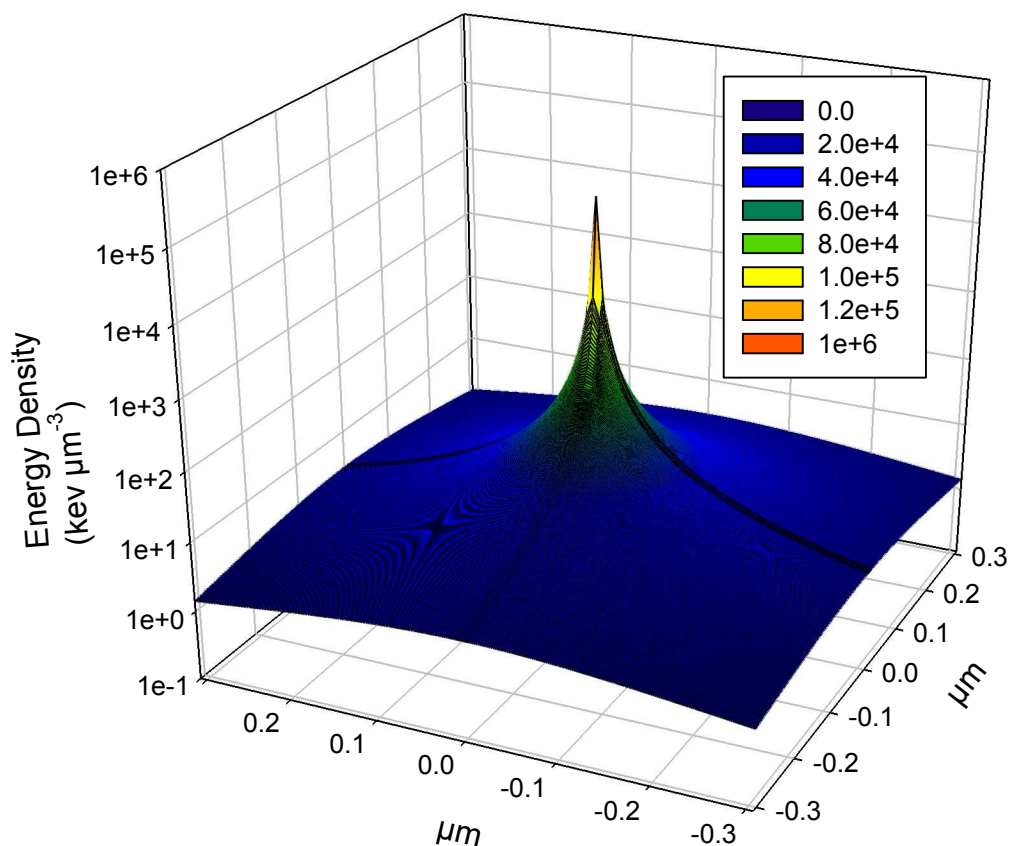


Fig 3. Chatterjee and Schaefer energy density for a radius of $0.3 \mu\text{m}$ surrounding the particle track of a $296 \text{ MeV } u^{-1} {}^{20}\text{Ne}$ ion as it enters a water volume. Total penumbra radius is $195 \mu\text{m}$. The high energy density in the core region accounts for about 50 % of the total imparted energy, the energy density then rapidly falls off as a function of distance away from the core. In the $0.3 \mu\text{m}$ radius shown, 69.6 % of the total energy is deposited.

Quality Factor for Charged Particles

By definition, a high LET particle transfer more energy to a cell as it passes through it compared to a lower LET particle. This allows for a comparatively lower quantity of high LET particles to be required for an equal dose. Furthermore, it has been seen that for the same dose to a cell, high LET radiations create a larger amount of complex DNA damage such as double strand breaks, chromosome aberrations, dicentric, lethal lesions, and a higher percentage of cell inactivation. (Nikjoo et al., 1999) These complex damages are due to the dense ionization track of the particle, creating numerous delta rays that will dissipate their energy in, and cause damage to, a DNA strand. (Hamada 2009)

The greater effects from an equal dose of high LET particles over that of low LET particles show that the quality factor (Q) of particles increase with LET, up to a point. The value of Q is strongly dependent on the RBE of a particle. The International Commission on Radiation Protection (ICRP) relates Q and LET together by eqn (9).

$$Q = \begin{cases} 1 & \text{if } LET \leq 10 \\ 0.32LET - 2.2 & \text{if } 10 < LET < 100 \\ 300/\sqrt{LET} & \text{if } LET \geq 100 \end{cases} \quad (9)$$

where LET is given in units of keV u⁻¹. (Valentin 2003)

The overall dose equivalence (H) is then given by:

$$H = Dose \cdot Q \quad (10)$$

when referring to dose equivalence the special unit Sievert (Sv) is used instead of the Gray (Gy). Both these metrics correspond to 1 J kg⁻¹, but the usage of the Sv attempts to

compensate for the relative damaging ability of the ion. An additional cellular or organ weighting term can be added on to eqn (10) if enough information is known about how the specific cell types being irradiated respond to that form of radiation.

The reduction of Q when LET is above $100 \text{ keV } \mu\text{m}^{-1}$ is indicative of a double event theory for cellular death. LETs around $100 \text{ keV } \mu\text{m}^{-1}$, on average, create two damage sites inside a cell which will cause cell death in a majority of cases. (Goodhead 1999) LETs greater than $100 \text{ keV } \mu\text{m}^{-1}$ will cause more damage sites in a cell, but the extra damage does little to increase the probability of lethality. In essence, LETs of $100 \text{ keV } \mu\text{m}^{-1}$ are most efficient at killing cells, as the LET increases past $100 \text{ keV } \mu\text{m}^{-1}$ a particle “wastes” its excess energy. It is important to note that eqn (9) is a simplified approximation made by the ICRP and although very useful to approximate Q , there are factors other than LET, such as delta ray creation, that influence Q for different ions.

The effects that charged particles have on specific cell types can potentially further increase their dose equivalence. Depending on the cellular makeup of a tumor, some cancers may be harder to treat with low LET radiations. Adenocarcinoma of the prostate, squamous cell carcinomas, fibrosarcomas, and neurofibrosarcomas are examples of tumors that show resistance to low LET radiations. (Bella et al., 2008) Higher LET radiations have been shown as an option to combat these difficult tumors.

The benefits from HCPT for use on low LET radioresistant tumors can be seen in a 2008 study that examined, the survival of different cell lines irradiated with ^{12}C beams of varying LET. (Bella et al., 2008) Two of the cell types (SCC25 and SQ20B) were derived from human tumors tissues and two (HF19 and H184B5-1M/10) were

derived from a healthy human cells. The results of this study are presented in Fig. 4 as survival curves.

When comparing the cell survival curves of the ^{12}C ions to that of photons, a substantial increase in cell killing can be seen for all LET's in the range of 94-303 keV/ μm . Regions of higher LET are characteristic of the Bragg Peak and this higher killing rate would occur in the target volume of HCPT. Of note is that the percentage of increase in cell inactivation between photon and HCP irradiation is greatest in the cell lines that showed the most radioresistance. This suggests that mechanisms such as Bcl-2 overexpression, p53 mutations and intratumor hypoxia that protect some tumor cells from radiation is bypassed by exposure to high LET radiations. (Hamada 2009) Thus, HCPT should be the therapy of choice when dealing with photon resistant tumors.

Effects of Dose Fractionation

The biological effects of how the dose is delivered must also be considered when comparing IMRT treatments to CPT. In IMRT, it is common to deliver the total dose in several small fractions separated by time. This fractionation allows for the repair of healthy tissues which reduces the potential long term damage from radiation. Cells in the tumor are not capable of properly repairing themselves and do not benefit as greatly from fractionizing the dose. The complex damage caused by high LET radiation is not as easily repaired and the healing of healthy tissues does not occur to as great of an extent when using HCPT. Not being able to gain the benefits of dose fractionation was

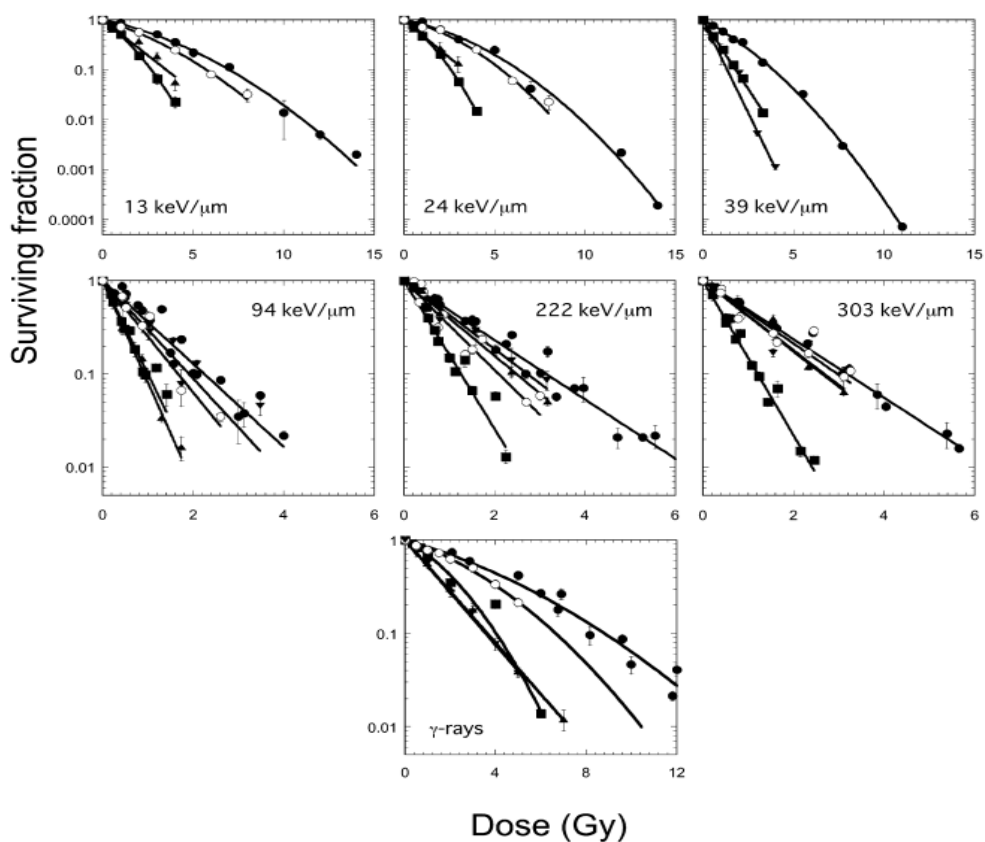


Fig 4. Survival curves for irradiation of (\blacktriangle) SCC25, (\blacksquare) H184B5-1M/10, (\circ) V79, (\bullet) SQ20B, and (\blacktriangledown) HF19 cell lines using ^{12}C beams of different LET and ^{60}Co photons. The greatest increase in cellular killing rate between ^{12}C and photons is seen to occur in the cells that had the highest survival rates in photon irradiation, suggesting that ion therapy would be greatly beneficial when dealing with tumors that display radioresistance to photons and other low LET radiations (Bella et al., 2008)

initially seen as a disadvantage to HCPT, however, studies have shown that there is some positive healing that occurs from fractionating heavy ion beams, thus reducing the probability of long term damage. (Wang et al., 2008)

The effects of fractionation on AG1522B cells for both 250 keV x-rays and a $16.6 \text{ keV } \mu\text{m}^{-1} \text{ }^{12}\text{C}$ beam (195 MeV u^{-1}) are presented in Fig. 5 where fractions were administered every 24 hours. The survival rates of cells are seen to increase similarly as fractionation amounts are increased for both x-rays and carbon, indicating that fractionizing dose in HCPT would lead to a reduction of secondary cancers. More research must be done in this field to determine at what LET fractionation no longer becomes beneficial and if the trends from this study apply to all cell types.

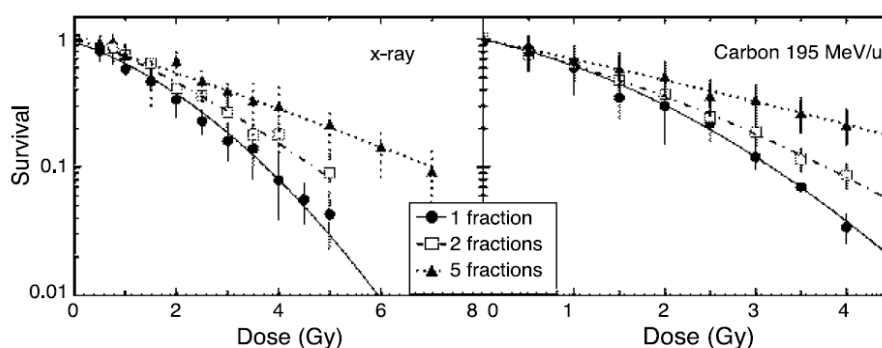


Fig 5. Comparison of AG1522B cell survival when irradiated with 250 keV x-rays and $16.6 \text{ keV } \mu\text{m}^{-1} \text{ }^{12}\text{C}$ ions in different fractions. Doses were delivered every 24 hours, the amount of repair in cells from ^{12}C irradiation was seen to be comparable to the amount of repair in cells from x-rays, suggesting that fractionation would be beneficial in HCPT. (Wang et al., 2008)

Fragmentation and Scattering

In addition to hard and soft collisions, energy is also transferred in the form of nuclear collisions. For every 4000 energy transfer events approximately one of them is a nuclear collision. (Fenrow 1989) Although this is a small yield, they become important if a medium is thick enough to produce an appreciable amount them. Fragmentation products will cause dose to be distributed away from the point of interest in clinical CPT situations. Fragment products are produced with some lateral deflection that is inversely dependent on fragment energy. Fragments with smaller energies tend to have larger deflection. The high energy fragments with small deflection may be able to travel further than the tumor boundary in the distal direction, reducing the benefit from the sharp drop of the Bragg Peak.

The majority of fragmentation particles will be single nucleons and light ions such as deuterons, tritons, ^3He , and alpha particles. Being composed of fewer nucleons and a lower energy to reach the same depth, lighter ions will experience smaller a degree of fragmentation than the heavy ions. Because they are lighter these radiations experience more lateral spread and scattering as they pass through a medium and depending on the degree of the spread, could cause unwanted dose outside of a tumor and a less precise beam. The low LET that helps accommodate the low levels of fragmentation, or no fragmentation in the case of proton, may actually make them undesirable. When the sheer quantity of ions needed to reach a potential dose is taken

into consideration, their total amount of energy lost by fragmentation and scattering may be greater than that of heavier ions.

CHAPTER III

METHODS AND MATERIALS

Particle Heavy Ion Transport System (PHITS)

PHITS is a Monte Carlo code specially designed for the transport of heavy ions and other charged particles in accelerator and galactic simulations. It was designed as a joint project between the Japan Atomic Energy Agency, Research Organization for Information Science and Technology, High Energy Accelerator Research Organization, and Chalmers University of Technology. PHITS is able to simulate all particle types across a wide breadth of energies. (PHITS 2011)

Phantom Geometry and Particle Beams

To simulate a human body, a 10 cm radius cylinder with a height of 24 cm was created. In the center of this cylinder a 1 cm radius sphere was placed to serve as a tumor. Both the cylinder and the sphere were filled with 1 g cm^{-3} water. Water was used as a medium because it closely resembles the density of a human body. A view of this phantom is given in Fig. 6.

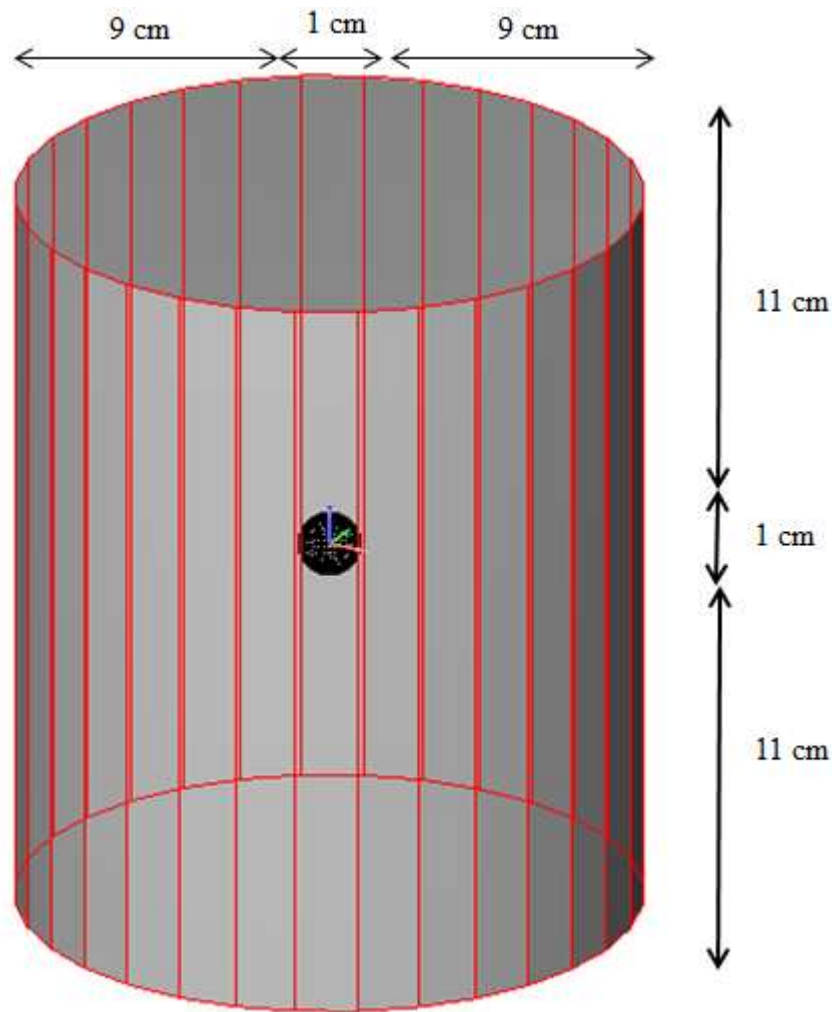


Fig 6. Geometry of water phantom used to simulate a human body and tumor for heavy ion transports. Radial dimension of 10 cm and height dimension of 24 cm were used for the cylindrical “body” and spherical radius of 1 cm used for the “tumor”. Entire phantom filled with 1 g cm^{-3} water.

Beams of different primary particles were individually delivered into the phantom. Beam energies were selected so that their Bragg peak would occur approximately 10 cm into the phantom, in the center of the tumor. For all beams, simulations were run with 500,000 particles and an initial beam radius of 0.1 cm was used. All the beams originated in a vacuum. The beams were directed normal to the

cylinder base and centered with the tumor sphere. Table 1 shows the ions and energies used for each beam. Depending on the beam species, the average run time for each simulation varied between 30 minutes to over 24 hours.

Table 1. List of ions and energies used for transport simulations. Energies were selected to have Bragg Peak occur at a depth of 10 cm in a 1 g cm^{-3} water phantom.

Ion	Energy (MeV u^{-1})
^1H	116.5
^4He	116.5
^7Li	134.5
^{12}C	219
^{16}O	259
^{20}Ne	296

Dose Calculations

To calculate dose, LET from the particles was tracked throughout the phantom. Inside the body phantom $1 \mu\text{m}$ thick bins were set up and centered at the depths shown in Table 2. For the 45 depth locations between 9.0005 and 10.9995 cm, LET was tracked both inside and outside of the tumor. The distance between bins were selected to have a larger gap in regions where the LET was not rapidly changing and a smaller gap in regions where the LET was expected to be rapidly changing.

Table 2. Depths in cm where LET was scored in μm bins for dose simulations. Distances between slabs were selected to so that any sudden change in LET would be noticed. For depths of 9.0005 through 10.9995 cm, LET was scored both inside and outside of the tumor volume.

0.0005	9.0005	9.86	9.98	10.04	10.9995
1.0	9.1	9.87	9.99	10.05	11.0005
2.0	9.2	9.89	10.0	10.1	12.0
2.5	9.3	9.9	10.01	10.2	13.0
3.0	9.4	9.91	10.02	10.3	14.0
4.0	9.5	9.92	10.03	10.4	15.0
5.0	9.6	9.93	10.04	10.5	16.0
6.0	9.7	9.94	10.05	10.6	17.0
7.0	9.75	9.95	10.1	10.7	18.0
8.0	9.8	9.96	10.2	10.8	19.0
8.9995	9.85	9.97	10.03	10.9	19.9995

All depths shown to four significant digits were placed so as to be the closest a $1\ \mu\text{m}$ bin could be placed to a geometric boundary.

In each bin the total energy transferred, as well as the energy transferred from only the primary particle across each width (LET) was scored. For the applicable ions, energy transferred from protons and alpha particles were also scored for each bin.

With knowledge of LET at each depth, dose was calculated in each bin by assuming that LET was constant over the $1\ \mu\text{m}$ distance, scattering was negligible, and charged particle equilibrium existed. With these assumptions dose can be calculated as (Attix 2004):

$$D = 1.602 \times 10^{-10} \Phi LET \quad (11)$$

where D is solved for is Gray (Gy)
 LET is given in $\text{keV}\ \mu\text{m}^{-1}$
 and Φ is particle fluence

The quality can also be solved for by using eqn (9) and the dose equivalence using eqn (10).

Fragmentation and Scattering Analysis

Complete particle fluences were taken at several depths. Circular planes of 0.1 cm were set up and centered around the beamline axis at depths of 0.0001, 1, 2, 3, 4, 5, 6, 7, 8, 9, 10, 11, and 12 cm. An additional two circular planes were placed 1 μm apart from each other surrounding the region of max LET for each beam variety. These planes served to determine the makeup of the forward current of particles within the width of the original beamline. Torus planes at the same depths were set up and centered around the beam with an inner radius of 0.1 cm and an outer radius of 1 cm. These planes served to determine the makeup of the forward current of particles that had the same radius as the tumor, which would consist of fragmentation products or primary particles scattered outside of the original beam width. The fluences through cylindrical planes extended between the sequential circular and torus planes were also found to determine the particle makeup sheering off from the original beam width and the particle make up traveling more than 1 cm from the beam line center.

CHAPTER IV

RESULTS AND DISCUSSION

LET and Dose Analysis

The LET as a function of depth, for the entire phantom, is shown in Fig. 7, for each ion variety. All the LET profiles follow the same pattern of a slow buildup to a sudden jump in LET followed by a rapid decline to almost zero. Because of the charge squared relationship of the Bethe approximation, the greatest magnitude LET is seen in the more massively charged particles. The LET exiting the tumor is from fragmentation products, the primary particles with the longest range all stop within 0.2 cm of the targets center.

For each individual ion, the total LET from all particles as well as the LET from only the primary particle are shown in Figs. 8 – 13. The bottom window of each figure shows a detailed tracking of LET in only the tumor volume. The LET at every depth tallied for each ion can be found in Appendix A.

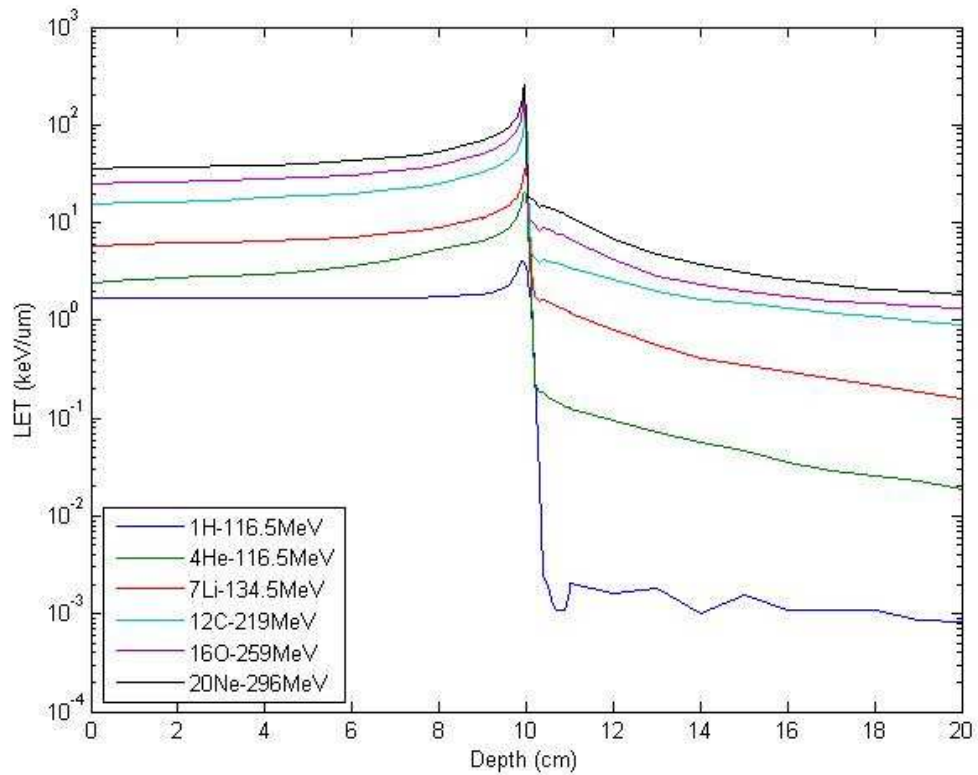


Fig 7. LET depth profiles for various ion beams, of concern in charged particle therapy, passing through a water phantom. All beams show characteristics of a slow LET buildup followed by a rapid rise in energy transfer near the end of the particle track and a rapid decline thereafter. Higher magnitude LETs are seen in ions with higher charges. LET values are averages taken from 500,000 particle simulations using PHITS.

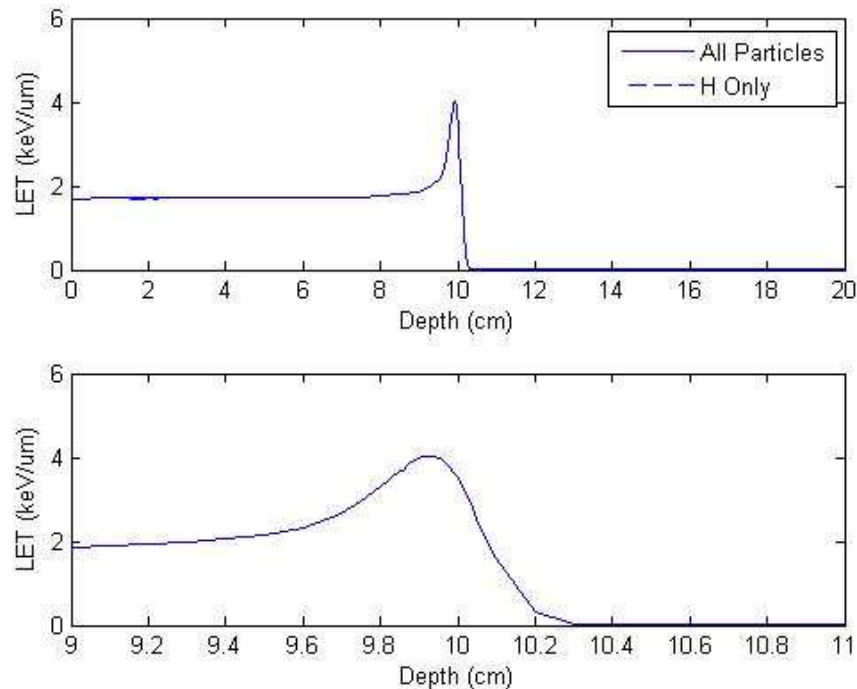


Fig 8. LET depth profile of ^1H 116.5 MeV u^{-1} traversing through 1 g cm^{-3} water. Maximum LET occurs at $1.86 \text{ keV } \mu\text{m}^{-1}$ at a depth of 9.94 cm , giving a 140% increase from the entrance LET.

For hydrogen, the beam enters the body with an average per particle LET of $1.67 \text{ keV } \mu\text{m}^{-1}$. The LET rises to $1.86 \text{ keV } \mu\text{m}^{-1}$ as it reaches the tumor. Upon entering the tumor the LET continues to rise to a maximum of $4.00 \text{ keV } \mu\text{m}^{-1}$ at a depth of 9.94 cm . The influence of non-primary particles is almost nonexistent because hydrogen cannot fragment. At a depth of 10.1 cm , an LET of $1.60 \text{ keV } \mu\text{m}^{-1}$ is seen, but quickly drops off to almost zero after that.

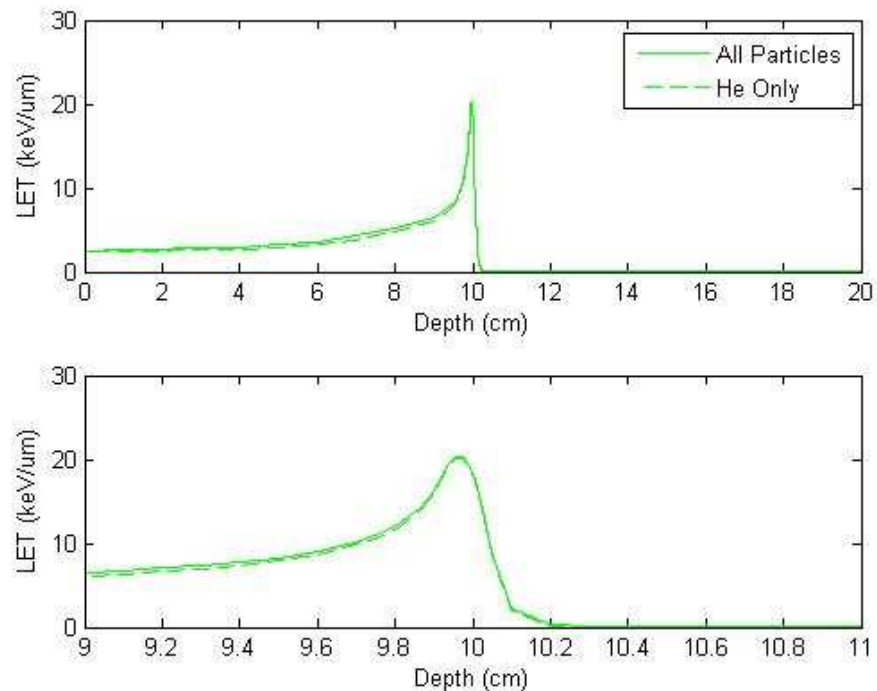


Fig 9. LET depth profile of ${}^4\text{He}$ 116.5 MeV u^{-1} traversing through 1 g cm^{-3} water. Maximum LET occurs at $20.3 \text{ keV } \mu\text{m}^{-1}$ at a depth of 9.96 cm , giving a 726% increase from the entrance LET. Dashed line shows LET from only primary particles, while solid line shows LET from all particles.

For helium, the beam enters the body with an average per particle LET of $2.46 \text{ keV } \mu\text{m}^{-1}$. The LET rises to $6.47 \text{ keV } \mu\text{m}^{-1}$ as it reaches the tumor. Upon entering the tumor the LET continues to rise to a maximum of $20.3 \text{ keV } \mu\text{m}^{-1}$ at a depth of 9.96 cm . At a depth of 10.1 cm , an LET of $2.15 \text{ keV } \mu\text{m}^{-1}$ is seen, but quickly drops off to almost zero after that. At a depth of 4 cm , a maximum of 10.8% of the LET is seen to come from non-primary particles.

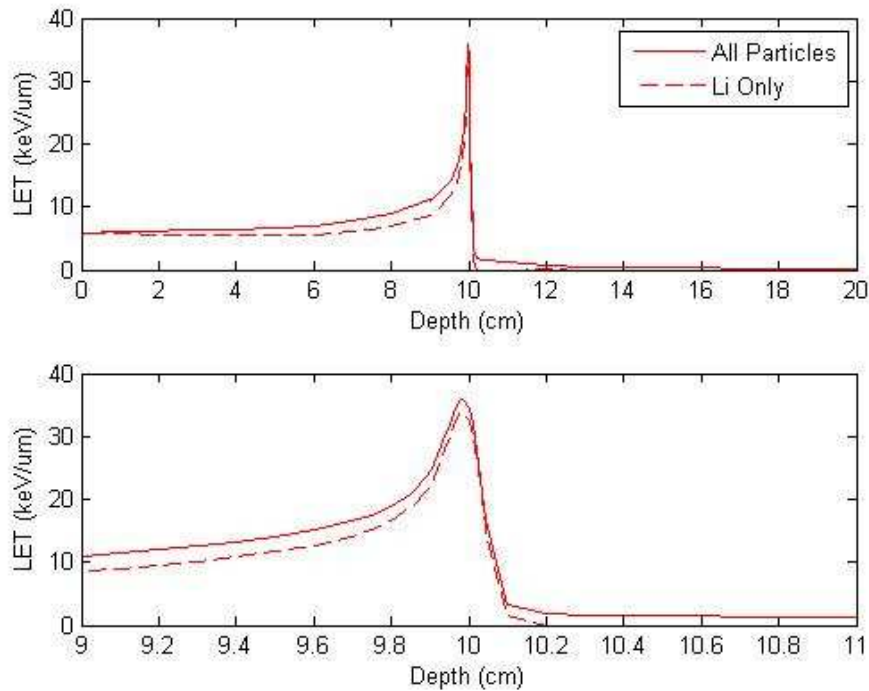


Fig 10. LET depth profile of ${}^7\text{Li}$ 134.5 MeV u^{-1} traversing through 1 g cm^{-3} water. Maximum LET occurs at $35.0 \text{ keV } \mu\text{m}^{-1}$ at a depth of 9.98 cm , giving a 509% increase from the entrance LET. Dashed line shows LET from only primary particles, while solid line shows LET from all particles.

For lithium, the beam enters the body with an average per particle LET of $5.75 \text{ keV } \mu\text{m}^{-1}$. The LET rises to $9.04 \text{ keV } \mu\text{m}^{-1}$ as it reaches the tumor, which is close to the threshold when Q begins to increase. Upon entering the tumor the LET continues to rise to a maximum of $35.0 \text{ keV } \mu\text{m}^{-1}$ at a depth of 9.98 cm . At a depth of 10.1 cm , an LET of $14.5 \text{ keV } \mu\text{m}^{-1}$ is still seen, but quickly drops off to $0.247 \text{ keV } \mu\text{m}^{-1}$ before exiting tumor. The effect of non-primary particles greatly attributes to lithium's LET, at a depth of 8 cm , a maximum of 23.5 % of the LET is seen to come from non-primary particles, mostly alpha particles. Beyond the tumor volume, non-primaries account for an LET between 0.16 and $1.21 \text{ keV } \mu\text{m}^{-1}$.

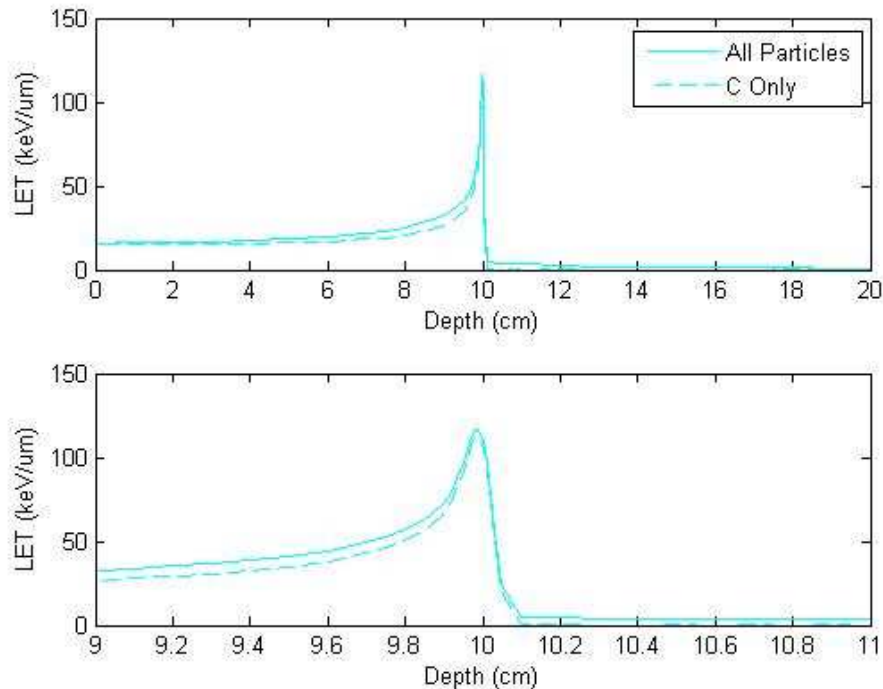


Fig 11. LET depth profile of ^{12}C 219 MeV u^{-1} traversing through 1 g cm^{-3} water. Maximum LET occurs at $116.26 \text{ keV } \mu\text{m}^{-1}$ at a depth of 9.98 cm, giving a 647% increase from the entrance LET. Dashed line shows LET from only primary particles, while solid line shows LET from all particles.

For carbon, the beam enters the body with an average per particle LET of $15.6 \text{ keV } \mu\text{m}^{-1}$. The LET rises to $32.5 \text{ keV } \mu\text{m}^{-1}$ as it reaches the tumor. Upon entering the tumor the LET continues to rise to a maximum of $116.2 \text{ keV } \mu\text{m}^{-1}$ at a depth of 9.98 cm. At a depth of 10.05 cm, an LET of $23.5 \text{ keV } \mu\text{m}^{-1}$ is still seen, but drops off to $1.44 \text{ keV } \mu\text{m}^{-1}$ before exiting tumor. At a depth of 9 cm, a maximum of 18.5 % of the LET is seen to come from non-primary particles. Beyond the tumor volume, non-primaries account for an LET between 0.893 and $3.34 \text{ keV } \mu\text{m}^{-1}$.

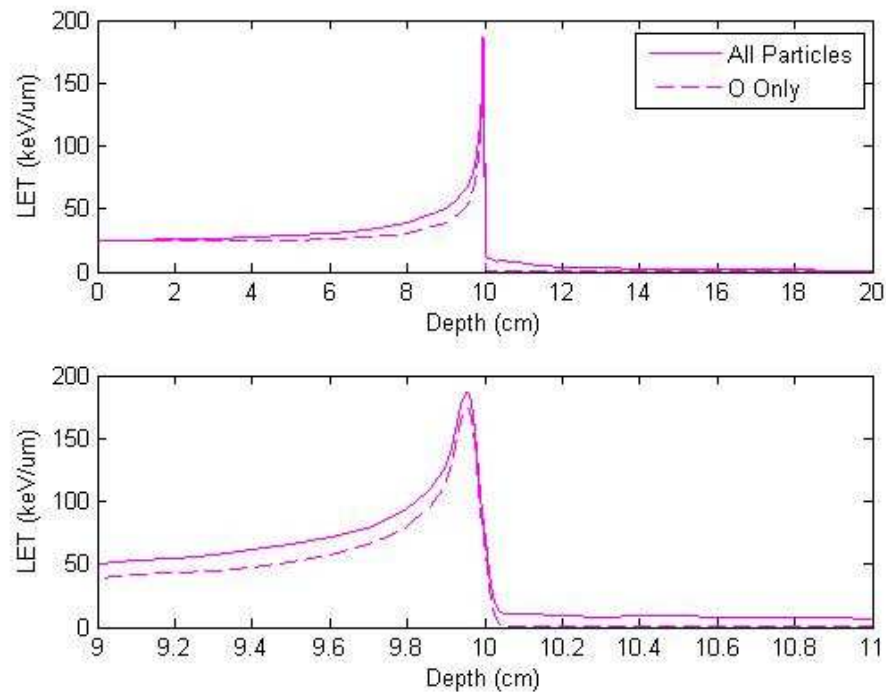


Fig 12. LET depth profile of ^{16}O 259 MeV u^{-1} traversing through 1 g cm^{-3} water. Maximum LET occurs at $185 \text{ keV } \mu\text{m}^{-1}$ at a depth of 9.95 cm, giving a 640% increase from the entrance LET. Dashed line shows LET from only primary particles, while solid line shows LET from all particles.

For oxygen, the beam enters the body with an average per particle LET of $25.0 \text{ keV } \mu\text{m}^{-1}$. The LET rises to $50.5 \text{ keV } \mu\text{m}^{-1}$ as it reaches the tumor. Upon entering the tumor the LET continues to rise to a maximum of $185 \text{ keV } \mu\text{m}^{-1}$ at a depth of 9.95 cm. At a depth of 10.0 cm, an LET of $68.9 \text{ keV } \mu\text{m}^{-1}$ is still seen, but drops off to $3.87 \text{ keV } \mu\text{m}^{-1}$ before exiting tumor. At a depth of 9 cm, a maximum of 21.4 % of the LET is seen to come from non-primary particles. Beyond the tumor volume, non-primaries account for an LET between 1.32 and $6.77 \text{ keV } \mu\text{m}^{-1}$.

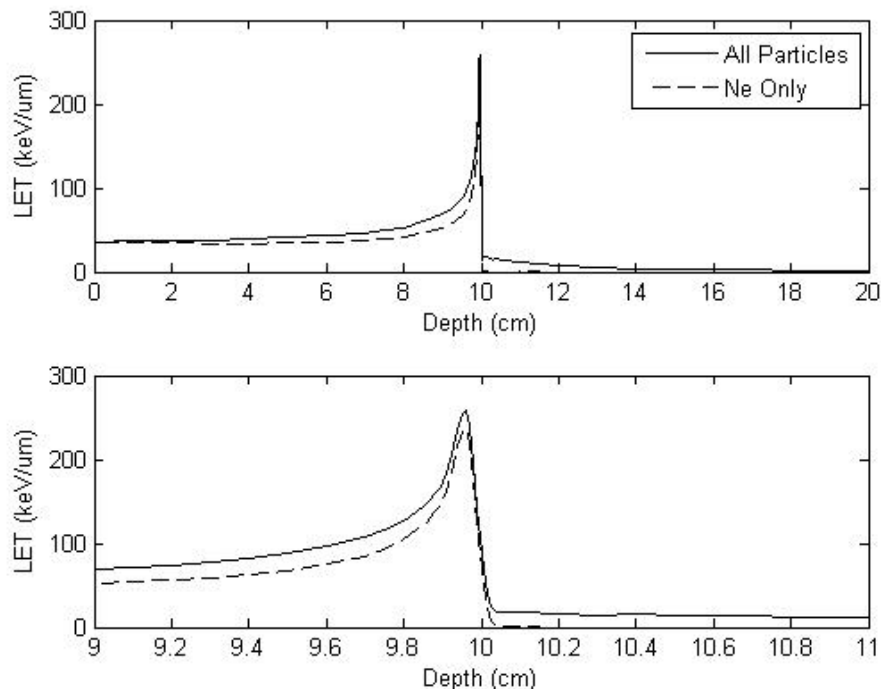


Fig 13. LET depth profile of ^{20}Ne 296 MeV u^{-1} traversing through 1 g cm^{-3} water. Maximum LET occurs at $256.8 \text{ keV } \mu\text{m}^{-1}$ at a depth of 9.94 cm , giving a 610% increase from the entrance LET. Dashed line shows LET from only primary particles, while solid line shows LET from all particles.

For neon, the beam enters the body with an average per particle LET of $36.2 \text{ keV } \mu\text{m}^{-1}$. The LET rises to $68.6 \text{ keV } \mu\text{m}^{-1}$ as it reaches the tumor. Upon entering the tumor the LET continues to rise to a maximum of $256.8 \text{ keV } \mu\text{m}^{-1}$ at a depth of 9.96 cm . At a depth of 10.0 cm , an LET of $89.0 \text{ keV } \mu\text{m}^{-1}$ is still seen, but drops off to $8.13 \text{ keV } \mu\text{m}^{-1}$ before exiting tumor. At a depth of 9 cm , a maximum of 24.1% of the LET is seen to come from non-primary particles. Beyond the tumor volume, non-primaries account for an LET between 1.86 and $11.4 \text{ keV } \mu\text{m}^{-1}$.

The LET contributions from non-primary particles vary for all the ions with lithium showing the greatest contribution from non-primaries and hydrogen showing the least because it cannot fragment. The percentage of LET contribution at different depths

in shown in Fig. 14, up to the ions maximum LET, after the particle stops 100% of the LET contribution is from non-primary particles and this is not shown in the figure.

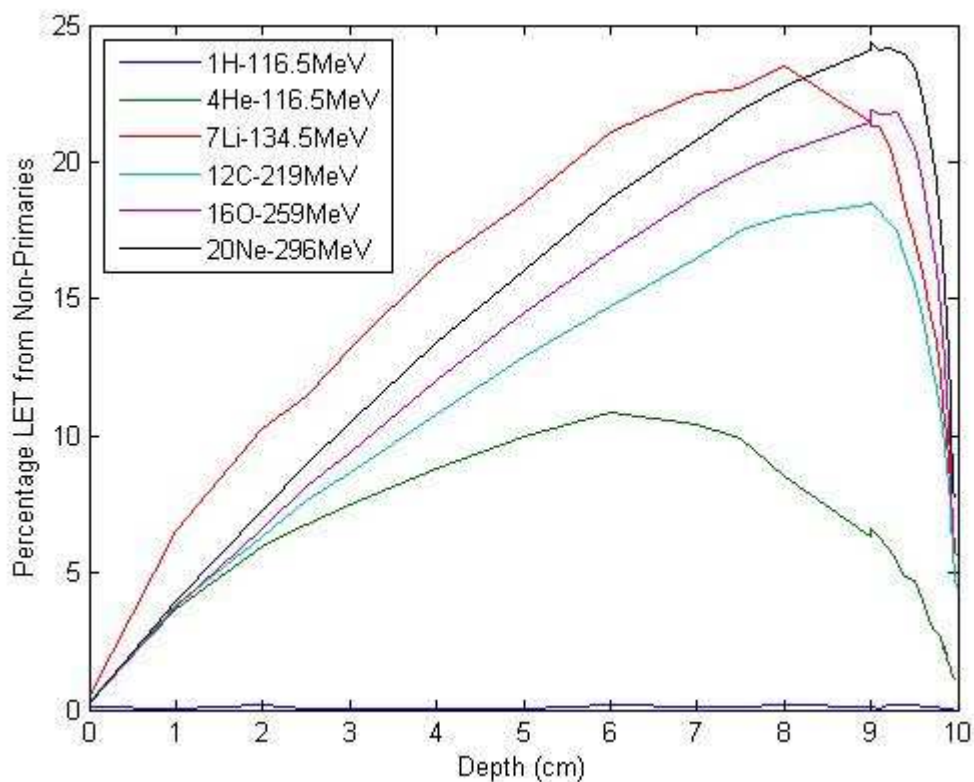


Fig 14. Percent of measured LET from non-primary particles in a water phantom for various ion beams. Being unfragmentable, ^1H is seen to not be influenced by secondary particles while ^7Li is seen to be most affected by secondary particles.

The non-primary LET rates may seem high, however, in the regions of max LET (within 80% of max LET) the rates drastically decrease. For neon and oxygen these rates fall below 10%, for carbon and lithium they fall below 5%, and for helium and hydrogen they are below 1%. Where LET is low the effects of non-primary particles is very prevalent because the particles are traveling at energies in which they can fragment and high energy delta rays are being created, however, in high LET regions the particles

have slowed down to a velocity where no fragmentation can occur and no high energy delta rays are being created.

Comparison of the LET values achieved from simulation to those that would result from the Bethe approximation shows that the Bethe approximation overexaggerates the true LET for all ions except hydrogen. Because of the additive effect of fragmentation, this overexaggeration increases with depth and is most noticeable in heavier ions. The percentage differences between the Bethe approximated LET and the simulated LETs are shown in Table 3 at various depths (positive values depict the Bethe approximation being larger than the simulated). The Bethe approximation used had a stepsize of 0.1 cm and assumed constant LET in each 0.1 cm increment.

Table 3. Percentage differences between PHITS simulated LETs and Bethe approximated LETs for charged particles. Positive values imply overapproximation of Bethe approximation. Overapproximation due to fragmentation of incident ion beam and the shell effect.

Depth (cm)	¹ H	⁴ He	⁷ Li	¹² C	¹⁶ O	²⁰ Ne
0	-157%	6%	-8%	-2%	-2%	-2%
1	-151%	5%	-10%	-1%	0%	1%
5	-97%	7%	5%	6%	8%	11%
9	-11%	3%	17%	12%	15%	18%
9.5	8%	7%	24%	16%	17%	20%
Max LET	38%	10%	28%	11%	-2%	2%

The overexaggeration of the Bethe approximation reduces the actual dose that would be delivered to tissues in CPT. Depending on the magnitude of the separation from the Bethe approximation, this deviance may be a favorable sign for CPT. A large

exaggeration in healthy tissues would decrease the dose to them; this would be beneficial if the maximum LET were not as highly overstated as the LETs in the healthy tissues. This is a clear-cut advantage for oxygen and neon and a clear-cut disadvantage for hydrogen and lithium and shows the importance of Monte Carlo calculations and simulations when working in RT. The majority of the lost LET is due to fragmentation but part of the over estimation can be contributed to the shell effect, which occurs when a projectile slows down to below the speed of the orbital electron of a target and the electron no longer interacts with the projectile, effectively reducing the mean excitation potential of the target

If one is not to consider Q , the therapeutic ratio for a treatment will be highest when the ratio of LET inside and outside the tumor is the greatest. Often this is simplified by comparing the entrance LET of the body to the maximum LET in the tumor. Using this analysis, helium is seen to be the most effective ion for CPT. The increase between entrance LET and maximum LET is 140, 726, 509, 647, 640, and 610 % for the ions in order of increasing mass. The lesser magnitude Bragg Peak experienced by hydrogen contributes to a relatively small increase LET. Although this increase would correspond to a higher therapeutic ratio for PT over IMRT it does not justify the usage of PT over HCPT.

When the total LET is integrated to show the entire spectrum of the phantom, the superiority of helium is once again seen. As shown in Fig. 15, 24.0% of the total LET from helium occurs within the tumor volume, greater than any other ion. The total LET distal to the tumor is also much lower for helium than any of the other HCPT ion.

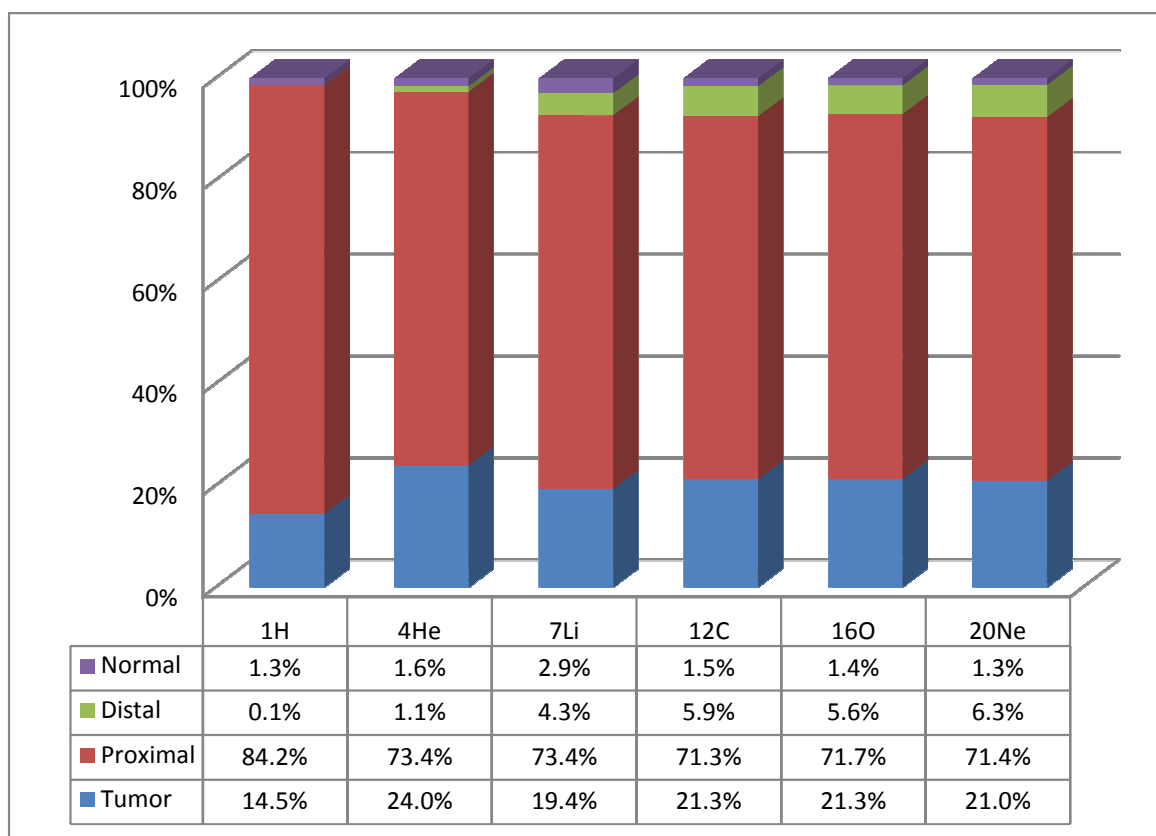


Fig 15. Dose percentage rates for various ion beams in a tumor and in different regions of a body relative to the tumor. Proximal refers to all depths prior to the tumor, distal refers to all depths beyond the tumor, normal refers to all regions neither proximal, distal, or inside the tumor. ^4He is seen to confine the greatest amount of dose inside the tumor volume.

Because dose is only affected by LET, and not Q, the percentages shown in Fig. 14 can also refer directly to dose for each ion.

The percentage of LET in the tumor for neon, oxygen, and carbon are all relatively similar at approximately 21.0%. Additionally, rates proximal, distal, and normal are nearly equivalent for these three ions. The inferiority of hydrogen and PT can be seen by its very low LET percentage in the tumor, although it does display almost zero dose behind the tumor due to its lack of fragmentation.

Although helium does show many favorable qualities when analyzing only LET and dose, it is imperative that other factors be taken into account when considering RT. The Bragg Peak has a very small width and to ensure that an entire tumor receives a uniform dose an ion beam must be passed through different filters or be composed of different energies to spread out the width of the Bragg Peak. Essentially, the depth dose profiles from several beams with slightly different energies have to be superimposed on each other. Due to this superimposition of dose, it is best for the Bragg Peak to be as sharp as possible and with a high magnitude. Being the most heavily charged particle, neon has the highest magnitude and it also has the highest increase in dose inside the tumor at 271% compared to 212% for helium. The percentage increase is higher for each ion of greater charge suggesting that the necessary spreading of the beam would be least detrimental with greater charged particles.

Using eqn (11) the average dose per particle at varying depth was solved for. Table 4 shows these doses at different depths for all ion varieties investigated. Notice the massive difference between average maximum dose for the three heavier ions compared to those of the three lighter ions, this difference allows for fewer primary particles to be necessary for equal tumor doses for heavier ions.

Table 4. Average dose in nGy per input particle at different depths for all ions used in PHITS analysis. Larger dose maximums for the heavier ions require that less of them must be used to achieve equal doses inside a tumor.

Depth (cm)	Dose (nGy/ input particle)					
	¹ H	⁴ He	⁷ Li	¹² C	¹⁶ O	²⁰ Ne
0	2.68	3.95	9.21	24.94	40.09	57.91
1.00	2.74	4.17	9.74	25.71	40.81	58.51
3.00	2.74	4.53	10.09	27.17	42.96	60.77
5.00	2.74	5.17	10.69	29.88	46.56	65.11
7.00	2.76	6.83	12.62	34.82	54.02	74.63
9.00	2.98	10.36	17.8	52.05	80.94	109.98
9.20	2.81	10.52	17.04	54.64	86.03	116.43
9.40	3.02	11.88	19.46	60.71	96.26	130.3
9.60	3.46	14.25	22.61	69.68	112.74	152.76
9.80	5.11	19	28.79	90.01	149.7	200.97
9.85	5.76	21.67	32.08	99.99	170.99	228.34
9.90	6.28	26.08	37.87	115.79	206.81	276.67
9.91	6.34	27.39	39.73	120.77	220.78	293.72
9.93	6.39	29.96	44.23	134.32	259.68	343.9
9.94	6.4	31.09	46.95	143.73	281.95	376.36
9.95	6.32	32.02	49.88	154.8	296.79	404.56
9.96	6.23	32.54	52.56	167.19	294.49	411.41
9.97	6.13	32.44	54.87	178.83	270.58	382.11
9.98	5.99	32.12	56.12	186.24	223.43	313.36
9.99	5.8	30.83	55.87	185.6	166.06	224.06
10	5.56	29.08	53.76	176.04	110.4	140.94
10.03	4.79	20.92	37.65	91.54	25.74	34.6
10.05	4.06	14.18	23.23	37.68	16.52	27.38
10.1	2.51	3.45	3.85	6.64	14.95	25.73
10.5	0	0.08	0.93	4.83	11.77	20.69
11	0	0.2	1.94	5.51	10.84	18.31
13	0	0.12	0.89	3.18	4.56	7.55
20	0	0.03	0.26	1.43	2.12	2.98

Dose Equivalence

The previous analysis did not take into account the quality factor for high LET radiations. Using eqn (9), Q was calculated for each ion and shown in Fig. 16. Notice that the maximum Q from any of the ions is 30, this maximum occurs when the LET of a particle is equal to $100 \text{ keV } \mu\text{m}^{-1}$ and corresponds to the most efficient use of energy in the terms of cell killing. Carbon, oxygen, and neon all reach a Q of 30 at some point along their paths. However, as LET increases past $100 \text{ keV } \mu\text{m}^{-1}$, Q begins to decrease. This decrease is most noticeable in neon, whose quality factor reaches 30 near 9.7 cm, but decrease to 18.7 at its maximum LET. It should be noted that even though Q decreases at LETs greater than $100 \text{ keV } \mu\text{m}^{-1}$, the dose equivalence will still increase, just at a slower rate than in the 10-100 $\text{keV } \mu\text{m}^{-1}$ regions. To optimize CPT, it would be ideal to have a spread out Bragg Peak at $100 \text{ keV } \mu\text{m}^{-1}$. A higher LET would result in too high of a dose in tissues before the tumor, while a lower LET would create too low of a ratio of therapeutic ratio.

The Q for hydrogen never exceeds unity and as thus, there is no change between dose and dose equivalence for PT because of the low LET of hydrogen. Helium also has a quality factor near unity for most of its track, but does increase to a value of 4.30 by the time it stops in the tumor. When only LET and dose were being investigated helium seemed to be the most apt particle for CPT, however, its low Q results in a low dose equivalence, which greatly reduces its appropriateness for CPT.

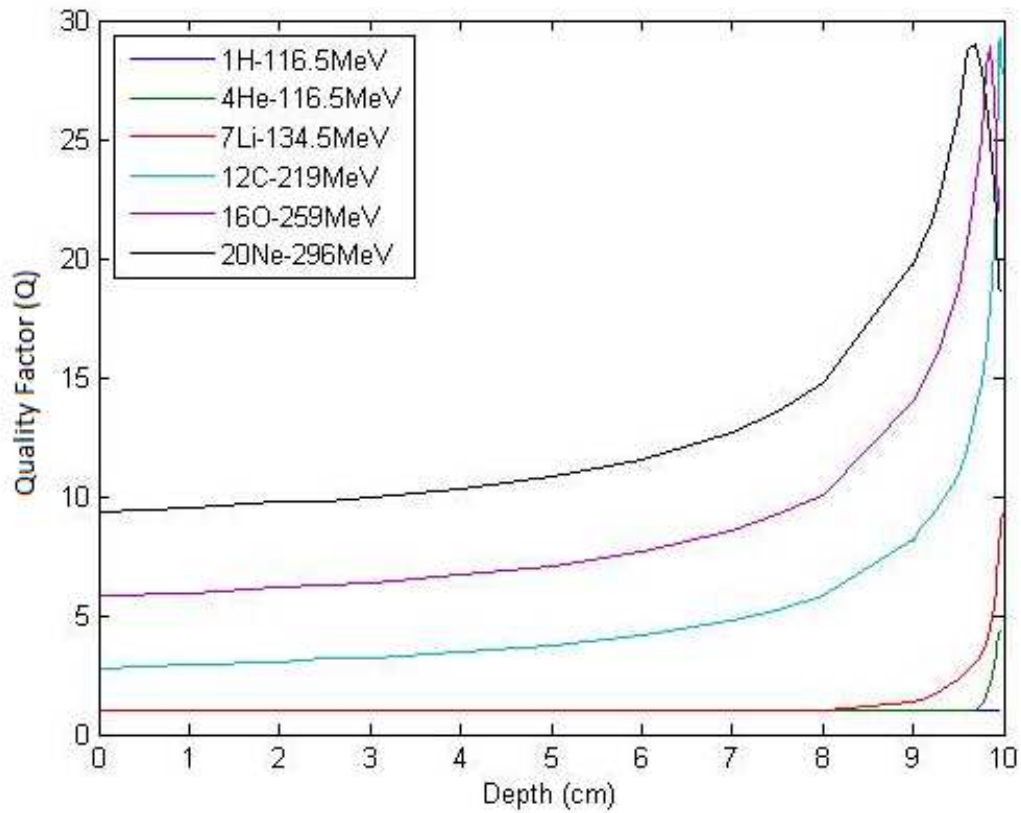


Fig 16. Quality factors (Q) for various ion beams as they approach their Bragg Peaks traversing through water. Maximum Q is 30 and occurs when LET is equal to $100 \text{ keV } \mu\text{m}^{-1}$. For hydrogen, Q never increases beyond unity. For heavier ions, the maximum Q is reached but falls off after LET increases past $100 \text{ keV } \mu\text{m}^{-1}$. Carbon is seen to have the highest Q when it reaches its maximum LET.

Lithium also displays low LET for most of its track but reaches a level above 10 $\text{keV } \mu\text{m}^{-1}$ immediately after entering the tumor, this sudden jump allows for the Q outside of the tumor to remain at one, while the Q inside the tumor increases from unity to 9.01. For the specific geometry used, lithium can be seen as a very efficient ion because it is sparing healthy tissue by maintaining a low Q in the regions that a low Q is desirable and harming cancerous tissues by having an increase in Q in the regions where a high Q is desirable. When Q was not being considered, lithium was shown to have a tumor confined dose concentration last to only protons. However, the Q increase shows that proper treatment planning in which Q is minimized outside the tumor can create a very high therapeutic ratio. Even though lithium was shown to overall be one of the less effective ions from an LET analysis, it seems quite suitable for this specific geometry and goes to illustrate that the best ion or mixture of ions to use in RT may be specific to the tumor depth and size rather than just the physical properties of the particles.

For the three heavier charged particles, all of them enter the body with an LET greater than 10 $\text{keV } \mu\text{m}^{-1}$ and thus an quality factor greater than 1. Because the max LET of carbon is closest to the desired 100 $\text{keV } \mu\text{m}^{-1}$ it is assumed that it will be the best treatment plan option. For oxygen and neon, oxygen remains closer to 100 $\text{keV } \mu\text{m}^{-1}$ and it is also assumed that it will be a better tumorcidal carrier than neon because the unnecessarily high LET is diminishing the effectiveness of the neon to kill cells in the tumor. This is indeed true and can be seen in Figs. 17 and 18 which shows the dose equivalence, normalized to the entrance, as it traverses both the body and tumor. Carbon is seen to be the most appropriate particle for use in HCPT increasing it dose

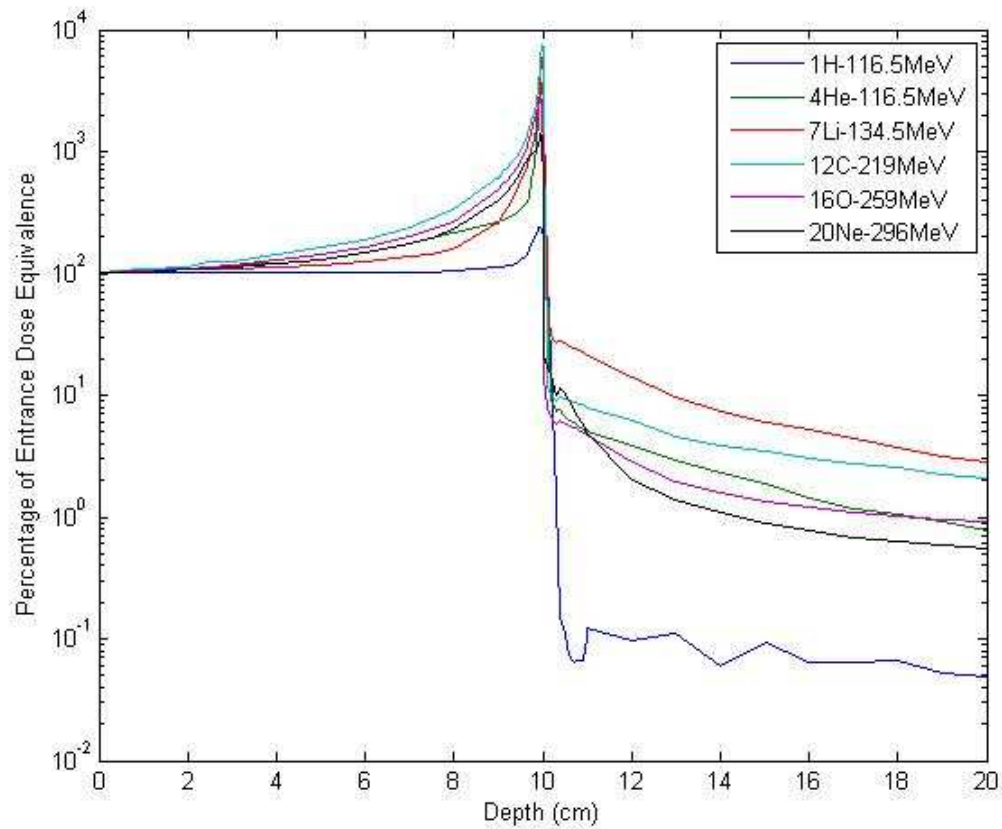


Fig 17. Dose equivalence normalized to entrance dose for various ion beams as they traverse water. Carbon is seen to have the greatest therapeutic benefit, increasing its dose equivalence 7367% while hydrogen only increases by 139 %.

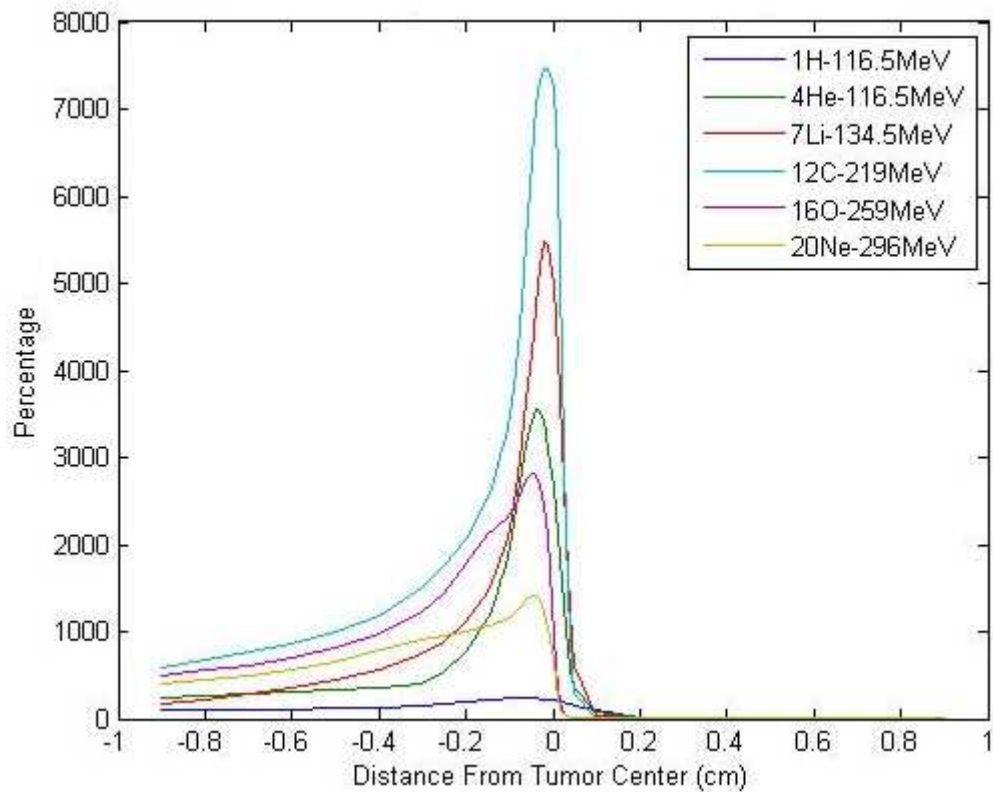


Fig 18. Percentage increases in dose equivalence, normalized to entrance dose equivalence as various ions pass through a tumor volume. Carbon is seen to have the greatest therapeutic benefit, increasing its dose equivalence 7367% while hydrogen only increases by 139 %.

equivalence over 7000%. In order of increasing mass, the rise in maximum dose equivalence is 139, 3445, 5390, 7367, 2709, and 1320 %. Exiting the tumor, the relative dose equivalence was seen to be highest in lithium, over 20%. In order of increasing mass, the relative exit doses were 0.12, 4.9, 20.9, 7.9, 4.7, and 4.9 %. Even though carbon has the second highest relative percentage of dose exiting the tumor its ratio of maximum dose equivalence to exit dose equivalence is greatest of all the HCPs. To reduce the late term effect of HCPT, both proximal and distal to the tumor, carbon is the ion of choice.

When the total dose equivalence is integrated to show the entire spectrum of the phantom, the dominance of carbon is seen. As shown in Fig. 19, 49.5% of the total dose equivalence from carbon occurs within the tumor volume. When comparing Fig. 15 and Fig. 19 some important differences must be noted. Firstly, the percentage of dose in the tumor increased for all ions other than hydrogen, this is a notable drawback for PT compared to HCPT. Also because of its low LET the increase from helium is minimal to that of heavier particles. Lithium and carbon both show doubling of their therapeutic ratios. Therapeutic ratios for oxygen and neon also show considerable increases. Of substantial importance is the reduction in dose equivalence beyond the tumor. Because the dose behind the tumor is predominantly from light fragments (protons and alpha particles) their LET and dose equivalence is low and their relative influence is diminished. For the three heavier ions, the dose behind the tumor was in the range of 6%, however, once Q was factored in the total was reduced to less than 1% for all ions.

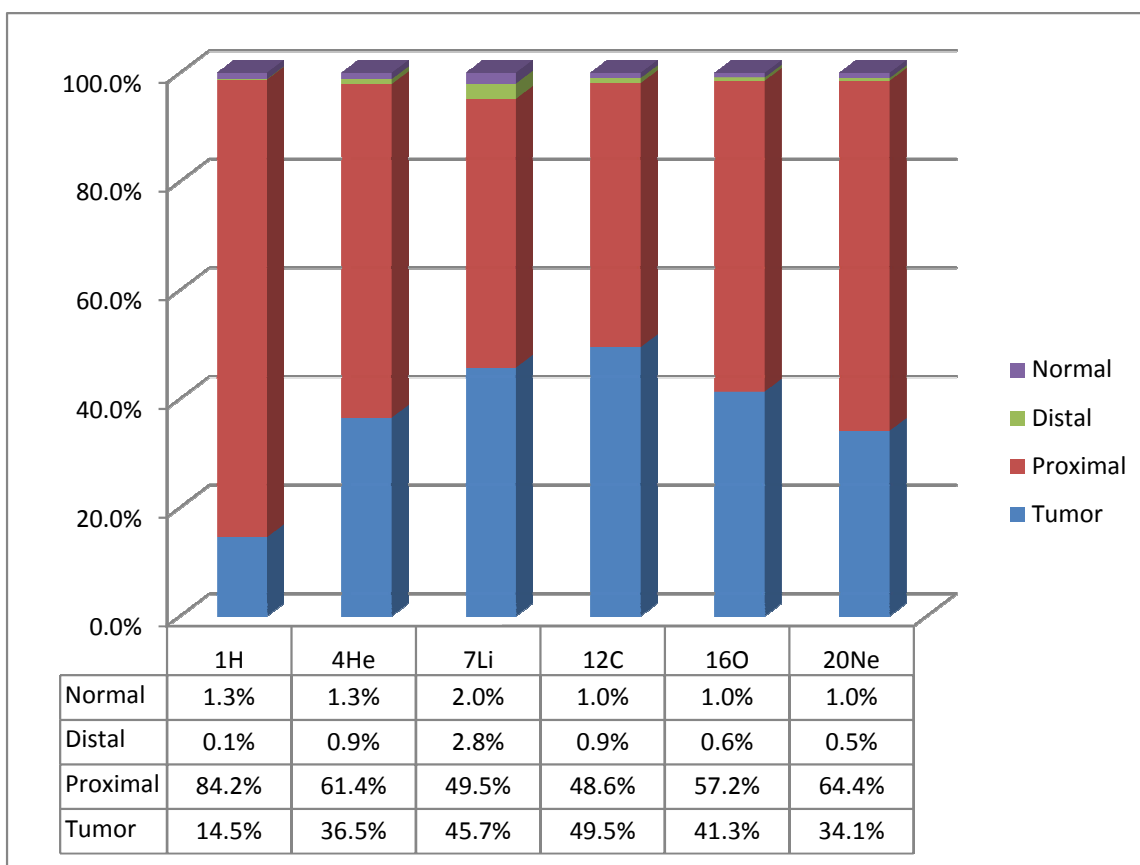


Fig 19. Dose equivalence percentage rates for various ion beams in a tumor and in different regions of a body relative to the tumor. When Q was taken into account, ^{12}C was seen to have the greatest therapeutic ratio of any ion. ^4He , which had the highest tumor contained dose when Q was not considered, has the 4th highest tumor dose equivalent containment. Proximal refers to all depths prior to the tumor, distal refers to all depths beyond the tumor, normal refers to all regions neither proximal, distal, or inside the tumor.

Lithium is seen to cause much higher dose equivalence beyond the tumor than any other ion. Additionally, in the regions normal to the tumor lithium has to highest percentage of lost dose. These facts show that lithium is affected by fragmentation and scattering to a greater extent than any of the other ion. Although its high dose-rate in the tumor makes it appear an applicable particle for this specific simulation, its use in general should not be recommended unless dictated by the geometry.

When the effects of Q are considered the discrepancy between the numbers of particles needed for a 10 Sv dose become even more pronounced than those needed for a 10 Gy dose, as shown in Table 5. For the three heavier ions, a factor of magnitude less particles must be used to achieve the same endpoints. This reduction will greatly reduce the overall effects of fragmentation and scattering in the heavier particle beams.

Table 5. Required particle fluencies to casue a maximum dose of 10 Gy and 10 Sv from various ions. The high LET and quality factors seen by heavier ion greatly reduces the amount of these particles required for equal doses from low LET particles.

Ion	Fluence Required For:	
	10 Gy	10 Sv
¹ H	1.562 x10 ⁸	1.562 x10 ⁸
⁴ He	3.073 x10 ⁷	7.150 x10 ⁶
⁷ Li	1.782 x10 ⁷	1.978 x10 ⁶
¹² C	5.370 x10 ⁶	1.930 x10 ⁵
¹⁶ O	3.369 x10 ⁶	1.529 x10 ⁵
²⁰ Ne	2.431 x10 ⁶	1.298 x10 ⁵

Fragmentation and Scattering

Being composed of the most nucleons and having the highest kinetic energy neon will create the largest amount of fragmentation products followed by oxygen, carbon, lithium, helium, and hydrogen. The complete fragmentation fluencies at various radial and lateral depths can be found in Appendix B-E. An overview of the scattering will be presented here, but a full summary is above the breadth of this paper.

Due to collision interactions and deflections the actual number of primary particles that reach the target depth will be low compared to the amounts that were input in the body. Because primary particles will have the highest LET and dose equivalence, it is desired to have the high percent of primaries remain within the beamline and reach the tumor. Table 6 shows the percentage of primaries to reach the proximal tumor boundary at radii of 0.1 and 1 cm from the center of the tumor and Fig. 20 shows the decrease in primary particles remaining in the original beamline width as they traverse the body.

The relatively light hydrogen is easily deflected and scatters to a much greater degree than any other ion. Lithium also displays markedly worse beam coherence in the 0.1 cm radius than all ions sans hydrogen. Being composed of three tightly bound alpha particles, carbon displays slightly less fragmentation than the other ions and has the highest yield of primaries staying within in the initial beam radius and entering the tumor. Along the entire depth, the other four heaviest ions display somewhat similar percentages losing between 5-10% of their remaining primary particles every centimeter

Table 6. Percentage of primary particles passing into the tumor at different radii centered around the tumor. Radii lengths correspond to the original beam radius (0.1 cm) and the tumor radius (1 cm). Being most influenced by scattering, ^1H is seen to have the lowest percent of primary particles remaining in a 0.1 cm radius, but the most in a 1 cm radius due to lack of fragmentation. Carbon is seen to have the lowest dependence on fragmentation and scattering from all the heavier charged particles.

Ion	Percentage	
	r=0.1 cm	r=1 cm
^1H	21.4	86.1
^4He	43.7	81.1
^7Li	39.3	60.3
^{12}C	47.7	65.7
^{16}O	46.9	61.6
^{20}Ne	45.1	57.2

until they all stop near their target depth. At the 1 cm radial scale 86% of hydrogen is entering that tumor, because hydrogen is not fragmenting it can be assumed that 14% of the hydrogen was scattered a great enough extent to fully miss the tumor. With lithium as an outlier, primary fluences at 1 cm are seen to decrease as a charge and mass are increased. This is due to a higher degree of fragmentation, and although the primary fluences are decreased, the heavier fragment will mostly pass through the tumor.

For energy deposition behind the tumor the three heavier ion experience the worse effects from fragmentation having yields of 0.5, 0.53, and 1% alpha particles with average energies of 79, 103, and 119 MeV amu^{-1} for carbon, oxygen, and neon respectively. These alpha particles have a potential range of 2.3, 8.2, and 10.1 cm in water (ASTAR-NIST).

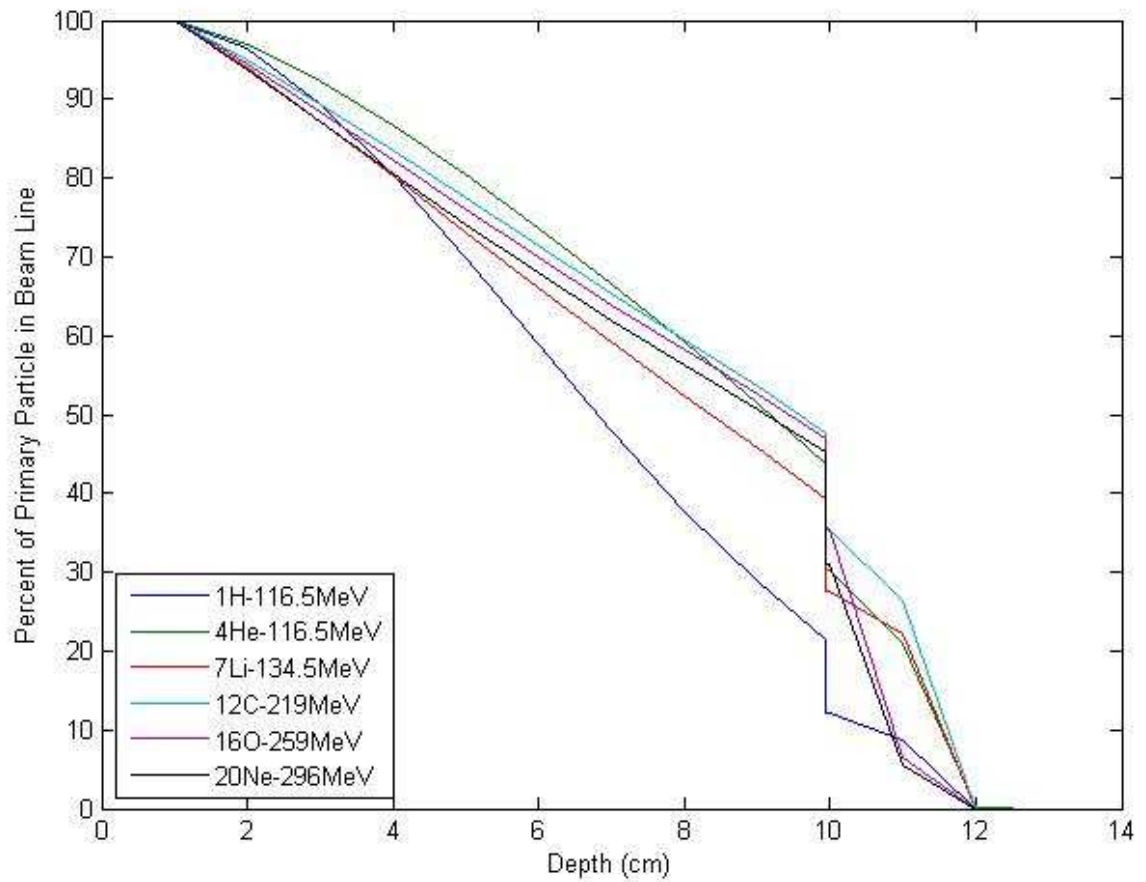


Fig 20. Percentage of primary particles remaining within the original beam width (0.1 cm) as they approach their Bragg Peak at 10 cm and continue until all stop. Due to scattering ^1H is seen “lose” the greatest percent of particles, while all other ions exhibit similar rates of primary particle losses, carbon is seen to have primary percentage while in the tumor.

When considering fragmentation in RT heavy particles are often initially regarded as undesirable because of their amount of fragmentation, this is an obvious truth based on a per particle basis as shown by Fig. 21 which compares the total amount of energy escaping the original beamline radius of 0.1 cm in the form of neutrons for each ion.

However, when normalized to dose equivalence, the amount of energy lost is actually larger for the lightest ions. Figs. 22-23 shows the total amount of energy lost out of a 0.1 and 1 cm radius centered on the beamline. It can be seen that for a 10 Sv dose, hydrogen gives off almost an order of magnitude more energy in the form of fragments and scattering than any other ion. Carbon, oxygen, and neon all lose approximately the same percentage of their energies. Carbon, having the least amount of required input energy to reach a 10 Sv dose is seen to have the most sparing effect on healthy tissues. The amount of particles required to reach equal dose equivalences for lower LET ions is so great that they do not benefit overall from their lower escaping energy on a per particle basis. The usage of these particles in CPT would raise the probability of secondary cancer induction.

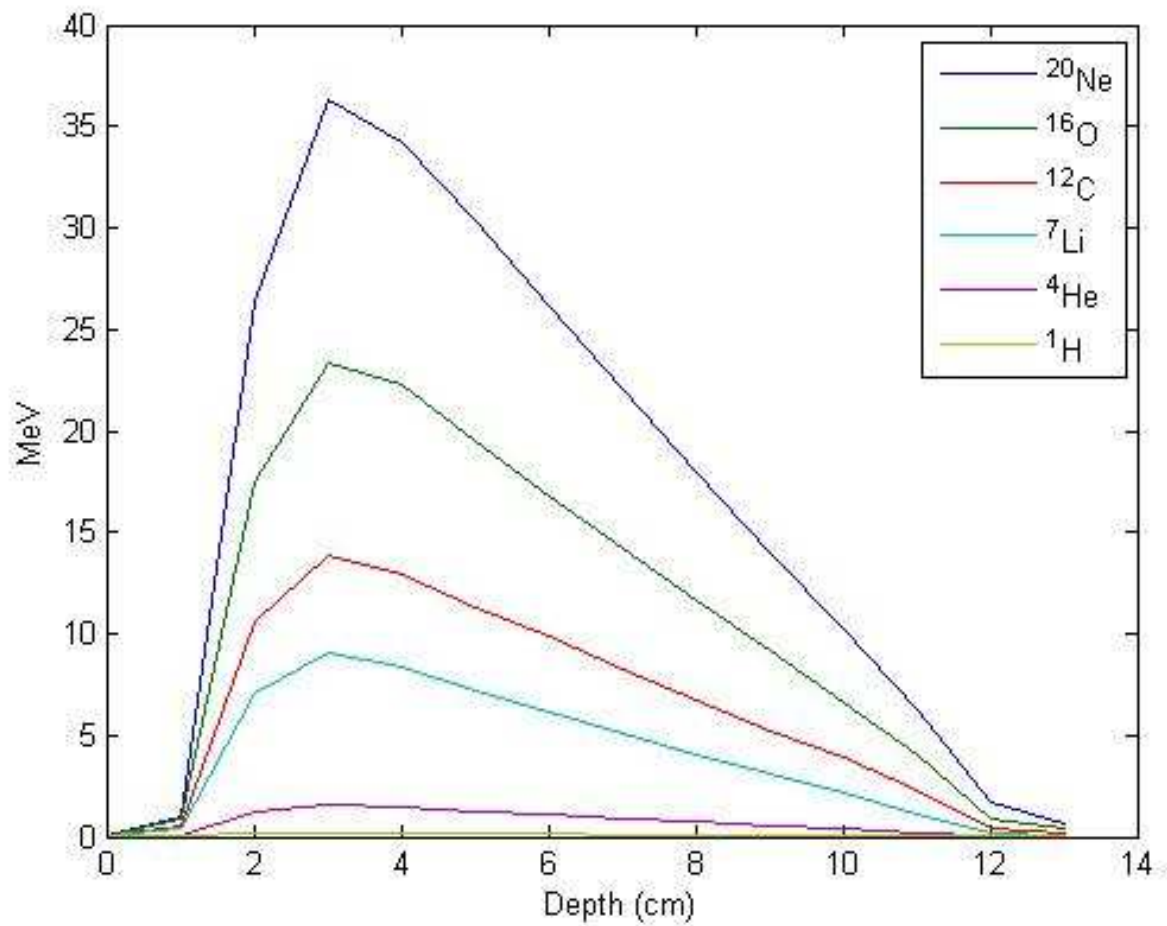


Fig 21. Total energy escaping a 0.1 cm radius in the form of neutrons for various ion beams having a depth of 10 cm, on a per particle basis. The more massive ions display a higher amount energy escaping.

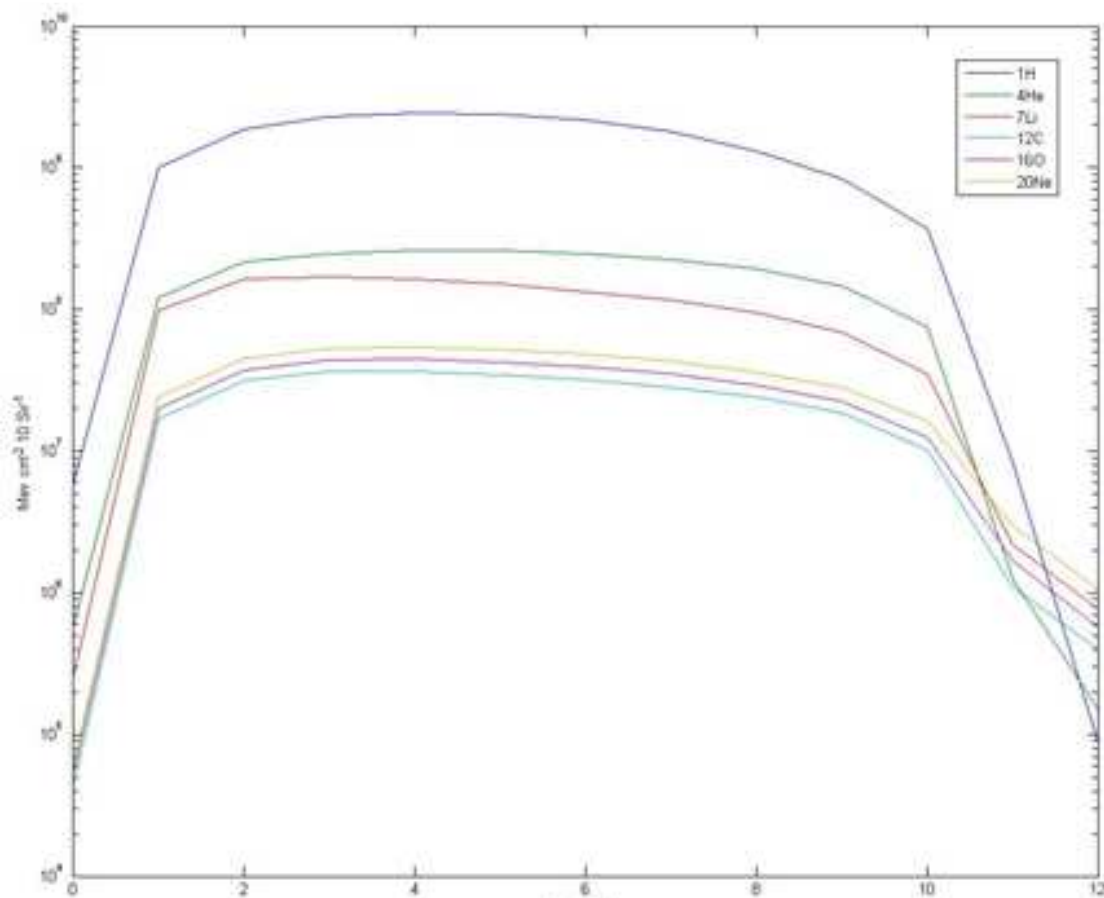


Fig 22. Total energy escaping a 0.1 cm radius for various ion beams having a depth of 10 cm, normalized to maximum dose equivalence. Because much great fluences are required for lower LET radiations to reach an equal dose equivalence, total energy escaping is greater for low LET radiations even though on a per particle basis they release less energy.

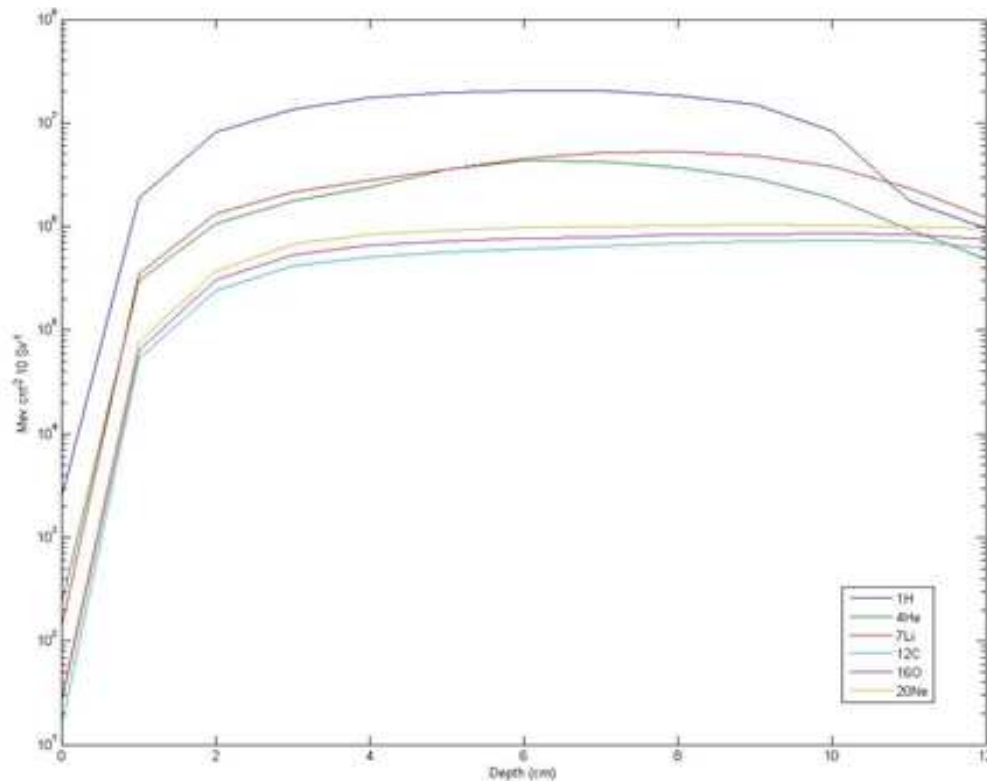


Fig 23. Total energy escaping a 1 cm radius for various ions having a depth of 10 cm, normalized to maximum dose equivalence. Because much great fluences are required for lower LET radiations to reach an equal dose equivalence, total energy escaping is greater for low LET radiations even though on a per particle basis they release less energy.

Due to the large spectrum of particles, a quality factor analysis was not taken for all fragmentation products. However, Figs. 24-29, show that the majority of the lost energy (leaving 1 cm radius) is being carried away is in the form of protons, neutrons, and isobars less than 5 amu, for all originating ions. Because these particles are low LET (except for neutrons) they will have comparable quality factors, and the dose equivalence in the surrounding tissue will be directly proportional to total energy lost. For the neutrons energies seen, the quality factors initially vary between 5 and 7 for all

beam types, and will all increase to approximately 11. (Attix 2004) Because the quality factors of neutrons and the percentage of escape energy from neutrons is similar for all ion beams, the dose equivalence from neutrons will also be directly proportional to escaped energy.

Figs. 24-29 show the amount of energy being carried away by different isobars, all isobars that carried away greater than 0.0001% of the total lost energy are shown. Although the specific isobar concentration is not solved for it can be assumed that the most prevalent ions at each mass are ^2H , ^4He , ^6Li , ^8Be , ^{10}B , ^{12}C , ^{13}C , ^{14}N , ^{16}O , ^{17}O , ^{18}F , and ^{20}Ne . While ^3H , ^3He , ^7Li , ^7B , ^{11}B , ^{11}C , ^{15}N , ^{15}O , ^{19}Ne , and ^{19}Ne all display near equal yields for their respective isobars. For this discussion, the term escape energy refers to the total energy being imparted greater than 1 cm away from the beam center.

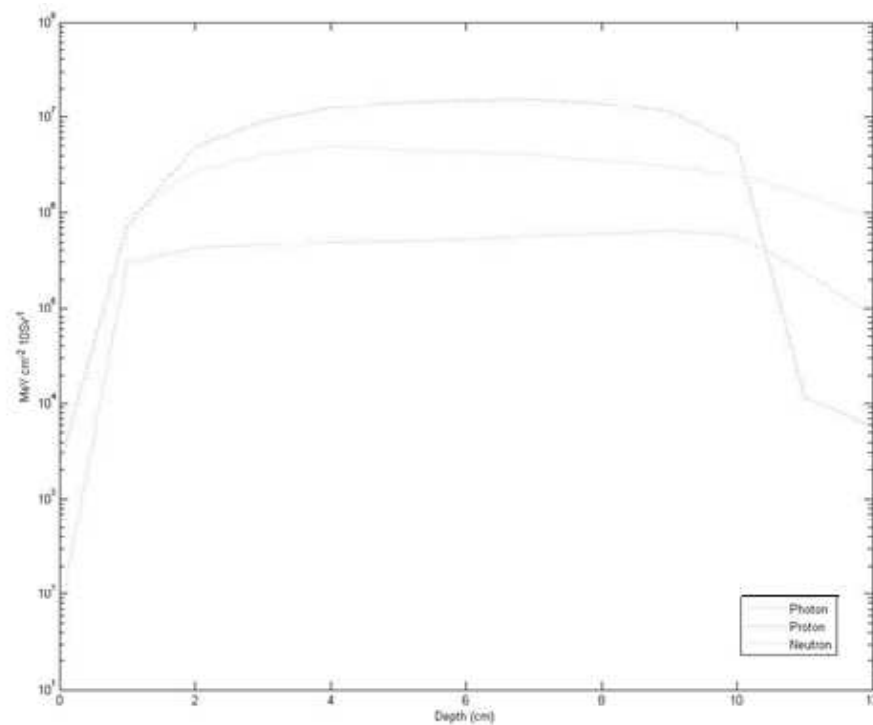


Fig 24. Total energy escaping a 1 cm radius from different particles for a beam of $116.5 \text{ MeV u}^{-1} \text{ } ^1\text{H}$ particles delivering a maximum dose of 10 Sv. Total energy escaping is $9.2 \times 10^8 \text{ MeV}$, an amount greater than any other ion under investigation.

Being unable to fragment, there are no particles greater than 1 amu in the hydrogen spectrum. For hydrogen, 70.8 % percent of the escape energy is in the form of hydrogen, while neutrons and photons account for 25.5 and 3.7 % of the escape energy. The average energy of each proton is 41.7 MeV, while average neutron energies are 22.73 Mev. With a total energy loss of $9.20 \times 10^8 \text{ MeV}$, hydrogen is seen to impart the greatest sum of energy outside a 1 cm radius to the tissues surrounding the tumor. The total energy loss accounts for 5 % of the input energy. The total energy being imparted out of the original beam radius is 57 %.

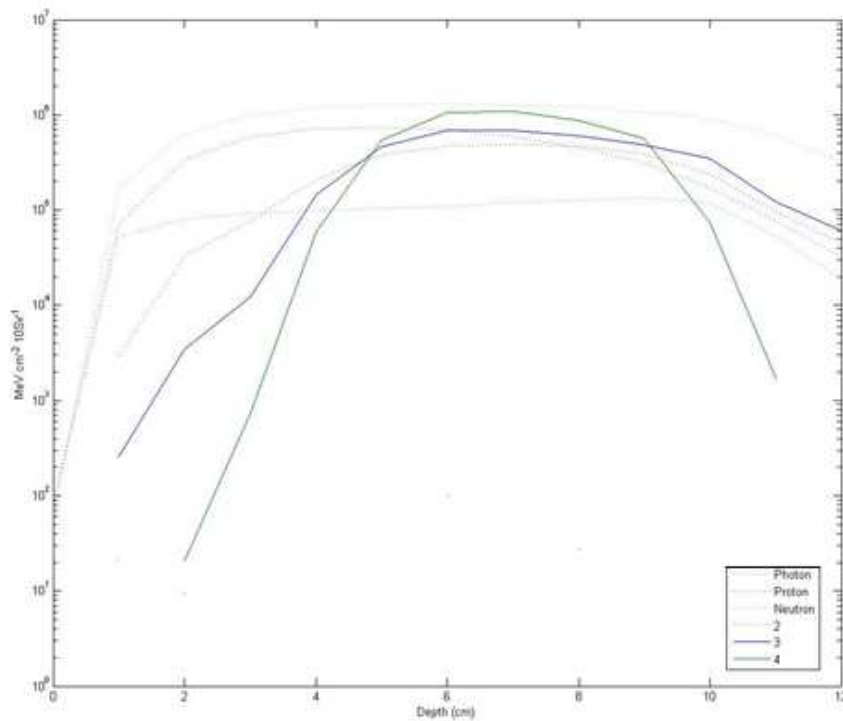


Fig 25. Total energy escaping a 1 cm radius from different fragmentation and scattering isobars for a beam of $116.5 \text{ MeV u}^{-1} \text{ } ^4\text{He}$ particles delivering a maximum dose of 10 Sv. Total energy escaping is $1.7 \times 10^8 \text{ MeV}$.

For helium 17.3 and 39.6 % of the escape energy are in the form of proton and neutrons, with average energies of 45.0 and 24.9 MeV. Alpha particles account for 15.4 % of the escaped energy, while isobars of 2 and 3 amu accounts for 10.5 and 13.1 % of the escape energy. Helium has a total energy loss of $1.74 \times 10^8 \text{ MeV}$, which equals 5 % of the input energy. The total energy being imparted out of the original beam radius is 38 %.

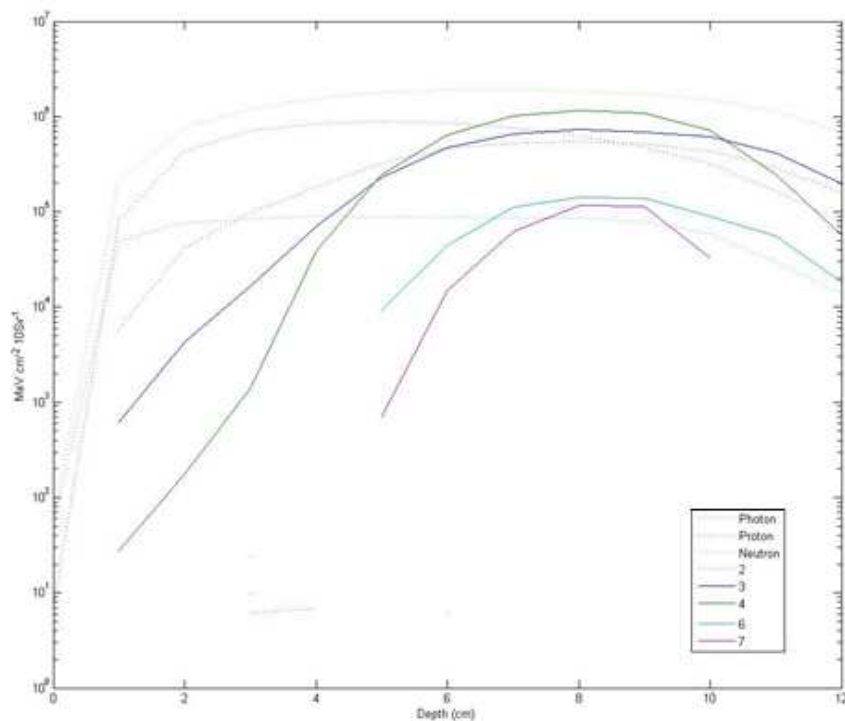


Fig 26. Total energy escaping a 1 cm radius from different fragmentation and scattering isobars for a beam of $134.5 \text{ MeV u}^{-1} {}^7\text{Li}$ particles delivering a maximum dose of 10 Sv. Total energy escaping is $2.3 \times 10^8 \text{ MeV}$

For lithium 16.8 and 43.8 % of the escape energy is in the form of proton and neutrons, with average energies of 54.0 and 37.2 MeV. Alpha particles account for 13.9 % of the escaped energy at 1 cm, while isobars of 2 and 3 amu accounts for 9.7 and 11.0 % of the escape energy. ${}^7\text{Li}$ only contributes 0.9 % of the escape energy. Isobars of 5 are not found in the lithium spectrum, or any other ions spectrum. Lithium has a total energy loss of $2.34 \times 10^8 \text{ MeV}$, which equals 13 % of its input energy, a higher percentage than any other ion. The total energy being imparted out of the original beam radius is 40 %.

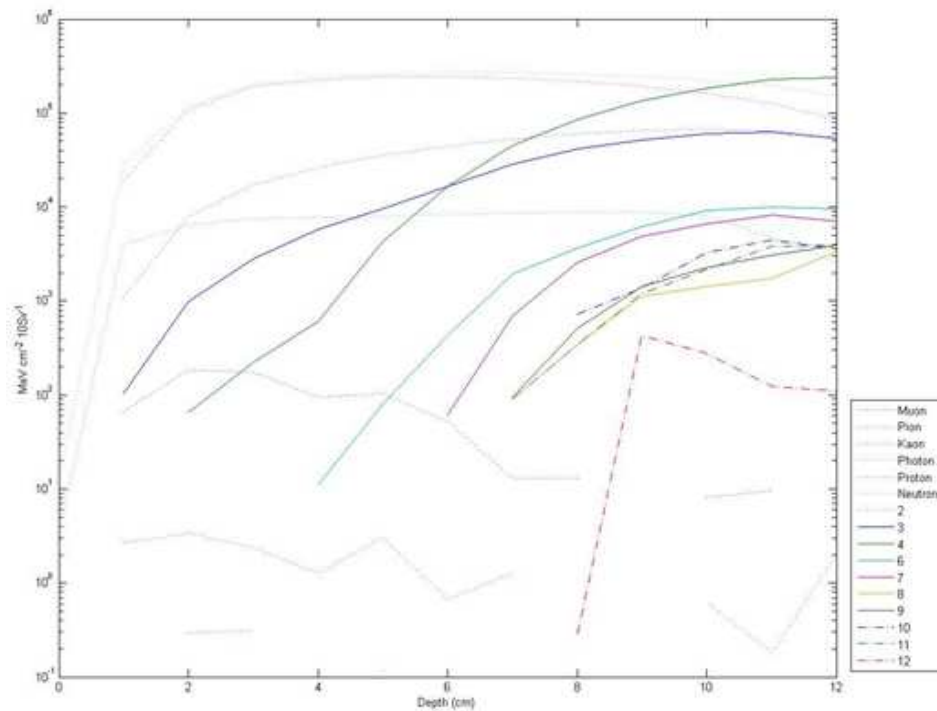


Fig 27. Total energy escaping a 1 cm radius from different fragmentation and scattering isobars for a beam of $219 \text{ MeV u}^{-1} \text{ }^{12}\text{C}$ particles delivering a maximum dose of 10 Sv. Total energy escaping is $4.1 \times 10^7 \text{ MeV}$, an amount less than any other ion under investigation.

For carbon 31.9 and 38.1 % of the escape energy are in the form of proton and neutrons, with average energies of 89.1 and 57.0 MeV. Alpha particles account for 14.5 % of the escaped energy, while isobars of 2 and 3 amu accounts for 7.6 and 5.2 % of the escape energy. The remaining isobars account for 1.78 % of the escape energy. ^{12}C is not seen to scatter pass a depth of 1 cm. Carbon has a total energy loss of $4.09 \times 10^7 \text{ MeV}$, which equals 8 % of the input energy. The total energy being imparted out of the original beam radius is 33 %.

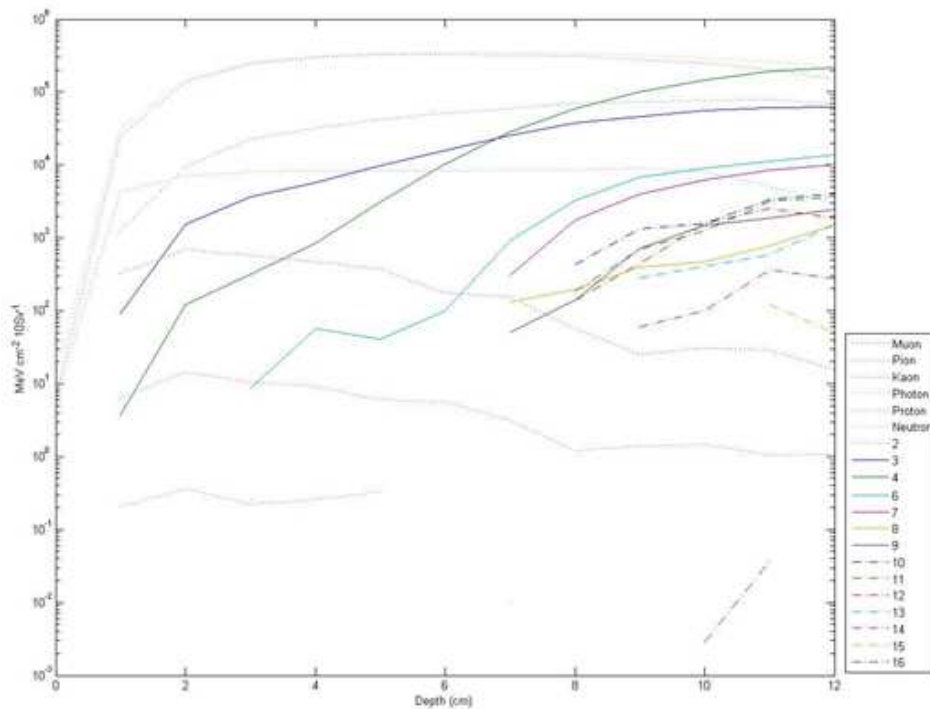


Fig 28. Total energy escaping a 1 cm radius from different fragmentation and scattering isobars for a beam of $259 \text{ MeV u}^{-1} {}^{16}\text{O}$ particles delivering a maximum dose of 10 Sv. Total energy escaping is $5.0 \times 10^7 \text{ MeV}$

For oxygen 36.3 and 40.2 % of the escape energy are in the form of proton and neutrons, with average energies of 107.2 and 71.6 MeV. Alpha particles account for 9.5 % of the escaped energy, while isobars of 2 and 3 amu accounts for 7.4 and 4.1% of the escape energy. The remaining isobars account for 1.4 % of the escape energy. Isobars greater than 12 amu are not seen to scatter pass a depth of 1 cm. Oxygen has a total energy loss of $5.01 \times 10^7 \text{ MeV}$, which equals 8 % of the input energy. The total energy being imparted out of the original beam radius is 33 %.

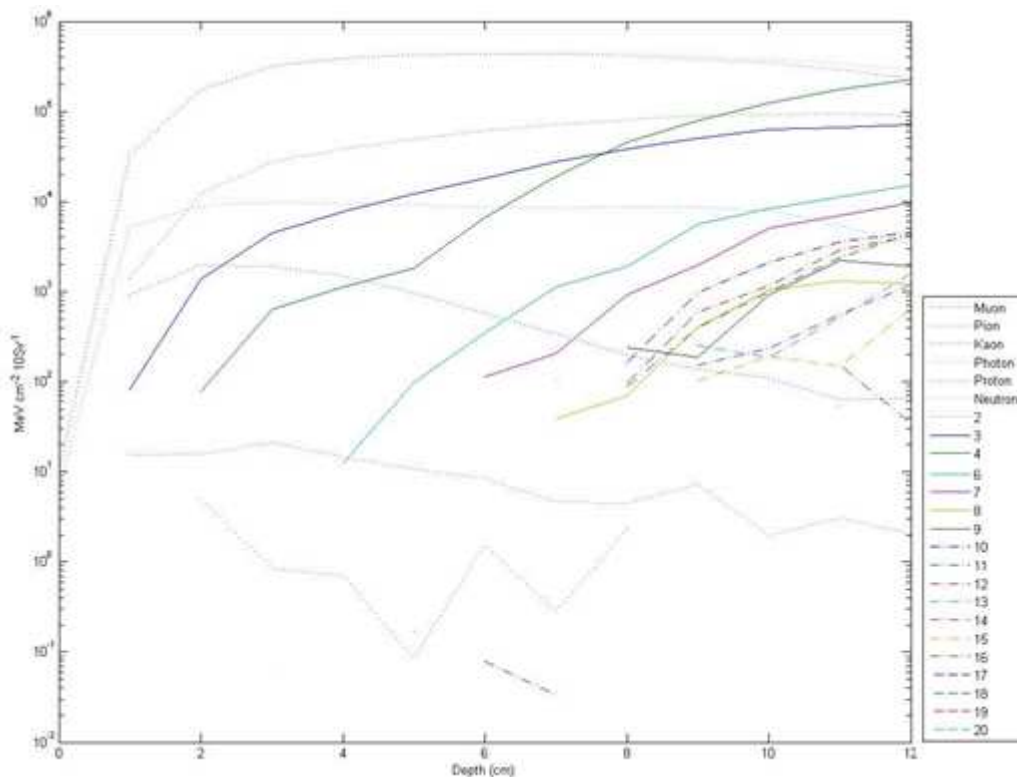


Fig 29. Total energy escaping a 1 cm radius from different fragmentation and scattering isobars for a beam of $296 \text{ MeV u}^{-1} {}^{20}\text{Ne}$ particles delivering a maximum dose of 10 Sv. Total energy escaping is $6.2 \times 10^7 \text{ MeV}$

For neon 39.1 and 41.1 % of the escape energy are in the form of proton and neutrons, with average energies of 124.5 and 85.7 MeV. Alpha particles account for 6.9 % of the escaped energy, while isobars of 2 and 3 amu accounts for 7.1 and 3.7 % of the escape energy. The remaining isobars account for 1.1 % of the escape energy. Isobars beaten 8 and 14 and greater than than 18 amu are not seen to scatter pass a depth of 1 cm. Neon has a total energy loss of $6.23 \times 10^7 \text{ MeV}$, which equals 8 % of the input energy. The total energy being imparted out of the original beam radius is 33 %.

Even though far more fragmentation products are produced for the heavier ion beams, the total energy lost to healthy tissues is greater for lighter ions. The concern of fragmentation and scattering from heavy ions should by no means be a bottleneck in the advancement of HCPT.

CHAPTER V

CONCLUSIONS

Through the analysis of several different parameters for several different ions it was verified that ^{12}C is that most appropriate ion for the advancement of charged particle therapy. Once the quality factor of heavy ions was accounted for in dose, ^{12}C showed markedly better therapeutic ratios than other ions. Supplementing its high therapeutic ratio, ^{12}C also showed the lowest amount of energy lost through fragmentation and scattering processes which are a corollary to reduction in secondary cancers in patients. With the benefits of the other biological effects discussed in the background, the advantages of carbon therapy would be even more pronounced when compared to IMRT. High LET ions, which are more prone to fragmentation exhibited less energy loss through fragmentation and scattering than lower LET ions, for equal doses delivered. Although this certainly would not be the case for all atomic masses, it seemingly holds true for any not composed of greater than 20 nucleons.

As beneficial as carbon therapy was shown to be, proton therapy was shown to be equally disadvantageous when compared to other ion therapies. In almost every pertinent consideration proton use was found to be significantly less helpful than the next worse option. Although much has been gained from the use to proton therapy in the previous years, when the current infrastructure of radiotherapy needs to be updated it should done with ions heavier than that of protons.

Even though ^{12}C was shown to be the most superior ion under investigation, usage and investigation of other ions should not be discouraged or considered imprudent. Depending on tumor location, size, movement, tissue, cellular cycles, and many other factors, the use of different ions whether individually or in combinations may be the most beneficial treatments on a case to case basis; improvements in cancer therapies would be impossible without the continued research into such ideas.

REFERENCES

- Amaldi U., Kraft G. European Developments in Radiotherapy with Beams of Large Radiobiological Effectiveness. *J. Radiat. Res.*, 48: Suppl., A27-A41; 2007.
- Attix F. Introduction to Radiological Physics and Radiation Dosimetry. Weinheim, Germany: Wiley-VCH Verlag GmbH & Co. KGaA; 2004.
- Bella M., Bettega D., Calzolari P., Cherubini G., Cuttone G., et al. Effectiveness of Monoenergetic and Spread-Out Bragg Peak Carbon-Ions for the Inactivation of Various Normal and Tumour Human Cell Lines. *J. Radiat. Res.* 49:591-607; 2008.
- Castro, J.R., Linstadt, D.E., Bahary, JP., Petti, P.L., Daftari, I., Collier, J.M., Gutin, P.H., Gauger, G., Phillips, T.L. Experience in Charged Particle Irradiation of Tumors of the Skull Base: 1977-1992. *Int. J. Radiation Oncology Biol. Phys* 29: 647-655; 1994.
- Chatterjee, A., Schaefer, H.J. Microdosimetric Structure of Heavy Ion Tracks in Tissue. *Rad. And Environm. Biophysics* 13: 215-227; 1976.
- Fenrow, R. Introduction to Experimental Particle Physics. New York: Cambridge University Press; 1989.
- Goodhead, D.T. Mechanisms for the Biological Effectiveness of High-Let Radiation. *J. Radiat. Res.* 40: Suppl., 1-13; 1999.
- Hamada N. Recent Insights into the Biological Action of Heavy-Ion Radiation. *J. Radiat Res.*, 50(1): 1-9; 2009
- Japanese National Institute of Radiological Sciences (NIRS). Research Center for Charged Particle Therapy.
<http://www.nirs.go.jp/ENG/research/charged_particle/index.shtml>.
Accessed 9 May 2001
- Linstadt, D.E., Castro, J.R., Phillips, T.L. Neon Ion Radiotherapy: Results of the Phase I/II Clinical Trial. *Int. J. Radiation Oncology Biol. Phys* 20: 761-769; 1991.
- Nikjoo, H., Munson, R.J., Bridges, B.A. RBE-LET Relationships in Mutagenesis by Ionizing Radiation. *J. Radiat. Res.*, 40: Suppl.: 85-105. 1999.

- Particle and Heavy Ion Transport System (PHITS). Overview of PHITS.
<<http://phits.jaea.go.jp/Overview.html>>. Accessed 9 May 2011.
- Particle Therapy Co-Operative Group (PTCOG). Particle therapy facilities in operation
<<http://ptcog.web.psi.ch/ptcentres.html>>. Accessed: 1 May 2011.
- Raju, M.R. Particle Radiotherapy: Historical Developments and Current Status. *Rad Res* 145: 391-407; 1996.
- Suit, H. Potential for Proton Beams in Clinical Radiation Oncology. *Radiation Research: A Twentieth Century Perspective, Vol II.* 3-13. San Diego: Academic Press; 1992.
- Valentin, J. Relative Biological Effectiveness (RBE), Quality Factor (Q), and Radiation Weighting Factor (w_R): ICRP Publication 92. *Annals of the ICRP, Volume 33, Issue 4, December 2003.*
- Wang J., Li R., Guo C., Fournier C., K-Weyrather W. The Influence of Fractionation on Cell Survival and Premature Differentiation after Carbon Ion Irradiation. *J. Radiat Res.*, 49, 391-398; 2008.
- Wilson, R.R. Radiological Use of Fast Protons. *Radiology* 47: 487-491; 1946.

APPENDIX A

Total, Primary, Alpha, and Proton LET Rates in Water Phantom

Table A. 1 LET Rates At Different Depths from All Particle, Neon, Alphas, and Protons from a ^{20}Ne Ion accelerated to 296 MeV u^{-1} in a Water Phantom. “Outside” refers to LET at tumor depths not located within the tumor described of page 20.

LET (keV/um)					LET (keV/um)				
Depth (cm)	Total	Neon	Alpha	Proton	Depth (cm)	All	Neon	Alpha	Proton
0.001	3.61E+01	3.61E+01	3.53E-03	5.65E-02	11.0005	1.14E+01	4.98E-03	1.02E+00	1.49E+00
1	3.65E+01	3.51E+01	8.12E-02	3.35E-01	12	6.71E+00	0.00E+00	9.43E-01	1.35E+00
2	3.73E+01	3.46E+01	1.32E-01	5.37E-01	13	4.71E+00	0.00E+00	8.72E-01	1.26E+00
2.5	3.75E+01	3.41E+01	1.78E-01	6.27E-01	14	3.75E+00	0.00E+00	8.26E-01	1.18E+00
3	3.79E+01	3.40E+01	1.99E-01	7.22E-01	15	3.02E+00	0.00E+00	8.05E-01	1.12E+00
4	3.91E+01	3.38E+01	2.69E-01	8.99E-01	16	2.62E+00	0.00E+00	7.63E-01	1.05E+00
5	4.06E+01	3.41E+01	3.45E-01	1.02E+00	17	2.31E+00	0.00E+00	7.05E-01	1.01E+00
6	4.30E+01	3.50E+01	4.22E-01	1.19E+00	18	2.10E+00	0.00E+00	6.82E-01	9.45E-01
7	4.66E+01	3.69E+01	5.02E-01	1.31E+00	19	1.97E+00	0.00E+00	6.43E-01	9.16E-01
7.5	4.92E+01	3.85E+01	5.65E-01	1.37E+00	20	1.86E+00	0.00E+00	6.06E-01	8.73E-01
8	5.32E+01	4.11E+01	6.19E-01	1.42E+00					
8.9995	6.86E+01	5.21E+01	8.35E-01	1.55E+00					
9.0005	5.81E-01	5.00E-01	2.05E-03	2.38E-03	9.0005	6.78E+01	5.12E+01	8.19E-01	1.53E+00
9.1	6.89E+01	5.41E+01	6.14E-01	3.99E-01	9.1	2.28E+00	1.28E-02	2.26E-01	1.26E+00
9.2	7.27E+01	5.64E+01	7.71E-01	5.18E-01	9.2	1.64E+00	0.00E+00	1.27E-01	1.18E+00
9.3	7.64E+01	5.91E+01	8.43E-01	5.86E-01	9.3	1.41E+00	0.00E+00	9.88E-02	1.09E+00
9.4	8.13E+01	6.28E+01	9.05E-01	6.38E-01	9.4	1.29E+00	0.00E+00	5.51E-02	1.06E+00
9.5	8.72E+01	6.77E+01	9.38E-01	6.80E-01	9.5	1.26E+00	0.00E+00	5.11E-02	1.04E+00
9.6	9.53E+01	7.50E+01	1.03E+00	7.33E-01	9.6	1.24E+00	0.00E+00	4.37E-02	1.05E+00
9.7	1.06E+02	8.49E+01	1.06E+00	7.57E-01	9.7	1.22E+00	0.00E+00	3.75E-02	1.02E+00
9.75	1.14E+02	9.28E+01	1.11E+00	7.60E-01	9.75	1.20E+00	0.00E+00	4.20E-02	9.98E-01
9.8	1.25E+02	1.04E+02	1.12E+00	7.65E-01	9.8	1.17E+00	0.00E+00	3.55E-02	1.01E+00
9.85	1.43E+02	1.22E+02	1.16E+00	7.79E-01	9.85	1.17E+00	0.00E+00	3.64E-02	9.97E-01
9.86	1.46E+02	1.25E+02	1.17E+00	8.06E-01	9.86	1.19E+00	0.00E+00	4.49E-02	1.00E+00
9.87	1.51E+02	1.30E+02	1.17E+00	7.88E-01	9.87	1.21E+00	0.00E+00	3.39E-02	1.05E+00
9.88	1.57E+02	1.36E+02	1.18E+00	7.87E-01	9.88	1.20E+00	0.00E+00	3.81E-02	1.02E+00
9.89	1.64E+02	1.44E+02	1.20E+00	7.99E-01	9.89	1.22E+00	0.00E+00	3.92E-02	1.03E+00
9.9	1.73E+02	1.52E+02	1.19E+00	7.92E-01	9.9	1.18E+00	0.00E+00	4.30E-02	9.92E-01
9.91	1.83E+02	1.63E+02	1.17E+00	8.00E-01	9.91	1.19E+00	0.00E+00	4.13E-02	1.01E+00
9.92	1.97E+02	1.77E+02	1.17E+00	7.94E-01	9.92	1.23E+00	0.00E+00	4.00E-02	1.02E+00
9.93	2.15E+02	1.95E+02	1.16E+00	7.97E-01	9.93	1.25E+00	0.00E+00	3.86E-02	1.04E+00
9.94	2.35E+02	2.15E+02	1.16E+00	7.78E-01	9.94	1.21E+00	0.00E+00	3.78E-02	1.03E+00
9.95	2.53E+02	2.33E+02	1.16E+00	7.75E-01	9.95	1.21E+00	0.00E+00	4.04E-02	1.02E+00
9.96	2.57E+02	2.38E+02	1.15E+00	7.74E-01	9.96	1.17E+00	0.00E+00	5.11E-02	9.81E-01
9.97	2.38E+02	2.20E+02	1.15E+00	7.61E-01	9.97	1.19E+00	0.00E+00	3.80E-02	9.96E-01
9.98	1.96E+02	1.77E+02	1.14E+00	7.75E-01	9.98	1.18E+00	0.00E+00	3.67E-02	9.86E-01
9.99	1.40E+02	1.22E+02	1.12E+00	7.55E-01	9.99	1.23E+00	0.00E+00	4.83E-02	1.01E+00
10	8.80E+01	7.05E+01	1.12E+00	7.37E-01	10	1.14E+00	0.00E+00	3.58E-02	9.70E-01
10.01	5.11E+01	3.38E+01	1.10E+00	7.39E-01	10.01	1.19E+00	0.00E+00	4.67E-02	9.88E-01
10.02	3.04E+01	1.34E+01	1.11E+00	7.27E-01	10.02	0.00E+00	0.00E+00	0.00E+00	0.00E+00
10.03	2.16E+01	4.66E+00	1.10E+00	7.35E-01	10.03	0.00E+00	0.00E+00	0.00E+00	0.00E+00
10.04	1.82E+01	1.38E+00	1.09E+00	7.21E-01	10.04	3.78E-02	0.00E+00	0.00E+00	2.26E-02
10.05	1.71E+01	3.40E-01	1.10E+00	7.13E-01	10.05	1.21E+00	0.00E+00	3.53E-02	1.03E+00
10.1	1.61E+01	1.56E-02	1.05E+00	6.92E-01	10.1	1.21E+00	0.00E+00	3.88E-02	1.01E+00
10.2	1.52E+01	0.00E+00	1.04E+00	6.55E-01	10.2	1.24E+00	0.00E+00	4.73E-02	1.05E+00
10.3	1.31E+01	0.00E+00	9.16E-01	5.51E-01	10.3	1.15E+00	0.00E+00	4.71E-02	9.55E-01
10.4	1.36E+01	0.00E+00	9.91E-01	5.78E-01	10.4	1.35E+00	0.00E+00	6.60E-02	1.07E+00
10.5	1.29E+01	0.00E+00	9.58E-01	5.17E-01	10.5	1.47E+00	0.00E+00	9.66E-02	1.16E+00
10.6	1.22E+01	0.00E+00	9.15E-01	4.78E-01	10.6	1.55E+00	0.00E+00	1.27E-01	1.15E+00
10.7	1.13E+01	0.00E+00	8.43E-01	4.06E-01	10.7	1.73E+00	0.00E+00	1.63E-01	1.19E+00
10.8	1.02E+01	0.00E+00	7.30E-01	3.14E-01	10.8	2.32E+00	0.00E+00	2.89E-01	1.26E+00
10.9	8.13E+00	0.00E+00	5.14E-01	2.03E-01	10.9	3.86E+00	0.00E+00	4.96E-01	1.33E+00
10.9995	2.18E-02	0.00E+00	6.50E-04	2.50E-04	10.9995	1.13E+01	0.00E+00	9.77E-01	1.48E+00

Outside

Table A. 2 LET Rates At Different Depths from All Particle, Oxygen, Alphas, and Protons from a ^{16}O Ion accelerated to 259 MeV u^{-1} in a Water Phantom. “Outside” refers to LET at tumor depths not located within the tumor described of page 20.

LET (keV/um)					LET (keV/um)				
Depth (cm)	Total	Neon	Alpha	Proton	Depth (cm)	All	Neon	Alpha	Proton
0.001	2.502E+01	2.497E+01	4.216E-03	3.310E-02	11.0005	6.767E+00	7.413E-03	8.698E-01	1.091E+00
1	2.547E+01	2.452E+01	7.829E-02	2.902E-01	12	4.183E+00	1.454E-03	8.111E-01	1.006E+00
2	2.607E+01	2.434E+01	1.221E-01	4.474E-01	13	2.845E+00	8.739E-03	7.654E-01	9.021E-01
2.5	2.642E+01	2.426E+01	1.722E-01	3.943E-01	14	2.290E+00	4.678E-04	6.823E-01	8.467E-01
3	2.682E+01	2.429E+01	1.756E-01	5.961E-01	15	1.967E+00	5.520E-04	6.523E-01	7.899E-01
4	2.789E+01	2.453E+01	2.320E-01	7.394E-01	16	1.782E+00	2.662E-03	6.119E-01	7.407E-01
5	2.906E+01	2.484E+01	3.276E-01	6.360E-01	17	1.591E+00	8.795E-04	5.652E-01	6.798E-01
6	3.087E+01	2.572E+01	3.478E-01	9.488E-01	18	1.478E+00	1.415E-04	5.324E-01	6.441E-01
7	3.371E+01	2.738E+01	4.934E-01	1.029E+00	19	1.370E+00	2.964E-03	4.915E-01	5.992E-01
7.5	3.583E+01	2.880E+01	5.664E-01	8.044E-01	20	1.324E+00	2.852E-03	4.822E-01	5.864E-01
8	3.840E+01	3.059E+01	5.592E-01	1.106E+00					
8.9995	5.052E+01	3.970E+01	7.617E-01	1.213E+00					
9.0005	4.198E-01	3.743E-01	1.981E-03	1.493E-03	9.0005	5.024E+01	3.921E+01	7.878E-01	1.242E+00
9.1	5.055E+01	4.126E+01	5.797E-01	3.358E-01	9.1	2.321E+00	9.237E-02	2.388E-01	9.988E-01
9.2	5.370E+01	4.317E+01	6.862E-01	4.160E-01	9.2	1.469E+00	1.821E-02	1.612E-01	9.134E-01
9.3	5.662E+01	4.522E+01	7.615E-01	4.798E-01	9.3	1.216E+00	6.719E-04	1.005E-01	8.718E-01
9.4	6.008E+01	4.813E+01	8.310E-01	5.166E-01	9.4	1.089E+00	4.459E-04	7.510E-02	8.227E-01
9.5	6.441E+01	5.197E+01	8.665E-01	5.612E-01	9.5	1.048E+00	3.023E-04	6.691E-02	8.089E-01
9.6	7.037E+01	5.763E+01	9.810E-01	5.872E-01	9.6	9.974E-01	9.957E-03	5.408E-02	7.748E-01
9.7	7.813E+01	6.531E+01	1.046E+00	6.255E-01	9.7	1.008E+00	1.903E-02	4.821E-02	7.945E-01
9.75	8.419E+01	7.142E+01	1.046E+00	6.266E-01	9.75	9.545E-01	4.142E-04	5.429E-02	7.637E-01
9.8	9.343E+01	8.065E+01	1.072E+00	6.302E-01	9.8	9.393E-01	5.916E-04	4.758E-02	7.562E-01
9.85	1.067E+02	9.404E+01	1.102E+00	6.326E-01	9.85	9.766E-01	6.235E-04	4.376E-02	7.797E-01
9.86	1.090E+02	9.640E+01	1.140E+00	5.155E-01	9.86	9.506E-01	7.749E-04	5.767E-02	7.579E-01
9.87	1.127E+02	1.002E+02	1.138E+00	4.709E-01	9.87	9.466E-01	1.037E-03	4.942E-02	7.493E-01
9.88	1.170E+02	1.047E+02	1.132E+00	4.710E-01	9.88	1.002E+00	1.408E-03	5.248E-02	7.883E-01
9.89	1.225E+02	1.102E+02	1.127E+00	4.709E-01	9.89	9.835E-01	7.988E-03	5.072E-02	7.727E-01
9.9	1.291E+02	1.170E+02	1.121E+00	4.662E-01	9.9	9.659E-01	4.648E-04	5.476E-02	7.744E-01
9.91	1.378E+02	1.259E+02	1.124E+00	4.688E-01	9.91	9.746E-01	2.561E-04	5.449E-02	7.727E-01
9.92	1.490E+02	1.371E+02	1.124E+00	4.688E-01	9.92	9.764E-01	7.802E-03	5.195E-02	7.739E-01
9.93	1.621E+02	1.504E+02	1.114E+00	4.675E-01	9.93	9.773E-01	6.991E-04	4.728E-02	7.768E-01
9.94	1.760E+02	1.645E+02	1.106E+00	4.712E-01	9.94	9.579E-01	1.873E-03	4.997E-02	7.726E-01
9.95	1.852E+02	1.739E+02	1.082E+00	4.564E-01	9.95	9.563E-01	6.756E-04	4.871E-02	7.679E-01
9.96	1.838E+02	1.727E+02	1.081E+00	4.539E-01	9.96	9.766E-01	6.235E-04	4.376E-02	7.797E-01
9.97	1.689E+02	1.581E+02	1.086E+00	4.505E-01	9.97	9.529E-01	7.815E-04	5.063E-02	7.569E-01
9.98	1.395E+02	1.289E+02	1.082E+00	4.443E-01	9.98	9.426E-01	9.799E-04	5.613E-02	7.488E-01
9.99	1.036E+02	9.328E+01	1.062E+00	4.347E-01	9.99	9.466E-01	3.129E-04	5.016E-02	7.523E-01
10	6.891E+01	5.866E+01	1.054E+00	4.314E-01	10	9.610E-01	4.072E-04	5.405E-02	7.669E-01
10.01	4.184E+01	3.167E+01	1.047E+00	4.254E-01	10.01	9.614E-01	2.975E-03	5.470E-02	7.458E-01
10.02	2.492E+01	1.495E+01	1.037E+00	4.208E-01	10.02	0.000E+00	0.000E+00	0.000E+00	0.000E+00
10.03	1.606E+01	6.106E+00	1.035E+00	4.124E-01	10.03	0.000E+00	0.000E+00	0.000E+00	0.000E+00
10.04	1.205E+01	2.194E+00	1.030E+00	4.061E-01	10.04	1.628E-02	0.000E+00	0.000E+00	1.578E-02
10.05	1.031E+01	5.613E-01	9.789E-01	5.565E-01	10.05	9.700E-01	1.613E-02	5.107E-02	7.562E-01
10.1	9.331E+00	5.519E-03	9.428E-01	5.450E-01	10.1	9.860E-01	1.585E-03	5.891E-02	7.729E-01
10.2	8.777E+00	8.753E-04	9.002E-01	5.174E-01	10.2	1.006E+00	6.373E-04	5.957E-02	7.919E-01
10.3	7.455E+00	2.464E-07	7.765E-01	4.354E-01	10.3	9.376E-01	7.498E-03	6.217E-02	7.131E-01
10.4	7.840E+00	1.614E-06	8.725E-01	4.230E-01	10.4	1.073E+00	6.539E-04	8.192E-02	7.954E-01
10.5	7.347E+00	1.073E-02	8.015E-01	4.070E-01	10.5	1.206E+00	2.313E-03	1.164E-01	8.486E-01
10.6	6.800E+00	0.000E+00	7.626E-01	3.506E-01	10.6	1.398E+00	2.734E-02	1.799E-01	8.573E-01
10.7	6.131E+00	0.000E+00	6.732E-01	2.981E-01	10.7	1.615E+00	3.105E-03	2.206E-01	8.978E-01
10.8	5.398E+00	0.000E+00	5.793E-01	2.430E-01	10.8	2.093E+00	9.662E-04	3.222E-01	9.443E-01
10.9	3.873E+00	0.000E+00	3.398E-01	1.461E-01	10.9	3.313E+00	8.547E-03	5.546E-01	9.903E-01
10.9995	9.285E-03	0.000E+00	1.500E-04	1.800E-04	10.9995	6.794E+00	5.399E-04	8.648E-01	1.091E+00

Outside

Table A. 3 LET Rates At Different Depths from All Particle, Carbon, Alphas, and Protons from a ^{12}C Ion accelerated to 219 MeV u^{-1} in a Water Phantom. “Outside” refers to LET at tumor depths not located within the tumor described of page 20.

LET (keV/um)					LET (keV/um)				
Depth (cm)	Total	Neon	Alpha	Proton	Depth (cm)	All	Neon	Alpha	Proton
0.001	1.557E+01	1.553E+01	4.216E-03	3.310E-02	11.0005	3.436E+00	0.000E+00	9.588E-01	7.108E-01
1	1.604E+01	1.543E+01	9.178E-02	2.274E-01	12	2.644E+00	2.192E-03	8.630E-01	6.243E-01
2	1.634E+01	1.531E+01	1.266E-01	3.447E-01	13	1.984E+00	0.000E+00	8.071E-01	5.680E-01
2.5	1.680E+01	1.552E+01	1.701E-01	3.943E-01	14	1.644E+00	0.000E+00	7.352E-01	5.127E-01
3	1.696E+01	1.549E+01	1.912E-01	4.489E-01	15	1.481E+00	0.000E+00	6.725E-01	4.622E-01
4	1.781E+01	1.589E+01	2.539E-01	5.461E-01	16	1.324E+00	0.000E+00	6.106E-01	4.246E-01
5	1.865E+01	1.625E+01	3.276E-01	6.360E-01	17	1.183E+00	0.000E+00	5.636E-01	3.856E-01
6	1.988E+01	1.696E+01	4.183E-01	7.055E-01	18	1.090E+00	1.483E-03	5.180E-01	3.638E-01
7	2.174E+01	1.815E+01	5.137E-01	7.708E-01	19	9.698E-01	0.000E+00	4.676E-01	3.303E-01
7.5	2.317E+01	1.911E+01	5.664E-01	8.044E-01	20	8.933E-01	4.448E-03	4.154E-01	3.099E-01
8	2.505E+01	2.054E+01	6.377E-01	8.279E-01					
8.9995	3.248E+01	2.649E+01	8.696E-01	8.960E-01					
9.0005	2.795E-01	2.566E-01	1.864E-03	1.117E-03	9.0005	3.206E+01	2.610E+01	8.865E-01	8.744E-01
9.1	3.190E+01	2.748E+01	5.459E-01	2.555E-01	9.1	2.130E+00	3.373E-01	3.247E-01	6.945E-01
9.2	3.410E+01	2.904E+01	7.226E-01	3.182E-01	9.2	1.334E+00	1.015E-01	2.091E-01	6.452E-01
9.3	3.603E+01	3.055E+01	8.082E-01	3.711E-01	9.3	1.062E+00	3.233E-02	1.607E-01	6.089E-01
9.4	3.789E+01	3.237E+01	9.035E-01	4.196E-01	9.4	9.065E-01	1.257E-02	1.231E-01	5.749E-01
9.5	4.025E+01	3.469E+01	9.515E-01	4.351E-01	9.5	8.143E-01	5.190E-03	1.000E-01	5.475E-01
9.6	4.349E+01	3.794E+01	9.922E-01	4.388E-01	9.6	7.902E-01	1.470E-03	9.159E-02	5.484E-01
9.7	4.869E+01	4.314E+01	1.056E+00	4.521E-01	9.7	7.610E-01	3.300E-03	8.248E-02	5.416E-01
9.75	5.222E+01	4.672E+01	1.087E+00	4.550E-01	9.75	7.250E-01	5.790E-03	7.641E-02	5.168E-01
9.8	5.618E+01	5.076E+01	1.104E+00	4.709E-01	9.8	7.467E-01	0.000E+00	8.117E-02	5.422E-01
9.85	6.241E+01	5.707E+01	1.117E+00	4.674E-01	9.85	7.540E-01	0.000E+00	7.943E-02	5.293E-01
9.86	6.361E+01	5.831E+01	1.140E+00	5.155E-01	9.86	7.303E-01	0.000E+00	8.051E-02	5.204E-01
9.87	6.530E+01	6.011E+01	1.138E+00	4.709E-01	9.87	7.474E-01	0.000E+00	8.141E-02	5.319E-01
9.88	6.738E+01	6.216E+01	1.132E+00	4.710E-01	9.88	7.508E-01	0.000E+00	7.743E-02	5.405E-01
9.89	6.956E+01	6.445E+01	1.127E+00	4.709E-01	9.89	7.578E-01	0.000E+00	8.215E-02	5.322E-01
9.9	7.227E+01	6.717E+01	1.121E+00	4.662E-01	9.9	7.437E-01	0.000E+00	7.914E-02	5.328E-01
9.91	7.538E+01	7.032E+01	1.124E+00	4.688E-01	9.91	7.225E-01	0.000E+00	7.687E-02	5.178E-01
9.92	7.926E+01	7.421E+01	1.108E+00	4.613E-01	9.92	7.371E-01	0.000E+00	8.112E-02	5.192E-01
9.93	8.384E+01	7.889E+01	1.106E+00	4.712E-01	9.93	7.351E-01	0.000E+00	8.057E-02	5.203E-01
9.94	8.971E+01	8.485E+01	1.114E+00	4.675E-01	9.94	7.522E-01	0.000E+00	7.845E-02	5.235E-01
9.95	9.662E+01	9.189E+01	1.082E+00	4.564E-01	9.95	7.415E-01	0.000E+00	8.116E-02	5.246E-01
9.96	1.044E+02	9.969E+01	1.076E+00	4.538E-01	9.96	7.300E-01	0.000E+00	7.980E-02	5.179E-01
9.97	1.116E+02	1.071E+02	1.086E+00	4.505E-01	9.97	7.713E-01	0.000E+00	8.250E-02	5.292E-01
9.98	1.162E+02	1.118E+02	1.082E+00	4.443E-01	9.98	7.535E-01	0.000E+00	8.620E-02	5.244E-01
9.99	1.158E+02	1.115E+02	1.062E+00	4.347E-01	9.99	7.307E-01	0.000E+00	8.108E-02	5.143E-01
10	1.099E+02	1.056E+02	1.054E+00	4.314E-01	10	7.548E-01	0.000E+00	9.022E-02	5.261E-01
10.01	9.589E+01	9.171E+01	1.047E+00	4.254E-01	10.01	7.392E-01	0.000E+00	8.790E-02	5.109E-01
10.02	7.740E+01	7.329E+01	1.037E+00	4.208E-01	10.02	0.000E+00	0.000E+00	0.000E+00	0.000E+00
10.03	5.713E+01	5.306E+01	1.035E+00	4.124E-01	10.03	0.000E+00	0.000E+00	0.000E+00	0.000E+00
10.04	3.845E+01	3.442E+01	1.030E+00	4.061E-01	10.04	7.770E-03	0.000E+00	0.000E+00	7.305E-03
10.05	2.352E+01	1.953E+01	1.022E+00	3.993E-01	10.05	7.541E-01	0.000E+00	7.944E-02	5.335E-01
10.1	4.147E+00	2.905E-01	9.897E-01	3.743E-01	10.1	7.798E-01	0.000E+00	9.262E-02	5.407E-01
10.2	3.656E+00	3.938E-03	9.512E-01	3.414E-01	10.2	7.829E-01	0.000E+00	9.740E-02	5.315E-01
10.3	3.088E+00	0.000E+00	8.311E-01	2.874E-01	10.3	7.939E-01	0.000E+00	1.099E-01	5.185E-01
10.4	3.287E+00	0.000E+00	8.848E-01	2.849E-01	10.4	9.110E-01	0.000E+00	1.517E-01	5.510E-01
10.5	3.014E+00	0.000E+00	8.245E-01	2.548E-01	10.5	9.837E-01	9.542E-04	1.839E-01	5.762E-01
10.6	2.779E+00	0.000E+00	7.554E-01	2.211E-01	10.6	1.115E+00	0.000E+00	2.471E-01	5.699E-01
10.7	2.454E+00	4.537E-03	6.553E-01	1.851E-01	10.7	1.361E+00	0.000E+00	3.162E-01	6.154E-01
10.8	1.998E+00	0.000E+00	4.977E-01	1.369E-01	10.8	1.673E+00	0.000E+00	4.609E-01	6.287E-01
10.9	1.439E+00	0.000E+00	2.989E-01	7.921E-02	10.9	2.178E+00	2.392E-04	6.763E-01	6.749E-01
10.9995	3.270E-03	0.000E+00	2.700E-04	8.250E-05	10.9995	3.439E+00	0.000E+00	9.653E-01	7.067E-01

Outside

Table A. 4 LET Rates At Different Depths from All Particle, Lithium, Alphas, and Protons from a ${}^7\text{Li}$ Ion accelerated to 134.5 MeV u^{-1} in a Water Phantom. “Outside” refers to LET at tumor depths not located within the tumor described of page 20.

LET (keV/um)					LET (keV/um)				
Depth (cm)	Total	Neon	Alpha	Proton	Depth (cm)	All	Neon	Alpha	Proton
0.001	5.749E+00	5.719E+00	2.090E-03	2.378E-02	11.0005	1.209E+00	0.000E+00	5.550E-01	2.643E-01
1	6.076E+00	5.677E+00	7.792E-02	2.039E-01	12	7.960E-01	4.730E-04	2.506E-01	1.938E-01
2	6.205E+00	5.569E+00	1.430E-01	3.084E-01	13	5.525E-01	0.000E+00	8.926E-02	1.535E-01
2.5	6.304E+00	5.581E+00	1.758E-01	3.409E-01	14	4.165E-01	0.000E+00	2.474E-02	1.210E-01
3	6.301E+00	5.469E+00	2.092E-01	3.745E-01	15	3.499E-01	0.000E+00	6.220E-03	1.028E-01
4	6.475E+00	5.422E+00	2.834E-01	4.330E-01	16	2.961E-01	0.000E+00	1.018E-02	8.182E-02
5	6.674E+00	5.437E+00	3.609E-01	4.820E-01	17	2.577E-01	0.000E+00	2.199E-03	7.378E-02
6	7.061E+00	5.573E+00	4.674E-01	5.184E-01	18	2.145E-01	0.000E+00	1.673E-03	6.433E-02
7	7.876E+00	6.103E+00	6.072E-01	5.352E-01	19	1.825E-01	0.000E+00	1.030E-03	5.557E-02
7.5	8.364E+00	6.468E+00	6.806E-01	5.451E-01	20	1.608E-01	0.000E+00	2.777E-03	5.090E-02
8	9.074E+00	6.939E+00	7.846E-01	5.586E-01					
8.9995	1.111E+01	8.725E+00	1.062E+00	5.367E-01					
9.0005	7.678E-02	7.389E-02	7.897E-04	5.193E-04	9.0005	1.093E+01	8.582E+00	1.051E+00	5.281E-01
9.1	9.943E+00	8.951E+00	4.164E-01	1.551E-01	9.1	1.581E+00	1.167E-01	7.246E-01	3.906E-01
9.2	1.064E+01	9.397E+00	5.115E-01	1.922E-01	9.2	1.362E+00	1.209E-01	6.200E-01	3.393E-01
9.3	1.130E+01	9.965E+00	5.826E-01	2.138E-01	9.3	1.268E+00	1.270E-01	5.603E-01	3.136E-01
9.4	1.214E+01	1.073E+01	6.499E-01	2.247E-01	9.4	1.174E+00	1.390E-01	5.132E-01	2.911E-01
9.5	1.306E+01	1.159E+01	6.944E-01	2.274E-01	9.5	1.092E+00	1.388E-01	4.737E-01	2.664E-01
9.6	1.411E+01	1.263E+01	7.111E-01	2.316E-01	9.6	1.025E+00	9.866E-02	4.557E-01	2.702E-01
9.7	1.550E+01	1.405E+01	7.129E-01	2.199E-01	9.7	9.622E-01	5.123E-02	4.502E-01	2.587E-01
9.75	1.653E+01	1.510E+01	7.105E-01	2.259E-01	9.75	9.362E-01	2.533E-02	4.579E-01	2.559E-01
9.8	1.797E+01	1.655E+01	7.005E-01	2.168E-01	9.8	8.904E-01	1.581E-02	4.408E-01	2.478E-01
9.85	2.002E+01	1.872E+01	6.913E-01	1.971E-01	9.85	8.680E-01	4.500E-03	4.220E-01	2.452E-01
9.86	2.064E+01	1.921E+01	6.837E-01	2.310E-01	9.86	8.842E-01	2.775E-03	4.282E-01	2.523E-01
9.87	2.118E+01	1.984E+01	6.952E-01	2.001E-01	9.87	8.664E-01	3.075E-03	4.233E-01	2.497E-01
9.88	2.191E+01	2.057E+01	6.873E-01	1.987E-01	9.88	8.605E-01	3.465E-03	4.198E-01	2.438E-01
9.89	2.271E+01	2.139E+01	6.836E-01	1.999E-01	9.89	8.870E-01	4.935E-03	4.214E-01	2.531E-01
9.9	2.364E+01	2.234E+01	6.841E-01	1.879E-01	9.9	8.850E-01	0.000E+00	4.331E-01	2.457E-01
9.91	2.480E+01	2.352E+01	6.811E-01	1.903E-01	9.91	8.671E-01	2.730E-03	4.219E-01	2.480E-01
9.92	2.609E+01	2.481E+01	6.864E-01	1.874E-01	9.92	8.637E-01	3.435E-03	4.187E-01	2.447E-01
9.93	2.760E+01	2.633E+01	6.820E-01	1.867E-01	9.93	8.651E-01	6.450E-04	4.130E-01	2.541E-01
9.94	2.930E+01	2.807E+01	6.798E-01	1.757E-01	9.94	8.624E-01	7.950E-04	4.135E-01	2.495E-01
9.95	3.113E+01	2.992E+01	6.626E-01	1.709E-01	9.95	8.584E-01	1.185E-03	4.141E-01	2.475E-01
9.96	3.281E+01	3.161E+01	6.716E-01	1.684E-01	9.96	8.511E-01	2.985E-03	4.125E-01	2.407E-01
9.97	3.425E+01	3.308E+01	6.538E-01	1.666E-01	9.97	8.598E-01	0.000E+00	4.182E-01	2.472E-01
9.98	3.503E+01	3.388E+01	6.516E-01	1.627E-01	9.98	8.729E-01	0.000E+00	4.270E-01	2.489E-01
9.99	3.487E+01	3.373E+01	6.402E-01	1.591E-01	9.99	8.724E-01	0.000E+00	4.259E-01	2.465E-01
10	3.356E+01	3.243E+01	6.384E-01	1.560E-01	10	8.886E-01	0.000E+00	4.496E-01	2.446E-01
10.01	3.111E+01	3.001E+01	6.276E-01	1.558E-01	10.01	8.775E-01	0.000E+00	4.305E-01	2.439E-01
10.02	2.769E+01	2.661E+01	6.164E-01	1.507E-01	10.02	0.000E+00	0.000E+00	0.000E+00	0.000E+00
10.03	2.350E+01	2.243E+01	6.144E-01	1.478E-01	10.03	0.000E+00	0.000E+00	0.000E+00	0.000E+00
10.04	1.877E+01	1.771E+01	5.986E-01	1.496E-01	10.04	3.870E-03	0.000E+00	0.000E+00	2.760E-03
10.05	1.450E+01	1.346E+01	5.922E-01	1.405E-01	10.05	8.790E-01	0.000E+00	4.353E-01	2.459E-01
10.1	2.401E+00	1.432E+00	5.487E-01	1.325E-01	10.1	8.850E-01	0.000E+00	4.331E-01	2.457E-01
10.2	8.655E-01	0.000E+00	4.817E-01	1.163E-01	10.2	9.187E-01	0.000E+00	4.374E-01	2.499E-01
10.3	6.913E-01	0.000E+00	3.751E-01	9.194E-02	10.3	8.451E-01	0.000E+00	3.930E-01	2.308E-01
10.4	6.768E-01	0.000E+00	3.659E-01	8.428E-02	10.4	9.418E-01	0.000E+00	4.552E-01	2.505E-01
10.5	5.814E-01	0.000E+00	3.054E-01	6.844E-02	10.5	9.713E-01	0.000E+00	4.756E-01	2.499E-01
10.6	4.938E-01	0.000E+00	2.566E-01	5.904E-02	10.6	9.741E-01	0.000E+00	4.558E-01	2.592E-01
10.7	3.993E-01	0.000E+00	2.084E-01	3.797E-02	10.7	9.998E-01	0.000E+00	4.720E-01	2.603E-01
10.8	3.367E-01	0.000E+00	1.762E-01	2.504E-02	10.8	1.009E+00	0.000E+00	4.605E-01	2.649E-01
10.9	2.471E-01	0.000E+00	1.237E-01	1.391E-02	10.9	1.035E+00	0.000E+00	4.788E-01	2.677E-01
10.9995	2.400E-04	0.000E+00	3.000E-05	0.000E+00	10.9995	1.223E+00	0.000E+00	5.391E-01	2.721E-01

Outside

Table A. 5 LET Rates At Different Depths from All Particle, Helium, and Protons from a ^4He Ion accelerated to 116.5 MeV u^{-1} in a Water Phantom. “Outside” refers to LET at tumor depths not located within the tumor described of page 20.

Depth (cm)	LET (keV/um)			Depth (cm)	LET (keV/um)		
	Total	Neon	Alpha		All	Neon	Alpha
0.001	2.463E+00	2.456E+00	6.059E-03	11.0005	1.243E-01	1.236E-03	4.571E-02
1	2.603E+00	2.506E+00	6.425E-02	12	9.362E-02	5.408E-04	3.186E-02
2	2.684E+00	2.524E+00	1.012E-01	13	7.322E-02	1.705E-03	2.241E-02
2.5	2.778E+00	2.591E+00	1.140E-01	14	5.756E-02	5.273E-04	1.762E-02
3	2.828E+00	2.618E+00	1.259E-01	15	4.682E-02	3.113E-04	1.367E-02
4	2.976E+00	2.714E+00	1.473E-01	16	3.552E-02	0.000E+00	1.087E-02
5	3.225E+00	2.904E+00	1.694E-01	17	2.900E-02	0.000E+00	9.325E-03
6	3.603E+00	3.213E+00	1.823E-01	18	2.558E-02	1.494E-04	9.010E-03
7	4.265E+00	3.820E+00	1.913E-01	19	2.278E-02	6.822E-04	7.893E-03
7.5	4.767E+00	4.296E+00	1.940E-01	20	1.885E-02	0.000E+00	8.168E-03
8	5.294E+00	4.845E+00	1.868E-01				
8.9995	6.468E+00	6.058E+00	1.700E-01				
9.0005	4.025E-02	3.978E-02	2.077E-04	9.0005	6.460E+00	6.031E+00	1.666E-01
9.1	6.213E+00	5.985E+00	6.669E-02	9.1	5.413E-01	3.419E-01	9.448E-02
9.2	6.568E+00	6.315E+00	8.173E-02	9.2	4.541E-01	2.929E-01	7.976E-02
9.3	6.911E+00	6.664E+00	8.508E-02	9.3	3.868E-01	2.357E-01	7.415E-02
9.4	7.414E+00	7.181E+00	8.604E-02	9.4	2.867E-01	1.424E-01	6.418E-02
9.5	8.074E+00	7.817E+00	9.235E-02	9.5	2.042E-01	7.345E-02	5.940E-02
9.6	8.894E+00	8.660E+00	9.048E-02	9.6	1.644E-01	3.988E-02	5.664E-02
9.7	1.002E+01	9.826E+00	8.237E-02	9.7	1.379E-01	1.666E-02	5.403E-02
9.75	1.077E+01	1.058E+01	8.374E-02	9.75	1.250E-01	9.168E-03	4.934E-02
9.8	1.186E+01	1.166E+01	8.189E-02	9.8	1.255E-01	8.405E-03	4.760E-02
9.85	1.353E+01	1.335E+01	7.545E-02	9.85	1.183E-01	4.758E-03	4.619E-02
9.86	1.386E+01	1.366E+01	8.268E-02	9.86	1.210E-01	4.932E-03	4.807E-02
9.87	1.434E+01	1.417E+01	7.236E-02	9.87	1.198E-01	4.632E-03	4.778E-02
9.88	1.494E+01	1.477E+01	7.275E-02	9.88	1.185E-01	2.802E-03	4.837E-02
9.89	1.557E+01	1.542E+01	7.023E-02	9.89	1.181E-01	3.024E-03	4.807E-02
9.9	1.628E+01	1.611E+01	6.718E-02	9.9	1.170E-01	3.288E-03	4.823E-02
9.91	1.709E+01	1.695E+01	6.483E-02	9.91	1.173E-01	2.868E-03	4.799E-02
9.92	1.791E+01	1.777E+01	6.437E-02	9.92	1.162E-01	2.982E-03	4.608E-02
9.93	1.870E+01	1.856E+01	6.015E-02	9.93	1.193E-01	5.014E-03	4.665E-02
9.94	1.941E+01	1.927E+01	6.165E-02	9.94	1.177E-01	3.373E-03	4.544E-02
9.95	1.999E+01	1.985E+01	5.875E-02	9.95	1.203E-01	3.042E-03	4.855E-02
9.96	2.031E+01	2.018E+01	5.874E-02	9.96	1.168E-01	2.808E-03	4.696E-02
9.97	2.025E+01	2.013E+01	5.626E-02	9.97	1.155E-01	2.562E-03	4.707E-02
9.98	2.005E+01	1.993E+01	5.577E-02	9.98	1.132E-01	2.418E-03	4.466E-02
9.99	1.924E+01	1.913E+01	5.391E-02	9.99	1.144E-01	2.298E-03	4.697E-02
10	1.815E+01	1.804E+01	5.233E-02	10	1.163E-01	2.046E-03	4.666E-02
10.01	1.669E+01	1.659E+01	5.057E-02	10.01	1.167E-01	2.238E-03	4.472E-02
10.02	1.496E+01	1.486E+01	5.034E-02	10.02	0.000E+00	0.000E+00	0.000E+00
10.03	1.306E+01	1.296E+01	4.971E-02	10.03	0.000E+00	0.000E+00	0.000E+00
10.04	1.089E+01	1.079E+01	4.672E-02	10.04	5.100E-04	0.000E+00	5.100E-04
10.05	8.848E+00	8.758E+00	4.465E-02	10.05	1.170E-01	2.274E-03	4.643E-02
10.1	2.154E+00	2.074E+00	4.135E-02	10.1	1.131E-01	2.223E-03	4.282E-02
10.2	1.203E-01	5.402E-02	3.449E-02	10.2	1.106E-01	1.074E-03	4.133E-02
10.3	7.886E-02	2.634E-02	2.558E-02	10.3	1.036E-01	2.136E-03	3.865E-02
10.4	6.993E-02	1.753E-02	2.375E-02	10.4	1.150E-01	9.780E-04	4.441E-02
10.5	4.962E-02	8.310E-03	1.939E-02	10.5	1.150E-01	1.798E-03	4.172E-02
10.6	4.037E-02	6.169E-03	1.612E-02	10.6	1.133E-01	1.586E-03	4.292E-02
10.7	2.941E-02	3.259E-03	1.127E-02	10.7	1.196E-01	5.093E-03	4.640E-02
10.8	2.185E-02	1.155E-03	8.974E-03	10.8	1.162E-01	2.968E-03	4.169E-02
10.9	1.150E-02	5.213E-04	4.261E-03	10.9	1.187E-01	2.724E-03	4.233E-02
10.9995	0.000E+00	0.000E+00	0.000E+00	10.9995	1.297E-01	1.845E-03	4.714E-02

Table A. 6 LET Rates At Different Depths from All Particle, Helium, and Protons from a ^4He Ion accelerated to 116.5 MeV u^{-1} in a Water Phantom. “Outside” refers to LET at tumor depths not located within the tumor described of page 20.

Depth (cm)	LET (keV/um)	Depth (cm)	LET (keV/um)
	Total		All
0.001	1.675E+00	11.0005	2.028E-03
1	1.710E+00	12	1.599E-03
2	1.705E+00	13	1.851E-03
2.5	1.707E+00	14	9.990E-04
3	1.708E+00	15	1.539E-03
4	1.709E+00	16	1.092E-03
5	1.707E+00	17	1.089E-03
6	1.710E+00	18	1.101E-03
7	1.725E+00	19	8.670E-04
7.5	1.726E+00	20	8.250E-04
8	1.752E+00		
8.9995	1.859E+00		Outside
9.0005	6.663E-03	9.0005	1.853E+00
9.1	1.669E+00	9.1	2.276E-01
9.2	1.754E+00	9.2	1.736E-01
9.3	1.802E+00	9.3	1.599E-01
9.4	1.887E+00	9.4	1.596E-01
9.5	1.989E+00	9.5	1.599E-01
9.6	2.158E+00	9.6	1.665E-01
9.7	2.513E+00	9.7	1.575E-01
9.75	2.819E+00	9.75	1.437E-01
9.8	3.189E+00	9.8	1.233E-01
9.85	3.593E+00	9.85	1.005E-01
9.86	3.580E+00	9.86	9.462E-02
9.87	3.741E+00	9.87	8.379E-02
9.88	3.816E+00	9.88	7.996E-02
9.89	3.871E+00	9.89	7.170E-02
9.9	3.919E+00	9.9	6.497E-02
9.91	3.955E+00	9.91	6.322E-02
9.92	3.982E+00	9.92	5.687E-02
9.93	3.986E+00	9.93	5.194E-02
9.94	3.996E+00	9.94	4.499E-02
9.95	3.942E+00	9.95	4.142E-02
9.96	3.891E+00	9.96	3.612E-02
9.97	3.824E+00	9.97	3.211E-02
9.98	3.739E+00	9.98	3.004E-02
9.99	3.621E+00	9.99	2.517E-02
10	3.468E+00	10	2.307E-02
10.01	3.322E+00	10.01	1.803E-02
10.02	3.161E+00	10.02	0.000E+00
10.03	2.991E+00	10.03	0.000E+00
10.04	2.781E+00	10.04	4.875E-05
10.05	2.534E+00	10.05	1.159E-02
10.1	1.569E+00	10.1	5.336E-03
10.2	3.220E-01	10.2	1.493E-03
10.3	2.258E-02	10.3	1.069E-03
10.4	6.660E-04	10.4	1.834E-03
10.5	2.100E-05	10.5	1.860E-03
10.6	3.000E-06	10.6	1.215E-03
10.7	3.000E-06	10.7	1.069E-03
10.8	6.000E-06	10.8	1.103E-03
10.9	6.000E-06	10.9	1.088E-03
10.9995	0.000E+00	10.9995	1.710E-03

APPENDIX B

Particle Fluences through circular areas with 0.1 cm radius centered on an ion beam
passing through a water phantom.

Table B. 1. Particle fluences through circular 0.031416 cm² areas centered on an ion beam passing through different depths (cm) in a water phantom. Initial fluence equal to 500,000 ²⁰Ne particles, accelerated to 296 MeV/u

Depth 0.001			Depth 1			Depth 1		
Particle	Quantity	Avg. E	Particle	Quantity	Avg. E	Particle	Quantity	Avg. E
π^-	4	131.87426	π^-	56	83.766914	18O	356	277.34944
γ	327	4.2168777	β^+	1	38.43207	19O	9	275.51387
π^+	1	106.20482	(ν_μ)	3	35.961917	17F	209	274.60558
neutron	1223	171.20523	γ	4425	6.9894973	18F	1320	275.82772
1H	1330	178.48431	π^+	47	78.950066	19F	2518	278.93528
2H	165	148.48638	neutron	36166	219.41194	20F	14	275.06476
3H	51	158.14813	1H	37379	227.67321	16Ne	18	268.95392
3He	31	214.57323	2H	6892	224.21426	17Ne	116	270.94595
4He	219	221.59383	3H	1926	232.63569	18Ne	479	274.53943
6He	1	310.69763	6H	8	257.60777	19Ne	2626	277.24594
6Li	11	260.33563	3He	1947	239.86594	20Ne	468233	277.74754
7Li	5	204.36448	4He	14246	267.69005	20Na	229	276.66087
6B	1	281.77403	6He	84	262.47263			
7B	6	220.89848	8He	5	253.16278			
9B	5	116.61389	6Li	737	263.7332			
10B	1	273.76398	7Li	325	263.32515			
8Be	1	296.22098	8Li	51	263.83406			
10Be	6	181.48906	9Li	12	254.09454			
11Be	6	269.99478	6B	135	246.58209			
13Be	2	287.70699	7B	278	262.53323			
8C	1	1.5519252	9B	179	268.82017			
11C	2	271.46006	10B	113	266.50754			
12C	13	281.42152	11B	7	255.60606			
13C	9	288.30154	12B	4	257.51596			
14C	4	285.0708	14B	1	275.09281			
13N	4	216.2502	6Be	6	254.40623			
14N	15	286.1451	8Be	39	256.44898			
15N	6	291.90725	10Be	362	266.51614			
13O	1	281.91662	11Be	288	267.63686			
14O	2	288.94807	12Be	48	268.96301			
15O	5	290.44955	13Be	27	271.19864			
16O	37	292.47378	14Be	2	259.54245			
17O	3	293.38829	15Be	5	280.98838			
18O	4	288.87391	8C	8	258.81699			
17F	2	296.78657	9C	8	245.90253			
18F	19	293.55989	10C	75	261.01339			
19F	31	295.57112	11C	260	266.0496			
17Ne	1	287.70279	12C	1527	271.08301			
18Ne	8	291.40719	13C	589	272.20654			
19Ne	33	296.01685	14C	202	274.29098			
20Ne	499669	295.82058	15C	15	271.36062			
20Na	2	296.04708	16C	13	273.4366			

Depth 2			Depth 2			Depth 3			Depth 3		
Particle	Quantity	Avg. E	Particle	Quantity	Avg. E	Particle	Quantity	Avg. E	Particle	Quantity	Avg. E
π^-	37	76.6453	12O	6	243.014	π^-	23	67.0623	12O	6	227.177
β^-	1	50.3773	13O	32	243.919	μ^+	1	2.00528	13O	42	225.841
(ν_μ)	1	32.1962	14O	215	252.808	(ν_μ)	1	42.6878	14O	264	233.764
γ	4455	5.69204	15O	1073	256.163	γ	4350	5.1386	15O	1408	237.812
π^+	42	97.1058	16O	3969	259.092	π^+	13	114.128	16O	4958	241.072
neutron	41445	213.281	17O	768	258.709	neutron	41827	201.405	17O	980	241.609
1H	42112	220.164	18O	642	261.443	1H	42288	206.997	18O	898	244.319
2H	8799	218.096	19O	13	258.374	2H	9191	206.843	19O	17	243.28
3H	2516	225.161	17F	360	255.48	3H	2749	213.243	17F	511	236.554
6H	17	240.028	18F	2254	257.838	6H	15	225.128	18F	2996	239.035
3He	2677	231.405	19F	4505	261.469	3He	2800	219.705	19F	5875	243.265
4He	21457	255.896	20F	21	257.569	4He	24038	241.707	20F	25	240.259
6He	124	251.842	16Ne	38	246.485	6He	131	234.69	16Ne	52	224.503
8He	9	215.059	17Ne	198	250.277	8He	7	221.123	17Ne	264	228.489
10He	1	226.895	18Ne	890	254.839	10He	1	225.141	18Ne	1187	233.951
6Li	1019	251.027	19Ne	4796	257.834	6Li	1075	234.97	19Ne	6357	237.515
7Li	512	250.305	20Ne	435178	258.822	7Li	584	234.955	20Ne	402368	239.029
8Li	93	244.693	20Na	447	255.765	8Li	101	231.789	20Na	597	233.479
9Li	21	241.526				9Li	33	228.694	20Mg	1	236.938
11Li	2	253.202				11Li	2	249.911			
6B	188	228.906				6B	221	214.658			
7B	442	247.938				7B	507	231.345			
9B	312	252.777				9B	329	238.304			
10B	162	253.136				10B	205	237.006			
11B	14	248.544				11B	17	237.721			
12B	6	247.593				12B	6	230.895			
14B	2	252.722				14B	1	229.827			
6Be	7	242.437				6Be	7	203.583			
8Be	50	241.422				8Be	66	228.75			
10Be	567	252.874				10Be	676	237.386			
11Be	507	253.5				11Be	582	237.304			
12Be	66	253.979				12Be	83	239.13			
13Be	30	256.314				13Be	31	244.202			
14Be	5	252.679				14Be	8	242.53			
15Be	8	259.749				15Be	8	239.627			
8C	16	224.765				8C	19	211.581			
9C	10	234.839				9C	17	223.844			
10C	103	245.897				10C	119	228.621			
11C	431	249.318				11C	508	232.197			
12C	2539	255.487				12C	3087	238.979			
13C	957	257.583				13C	1149	241.103			
14C	337	259.465				14C	400	244.905			
15C	23	257.622				15C	21	248.048			
16C	23	263.563				16C	26	246.792			
17C	2	247.73				17C	2	239.195			
18C	1	253.202				18C	1	245.254			
12N	46	245.916				12N	54	227.831			
13N	385	253.268				13N	462	235.663			
14N	2172	257.12				14N	2833	239.915			
15N	1551	260.45				15N	1930	243.883			
16N	108	257.901				16N	159	241.333			
17N	124	260.976				17N	173	245.552			
18N	4	257.174				18N	4	242.74			

Depth 4			Depth 4			Depth 5			Depth 5		
Particle	Quantity	Avg. E	Particle	Quantity	Avg. E	Particle	Quantity	Avg. E	Particle	Quantity	Avg. E
π^-	(ν_μ)	68.3415	14O	288	213.917	π^-	5	74.9634	14O	314	193.099
(ν_μ)	3	39.7267	15O	1555	218.261	(ν_e) \square	2	32.5205	15O	1645	197.723
γ	4241	4.58732	16O	5366	221.892	(ν_μ)	1	32.3115	16O	5332	201.461
π^+	10	105.551	17O	1126	223.338	γ	4191	3.94466	17O	1170	204.367
neutron	40051	187.599	18O	1054	226.531	π^+	7	79.2392	18O	1145	207.871
1H	39931	192.87	19O	15	226.786	neutron	37617	171.354	19O	16	205.145
2H	8923	192.021	17F	586	216.155	1H	37463	175.892	17F	653	194.059
3H	2738	196.9	18F	3438	219.352	2H	8598	175.727	18F	3716	198.351
6H	13	204.055	19F	6891	224.084	3H	2612	179.078	19F	7665	203.766
3He	2908	200.655	20F	25	221.608	6H	16	208.423	20F	27	200.467
4He	24546	225.264	16Ne	60	198.781	3He	2851	181.863	16Ne	62	170.784
6He	135	222.43	17Ne	314	205.556	4He	24062	206.355	17Ne	323	180.946
8He	5	199.113	18Ne	1414	211.647	6He	123	203.969	18Ne	1557	187.955
10He	1	205.779	19Ne	7584	216.096	8He	9	181.657	19Ne	8375	193.227
6Li	1130	217.306	20Ne	370430	218.171	10He	2	196.157	20Ne	339722	195.987
7Li	588	219.34	20Na	731	210.475	6Li	1097	199.441	20Na	843	185.606
8Li	94	218.281	20Mg	2	210.774	7Li	549	200.746	20Mg	2	177.263
9Li	41	216.359				8Li	90	195.816			
11Li	4	228.037				9Li	36	201.227			
6B	234	199.009				11Li	1	202.286			
7B	541	214.615				6B	220	177.836			
9B	350	220.29				7B	501	196.644			
10B	192	220.991				9B	336	202.237			
11B	15	225.272				10B	183	201.657			
12B	9	212.511				11B	20	207.106			
14B	2	216.432				12B	10	197.561			
6Be	10	183.58				6Be	10	159.351			
8Be	68	208.942				8Be	67	185.692			
10Be	723	219.557				10Be	701	200.687			
11Be	591	221.317				11Be	583	203.064			
12Be	107	222.379				12Be	109	204.293			
13Be	36	228.592				13Be	32	210.36			
14Be	4	235.472				14Be	3	215.591			
15Be	7	232.547				15Be	11	207.3			
8C	19	185.954				8C	14	171.854			
9C	18	204.693				9C	11	176.231			
10C	142	209.665				10C	137	189.307			
11C	528	213.746				11C	485	195.148			
12C	3328	221.388				12C	3360	202.069			
13C	1290	223.602				13C	1249	205.09			
14C	423	228.119				14C	455	210.193			
15C	26	231.42				15C	30	213.605			
16C	24	232.034				16C	33	213.163			
17C	2	230.419				17C	1	222.575			
12N	55	208.052				12N	52	188.476			
13N	484	216.84				13N	521	196.935			
14N	3012	221.76				14N	3094	201.845			
15N	2223	226.032				15N	2339	207.385			
16N	167	223.944				16N	173	206.458			
17N	208	228.574				17N	207	211.617			
18N	2	229.608				18N	2	211.588			
12O	5	211.224				12O	8	177.159			
13O	38	203.825				13O	38	181.693			

Depth 6			Depth 6			Depth 7			Depth 7		
Particle	Quantity	Avg. E	Particle	Quantity	Avg. E	Particle	Quantity	Avg. E	Particle	Quantity	Avg. E
π^-	2	31.8709	13O	38	158.173	γ	4015	3.39185	17O	1187	160.114
μ^+	1	3.15977	14O	321	170.015	π^+	1	63.4791	18O	1227	166.335
(ν_e) \square	1	42.1207	15O	1651	175.541	neutron	32200	135.778	19O	14	159.164
(ν_μ)	1	30.6172	16O	5227	179.198	1H	31407	137.718	17F	693	145.256
γ	4117	3.61863	17O	1205	183.448	2H	7603	136.054	18F	3847	150.959
π^+	5	43.6538	18O	1197	187.895	3H	2377	138.964	19F	8330	158.511
neutron	35464	153.716	19O	13	184.972	6H	20	129.942	20F	27	152.254
1H	35014	157.152	17F	697	170.9	3He	2592	137.817	16Ne	58	106.081
2H	8222	156.337	18F	3856	175.733	4He	20845	165.166	17Ne	328	123.129
3H	2514	160.938	19F	8112	182.104	6He	125	154.735	18Ne	1719	133.087
6H	11	164.155	20F	29	176.815	8He	7	142.981	19Ne	9144	140.826
3He	2691	161.181	16Ne	58	142.797	10He	1	105.961	20Ne	280675	145.621
4He	22598	186.92	17Ne	336	154.575	6Li	971	158.016	20Na	1018	127.49
6He	115	181.984	18Ne	1644	162.231	7Li	439	158.521			
8He	11	168.088	19Ne	8901	168.399	8Li	89	156.772			
10He	1	186.31	20Ne	309621	172.049	9Li	30	160.155			
6Li	1065	179.851	20Na	931	158.406	11Li	2	182.326			
7Li	511	180.028	20Mg	2	138.961	6B	165	130.021			
8Li	95	180.034				7B	483	150.271			
9Li	34	181.345				9B	284	160.344			
11Li	3	187.084				10B	168	159.674			
6B	192	150.844				11B	20	167.785			
7B	484	174.505				12B	4	165.063			
9B	316	182.777				6Be	7	109.532			
10B	165	181.879				8Be	49	142.56			
11B	17	190.94				10Be	614	156.451			
12B	6	181.887				11Be	495	160.828			
6Be	7	136.965				12Be	97	157.686			
8Be	64	164.767				13Be	37	168.415			
10Be	663	178.958				14Be	6	186.303			
11Be	552	182.625				15Be	7	185.339			
12Be	92	184.818				8C	7	111.681			
13Be	26	199.584				9C	11	145.001			
14Be	2	220.351				10C	111	145.172			
15Be	9	194.02				11C	486	148.549			
8C	14	142.033				12C	3069	158.342			
9C	10	163.188				13C	1173	162.622			
10C	128	165.219				14C	442	171.008			
11C	483	173.893				15C	14	183.07			
12C	3297	181.16				16C	31	182.489			
13C	1240	184.262				17C	2	188.088			
14C	473	190.935				12N	57	144.5			
15C	23	191.099				13N	488	150.214			
16C	34	199.24				14N	3020	157.148			
17C	2	198.019				15N	2253	165.338			
12N	59	168.098				16N	150	167.856			
13N	492	174.871				17N	222	173.823			
14N	3102	180.562				18N	10	161.601			
15N	2371	187.237				12O	2	121.26			
16N	160	186.478				13O	44	135.472			
17N	214	193.685				14O	332	144.427			
18N	7	178.426				15O	1586	151.193			
12O	6	148.197				16O	4905	154.997			

Depth 8			Depth 8			Depth 9			Depth 9		
Particle	Quantity	Avg. E	Particle	Quantity	Avg. E	Particle	Quantity	Avg. E	Particle	Quantity	Avg. E
β^+	1	46.6443	16O	4432	127.894	γ	3800	3.01978	18O	1142	116.179
γ	3809	3.026	17O	1148	134.823	neutron	26164	89.6124	19O	11	100.726
neutron	29506	112.959	18O	1165	142.676	1H	25054	89.953	17F	633	79.5613
1H	28809	114.852	19O	13	127.584	2H	6545	88.3336	18F	3540	88.9033
2H	7130	112.795	17F	679	115.83	3H	2213	87.028	19F	8267	101.082
3H	2415	112.58	18F	3728	122.887	6H	15	80.2765	20F	18	82.6857
6H	16	130.928	19F	8409	132.203	3He	2187	85.169	16Ne	15	40.2274
3He	2402	113.948	20F	20	122.504	4He	18336	108.734	17Ne	174	49.1507
4He	19586	139.356	16Ne	41	68.8014	6He	123	95.8544	18Ne	1471	52.1858
6He	121	126.116	17Ne	326	85.6806	8He	12	78.7517	19Ne	9089	66.8755
8He	6	119.624	18Ne	1698	98.2008	6Li	793	96.6743	20Ne	225619	77.3846
10He	1	94.8939	19Ne	9176	108.694	7Li	449	92.1933	21Ne	1	50.4497
6Li	888	131.087	20Ne	252932	115.285	8Li	80	90.4343	20Na	749	53.9476
7Li	430	129.545	20Na	1080	89.2892	9Li	40	86.0655			
8Li	78	138.56	19Mg	1	96.6236	11Li	2	27.4707			
9Li	29	136.687				6B	142	74.6468			
11Li	2	178.239				7B	372	93.2681			
6B	195	101.203				9B	236	103.533			
7B	421	124.871				10B	149	99.8737			
9B	271	132.572				11B	8	130.623			
10B	146	134.3				12B	4	106.935			
11B	16	145.044				14B	1	152.247			
12B	7	122.824				6Be	9	45.0534			
14B	1	158.607				8Be	40	74.9701			
6Be	6	89.0504				10Be	504	96.4491			
8Be	50	109.059				11Be	425	100.828			
10Be	581	129.76				12Be	83	107.471			
11Be	458	134.259				13Be	34	123.414			
12Be	89	135.555				14Be	4	123.73			
13Be	35	141.376				15Be	6	136.794			
14Be	7	156.621				8C	4	43.5061			
15Be	6	161.552				9C	12	68.5443			
8C	6	90.5947				10C	100	84.3224			
9C	11	115.634				11C	353	88.9129			
10C	100	118.575				12C	2529	100.702			
11C	435	122.726				13C	955	107.978			
12C	2837	132.501				14C	369	125.588			
13C	1077	138.275				15C	15	128.933			
14C	406	149.699				16C	18	151.3			
15C	16	154.099				17C	1	87.1933			
16C	22	167.49				12N	37	80.9729			
17C	1	194.099				13N	425	88.9924			
12N	47	114.843				14N	2578	99.5509			
13N	443	123.132				15N	1954	112.154			
14N	2826	130.825				16N	129	121.914			
15N	2167	140.458				17N	206	130.302			
16N	141	146.085				18N	7	110.346			
17N	230	153.048				12O	3	59.6552			
18N	11	142.009				13O	39	70.3158			
12O	2	107.695				14O	277	79.0453			
13O	40	101.759				15O	1425	89.4314			
14O	310	114.839				16O	3950	95.5806			
15O	1518	123.34				17O	1100	104.626			

Depth 9.95995			Depth 9.95995			Depth 9.96005			Depth 9.96005		
Particle	Quantity	Avg. E	Particle	Quantity	Avg. E	Particle	Quantity	Avg. E	Particle	Quantity	Avg. E
(v_e)	1	44.5827	20O	1	12.6556	(v_e)	1	44.5827	20O	1	12.6436
□						□					
γ	3007	2.65078	17F	354	33.4034	γ	3005	2.65219	17F	354	33.3916
neutron	18570	68.0888	18F	2856	44.2005	neutron	18566	68.1046	18F	2856	44.1919
1H	16276	66.6556	19F	7921	59.828	1H	16271	66.6628	19F	7921	59.822
2H	4387	68.8387	20F	5	27.9957	2H	4383	68.8395	20F	5	27.9821
3H	1477	71.1009	17Ne	1	52.4204	3H	1477	71.1	17Ne	1	52.4139
6H	8	54.0371	18Ne	17	20.1846	6H	8	54.0366	18Ne	17	20.1565
3He	1274	71.8779	19Ne	441	8.18349	3He	1274	71.8821	19Ne	439	8.1854
4He	13528	82.9819	20Ne	155097	8.56004	4He	13526	82.9827	20Ne	154708	8.55251
6He	87	82.5311	21Ne	1	2.85245	6He	87	82.5296	21Ne	1	2.81019
8He	10	47.9883	22Ne	3	3.16358	8He	10	47.9864	22Ne	3	3.12144
6Li	524	72.9677	20Na	120	6.80396	6Li	524	72.9645	20Na	120	6.76417
7Li	251	74.4083	22Na	1	0.92131	7Li	251	74.4061	22Na	1	0.84579
8Li	46	89.8045	23Na	2	2.13631	8Li	46	89.8028	23Na	2	2.08103
9Li	19	60.1925	24Mg	3	2.80053	9Li	18	63.5324	24Mg	3	2.74101
11Li	3	24.0518	25Mg	4	2.76052	11Li	3	24.0485	25Mg	4	2.70316
6B	65	62.4438	26Al	1	1.2058	6B	65	62.4386	26Al	1	1.13402
7B	201	79.3632	27Al	3	1.23154	7B	201	79.359	27Al	3	1.18199
9B	120	84.6389	28Al	2	2.37631	9B	120	84.6355	28Al	2	2.33107
10B	91	77.5349	27Si	1	0.07364	10B	91	77.5322	27Si	1	0.0396
11B	10	93.9604	28Si	3	1.16555	11B	10	93.9587	28Si	3	1.0875
12B	4	79.7092	29Si	2	2.08152	12B	4	79.7078	29Si	2	2.01521
14B	1	146.067	30P	1	0.63277	14B	1	146.064	30P	1	0.54918
8Be	18	60.4696				8Be	18	60.4635			
10Be	303	77.4566				10Be	303	77.4523			
11Be	263	80.575				11Be	263	80.5711			
12Be	55	92.9105				12Be	55	92.9082			
13Be	23	106.459				13Be	24	105.803			
14Be	4	107.171				14Be	4	107.169			
15Be	4	85.6504				15Be	4	85.6474			
8C	1	51.8991				8C	1	51.8928			
9C	5	61.3642				9C	5	61.3595			
10C	53	62.9919				10C	53	62.9848			
11C	165	69.7845				11C	165	69.7788			
12C	1602	75.7506				12C	1602	75.7461			
13C	613	86.95				13C	613	86.9462			
14C	286	102.958				14C	286	102.955			
15C	10	120.087				15C	10	120.084			
16C	19	128.347				16C	19	128.345			
12N	25	60.7069				12N	25	60.7006			
13N	255	61.5088				13N	255	61.5032			
14N	1742	70.3464				14N	1742	70.3417			
15N	1599	81.9522				15N	1599	81.9484			
16N	102	104.816				16N	102	104.813			
17N	163	110.047				17N	163	110.045			
18N	4	92.699				18N	4	92.696			
13O	12	48.7858				13O	12	48.7785			
14O	149	42.2242				14O	149	42.2154			
15O	1054	50.2603				15O	1053	50.3004			
16O	3518	50.322				16O	3518	50.3138			
17O	894	72.7794				17O	894	72.7747			
18O	1016	87.5698				18O	1016	87.5665			
19O	6	80.599				19O	6	80.5935			

Depth 10			Depth 10			Depth 11			Depth 11		
Particle	Quantity	Avg. E	Particle	Quantity	Avg. E	Particle	Quantity	Avg. E	Particle	Quantity	Avg. E
(v_e)	1	44.5827	13O	12	45.5594	γ	1369	1.36645	17O	405	61.6639
□											
γ	2623	2.53874	14O	138	41.3449	neutron	5658	111.628	18O	608	68.9639
neutron	16826	71.7181	15O	991	50.1575	1H	4369	109.12	19O	2	92.3431
1H	14359	71.0218	16O	3135	52.359	2H	1340	112.472	17F	4	27.2814
2H	3955	73.1347	17O	871	71.9909	3H	522	109.077	18F	211	29.4115
3H	1357	75.5657	18O	1007	86.2218	6H	2	123.892	19F	2437	39.4708
6H	8	53.8651	19O	6	78.7771	3He	436	103.733	18Ne	1	46.4798
3He	1133	76.839	20O	1	6.70718	4He	4890	118.626	19Ne	9	24.3015
4He	12535	86.2251	17F	307	33.2562	6He	34	109.013			
6He	80	87.0468	18F	2636	43.8151	8He	2	35.3131			
8He	10	47.5862	19F	7675	58.8132	6Li	171	114.78			
6Li	479	76.6233	20F	4	30.9096	7Li	90	103.103			
7Li	224	78.606	17Ne	1	49.5588	8Li	16	115.348			
8Li	42	89.3157	18Ne	7	37.8441	9Li	9	99.5962			
9Li	17	66.5136	19Ne	40	21.1436	11Li	1	27.265			
11Li	3	23.1525	20Ne	28019	4.90925	6B	25	62.4217			
6B	56	67.6229	22Ne	1	3.15302	7B	75	89.9871			
7B	181	84.4048	20Na	7	6.23294	9B	51	111.647			
9B	107	88.049	24Mg	1	2.75341	10B	30	98.4993			
10B	80	81.1577				11B	6	106.132			
11B	10	93.1215				12B	1	24.8229			
12B	4	79.0767				8Be	4	77.6416			
14B	1	145.818				10Be	103	95.6542			
8Be	17	62.0919				11Be	104	99.7518			
10Be	266	82.0699				12Be	32	99.0362			
11Be	243	84.4303				13Be	11	119.94			
12Be	54	93.4198				14Be	2	145.53			
13Be	24	105.715				15Be	1	116.487			
14Be	4	106.583				9C	1	51.3423			
15Be	3	111.064				10C	13	70.8586			
8C	1	49.6367				11C	66	78.496			
9C	5	59.1236				12C	660	83.2846			
10C	50	64.489				13C	301	90.0737			
11C	152	73.2521				14C	183	98.4633			
12C	1506	77.4395				15C	4	141.427			
13C	586	88.6871				16C	15	126.979			
14C	273	105.801				12N	6	49.9405			
15C	10	118.328				13N	79	56.3937			
16C	19	127.741				14N	681	65.8927			
12N	24	60.9253				15N	760	78.7471			
13N	245	60.6954				16N	76	90.3628			
14N	1680	70.343				17N	120	93.5058			
15N	1556	81.6434				18N	1	23.1623			
16N	101	104.803				14O	13	36.2503			
17N	158	111.224				15O	198	36.2929			
18N	4	91.7202				16O	746	49.207			

Depth 12

Particle	Quantity	Avg. E
γ	1224	0.8131168
neutron	3385	126.6755
1H	2495	121.29316
2H	778	128.53074
3H	319	123.98213
6H	1	222.07176
3He	275	114.94603
4He	2892	129.85599
6He	22	118.22707
8He	1	25.292415
6Li	108	124.54926
7Li	40	119.25428
8Li	9	128.70942
9Li	4	111.96025
6B	10	52.279317
7B	41	96.257613
9B	27	120.70402
10B	15	110.78479
11B	2	118.51555
14B	1	106.1422
8Be	1	56.043785
10Be	63	90.687462
11Be	68	104.1205
12Be	22	91.669789
13Be	12	108.36917
14Be	2	135.15053
10C	5	47.706845
11C	31	72.299565
12C	353	76.750079
13C	161	87.208794
14C	128	92.451324
15C	4	90.576873
16C	9	123.59208
12N	1	52.631665
13N	21	43.598672
14N	269	59.124208
15N	382	69.771781
16N	44	77.489719
17N	82	83.915717
14O	1	27.121868
15O	5	29.978973
16O	144	33.299915
17O	146	47.082078
18O	276	56.329487
17F	1	26.826476
19F	26	14.065944

Table B. 2. Particle fluences through circular 0.031416 cm² areas centered on an ion beam passing through different depths (cm) in a water phantom. Initial fluence equal to 500,000 ¹⁶O particles, accelerated to 259 MeV/u

Depth 0.001			Depth 1			Depth 2			Depth 3		
Particle	Quantity	Avg. E	Particle	Quantity	Avg. E	Particle	Quantity	Avg. E	Particle	Quantity	Avg. E
π^-	1	26.1282	π^-	19	96.7303	π^-	μ^-	77.5447	π^-	6	69.627
γ	280	5.31275	(ν_e) \square	1	44.9821	μ^+	1	6.63738	γ	3582	4.47547
π^+	1	27.1561	γ	3544	5.07862	(ν_μ)	1	3.91084	π^+	5	82.8533
neutron	958	135.83	π^+	13	101.063	γ	3602	5.11709	neutron	29194	170.12
1H	1050	154.312	neutron	26100	184.786	π^+	6	139.019	1H	29875	176.976
2H	142	133.334	1H	27081	195.083	neutron	29405	181.657	2H	6385	174.591
3H	34	144.428	2H	5159	190.851	1H	30275	188.114	3H	2100	181.602
3He	32	139.599	3H	1504	201.443	2H	6260	184.503	6H	6	187.006
4He	182	194.77	6H	8	217.738	3H	1986	196.943	3He	2149	186.085
6He	1	222.288	3He	1517	207.673	6H	6	203.493	4He	17211	207.942
8He	1	247.958	4He	10686	230.999	3He	2042	198.406	6He	90	201.373
6Li	7	204.993	6He	68	229.801	4He	15757	221.214	8He	8	202.33
7Li	4	120.936	8He	4	215.412	6He	108	217.679	10He	1	202.073
8Li	1	224.175	6Li	546	233.606	8He	7	213.435	6Li	927	205.321
6B	2	248.894	7Li	310	233.738	6Li	856	220.422	7Li	536	206.484
7B	4	245.475	8Li	49	228.304	7Li	484	220.429	8Li	72	204.62
9B	3	247.421	9Li	17	227.119	8Li	70	218.275	9Li	26	194.962
10B	1	241.374	11Li	3	232.609	9Li	21	217.029	11Li	1	230.801
11B	1	236.461	6B	128	213.493	11Li	2	234.236	6B	185	188.408
8Be	1	273.085	7B	280	229.133	6B	185	201.198	7B	429	200.786
10Be	4	248.431	9B	159	236.429	7B	455	217.093	9B	269	208.944
11Be	12	249.683	10B	91	232.704	9B	248	222.545	10B	164	207.39
10C	1	235.51	11B	7	227.596	10B	138	221.645	11B	21	207.761
11C	3	250.274	12B	7	231.621	11B	10	219.422	12B	17	206.211
12C	27	228.221	14B	1	226.52	12B	9	216.819	6Be	7	185.141
13C	5	256.644	6Be	6	220.484	6Be	7	165.683	8Be	57	200.405
14C	1	252.918	8Be	29	226.91	8Be	44	217.083	10Be	508	205.984
13N	5	255.176	10Be	276	234.471	10Be	437	220.594	11Be	606	209.687
14N	29	245.558	11Be	353	236.099	11Be	574	223.39	12Be	157	210.641
15N	34	257.614	12Be	72	237.369	12Be	123	225.316	13Be	160	215.336
14O	6	252.605	13Be	70	240.505	13Be	124	227.955	14Be	2	209.454
15O	29	257.301	14Be	1	237.217	14Be	2	231.479	8C	11	180.732
16O	499711	258.846	8C	16	219.415	8C	14	197.604	9C	22	194.541
			9C	11	224.242	9C	22	211.864	10C	135	200.854
			10C	72	229.716	10C	123	215.708	11C	559	204.177
			11C	291	234.256	11C	478	219.518	12C	4278	209.818
			12C	2265	239.744	12C	3583	225.215	13C	1383	210.698
			13C	631	239.731	13C	1085	225.431	14C	895	214.528
			14C	375	241.714	14C	667	228.673	15C	11	213.239
			15C	6	233.912	15C	11	225.598	12N	147	199.351
			12N	69	234.787	12N	122	216.88	13N	687	204.984
			13N	337	237.476	13N	551	221.793	14N	3647	208.961
			14N	1686	240.403	14N	2891	225.004	15N	6019	213.346
			15N	2535	243.652	15N	4539	228.889	16N	15	211.693
			16N	10	239.399	16N	18	227.115	12O	35	186.398
			12O	17	228.563	12O	25	205.58	13O	234	196.246
			13O	110	234.026	13O	214	215.526	14O	1009	202.56
			14O	399	238.232	14O	759	221.15	15O	6535	207.43
			15O	2756	242.076	15O	4922	225.146	16O	410695	209.672
			16O	472142	243.236	16O	441857	226.826			

Depth 4			Depth 5			Depth 6			Depth 7		
Particle	Quantity	Avg. E	Particle	Quantity	Avg. E	Particle	Quantity	Avg. E	Particle	Quantity	Avg. E
π^-	6	112.494	π^-	1	26.5334	π^-	1	32.7534	(ν_μ)	1	36.9513
γ	3616	4.05929	γ	3408	3.7955	γ	3561	3.62828	γ	3369	3.31298
π^+	9	82.2051	π^+	1	106.983	π^+	1	48.0843	π^+	1	56.5961
neutron	28324	158.287	neutron	27005	143.401	neutron	25401	128.548	neutron	23592	111.91
1H	29097	163.772	1H	27449	149.25	1H	25902	132.671	1H	23722	116.314
2H	6413	161.14	2H	6304	144.55	2H	6001	127.869	2H	5570	112.732
3H	2096	169.056	3H	2017	152.36	3H	2028	133.706	3H	1940	114.449
6H	10	177.429	6H	16	159.959	6H	20	140.172	6H	15	115.36
3He	2159	169.397	3He	2118	152.829	3He	1966	136.882	3He	1933	114.233
4He	17224	193.411	4He	16823	176.872	4He	16062	158.806	4He	15244	138.477
6He	104	185.46	6He	115	168.054	6He	107	154.509	6He	108	131.438
8He	9	197.756	8He	7	163.037	8He	6	166.952	8He	5	143.025
6Li	949	190.791	6Li	982	172.6	6Li	857	155.903	6Li	789	133.442
7Li	532	190.817	7Li	513	173.129	7Li	475	155.3	7Li	421	136.66
8Li	67	189.009	8Li	84	171.466	8Li	76	156.292	8Li	66	130
9Li	25	186.305	9Li	33	166.878	9Li	29	152.858	9Li	20	122.005
11Li	2	209.897	11Li	1	223.819	11Li	2	178.985	11Li	4	165.425
6B	174	170.146	6B	170	151.177	6B	189	132.498	6B	168	112.008
7B	494	185.454	7B	498	167.281	7B	448	148.691	7B	422	127.978
9B	263	191.158	9B	257	176.14	9B	232	158.45	9B	242	136.117
10B	154	193.651	10B	143	178.252	10B	165	158.403	10B	164	138.514
11B	18	197.035	11B	22	183.049	11B	19	161.883	11B	22	143.442
12B	21	192.687	12B	25	182.064	12B	27	169.696	12B	25	154.375
6Be	3	135.49	6Be	4	132.889	6Be	3	139.924	6Be	5	92.5374
8Be	56	182.806	8Be	61	162.756	8Be	58	140.652	8Be	61	116.657
10Be	497	189.173	10Be	520	172.239	10Be	486	152.82	10Be	511	131.448
11Be	654	192.768	11Be	643	176.13	11Be	643	158.352	11Be	605	139.042
12Be	161	195.41	12Be	156	179.578	12Be	160	162.297	12Be	143	142.468
13Be	182	201.604	13Be	213	187.57	13Be	202	173.052	13Be	193	155.471
14Be	1	188.428	14Be	4	172.568	14Be	3	151.155	14Be	3	122.859
8C	12	164.516	8C	16	146.38	8C	15	120.058	8C	11	97.5299
9C	28	174.72	9C	22	153.169	9C	27	136.871	9C	24	107.278
10C	139	183.778	10C	137	164.75	10C	140	144.252	10C	139	120.912
11C	565	187.162	11C	604	168.375	11C	570	148.657	11C	529	126.725
12C	4466	192.999	12C	4404	175.322	12C	4234	155.883	12C	4026	134.632
13C	1449	194.825	13C	1539	177.933	13C	1519	160.28	13C	1469	140.502
14C	1030	199.586	14C	1093	184.212	14C	1129	167.288	14C	1131	149.041
15C	6	200.532	15C	7	177.523	15C	7	156.946	15C	8	138.894
12N	156	180.838	12N	154	161.831	12N	146	139.817	12N	151	116.639
13N	803	187.523	13N	857	168.409	13N	870	148.046	13N	815	125.943
14N	4046	191.843	14N	4256	173.916	14N	4308	154.269	14N	4220	132.705
15N	7042	197.094	15N	7632	179.852	15N	8052	161.208	15N	8142	141.086
16N	21	193.105	16N	22	173.759	16N	17	151.767	16N	11	132.428
12O	35	166.021	12O	37	145.483	12O	36	123.184	12O	24	89.9306
13O	279	176.393	13O	286	154.843	13O	276	130.779	13O	251	101.994
14O	1164	183.385	14O	1288	162.463	14O	1356	139.707	14O	1381	113.836
15O	7659	188.692	15O	8458	168.62	15O	9006	146.81	15O	9176	122.393
16O	380179	191.558	16O	349903	172.251	16O	319841	151.374	16O	290881	128.273

Depth 8			Depth 9			Depth 9.5005			Depth 9.4995		
Particle	Quantity	Avg. E	Particle	Quantity	Avg. E	Particle	Quantity	Avg. E	Particle	Quantity	Avg. E
γ	3336	3.20244	γ	3313	2.94548	γ	2615	2.4478	γ	2616	2.44449
neutron	20947	93.6706	neutron	18530	72.6182	neutron	12648	55.3623	neutron	12648	55.3625
1H	21100	96.839	1H	18186	75.0421	1H	11527	55.5517	1H	11526	55.5564
2H	5230	92.206	2H	4705	69.8991	2H	2916	56.7137	2H	2918	56.6762
3H	1908	92.1502	3H	1669	68.3988	3H	1026	55.0366	3H	1026	55.0356
6H	16	98.4804	6H	23	66.0137	6H	12	60.7754	6H	12	60.7751
3He	1873	90.4878	3He	1554	67.8517	3He	831	58.5707	3He	831	58.5672
4He	14201	116.015	4He	12805	87.5616	4He	8156	68.9197	4He	8156	68.9181
6He	96	113.878	6He	74	78.2283	6He	40	73.5866	6He	40	73.5853
8He	9	86.8648	8He	6	46.8235	8He	4	39.3016	8He	4	39.3008
6Li	777	109.491	6Li	691	79.8622	6Li	331	68.7816	6Li	330	68.9441
7Li	400	112.58	7Li	395	82.1668	7Li	187	70.4855	7Li	187	70.4824
8Li	75	105.295	8Li	63	69.257	8Li	30	46.908	8Li	30	46.9051
9Li	23	111.442	9Li	21	89.198	9Li	14	78.3953	9Li	14	78.3935
11Li	2	139.021	11Li	2	134.246	6B	38	46.9733	6B	38	46.9678
6B	147	84.5361	6B	129	54.8057	7B	120	60.5931	7B	120	60.5881
7B	354	103.929	7B	348	70.5869	9B	85	80.9468	9B	85	80.944
9B	211	115.739	9B	200	82.8214	10B	69	78.4565	10B	69	78.4537
10B	148	115.496	10B	117	90.4955	11B	10	72.6188	11B	10	72.616
11B	14	129.105	11B	12	94.5873	12B	9	125.959	12B	9	125.958
12B	24	135.106	12B	14	116.375	14B	1	6.02332	14B	1	6.01651
6Be	4	52.6239	6Be	4	17.8608	8Be	8	64.2495	8Be	8	64.2442
8Be	40	91.2187	8Be	39	55.6582	10Be	197	61.5836	10Be	197	61.5787
10Be	461	107.157	10Be	419	77.3236	11Be	305	74.3872	11Be	305	74.3841
11Be	558	116.795	11Be	512	88.6438	12Be	67	99.8019	12Be	67	99.8001
12Be	136	126.613	12Be	105	106.348	13Be	103	108.23	13Be	103	108.228
13Be	179	138.308	13Be	152	118.201	9C	4	34.2341	9C	4	34.2247
14Be	3	107.519	14Be	1	66.7408	10C	30	37.2816	10C	30	37.2721
8C	11	47.472	15Be	1	64.0474	11C	223	45.8453	11C	223	45.8381
9C	17	78.087	8C	6	35.793	12C	2474	47.6612	12C	2474	47.6573
10C	114	96.0373	9C	14	44.4327	13C	923	70.6738	13C	923	70.6703
11C	498	101.036	10C	106	62.0078	14C	899	83.117	14C	899	83.1144
12C	3596	110.989	11C	445	71.3223	15C	2	129.145	15C	2	129.144
13C	1433	117.869	12C	3097	82.692	16C	1	5.07886	16C	1	5.06223
14C	1102	128.78	13C	1272	92.6356	12N	19	34.9569	12N	19	34.9469
15C	9	118.499	14C	1023	106.091	13N	337	31.2181	13N	337	31.2078
12N	125	89.8387	15C	7	86.4091	14N	2990	41.8734	14N	2989	41.8722
13N	806	99.801	12N	97	57.1324	15N	7808	57.6935	15N	7808	57.6888
14N	3979	108.371	13N	702	67.721	16N	3	22.9186	16N	3	22.9013
15N	8122	118.514	14N	3830	78.6938	13O	1	35.6287	13O	1	35.6189
16N	16	106.039	15N	8103	91.8124	14O	11	14.2623	14O	11	14.2286
12O	16	52.8565	16N	15	68.1598	15O	618	7.22985	15O	617	7.21104
13O	243	68.188	12O	2	18.9816	16O	177028	9.11593	16O	176775	9.10634
14O	1394	82.4325	13O	122	42.101	17O	1	1.87574	17O	1	1.82775
15O	9256	93.7879	14O	1065	47.0308	18F	1	2.64898	18F	1	2.59928
16O	262564	101.697	15O	9188	55.9964	19F	1	3.24547	19F	1	3.20621
			16O	234298	68.3938	20F	1	3.14602	20F	1	3.10789
			17O	1	61.2063	20Ne	3	2.39246	20Ne	3	2.33738
						22Ne	2	3.27918	22Ne	2	3.23833
						22Na	2	3.09835	22Na	2	3.04667
						23Na	4	1.72638	23Na	4	1.66168
						24Na	1	0.42267	24Na	1	0.34419
						25Na	1	4.12669	25Na	1	4.08898
						23Mg	1	0.59844	23Mg	1	0.50772
						24Mg	5	1.13753	24Mg	5	1.06366
						25Mg	1	1.21481	25Mg	1	1.14403
						26Mg	4	1.51645	26Mg	4	1.45286
						24Al	1	1.62727	24Al	1	1.55143
						25Al	1	3.34657	25Al	1	3.29253
						26Al	1	1.25018	26Al	1	1.17774

Depth 10			Depth 11			Depth 12		
Particle	Quantity	Avg. E	Particle	Quantity	Avg. E	Particle	Quantity	Avg. E
γ	2212	2.32459	γ	1155	1.03057	γ	1005	0.76391
neutron	11102	59.3289	neutron	3518	93.905	neutron	2096	103.701
1H	9801	60.0386	1H	2808	93.4004	1H	1558	103.18
2H	2525	61.1317	2H	782	92.9551	2H	464	103.701
3H	909	58.2161	3H	293	93.8153	3H	166	108.885
6H	10	69.3808	6H	4	96.003	6H	3	98.4738
3He	720	63.2874	3He	259	90.859	3He	166	91.9271
4He	7195	73.9992	4He	2671	102.848	4He	1685	110.164
6He	37	78.6319	6He	19	95.2016	6He	10	107.123
8He	4	38.8432	8He	1	11.4638	6Li	65	96.9953
6Li	285	74.5996	6Li	109	90.0085	7Li	32	99.4436
7Li	163	75.9489	7Li	80	85.5289	8Li	5	89.4685
8Li	25	60.482	8Li	11	85.8277	9Li	3	120.206
9Li	14	77.2922	9Li	6	100.933	6B	2	43.7686
6B	31	48.3263	6B	7	49.233	7B	24	63.3849
7B	104	66.2888	7B	48	71.0012	9B	20	71.4675
9B	79	84.294	9B	36	90.2088	10B	21	92.1725
10B	64	82.415	10B	33	94.4589	11B	6	98.1315
11B	9	78.9425	11B	7	84.5695	12B	8	102.422
12B	9	125.07	12B	7	121.254	8Be	1	43.9986
8Be	7	68.4543	8Be	1	45.4937	10Be	34	54.5157
10Be	171	65.8899	10Be	68	57.9531	11Be	65	69.4657
11Be	294	74.8948	11Be	133	75.702	12Be	31	75.9514
12Be	65	100.252	12Be	52	83.6907	13Be	64	83.8193
13Be	102	107.874	13Be	87	94.0786	11C	12	47.0297
9C	3	39.2048	10C	2	34.1267	12C	180	42.1286
10C	25	38.0575	11C	58	39.6705	13C	199	53.2227
11C	199	46.8804	12C	598	52.2254	14C	300	63.4546
12C	2187	49.3527	13C	453	61.2947	12N	1	34.0767
13C	896	69.7531	14C	553	71.8872	13N	2	38.4043
14C	884	81.9268	12N	2	36.4435	14N	3	22.604
15C	1	124.606	13N	5	28.3492	15N	510	24.5013
12N	16	36.1027	14N	396	30.9006	15O	1	5.5495
13N	271	32.4908	15N	2907	44.625			
14N	2710	41.6531	15O	3	34.9922			
15N	7592	56.3031						
16N	2	30.4956						
13O	1	31.3935						
14O	4	25.7115						
15O	45	11.1132						
16O	32746	4.92821						
18F	1	3.00318						

Table B. 3. Particle fluences through circular 0.031416 cm² areas centered on an ion beam passing through different depths (cm) in a water phantom. Initial fluence equal to 500,000 ¹²C particles, accelerated to 219 MeV/u

Depth 0.001			Depth 1			Depth 2			Depth 3		
Particle	Quantity	Avg. E	Particle	Quantity	Avg. E	Particle	Quantity	Avg. E	Particle	Quantity	Avg. E
π^-	3	93.284	π^-	6	78.6576	π^-	3	72.6553	π^-	7	63.5093
γ	220	3.72043	(v_e) \square	1	40.3397	γ	2614	4.17677	(v_μ)	1	30.1611
neutron	651	112.384	(v_μ)	2	31.8596	π^+	2	72.9206	γ	2603	4.05864
1H	727	120.632	γ	2479	4.65	neutron	19010	144.683	π^+	1	65.5301
2H	121	96.0597	π^+	5	42.887	1H	19110	152.008	neutron	18842	135.939
3H	35	113.166	neutron	17441	148.675	2H	4400	152.705	1H	18958	141.844
3He	19	160.57	1H	17679	156.424	3H	1602	166.286	2H	4591	143.436
4He	191	165.236	2H	3639	155.403	6H	9	157.286	3H	1679	153.484
6He	1	186.922	3H	1210	169.939	3He	1640	167.249	6H	7	117.765
6Li	6	100.803	6H	7	159.473	4He	14584	187.671	3He	1702	154.069
7Li	5	205.482	3He	1334	173.911	6He	88	178.335	4He	15982	176.329
9Li	1	181.219	4He	10060	196.636	8He	12	183.475	6He	92	172.992
6B	6	212.642	6He	63	192.45	6Li	535	187.453	8He	15	177.532
7B	7	181.965	8He	10	193.316	7Li	404	187.935	6Li	547	174.34
9B	1	224.177	6Li	374	195.321	8Li	88	186.964	7Li	479	176.369
10B	9	210.96	7Li	299	199.259	9Li	140	190.203	8Li	103	172.823
8Be	1	205.038	8Li	65	192.736	6B	220	175.77	9Li	145	180.552
10Be	8	185.523	9Li	87	199.917	7B	385	184.64	6B	221	158.829
11Be	39	211.34	6B	157	185.414	9B	304	188.697	7B	432	171.121
8C	1	199.908	7B	242	197.45	10B	569	192.806	9B	340	176.125
10C	9	213.447	9B	181	198.86	11B	11	186.986	10B	741	181.384
11C	17	216.628	10B	352	201.879	6Be	6	142.53	11B	7	173.282
12C	499755	218.871	11B	3	199.276	8Be	80	181.391	6Be	8	153.536
13C	1	0.89286	6Be	6	180.97	10Be	1375	188.147	8Be	86	166.532
12N	5	218.622	8Be	60	193.147	11Be	4188	193.551	10Be	1626	175.203
			10Be	836	200.88	12Be	17	190.734	11Be	5361	180.88
			11Be	2440	205.362	8C	23	167.776	12Be	28	176.699
			12Be	16	202.279	9C	121	178.103	8C	27	156.17
			8C	11	178.851	10C	656	184.551	9C	143	161.596
			9C	96	194.719	11C	4286	189.181	10C	826	168.814
			10C	396	199.683	12C	447141	192.243	11C	5510	174.417
			11C	2468	203.217	12N	410	186.831	12C	417423	177.916
			12C	475328	205.898				13C	1	0.4593
			12N	226	201.813				12N	550	170.194
			16O	1	0.09071				12O	1	173.704

Depth 4			Depth 5			Depth 6			Depth 7		
Particle	Quantity	Avg. E	Particle	Quantity	Avg. E	Particle	Quantity	Avg. E	Particle	Quantity	Avg. E
π^-	1	94.2133	π^-	2	43.8451	γ	2641	3.43341	γ	2537	3.11508
(ν_μ)	1	54.9772	γ	2727	3.59039	neutron	15952	100.348	neutron	14911	87.5686
γ	2641	3.76662	π^+	1	23.6215	1H	15947	106.165	1H	14577	91.9693
neutron	18294	124.598	neutron	17314	114.365	2H	4121	106.355	2H	3924	90.1608
1H	18337	130.286	1H	17570	119.098	3H	1634	112.541	3H	1495	93.1553
2H	4536	131.1	2H	4376	118.41	6H	4	87.2761	6H	7	89.922
3H	1644	141.442	3H	1690	125.489	3He	1564	110.72	3He	1518	93.5641
6H	6	162.088	6H	7	136.52	4He	14670	133.384	4He	13495	115.879
3He	1671	142.096	3He	1631	126.848	6He	80	130.581	6He	71	116.559
4He	15980	163.607	4He	15598	148.904	8He	31	144.184	8He	26	134.696
6He	98	157.683	6He	103	148.938	6Li	514	130.631	6Li	474	110.067
8He	20	153.792	8He	22	157.058	7Li	422	135.04	7Li	407	116.777
6Li	571	160.573	6Li	604	145.409	8Li	75	134.218	8Li	80	118.69
7Li	456	164.098	7Li	464	149.576	9Li	151	143.208	9Li	135	130.887
8Li	98	163.423	8Li	92	148.94	6B	179	112.374	6B	137	91.1574
9Li	146	168.651	9Li	146	156.835	7B	408	123.648	7B	432	106.776
6B	191	142.989	6B	184	130.277	9B	342	134.768	9B	322	118.752
7B	458	156.431	7B	457	140.752	10B	902	142.858	10B	875	127.898
9B	361	163.391	9B	364	149.577	11B	3	133.845	11B	7	110.897
10B	840	169.171	10B	910	156.531	6Be	2	70.424	6Be	2	47.3936
11B	6	162.561	11B	6	151.188	8Be	69	111.386	8Be	57	90.8394
6Be	8	143.34	6Be	5	120.495	10Be	1821	130.31	10Be	1761	112.608
8Be	94	148.534	8Be	70	132	11Be	6902	138.617	11Be	6976	122.197
10Be	1780	161.243	10Be	1831	146.607	12Be	14	127.5	12Be	11	108.599
11Be	6088	167.71	11Be	6567	153.758	8C	26	87.77	8C	13	70.1817
12Be	25	161.892	12Be	16	146.643	9C	177	102.554	9C	154	78.4599
8C	33	134.143	8C	26	107.306	10C	1075	114.715	10C	1027	91.7944
9C	173	144.648	9C	172	124.197	11C	7097	123.136	11C	7219	102.316
10C	974	152.342	10C	1040	134.343	12C	327057	129.151	12C	297685	109.766
11C	6295	158.627	11C	6809	141.672	13C	1	0.06068	13C	1	91.3594
12C	387359	162.802	12C	357141	146.652	12N	791	111.402	12N	839	86.3616
12N	654	152.294	13C	1	0.94563	14N	1	0.14418	14N	1	0.10265
12O	1	145.483	12N	744	132.697	12O	2	69.342	15N	1	0.39285
			14N	1	0.17102				12O	1	101.271
			12O	2	111.975						

Depth 8			Depth 9			Depth 9.97995			Depth 9.98005		
Particle	Quantity	Avg. E	Particle	Quantity	Avg. E	Particle	Quantity	Avg. E	Particle	Quantity	Avg. E
π^-	1	17.6067	γ	2520	2.95233	γ	2114	2.24793	γ	2111	2.25049
γ	2641	3.14708	neutron	12075	55.2531	neutron	7740	40.6887	neutron	7736	40.7042
neutron	13738	72.3027	1H	11134	56.6554	1H	5705	43.0786	1H	5700	43.1088
1H	13088	75.2594	2H	3219	54.9804	2H	1609	46.1412	2H	1609	46.1392
2H	3679	73.2889	3H	1290	54.9856	3H	578	50.6531	3H	578	50.652
3H	1447	75.1559	6H	6	47.3007	6H	2	39.8064	6H	2	39.806
6H	10	57.7804	3He	1197	53.6211	3He	426	48.9158	3He	426	48.9115
3He	1394	75.4335	4He	10885	72.8241	4He	6784	57.6155	4He	6782	57.626
4He	12381	96.1086	6He	75	70.5464	6He	21	88.8166	6He	21	88.8152
6He	69	95.9289	8He	14	99.7176	8He	6	118.558	8He	6	118.557
8He	15	128.78	10He	1	8.82948	6Li	177	55.8675	6Li	177	55.8638
6Li	459	88.5026	6Li	443	64.6524	7Li	164	63.9638	7Li	164	63.9618
7Li	351	95.5458	7Li	322	71.6617	8Li	33	83.7351	8Li	33	83.7336
8Li	61	99.068	8Li	64	74.4097	9Li	65	97.0913	9Li	65	97.0904
9Li	112	117.33	9Li	92	98.7785	6B	10	39.9805	6B	10	39.9736
6B	129	65.9876	11Li	1	47.6634	7B	152	37.7161	7B	152	37.7112
7B	374	85.307	6B	109	41.2541	9B	161	71.5757	9B	161	71.5736
9B	284	101.663	7B	337	59.2758	10B	563	76.8437	10B	563	76.842
10B	782	111.587	9B	258	81.662	11B	1	17.371	11B	1	17.3664
11B	7	92.2735	10B	742	92.1915	8Be	3	37.8396	8Be	3	37.8325
6Be	2	46.5138	11B	5	45.9148	10Be	1020	40.2718	10Be	1020	40.2664
8Be	53	71.2509	6Be	5	33.9042	11Be	6324	54.3429	11Be	6323	54.3389
10Be	1614	92.5304	8Be	42	42.6636	10C	4	29.8726	10C	4	29.861
11Be	6933	103.764	10Be	1470	67.9178	11C	228	7.38692	11C	225	7.45951
12Be	8	83.9153	11Be	6756	82.1882	12C	177791	8.67552	12C	177569	8.66763
13Be	1	1.77859	12Be	13	54.4494	12N	67	7.29216	12N	67	7.264
8C	5	48.5696	8C	5	29.8952	14N	1	3.1859	14N	1	3.15241
9C	103	59.4193	9C	45	36.188	18F	1	1.39262	16O	1	0.06303
10C	944	64.7604	10C	583	39.0867	19F	2	1.19645	18F	1	1.3283
11C	7046	77.5145	11C	6644	45.0135	21F	1	1.46885	19F	2	1.13094
12C	268235	87.4376	12C	238551	59.4948	20Ne	3	0.74074	21F	1	1.41638
13C	2	1.02172	12N	519	40.4333	21Ne	1	0.01967	20Ne	3	0.66323
12N	749	63.2785	13N	1	0.01928	22Ne	2	1.81448	21Ne	1	0.00313
14N	1	0.4774	14N	2	5.5648	22Na	2	1.09253	22Ne	2	1.7601
15N	1	0.45416	15N	1	0.77966	23Na	2	0.13182	22Na	2	1.01995
12O	1	53.3633				24Mg	1	1.37584	23Na	2	0.06666
16O	1	1.17889							24Mg	1	1.30385

Depth 10			Depth 11			Depth 12		
Particle	Quantity	Avg. E	Particle	Quantity	Avg. E	Particle	Quantity	Avg. E
γ	1996	2.22115	γ	883	0.79225	γ	794	0.66999
neutron	7259	41.9687	neutron	1923	73.5577	neutron	1116	85.6005
1H	5249	44.7957	1H	1188	78.8264	1H	693	86.7607
2H	1507	48.176	2H	431	81.4292	2H	247	88.9245
3H	546	52.3071	3H	185	84.6869	3H	101	92.5679
6H	2	39.6618	3He	148	65.5865	3He	79	73.2295
3He	395	51.4093	4He	2480	78.8866	4He	1439	86.3789
4He	6563	58.4282	6He	9	113.578	6He	3	135.134
6He	21	88.5919	8He	4	128.496	8He	6	100.902
8He	6	118.418	6Li	59	63.7329	6Li	33	60.1909
6Li	168	57.2034	7Li	81	65.3887	7Li	41	65.0833
7Li	162	65.631	8Li	17	95.0642	8Li	11	90.2173
8Li	32	85.2103	9Li	47	91.9429	9Li	37	80.7335
9Li	65	96.7363	6B	2	31.6308	7B	4	50.7347
6B	9	42.7553	7B	31	37.8501	9B	47	58.5698
7B	147	37.8416	9B	94	66.2586	10B	214	65.1418
9B	160	71.3332	10B	363	69.0124	8Be	1	35.9892
10B	558	76.6122	10Be	214	36.4377	10Be	37	26.1235
8Be	3	36.2738	11Be	2680	48.527	11Be	1079	37.0558
10Be	985	40.5329	10C	1	24.694	11C	1	44.3646
11Be	6282	53.8375	11C	6	45.2811			
10C	3	36.1984						
11C	101	8.21058						
12C	132195	6.93789						
12N	39	5.33417						
16O	1	2.22402						
18F	1	2.92718						
19F	1	0.43362						
20Ne	2	1.40114						
22Ne	1	1.21819						
23Na	1	0.70057						

Table B. 4. Particle fluences through circular 0.031416 cm² areas centered on an ion beam passing through different depths (cm) in a water phantom. Initial fluence equal to 500,000 ⁷Li particles, accelerated to 134.5 MeV/u

Depth 0.001			Depth 1			Depth 2			Depth 3		
Particle	Quantity	Avg. E	Particle	Quantity	Avg. E	Particle	Quantity	Avg. E	Particle	Quantity	Avg. E
γ	226	4.05929	γ	2735	3.88095	γ	2654	3.76326	γ	2541	3.7765
neutron	703	69.0769	neutron	18081	90.9006	neutron	18895	88.149	neutron	18182	82.5639
1H	593	64.3018	1H	11525	86.9164	1H	11678	84.3027	1H	11219	78.6491
2H	150	74.577	2H	4374	100.237	2H	4920	96.9423	2H	4906	90.8769
3H	53	96.5119	3H	2849	113.962	3H	3054	108.205	3H	2877	100.563
3He	17	81.6274	6H	9	89.9164	6H	4	82.4142	6H	6	67.2312
4He	177	83.449	3He	1017	103.034	3He	1080	96.4971	3He	1067	88.7788
6He	20	118.494	4He	6760	116.935	4He	8045	110.146	4He	8206	102.579
6Li	23	102.758	6He	1064	125.137	6He	1664	119.165	6He	2117	112.478
7Li	499715	134.424	6Li	1044	122.13	6Li	1508	113.51	6Li	1778	104.765
6B	3	83.5761	7Li	469980	126.679	7Li	436195	118.518	7Li	401039	109.913
7B	2	0.96466	8Li	2	1.53631	6B	127	101.808	6B	133	88.9601
9B	1	0.82677	6B	85	113.158	7B	147	110.427	7B	197	99.8325
10Be	1	0.41671	7B	103	118.378	10B	2	1.13551	10Be	1	1.97962
11C	1	1.27747	8Be	1	1.59362	11Be	1	2.23314	11Be	2	1.02687
12C	1	0.01371	10Be	1	0.23986	12Be	1	1.15985	12C	1	0.03006
13C	1	0.19421	11Be	3	0.49369	13C	1	0.778	16O	1	0.53673
			8C	1	2.92481	14N	1	0.02583			
			16O	1	0.01454	15N	1	0.08353			
Depth 4			Depth 5			Depth 6			Depth 7		
Particle	Quantity	Avg. E	Particle	Quantity	Avg. E	Particle	Quantity	Avg. E	Particle	Quantity	Avg. E
γ	2425	3.40794	γ	2560	3.0825	γ	2498	3.17282	γ	2376	2.91073
neutron	17036	76.3164	neutron	15516	69.6298	neutron	14155	61.5856	neutron	12550	52.8655
1H	10274	71.7303	1H	9345	64.7198	1H	8326	57.0939	1H	7184	49.3661
2H	4435	84.1736	2H	4262	75.0768	2H	3797	66.6728	2H	3357	56.9141
3H	2667	91.356	3H	2410	82.5067	3H	2199	73.0224	3H	1987	63.1345
6H	7	91.2281	6H	5	76.3265	6H	1	10.7101	6H	4	53.5429
3He	1069	80.2371	3He	971	72.1474	3He	924	62.3401	3He	835	51.9415
4He	7881	93.8818	4He	7405	85.033	4He	6662	74.5834	4He	6131	63.6303
6He	2395	104.984	6He	2461	97.5944	6He	2409	89.6728	6He	2251	80.4972
6Li	1840	94.882	6Li	1908	84.4851	6Li	1881	72.8782	6Li	1760	59.685
7Li	365726	100.786	7Li	330492	91.0022	7Li	295928	80.3472	7Li	261909	68.482
8Li	1	0.06802	8Li	4	3.92436	8Li	1	0.93546	6B	110	43.2069
6B	162	77.3452	9Li	3	5.01737	6B	130	56.8346	7B	146	50.1947
7B	202	86.278	6B	129	66.4332	7B	178	57.4861	9B	3	2.66264
9B	3	1.33976	7B	193	73.1406	8Be	1	3.4403	10Be	3	3.00874
11Be	1	1.49836	10B	1	10.6633	11Be	1	3.23689	12C	5	1.50615
12Be	1	1.91444	10Be	1	0.29196	11C	3	1.65701	14C	1	0.85947
10C	1	0.13417	11Be	1	0.01476	12C	3	0.46009	16N	1	0.0748
11C	1	3.00395	10C	1	2.90418	13N	1	0.5604			
13C	1	0.46985	12C	2	1.69276	14N	2	1.42753			
14N	2	0.77402	15N	1	1.1467	15N	1	1.03486			
			16N	1	0.32328	14O	1	0.3808			
			14O	1	1.08127						

Depth 8			Depth 9			Depth 9.97995			Depth 9.98005		
Particle	Quantity	Avg. E	Particle	Quantity	Avg. E	Particle	Quantity	Avg. E	Particle	Quantity	Avg. E
γ	2359	2.85341	γ	2142	2.54058	γ	1530	1.52286	γ	1529	1.52385
neutron	10579	44.0386	neutron	7990	34.254	neutron	3685	31.0568	neutron	3683	31.0622
1H	5894	40.2688	1H	4225	30.2982	1H	982	26.4469	1H	979	26.5161
2H	2812	46.742	2H	2127	36.5065	2H	814	35.371	2H	814	35.3692
3H	1657	52.2155	3H	1433	41.0312	3H	1179	29.6839	3H	1179	29.6829
6H	2	35.5518	6H	4	19.7873	3He	222	14.4789	3He	222	14.4714
3He	698	40.9534	3He	521	29.1487	4He	3018	21.2178	4He	3019	21.2079
4He	5491	51.0999	4He	4743	36.2336	6He	1778	44.8348	6He	1778	44.8337
6He	2200	69.9316	6He	2052	58.0378	6Li	24	3.57274	6Li	24	3.55335
6Li	1591	44.0781	8He	1	14.1823	7Li	137710	6.42389	7Li	137569	6.42022
7Li	228683	54.7384	6Li	1239	27.0495	7B	12	4.6236	7B	12	4.59792
8Li	2	9.11653	7Li	196265	37.4308						
6B	77	34.0601	8Li	2	20.6862						
7B	142	37.3381	6B	48	22.5139						
9B	1	1.88944	7B	105	23.26						
10Be	2	1.73275	9B	6	4.459						
11Be	2	1.12069	10B	1	3.53795						
11C	2	2.72141	10Be	1	1.16305						
12C	2	0.86357	11Be	3	1.91134						
14C	1	0.67342	11C	2	2.29568						
14N	2	0.7402	12C	7	1.27269						
			13C	5	1.3322						
			14C	1	2.67546						
			14N	1	2.6082						
			15O	1	2.99246						
			16O	2	0.56613						
Depth 10			Depth 11			Depth 12					
Particle	Quantity	Avg. E	Particle	Quantity	Avg. E	Particle	Quantity	Avg. E			
γ	1503	1.50845	(ν_{μ})	1	43.5081	γ	856	0.3931			
neutron	3474	31.9521	γ	853	0.53905	neutron	628	56.0333			
1H	869	28.0431	neutron	1053	51.945	1H	62	47.2276			
2H	774	36.1879	1H	149	42.3274	2H	125	52.2715			
3H	1152	29.5797	2H	223	47.7496	3H	150	47.9768			
3He	192	14.7808	3H	314	43.0667	3He	2	37.9898			
4He	2850	21.4494	3He	9	28.1836	4He	149	28.9572			
6He	1766	44.6303	4He	434	29.0063	6He	534	44.6651			
6Li	9	2.26715	6He	985	44.2283						
7Li	110774	5.48874									
7B	7	3.64249									

Table B. 5. Particle fluences through circular 0.031416 cm² areas centered on an ion beam passing through different depths (cm) in a water phantom. Initial fluence equal to 500,000 ⁴He particles, accelerated to 116.5 MeV/u

Depth 0.001			Depth 1			Depth 2			Depth 3		
Particle	Quantity	Avg. E	Particle	Quantity	Avg. E	Particle	Quantity	Avg. E	Particle	Quantity	Avg. E
γ	78	2.89193	γ	627	3.56461	γ	705	3.74207	γ	741	3.51887
neutron	206	50.9826	neutron	3246	68.1052	neutron	3477	64.9305	neutron	3521	60.0117
1H	222	53.6906	1H	3690	78.0367	1H	4075	74.69	1H	4058	68.4897
2H	43	64.0733	2H	986	83.2899	2H	1115	78.7412	2H	1188	72.2781
3H	16	86.1455	3H	495	95.5501	3H	593	89.4178	3H	576	85.1567
3He	34	89.7427	3He	1127	98.3083	3He	1324	92.6248	3He	1406	83.6628
4He	499887	116.427	4He	484666	109.749	4He	461265	102.705	4He	433350	95.2814
7B	1	0.63589	7Li	2	1.50295	6Li	4	4.26602	6Li	1	2.56569
9B	1	2.13155	11Be	1	0.13515	11Be	3	1.05126	12C	2	0.94321
10B	1	0.62448	12C	2	0.4825	14C	1	0.04448	14O	1	0.27251
Depth 4			Depth 5			Depth 6			Depth 7		
Particle	Quantity	Avg. E	Particle	Quantity	Avg. E	Particle	Quantity	Avg. E	Particle	Quantity	Avg. E
γ	812	3.55834	γ	783	3.01923	γ	860	3.16213	γ	842	2.91067
neutron	3291	55.9019	neutron	3227	48.7774	neutron	2976	43.1605	neutron	2632	37.4621
1H	3748	62.9662	1H	3567	56.7624	1H	3256	49.5098	1H	2857	42.2432
2H	1119	65.5722	2H	1109	57.7297	2H	1022	50.4015	2H	857	42.1717
3H	576	78.4619	3H	553	69.9262	3H	497	60.6939	3H	479	52.1308
3He	1460	76.69	3He	1459	66.963	3He	1445	57.772	3He	1336	46.6937
4He	402196	87.3928	4He	368219	78.9301	4He	332708	69.7022	4He	295383	59.4132
7B	2	1.65938	6He	1	6.40299	6He	1	0.80681	6Li	2	1.58895
12Be	1	0.01117	6Li	2	1.58905	6Li	3	2.79365	7Li	2	1.88758
9C	1	0.39919	8Li	1	1.2451	12C	2	1.72677	7B	1	2.30758
11C	2	2.05155	9B	1	1.57251				11C	1	1.65534
14N	1	1.4043	11Be	2	0.60491				12C	4	1.33264
15N	1	0.89284	12C	1	0.0137				13N	1	1.19802
16O	1	0.10065	13N	1	0.19521						
			15O	1	0.05529						
Depth 8			Depth 9			Depth 9.95995			Depth 9.96005		
Particle	Quantity	Avg. E	Particle	Quantity	Avg. E	Particle	Quantity	Avg. E	Particle	Quantity	Avg. E
γ	895	3.27782	γ	902	3.00764	γ	735	2.37825	γ	736	2.39291
neutron	2223	29.8328	neutron	1817	23.8202	neutron	875	20.1754	neutron	873	20.1721
1H	2328	34.1706	1H	1776	25.8484	1H	657	19.6687	1H	657	19.6638
2H	786	32.4821	2H	485	23.5161	2H	111	25.3527	2H	111	25.3505
3H	473	41.1259	3H	388	31.2552	3H	150	29.528	3H	150	29.527
3He	1257	34.8531	3He	1003	20.8701	3He	128	8.72179	3He	128	8.71285
4He	257203	47.4726	4He	218638	32.3957	4He	150982	6.68648	4He	150870	6.68372
6Li	4	2.11331	7Li	1	4.30903	15N	1	0.42269	15N	1	0.34528
7Li	1	1.76284	12C	3	0.06372				16O	1	0.44212
11Be	1	1.29883	13C	1	0.00325						
12C	4	0.68988	14N	1	0.79924						
15O	2	0.44246	15O	1	0.35852						
16O	1	0.48201									
Depth 10			Depth 11			Depth 12					
Particle	Quantity	Avg. E	Particle	Quantity	Avg. E	Particle	Quantity	Avg. E			
γ	640	2.342	γ	312	0.52834	γ	325	0.32433			
neutron	784	21.444	neutron	225	34.026	neutron	123	39.7748			
1H	553	20.0098	1H	36	36.2405	1H	15	41.1353			
2H	100	26.4636	2H	32	36.3168	2H	18	36.951			
3H	146	29.2657	3H	42	37.752	3H	20	45.5799			
3He	88	7.92959	4He	1	13.9922						
4He	104300	5.32309									

Table B. 6. Particle fluences through circular 0.031416 cm² areas centered on an ion beam passing through different depths (cm) in a water phantom. Initial fluence equal to 500,000 ¹H particles, accelerated to 116.5 MeV/u

Depth 0.001			Depth 1			Depth 2			Depth 3		
Particle	Quantity	Avg. E	Particle	Quantity	Avg. E	Particle	Quantity	Avg. E	Particle	Quantity	Avg. E
γ	19	1.6219	γ	129	2.94444	γ	137	2.70888	γ	142	2.94905
neutron	42	34.1267	neutron	343	55.5073	neutron	378	51.3379	neutron	360	47.3619
1H	499952	116.42	1H	481775	109.69	1H	446921	102.642	1H	401774	95.2207
4He	1	0.76243	2H	1	5.40937	15N	1	0.03357	2H	1	4.84406
			4He	3	1.77182				4He	2	1.47517
			6Li	1	0.02574				15N	1	0.01377
Depth 4			Depth 5			Depth 6			Depth 7		
Particle	Quantity	Avg. E	Particle	Quantity	Avg. E	Particle	Quantity	Avg. E	Particle	Quantity	Avg. E
γ	115	2.84854	γ	162	2.53923	γ	142	2.82928	γ	153	2.71908
neutron	332	44.3303	neutron	324	38.3148	neutron	304	30.2179	neutron	266	29.4944
1H	350296	87.3486	1H	295218	78.8971	1H	239807	69.6748	1H	187944	59.4011
4He	2	2.53954	2H	1	11.3254	2H	1	2.13658			
			4He	1	1.27539	4He	2	0.33511			
Depth 8			Depth 9			Depth 9.945			Depth 9.95995		
Particle	Quantity	Avg. E	Particle	Quantity	Avg. E	Particle	Quantity	Avg. E	Particle	Quantity	Avg. E
γ	140	2.53473	γ	133	2.67154	γ	133	2.11816	γ	132	2.09946
neutron	246	23.4082	neutron	202	16.9858	neutron	118	10.9382	neutron	118	10.9382
1H	143569	47.4799	1H	107048	32.4412	1H	61217	9.26588	1H	61190	9.26311
15O	1	0.00066	2H	1	6.04257	4He	1	0.26481	4He	1	0.13389
16O	2	0.00289	4He	1	3.58155						
			16O	1	0.01069						
Depth 10			Depth 11			Depth 12					
Particle	Quantity	Avg. E	Particle	Quantity	Avg. E	Particle	Quantity	Avg. E			
γ	122	1.66868	γ	58	0.44056	γ	61	0.19422			
neutron	92	11.4905	neutron	18	13.9455	neutron	11	24.2174			
1H	43932	7.83985									

APPENDIX C

Particle Fluences through torus areas with 0.1 cm inner radius and 1 cm outer radius
centered on an ion beam passing through a water phantom.

Table C. 1. Particle fluences through torus 3.11 cm^2 areas centered on an ion beam passing through different depths (cm) in a water phantom. Initial fluence equal to $500,000 \text{ }^{20}\text{Ne}$ ions accelerated to 296 MeV/u .

Depth 0.001			Depth 1			Depth 1		
Particle	Quantity	Avg. E	Particle	Quantity	Avg. E	Particle	Quantity	Avg. E
γ	31	7.44802	π^-	288	85.2249	17N	3	272.065
π^+	1	51.0663	μ^+	2	1.92107	18N	1	280.378
neutron	43	65.3295	$(\nu_e) \square$	7	36.8646	13O	1	268.532
1H	40	92.6259	β^+	5	40.9007	14O	18	267.183
2H	2	43.961	β^-	2	23.0605	15O	70	272.853
3H	1	238.086	(ν_μ)	22	33.3752	16O	257	276.576
3He	1	7.46452	γ	25336	5.62842	17O	26	274.5
4He	3	92.4024	π^+	243	102.28	18O	20	276.246
20Ne	21	295.822	neutron	79326	155.554	17F	20	273.178
			1H	76317	177.8	18F	83	273.499
			2H	7506	159.091	19F	109	277.691
			3H	1218	180.153	20F	2	278.917
			6H	3	265.11	17Ne	7	268.104
			3He	1069	202.468	18Ne	26	273.58
			4He	3730	264.269	19Ne	118	275.179
			6He	23	245.778	20Ne	2384	277.66
			8He	2	260.636	20Na	15	275.444
			6Li	166	262.489			
			7Li	70	263.862			
			8Li	18	267.867			
			9Li	6	248.489			
			6B	47	244.797			
			7B	66	262.32			
			9B	38	269.346			
			10B	29	263.038			
			11B	1	270.064			
			6Be	1	262.139			
			8Be	10	262.622			
			10Be	72	266.442			
			11Be	50	264.919			
			12Be	10	263.989			
			13Be	2	285.062			
			14Be	2	264.505			
			15Be	2	270.127			
			8C	4	260.548			
			9C	1	242.951			
			10C	12	262.433			
			11C	62	266.631			
			12C	215	271.715			
			13C	88	272.514			
			14C	19	269.471			
			16C	1	279.257			
			12N	4	267.721			
			13N	45	269.913			
			14N	155	271.444			
			15N	93	273.645			
			16N	9	270.131			

Depth 2			Depth 2			Depth 3			Depth 3		
Particle	Quantity	Avg. E	Particle	Quantity	Avg. E	Particle	Quantity	Avg. E	Particle	Quantity	Avg. E
π^-	333	79.6527	13N	136	253.663	π^-	262	80.1993	13N	301	236.269
μ^+	2	4.15351	14N	612	256.971	μ^+	3	4.84539	14N	1312	241.328
(ν_e) \square	24	33.8665	15N	370	261.452	(ν_e) \square	21	40.3252	15N	827	245.776
β^+	13	34.9861	16N	29	258.787	β^+	11	37.4041	16N	52	243.19
β^-	1	52.9772	17N	22	257.831	β^-	1	51.7422	17N	43	244.95
μ^-	2	3.99957	18N	4	261.984	(ν_μ)	50	31.9946	18N	5	251.866
(ν_μ)	36	32.9017	12O	2	240.026	γ	53157	4.12749	12O	5	214.211
γ	41544	4.97639	13O	5	247.185	π^+	272	102.472	13O	18	226.078
π^+	285	103.16	14O	64	249.349	neutron	204621	178.69	14O	135	231.667
neutron	152824	173.254	15O	286	255.935	1H	199449	194.912	15O	592	237.584
1H	148652	192.342	16O	997	259.777	2H	26776	188.582	16O	2142	242.584
2H	17520	181.141	17O	133	258.503	3H	5688	206.85	17O	314	242.068
3H	3303	202.781	18O	101	260.716	6H	28	198.77	18O	201	245.778
6H	12	193.497	19O	2	264.066	3He	5878	211.667	19O	8	242.49
3He	3295	213.935	17F	66	256.147	4He	28574	249.33	17F	134	236.254
4He	14129	258.423	18F	382	256.945	6He	162	245.937	18F	852	238.423
6He	86	249.937	19F	468	260.693	8He	16	238.782	19F	1031	242.798
8He	9	250.106	20F	7	260.702	6Li	1386	244.591	20F	10	244.705
6Li	691	255.039	16Ne	4	253.301	7Li	602	244.442	16Ne	13	224.585
7Li	311	254.415	17Ne	31	246.113	8Li	108	244.243	17Ne	59	224.024
8Li	49	254.023	18Ne	111	252.388	9Li	31	238.898	18Ne	233	230.708
9Li	18	249.843	19Ne	440	255.874	6B	299	219.381	19Ne	935	235.342
6B	160	233.12	20Ne	7445	258.705	7B	553	236.315	20Ne	14166	238.898
7B	276	249.204	20Na	48	253.318	9B	306	247.06	20Na	92	230.709
9B	138	260.781				10B	188	246.602			
10B	95	257.035				11B	12	243.62			
11B	4	257.353				12B	8	250.698			
12B	5	258.4				14B	1	266.218			
6Be	6	241.235				6Be	14	220.046			
8Be	39	243.558				8Be	69	226.027			
10Be	258	253.927				10Be	540	240.498			
11Be	201	255.552				11Be	489	242.321			
12Be	39	254.81				12Be	78	244.589			
13Be	13	265.917				13Be	26	252.519			
14Be	3	259.041				14Be	5	244.856			
15Be	3	263.75				15Be	7	257.109			
8C	10	243.383				8C	15	209.447			
9C	8	236.71				9C	16	222.141			
10C	67	245.148				10C	124	229.065			
11C	198	250.877				11C	405	235.946			
12C	893	256.925				12C	1913	242.577			
13C	330	258.616				13C	711	244.821			
14C	94	259.692				14C	212	246.334			
15C	4	255.519				15C	13	239.597			
16C	2	267.285				16C	8	255.647			
17C	1	271.318				17C	1	263.273			
12N	18	247.441				12N	45	228.332			

Depth 4			Depth 4			Depth 5			Depth 5		
Particle	Quantity	Avg. E	Particle	Quantity	Avg. E	Particle	Quantity	Avg. E	Particle	Quantity	Avg. E
π^-	200	81.4394	17C	1	255.254	π^-	144	73.4526	17C	2	233.774
μ^+	2	5.36506	18C	1	236.963	$(\nu_e) \square$	13	39.3455	18C	1	228.819
$(\nu_e) \square$	18	38.4205	12N	73	211.034	β^+	14	35.6548	12N	109	191.131
β^+	10	34.5669	13N	482	219.232	β^-	3	38.943	13N	680	200.91
β^-	2	28.6965	14N	2325	224.79	μ^-	2	4.54741	14N	3445	206.821
(ν_μ)	46	35.0979	15N	1373	229.468	(ν_μ)	30	32.6629	15N	2029	212.38
γ	64329	3.35424	16N	107	227.445	γ	74898	2.71573	16N	156	211.569
π^+	173	106.035	17N	79	232.389	π^+	135	98.3492	17N	129	216.127
neutron	242486	178.194	18N	5	239.551	neutron	269700	174.812	18N	8	215.85
1H	236259	191.946	12O	7	191.578	1H	262395	185.836	12O	8	171.136
2H	35290	189.112	13O	37	207.773	2H	42732	185.323	13O	51	184.999
3H	8116	205.339	14O	232	212.204	3H	10482	199.492	14O	319	191.435
6H	32	209.995	15O	992	218.925	6H	40	199.239	15O	1438	198.738
3He	8373	205.979	16O	3574	224.632	3He	10895	197.323	16O	5218	205.576
4He	44354	239.456	17O	551	224.934	4He	60988	228.215	17O	830	206.461
6He	252	236.19	18O	340	228.685	6He	352	226.279	18O	516	211.323
8He	23	230.752	19O	13	228.157	8He	28	223.108	19O	20	212.965
10He	2	203.68	17F	247	215.287	10He	3	186.865	17F	350	194.108
6Li	2020	232.592	18F	1434	219.018	6Li	2732	219.551	18F	2084	198.399
7Li	938	233.299	19F	1689	224.148	7Li	1308	220.542	19F	2425	204.401
8Li	161	232.113	20F	17	225.779	8Li	220	220.419	20F	27	204.539
9Li	52	227.536	16Ne	19	195.953	9Li	74	217.527	16Ne	22	166.013
11Li	1	242.05	17Ne	96	200.569	11Li	3	241.805	17Ne	156	176.075
6B	479	203.142	18Ne	406	208.529	6B	648	188.829	18Ne	609	184.351
7B	854	222.553	19Ne	1558	213.611	7B	1211	207.081	19Ne	2338	190.538
9B	470	235.164	20Ne	21793	218.024	9B	664	221.171	20Ne	29548	195.824
10B	281	235.876	20Na	152	206.246	10B	400	222.413	20Na	220	179.925
11B	19	236.792				11B	27	221.863			
12B	13	234.652				12B	20	222.626			
14B	1	261.746				14B	3	226.732			
6Be	19	202.731				6Be	31	176.231			
8Be	109	212.844				8Be	150	197.209			
10Be	886	226.605				10Be	1260	211.31			
11Be	809	228.847				11Be	1126	214.914			
12Be	128	230.886				12Be	191	216.085			
13Be	40	238.245				13Be	61	222.247			
14Be	9	234.868				14Be	12	224.657			
15Be	11	239.561				15Be	14	230.164			
8C	24	188.058				8C	14	162.061			
9C	29	207.336				9C	49	187.405			
10C	199	212.327				10C	280	195.078			
11C	683	218.616				11C	996	202.106			
12C	3156	227.023				12C	4587	210.613			
13C	1131	230.261				13C	1702	214.275			
14C	358	233.661				14C	494	218.347			
15C	18	231.213				15C	23	215.439			
16C	17	239.677				16C	20	226.816			

Depth 6			Depth 6			Depth 7			Depth 7		
Particle	Quantity	Avg. E	Particle	Quantity	Avg. E	Particle	Quantity	Avg. E	Particle	Quantity	Avg. E
π^-	99	71.6394	12N	141	170.696	π^-	68	65.3744	17C	2	215.948
(ν_e) \square	15	33.2057	13N	931	181.032	(ν_e) \square	14	35.799	12N	184	147.636
β^+	11	30.4844	14N	4529	187.832	β^+	9	31.032	13N	1161	159.56
β^-	2	36.4325	15N	2720	194.249	β^-	3	36.2537	14N	5720	167.093
(ν_μ)	34	31.6143	16N	209	195.062	μ^-	2	40.4059	15N	3422	174.674
γ	85948	2.26251	17N	172	199.791	(ν_μ)	26	33.4836	16N	258	176.025
π^+	87	104.433	18N	11	193.061	γ	96549	1.92972	17N	219	182.132
neutron	292391	168.021	12O	12	142.405	π^+	72	95.4136	18N	11	175.906
1H	282105	177.115	13O	76	160.934	neutron	308265	159.527	12O	18	113.277
2H	49327	178.967	14O	433	168.725	1H	294383	166.677	13O	99	133.808
3H	12864	189.953	15O	1919	177.493	2H	55218	169.94	14O	538	143.318
6H	54	204.928	16O	6829	185.185	3H	15132	179.097	15O	2484	153.424
3He	13494	185.871	17O	1109	186.928	6H	65	188.902	16O	8478	162.824
4He	78171	215.492	18O	704	192.526	3He	15779	173.13	17O	1409	165.6
6He	440	214.466	19O	30	191.99	4He	95377	201.943	18O	863	172.752
8He	40	204.344	17F	466	170.469	6He	534	201.197	19O	31	174.957
10He	4	189.198	18F	2808	176.191	8He	50	193.546	17F	631	144.538
6Li	3392	205.447	19F	3224	183.075	10He	5	186.724	18F	3547	151.754
7Li	1639	207.169	20F	35	184.867	6Li	4076	189.436	19F	4076	159.958
8Li	260	209.593	16Ne	41	134.728	7Li	1946	192.17	20F	40	162.407
9Li	88	206.079	17Ne	213	146.702	8Li	325	195.222	16Ne	52	97.6095
11Li	6	217.897	18Ne	822	157.577	9Li	111	189.165	17Ne	280	114.589
6B	835	171.732	19Ne	3200	165.423	11Li	8	205.445	18Ne	1029	127.669
7B	1552	191.342	20Ne	37638	171.872	6B	1013	153	19Ne	4149	137.493
9B	866	206.107	20Na	297	151.995	7B	1896	173.729	20Ne	45777	145.425
10B	527	207.82				9B	1064	190.954	20Na	392	118.831
11B	46	205.481				10B	630	193.158	20Mg	1	81.4235
12B	29	202.254				11B	57	189.502			
14B	3	221.855				12B	34	190.865			
6Be	43	145.81				14B	3	201.696			
8Be	192	178.011				6Be	45	120.479			
10Be	1662	195.231				8Be	233	159.393			
11Be	1455	199.923				10Be	2027	177.362			
12Be	254	201.217				11Be	1825	182.796			
13Be	79	207.813				12Be	318	184.858			
14Be	14	209.848				13Be	100	193.264			
15Be	18	215.761				14Be	12	201.504			
8C	49	140.653				15Be	22	191.917			
9C	68	164.054				8C	57	117.585			
10C	354	175.286				9C	88	139.851			
11C	1269	183.871				10C	427	155.081			
12C	6128	192.839				11C	1612	163.26			
13C	2266	196.862				12C	7699	173.439			
14C	643	202.819				13C	2794	178.621			
15C	36	203.955				14C	805	185.825			
16C	26	211.1				15C	53	182.197			
17C	2	224.994				16C	34	196.54			

Depth 8			Depth 8			Depth 9			Depth 9		
Particle	Quantity	Avg. E	Particle	Quantity	Avg. E	Particle	Quantity	Avg. E	Particle	Quantity	Avg. E
π^-	44	66.8644	12N	227	122.057	π^-	31	67.782	13N	1683	106.175
(ν_e) \square	13	36.8656	13N	1435	134.782	(ν_e) \square	12	36.6955	14N	8314	116.549
β^+	7	40.4583	14N	6954	143.821	β^+	5	35.8123	15N	4867	128.157
β^-	2	39.6192	15N	4131	153.099	(ν_μ)	17	36.8329	16N	350	132.023
(ν_μ)	23	32.6294	16N	303	155.674	γ	116081	1.50964	17N	291	142.485
γ	106140	1.70096	17N	253	163.664	π^+	43	98.1729	18N	21	132.175
π^+	48	107.706	18N	15	153.785	neutron	324653	136.542	12O	12	50.136
neutron	318896	149.067	12O	20	74.554	1H	297466	139.993	13O	134	70.9504
1H	299575	154.122	13O	129	104.019	2H	63670	144.724	14O	774	80.1179
2H	60165	158.21	14O	653	115.183	3H	19198	150.943	15O	3586	95.3116
3H	17132	166.785	15O	3044	126.829	6H	106	143.767	16O	11565	108.909
6H	83	164.037	16O	10105	137.977	3He	19797	140.974	17O	1979	114.337
3He	17952	158.074	17O	1703	141.572	4He	129193	168.502	18O	1237	124.524
4He	111989	186.686	18O	1054	150.593	6He	741	165.971	19O	37	127.479
6He	617	186.666	19O	35	153.92	8He	58	175.834	17F	912	77.9784
8He	57	183.447	17F	758	114.756	10He	7	162.268	18F	5191	90.5566
10He	7	164.519	18F	4333	124.058	6Li	5516	150.81	19F	5994	103.241
6Li	4740	172.593	19F	5001	133.772	7Li	2621	155.275	20F	61	107.382
7Li	2236	176.441	20F	52	137.255	8Li	459	154.618	16Ne	6	23.6361
8Li	377	178.369	16Ne	38	59.5609	9Li	158	157.212	17Ne	174	41.828
9Li	135	172.337	17Ne	326	73.2998	11Li	9	172.262	18Ne	1223	45.9365
11Li	10	184.599	18Ne	1291	91.1231	6B	1252	110.54	19Ne	5993	61.1447
6B	1127	133.124	19Ne	5108	104.643	7B	2607	131.382	20Ne	60519	77.095
7B	2258	154.573	20Ne	53332	115.063	9B	1493	150.116	20Na	319	47.5085
9B	1279	172.27	20Na	506	77.6575	10B	877	156.197			
10B	743	176.867				11B	84	156.193			
11B	69	175.285				12B	46	157.5			
12B	35	182.87				14B	3	190.812			
14B	3	196.35				6Be	45	63.5269			
6Be	47	92.0853				8Be	330	107.753			
8Be	273	137.479				10Be	2918	133.786			
10Be	2418	157.54				11Be	2606	142.081			
11Be	2205	163.511				12Be	460	146.729			
12Be	389	167.304				13Be	156	153.558			
13Be	127	174.116				14Be	20	165.729			
14Be	13	194.667				15Be	29	156.856			
15Be	26	174.535				8C	54	63.2193			
8C	58	91.9275				9C	114	88.5951			
9C	104	115.255				10C	593	102.875			
10C	518	130.95				11C	2338	114.374			
11C	1964	140.663				12C	11009	127.519			
12C	9320	152.245				13C	4014	134.942			
13C	3368	158.423				14C	1128	145.357			
14C	967	166.186				15C	62	144.74			
15C	55	168.055				16C	56	155.817			
16C	52	173.258				17C	5	169.399			
17C	4	176.642				12N	277	91.6991			

Depth 9.95995			Depth 9.95995			Depth 9.96005			Depth 9.96005		
Particle	Quantity	Avg. E	Particle	Quantity	Avg. E	Particle	Quantity	Avg. E	Particle	Quantity	Avg. E
π^-	21	75.4553	12N	254	65.9091	π^-	21	75.4549	12N	254	65.9035
(ν_e)						(ν_e)					
\square	9	40.9159	13N	1766	73.8099	\square	9	40.9159	13N	1766	73.8053
β^+	7	35.1842	14N	9220	85.8103	β^+	7	35.1842	14N	9220	85.8065
β^-	1	42.9146	15N	5467	99.4514	β^-	1	42.9146	15N	5467	99.4485
(ν_μ)	18	37.0721	16N	381	106.164	(ν_μ)	18	37.0721	16N	381	106.161
γ	122342	1.35042	17N	349	116.476	γ	122340	1.3503	17N	349	116.474
π^+	30	89.2203	18N	28	97.5783	π^+	30	89.22	18N	28	97.5754
neutron	325424	122.456	12O	3	32.8311	neutron	325414	122.457	12O	3	32.82
1H	281495	126.269	13O	59	52.6562	1H	281491	126.268	13O	59	52.6481
2H	65233	130.573	14O	570	47.5925	2H	65236	130.57	14O	570	47.5838
3H	20591	134.666	15O	3565	58.9243	3H	20591	134.666	15O	3564	58.9348
6H	123	126.497	16O	12432	73.8038	6H	123	126.497	16O	12432	73.7992
3He	20186	125.862	17O	2236	81.5383	3He	20184	125.873	17O	2236	81.5344
4He	145776	147.761	18O	1400	94.6691	4He	145776	147.761	18O	1400	94.6659
6He	834	144.872	19O	42	95.2848	6He	834	144.872	19O	42	95.2817
8He	70	147.342	17F	606	34.7564	8He	70	147.342	17F	605	34.8029
10He	6	158.131	18F	5240	47.1235	10He	6	158.13	18F	5240	47.1158
6Li	6037	128.373	19F	6747	64.2664	6Li	6037	128.371	19F	6747	64.261
7Li	2990	132.03	20F	74	65.715	7Li	2990	132.029	20F	74	65.7087
8Li	517	132.308	16Ne	1	70.0538	8Li	517	132.307	16Ne	1	70.0491
9Li	194	128.963	17Ne	3	43.6315	9Li	194	128.962	17Ne	3	43.6243
11Li	8	169.443	18Ne	18	27.8587	11Li	8	169.443	18Ne	18	27.8363
6B	1155	95.2252	19Ne	160	12.1713	6B	1155	95.2223	19Ne	159	12.2144
7B	2786	109.551	20Ne	47323	8.50565	7B	2786	109.549	20Ne	47231	8.49411
9B	1676	127.951	22Ne	1	3.9603	9B	1676	127.95	22Ne	1	3.91998
10B	1007	133.883	25Ne	1	2.02658	10B	1007	133.882	25Ne	1	1.98186
11B	92	134.097	20Na	36	7.35762	11B	92	134.095	20Na	36	7.31956
12B	44	145.142	23Na	1	3.98017	12B	44	145.141	23Na	1	3.93837
14B	4	153.074	24Mg	1	0.01147	14B	4	153.073	26Al	1	1.75675
6Be	18	59.7437	26Al	1	1.82053	6Be	18	59.7374	27Al	1	2.48723
8Be	309	86.8154	27Al	1	2.54511	8Be	309	86.8119	28Si	1	0.637
10Be	3247	108.93	28Si	1	0.72172	10Be	3247	108.928	31P	1	0.76943
11Be	2920	118.092	31P	1	0.85025	11Be	2920	118.091			
12Be	556	122.096				12Be	556	122.095			
13Be	196	128.7				13Be	195	128.893			
14Be	22	133.455				14Be	22	133.453			
15Be	30	150.295				15Be	30	150.294			
8C	24	46.7143				8C	24	46.7066			
9C	90	66.917				9C	90	66.9116			
10C	570	78.4425				10C	570	78.4382			
11C	2455	88.3114				11C	2455	88.3079			
12C	12323	99.9829				12C	12322	99.9881			
13C	4568	108.11				13C	4568	108.108			
14C	1281	120.973				14C	1282	120.877			
15C	70	120.653				15C	70	120.651			
16C	61	129.966				16C	61	129.964			
17C	7	142.367				17C	7	142.365			

Depth 10			Depth 10			Depth 11			Depth 11		
Particle	Quantity	Avg. E	Particle	Quantity	Avg. E	Particle	Quantity	Avg. E	Particle	Quantity	Avg. E
π^-	21	75.3041	12N	245	66.2135	π^-	18	79.1687	12N	114	56.2899
(v_e)						(v_e)					
\square	9	40.9159	13N	1742	73.1052	\square	7	41.1868	13N	1037	58.9504
β^+	7	35.1842	14N	9146	85.0774	β^+	3	28.5468	14N	6456	71.558
β^-	1	42.9146	15N	5454	98.6287	β^-	1	40.7152	15N	4517	83.7853
(v_μ)	17	37.5008	16N	378	105.662	(v_μ)	18	37.2572	16N	341	90.3708
γ	122088	1.33909	17N	352	114.678	γ	111880	0.93252	17N	324	100.364
π^+	29	89.1416	18N	27	99.7769	π^+	25	84.8488	18N	23	99.6608
neutron	324385	122.129	12O	3	28.2306	neutron	266209	124.425	12O	1	37.8701
1H	279190	126.146	13O	58	50.4866	1H	213413	128.626	13O	10	70.8965
2H	64978	130.363	14O	534	47.5459	2H	54743	132	14O	95	38.2846
3H	20527	134.418	15O	3474	58.0065	3H	18339	134.133	15O	1127	39.4307
6H	123	126.458	16O	12250	73.0211	6H	112	125.98	16O	6984	52.6078
3He	20118	125.587	17O	2234	79.9767	3He	17198	123.858	17O	1481	62.7964
4He	145855	147.341	18O	1403	93.3319	4He	137603	142.427	18O	1145	75.1842
6He	838	144.007	19O	42	94.0549	6He	792	141.343	19O	31	81.9775
8He	71	146.246	17F	551	33.9799	8He	73	142.629	17F	7	28.2246
10He	6	158.04	18F	5010	46.0777	10He	6	155.772	18F	405	26.1749
6Li	6023	128.129	19F	6670	62.9458	6Li	5254	123.698	19F	2807	37.9733
7Li	2999	131.406	20F	69	68.0636	7Li	2708	126.877	20F	35	44.4427
8Li	515	132.269	16Ne	1	67.598	8Li	483	125.265	21F	1	2.47987
9Li	191	129.48	17Ne	4	39.2472	9Li	185	124.674	19Ne	8	22.1485
11Li	8	169.264	18Ne	10	36.1221	11Li	7	169.096	22Ne	1	5.85299
6B	1138	95.1437	19Ne	39	28.0548	6B	851	89.5755	24Mg	1	3.61444
7B	2766	109.504	20Ne	8510	4.97332	7B	2290	102.458			
9B	1675	127.622	20Na	6	4.65343	9B	1499	121.339			
10B	1004	133.61	27Al	1	3.16579	10B	914	127.381			
11B	92	133.633				11B	90	130.338			
12B	44	144.799				12B	46	136.052			
14B	4	152.775				14B	4	149.831			
6Be	18	57.3415				6Be	7	46.6723			
8Be	306	86.3493				8Be	220	76.3661			
10Be	3231	108.671				10Be	2725	101.078			
11Be	2915	117.585				11Be	2650	109.36			
12Be	555	122.064				12Be	521	113.889			
13Be	192	130.16				13Be	179	122.983			
14Be	22	132.783				14Be	20	126.143			
15Be	31	145.134				15Be	32	134.365			
8C	23	45.3761				8C	3	39.4742			
9C	87	65.3632				9C	44	57.7742			
10C	564	77.9755				10C	377	65.0357			
11C	2429	87.9379				11C	1784	76.0343			
12C	12261	99.3864				12C	9870	88.4959			
13C	4557	107.432				13C	3907	96.843			
14C	1290	119.717				14C	1186	109.274			
15C	70	119.904				15C	69	113.71			
16C	61	129.27				16C	62	117.69			
17C	7	141.845				17C	7	127.873			

Depth 12			Depth 12		
Particle	Quantity	Avg. E	Particle	Quantity	Avg. E
π^-	14	70.9712	14N	3722	57.7096
(ν_e)					
\square	5	39.894	15N	3222	70.3682
β^+	4	35.9356	16N	274	75.5763
(ν_μ)	11	35.7267	17N	274	87.6778
γ	108156	0.6849	18N	18	87.6865
π^+	17	81.5864	12O	1	14.1149
neutron	209204	129.832	13O	4	59.5227
1H	161182	131.482	14O	11	37.7707
2H	44379	134.916	15O	71	28.6517
3H	15401	136.887	16O	1715	30.7099
6H	105	122.636	17O	694	42.0176
3He	13972	123.744	18O	740	59.3135
4He	122685	140.275	19O	18	75.1492
6He	707	140.638	18F	1	76.2312
8He	72	135.552	19F	20	13.0551
10He	6	153.464	20F	3	14.6558
6Li	4382	119.922			
7Li	2313	124.121			
8Li	419	123.989			
9Li	172	120.601			
11Li	7	164.468			
6B	595	82.2145			
7B	1764	96.8052			
9B	1318	116.607			
10B	832	120.015			
11B	85	126.66			
12B	42	130.584			
14B	4	140.031			
8Be	136	66.9237			
10Be	2178	94.2252			
11Be	2254	101.643			
12Be	467	104.114			
13Be	164	116.719			
14Be	17	131.182			
15Be	27	131.2			
8C	2	60.5058			
9C	19	52.3119			
10C	184	59.9628			
11C	1108	66.9241			
12C	7234	78.12			
13C	3095	87.6907			
14C	1021	98.3186			
15C	66	102.688			
16C	56	110.466			
17C	6	128.75			
12N	42	51.2465			
13N	418	46.3384			

Table C. 2. Particle fluences through torus 3.11 cm² areas centered on an ion beam passing through different depths (cm) in a water phantom. Initial fluence equal to 500,000 ¹⁶O ions accelerated to 259 MeV/u.

Depth 0.001			Depth 1			Depth 2			Depth 3		
Particle	Quantity	Avg. E	Particle	Quantity	Avg. E	Particle	Quantity	Avg. E	Particle	Quantity	Avg. E
γ	21	2.25045	π-	87	67.9139	π-	111	72.0388	π-	102	70.4712
neutron	47	65.8667	(v_e) □	10	34.5856	μ+	1	2.27501	μ+	1	5.28541
1H	29	76.6564	β+	4	31.496	(v_e) □	7	25.6428	(v_e) □	14	29.0862
2H	1	5.51293	β-	3	23.5665	β+	4	37.4851	β+	6	39.0439
4He	4	2.37472	(v_μ)	15	36.8596	β-	1	23.0964	β-	2	39.5087
16O	22	258.846	γ	20582	4.32578	(v_μ)	12	34.1705	(v_μ)	27	32.1771
			π+	91	79.54	γ	34021	3.9733	γ	44703	3.32441
			neutron	61713	130.855	π+	112	76.8387	π+	88	89.1704
			1H	57804	152.789	neutron	115959	145.571	neutron	154234	150.785
			2H	5851	136.454	1H	110665	165.353	1H	147340	166.957
			3H	1023	151.029	2H	13539	156.281	2H	20638	161.605
			6H	1	224.753	3H	2768	173.811	3H	4786	179.556
			3He	946	175.92	6H	7	212.601	6H	15	201.531
			4He	3334	227.666	3He	2709	185.325	3He	4834	183.452
			6He	19	220.835	4He	12134	222.902	4He	23984	214.712
			8He	2	229.719	6He	80	218.778	6He	180	212.122
			10He	1	228.609	8He	3	230.993	8He	10	191.37
			6Li	153	231.243	10He	1	226.918	10He	1	225.186
			7Li	79	231.846	6Li	583	224.9	6Li	1176	213.199
			8Li	10	233.403	7Li	293	222.644	7Li	557	214.505
			9Li	4	222.693	8Li	43	223.607	8Li	90	212.659
			11Li	2	219.658	9Li	17	221.813	9Li	37	214.883
			6B	34	210.921	11Li	2	216.12	11Li	2	212.534
			7B	80	227.904	6B	151	200.762	6B	316	187.297
			9B	29	234.789	7B	288	217.288	7B	621	205.136
			10B	19	234.06	9B	119	225.317	9B	248	213.781
			11B	4	237.648	10B	84	223.788	10B	154	213.871
			12B	2	235.229	11B	7	234.401	11B	15	217.09
			6Be	1	195.268	12B	8	227.314	12B	11	216.724
			8Be	3	241.226	14B	1	221.639	14B	1	216.604
			10Be	58	235.266	6Be	5	197.289	6Be	8	178.018
			11Be	61	236.49	8Be	29	208.542	8Be	53	196.575
			12Be	7	230.55	10Be	246	221.699	10Be	496	208.666
			13Be	11	238.645	11Be	276	224.323	11Be	605	212.017
			14Be	1	235.136	12Be	46	223.508	12Be	102	214.011
			8C	1	235.525	13Be	28	230.198	13Be	73	218.445
			9C	6	234.279	14Be	1	227.718	14Be	5	214.281
			10C	20	231.732	8C	10	200.239	8C	23	172.686
			11C	61	231.333	9C	24	206.637	9C	42	189.513
			12C	352	239.521	10C	65	212.141	10C	150	197.418
			13C	99	239.743	11C	224	217.802	11C	481	203.034
			14C	27	240.153	12C	1354	225.949	12C	2857	211.525
			15C	1	236.608	13C	342	226.257	13C	728	212.183
			12N	10	233.635	14C	128	229.284	14C	305	215.567
			13N	39	235.875	15C	4	219.19	15C	6	208.496
			14N	167	240.054	12N	39	215.257	12N	92	197.385
			15N	168	242.94	13N	166	220.317	13N	362	203.573
			16N	2	242.949	14N	709	224.344	14N	1574	208.211
			12O	5	219.915	15N	651	228.138	15N	1352	212.997
			13O	4	227.856	16N	7	224.466	16N	19	211.463
			14O	32	236.284	12O	9	200.59	12O	14	181.002
			15O	157	240.303	13O	29	213.272	13O	99	192.482
			16O	2723	243.097	14O	125	219.264	14O	283	200.093
						15O	597	222.981	15O	1345	205.033
						16O	8827	226.631	16O	17146	209.454

Depth 4			Depth 5			Depth 6			Depth 7		
Particle	Quantity	Avg. E	Particle	Quantity	Avg. E	Particle	Quantity	Avg. E	Particle	Quantity	Avg. E
π^-	72	74.1765	π^-	52	71.489	π^-	37	75.5362	π^-	18	77.9462
μ^+	1	3.02849	$(\nu_e) \square$	5	27.7782	$(\nu_e) \square$	5	37.8917	$(\nu_e) \square$	10	35.2991
$(\nu_e) \square$	8	32.4365	β^+	4	32.5849	β^+	4	24.2763	β^+	2	23.0729
β^+	4	30.3195	β^-	6	35.6246	β^-	2	27.5249	β^-	1	24.7003
β^-	2	37.4186	(ν_μ)	24	33.5236	(ν_μ)	13	31.1812	(ν_μ)	13	32.3375
(ν_μ)	17	32.1849	γ	63600	2.36533	γ	73295	2.01793	γ	82533	1.75039
γ	53875	2.76131	π^+	41	87.8145	π^+	30	85.0239	π^+	18	83.45
π^+	68	87.3513	neutron	201565	147.212	neutron	217145	141.014	neutron	228680	133.308
neutron	181600	150.429	1H	191283	158.249	1H	204297	150.293	1H	212682	140.599
1H	172638	164.211	2H	32625	157.536	2H	37652	150.961	2H	42074	142.566
2H	26938	161.355	3H	8820	170.439	3H	10748	163.275	3H	12672	152.864
3H	6851	175.899	6H	33	177.238	6H	46	162.312	6H	59	151.347
6H	25	168.153	3He	8928	167.805	3He	11020	157.11	3He	12895	144.902
3He	6915	176.545	4He	50043	194.774	4He	63580	183.168	4He	77135	170.196
4He	36908	205.105	6He	349	194.623	6He	444	183.506	6He	534	171.537
6He	247	205.86	8He	21	194.439	8He	23	184.704	8He	30	175.792
8He	14	201.204	10He	2	210.062	10He	2	155.144	10He	2	152.936
10He	2	211.836	6Li	2362	189.98	6Li	3046	175.855	6Li	3692	160.864
6Li	1773	201.779	7Li	1238	190.92	7Li	1601	177.596	7Li	1925	163.705
7Li	886	203.667	8Li	173	191.086	8Li	218	179.061	8Li	294	163.407
8Li	137	202.04	9Li	71	194.526	9Li	97	177.693	9Li	125	162.739
9Li	59	204.441	11Li	2	200.219	11Li	1	221.229	11Li	5	148.655
11Li	1	227.933	6B	619	159.963	6B	770	142.028	6B	945	123.928
6B	488	172.781	7B	1256	177.519	7B	1623	161.875	7B	1945	144.841
7B	913	192.093	9B	565	188.552	9B	744	174.146	9B	915	159.314
9B	408	201.692	10B	353	189.019	10B	460	176.079	10B	563	162.03
10B	255	202.071	11B	38	191.558	11B	54	179.363	11B	62	168.313
11B	24	207.816	12B	33	190.439	12B	43	179.317	12B	55	167.641
12B	19	204.957	14B	1	206.503	6Be	32	110.8	6Be	34	85.9409
14B	1	211.522	6Be	25	136.073	8Be	166	147.038	8Be	210	126.657
6Be	15	163.153	8Be	128	165.374	10Be	1438	164.245	10Be	1734	146.824
8Be	86	181.365	10Be	1086	180.038	11Be	1643	169.824	11Be	2046	153.219
10Be	811	194.853	11Be	1291	184.978	12Be	331	172.845	12Be	425	156.753
11Be	950	199.443	12Be	253	187.699	13Be	209	180.7	13Be	269	166.061
12Be	177	201.047	13Be	157	194.188	14Be	12	177.231	14Be	16	160.108
13Be	109	207.539	14Be	11	188.786	8C	46	104.774	8C	51	82.3987
14Be	7	205.54	8C	36	131.969	9C	91	126.551	9C	110	103.239
8C	31	153.518	9C	71	148.8	10C	410	141.369	10C	493	119.371
9C	50	169.349	10C	320	161.216	11C	1461	151.778	11C	1836	131.242
10C	241	179.446	11C	1136	170.309	12C	8657	162.825	12C	10646	143.71
11C	805	187.142	12C	6659	180.263	13C	2261	165.776	13C	2855	147.509
12C	4713	196.363	13C	1741	182.158	14C	983	171.863	14C	1225	155.18
13C	1226	197.805	14C	740	187.211	15C	17	172.445	15C	22	154.753
14C	521	201.808	15C	15	187.462	12N	266	137.129	12N	317	112.818
15C	12	199.467	12N	193	158.919	13N	1180	146.809	13N	1484	124.172
12N	142	178.672	13N	869	167.222	14N	5039	154.711	14N	6260	133.664
13N	597	185.662	14N	3832	173.787	15N	4548	162.21	15N	5751	142.515
14N	2664	191.544	15N	3435	180.144	16N	51	162.506	16N	62	142.516
15N	2293	197.013	16N	37	179.652	12O	55	100.516	12O	52	76.0515
16N	23	196.805	12O	46	133.916	13O	306	120.862	13O	384	88.6492
12O	31	160.68	13O	227	147.395	14O	1003	133.474	14O	1270	105.881
13O	151	170.778	14O	751	157.91	15O	4512	143.529	15O	5689	118.603
14O	496	179.304	15O	3353	165.683	16O	45603	151.105	16O	55268	127.982
15O	2300	185.926	16O	35588	171.996						
16O	26033	191.319									

Depth 8			Depth 9			Depth 9.5005			Depth 9.5005		
Particle	Quantity	Avg. E	Particle	Quantity	Avg. E	Particle	Quantity	Avg. E	Particle	Quantity	Avg. E
π^-	12	81.6122	π^-	9	90.386	π^-	8	77.6704	16O	62772	9.04792
μ^+	1	5.47024	$(\nu_e) \square$	2	11.933	β^+	3	31.481	19F	1	1.01847
$(\nu_e) \square$	3	23.2428	β^+	4	34.4602	(ν_μ)	4	35.8117	20F	1	1.37567
β^+	4	30.7981	(ν_μ)	8	33.476	γ	105915	1.2797	22F	1	2.10354
(ν_μ)	9	31.276	γ	99941	1.43913	π^+	6	106.316	20Ne	1	1.69256
γ	90868	1.58935	π^+	10	93.4992	neutron	240659	99.9647	22Ne	2	2.22106
π^+	11	92.6948	neutron	241139	112.559	1H	196284	104.59	23Na	2	2.40709
neutron	236053	124.028	1H	213552	115.944	2H	47721	107.764	24Mg	2	1.63929
1H	215735	129.281	2H	47723	119.789	3H	16892	112.607	26Mg	1	0.97794
2H	45247	132.354	3H	16091	125.98	6H	109	107.837	27Mg	1	3.10342
3H	14362	140.238	6H	96	117.09	3He	15617	101.365			
6H	73	135.007	3He	15968	114.01	4He	114902	119.138			
3He	14635	130.155	4He	104377	137.657	6He	781	122.024			
4He	90393	155.539	6He	726	138.24	8He	61	102.339			
6He	643	155.112	8He	48	126.747	10He	2	145.851			
8He	37	156.849	10He	2	148.137	6Li	5457	102.775			
10He	2	150.534	6Li	5017	123.451	7Li	2879	107.847			
6Li	4297	144.225	7Li	2632	127.356	8Li	498	108.025			
7Li	2247	147.865	8Li	432	128.559	9Li	218	107.94			
8Li	350	148.295	9Li	190	125.376	11Li	12	109.984			
9Li	148	148.001	11Li	10	119.91	6B	913	65.8538			
11Li	9	148.3	6B	1162	80.3452	7B	2634	82.551			
6B	1093	102.902	7B	2640	102.487	9B	1456	98.0762			
7B	2298	125.217	9B	1276	121.795	10B	926	105.513			
9B	1085	142.267	10B	848	124.736	11B	95	120.723			
10B	697	144.335	11B	80	140.811	12B	89	120.092			
11B	74	153.888	12B	81	134.986	14B	1	20.5855			
12B	59	157.995	6Be	18	51.027	6Be	3	57.3429			
6Be	32	64.9648	8Be	304	73.6599	8Be	210	53.6315			
8Be	268	101.313	10Be	2575	102.365	10Be	2712	78.9516			
10Be	2119	126.869	11Be	2948	112.592	11Be	3307	89.516			
11Be	2482	134.017	12Be	599	119.358	12Be	652	98.9141			
12Be	495	139.598	13Be	386	132.989	13Be	439	113.55			
13Be	324	150.408	14Be	18	130.171	14Be	21	106.651			
14Be	18	142.676	8C	15	40.5045	15Be	1	45.1929			
8C	40	59.9338	9C	91	50.633	8C	1	0.11253			
9C	124	75.1873	10C	672	63.5691	9C	29	44.1054			
10C	604	93.3787	11C	2602	80.3298	10C	377	43.8531			
11C	2205	108.414	12C	14575	97.151	11C	2303	54.0957			
12C	12670	122.237	13C	4019	103.929	12C	15168	69.442			
13C	3440	127.35	14C	1709	116.688	13C	4365	78.471			
14C	1477	137.326	15C	40	106.608	14C	1912	93.2986			
15C	27	135.367	12N	361	51.8386	15C	44	81.0515			
12N	379	83.2155	13N	2064	64.9895	16C	1	3.88049			
13N	1769	98.1059	14N	8725	80.8898	12N	98	38.3383			
14N	7499	109.805	15N	8130	94.8812	13N	1086	32.1009			
15N	6938	120.713	16N	88	93.9993	14N	8430	46.0636			
16N	68	121.882	12O	5	35.6061	15N	8970	63.2815			
12O	34	46.1427	13O	146	34.9672	16N	91	63.6548			
13O	334	58.1528	14O	1037	39.681	12O	1	32.8822			
14O	1499	71.76	15O	7928	49.4419	13O	7	35.3304			
15O	6896	89.0845	16O	73495	67.9716	14O	23	35.7154			
16O	64690	101.369	17F	1	51.9426	15O	269	10.4622			

Depth 9.4995			Depth 9.4995			Depth 10			Depth 11		
Particle	Quantity	Avg. E	Particle	Quantity	Avg. E	Particle	Quantity	Avg. E	Particle	Quantity	Avg. E
π^-	8	77.6701	16O	62672	9.03994	π^-	8	77.4128	π^-	8	80.8959
β^+	3	31.481	19F	1	0.95547	(ν_e) \square	1	15.9492	(ν_e) \square	1	15.9492
(ν_μ)	4	35.8117	20F	1	1.31851	β^+	3	31.481	β^+	1	27.9161
γ	105913	1.27985	22F	1	2.05602	(ν_μ)	5	36.6642	(ν_μ)	3	27.7047
π^+	6	106.316	20Ne	1	1.63384	γ	105765	1.26097	γ	96428	0.82225
neutron	240661	99.9634	22Ne	2	2.17122	π^+	5	125.658	π^+	3	62.956
1H	196282	104.59	23Na	2	2.35177	neutron	239289	99.6282	neutron	187294	103.35
2H	47720	107.765	24Mg	2	1.57279	1H	193604	104.628	1H	139301	108.553
3H	16892	112.607	26Mg	1	0.90473	2H	47361	107.701	2H	37643	110.422
6H	109	107.837	27Mg	1	3.05853	3H	16749	112.713	3H	14162	113.791
3He	15618	101.362				6H	113	105.319	6H	107	107.045
4He	114899	119.139				3He	15459	101.257	3He	12181	101.128
6He	781	122.023				4He	114443	118.909	4He	100939	115.945
8He	61	102.338				6He	778	121.939	6He	703	118.37
10He	2	145.851				8He	61	102.028	8He	52	104.33
6Li	5458	102.757				10He	2	145.733	10He	3	130.59
7Li	2879	107.846				6Li	5414	102.497	6Li	4407	99.3561
8Li	498	108.024				7Li	2858	107.775	7Li	2420	104.645
9Li	218	107.939				8Li	500	106.967	8Li	429	106.206
11Li	12	109.984				9Li	218	107.656	9Li	197	105.461
6B	913	65.8496				11Li	12	109.656	11Li	13	98.6031
7B	2634	82.5482				6B	884	66.019	6B	479	61.9062
9B	1456	98.0743				7B	2600	82.1857	7B	1858	75.9023
10B	926	105.511				9B	1448	97.6161	9B	1202	93.7759
11B	95	120.722				10B	923	104.852	10B	806	99.5327
12B	89	120.091				11B	95	120.954	11B	89	112.976
14B	1	20.5827				12B	89	121.056	12B	87	114.886
6Be	3	57.3344				14B	1	19.0047	6Be	1	43.2827
8Be	210	53.6264				6Be	2	78.0926	8Be	80	50.5127
10Be	2712	78.9487				8Be	205	51.8238	10Be	1896	70.584
11Be	3308	89.5198				10Be	2684	78.3459	11Be	2674	80.8196
12Be	652	98.9121				11Be	3281	89.0727	12Be	579	88.5037
13Be	439	113.548				12Be	642	98.7959	13Be	407	102.829
14Be	21	106.65				13Be	438	113.119	14Be	17	93.4278
15Be	1	45.1898				14Be	20	104.371	15Be	1	7.20325
8C	1	0.0246				15Be	2	23.5244	9C	7	34.9967
9C	29	44.0981				9C	28	45.8687	10C	86	37.7049
10C	377	43.8457				10C	351	43.6146	11C	868	42.9938
11C	2303	54.0903				11C	2206	53.7283	12C	9282	54.7255
12C	15169	69.4369				12C	14912	68.7402	13C	3158	64.2236
13C	4364	78.4596				13C	4336	77.5959	14C	1670	78.7941
14C	1912	93.2963				14C	1914	92.4504	15C	25	72.5987
15C	44	81.0489				15C	44	80.8422	12N	27	42.1465
16C	1	3.85843				12N	90	38.9802	13N	53	28.5408
12N	98	38.3291				13N	939	31.9815	14N	1511	28.4518
13N	1086	32.0913				14N	8053	45.1101	15N	4910	43.3969
14N	8430	46.0574				15N	8879	61.9541	16N	46	49.3884
15N	8969	63.2784				16N	90	62.2748	13O	1	9.97875
16N	91	63.6505				12O	1	27.8649	14O	1	17.6429
12O	1	32.8739				13O	7	33.8872	15O	9	35.4971
13O	7	35.3177				14O	21	34.4145			
14O	23	35.7051				15O	38	31.08			
15O	269	10.432				16O	11694	4.90285			

Depth 12

Particle	Quantity	Avg. E
π^-	5	100.302
(ν_e) \square	1	45.606
β^+	1	37.5296
β^-	1	33.2851
(ν_μ)	5	33.9263
γ	93750	0.56785
π^+	2	49.5983
neutron	142079	109.099
1H	101396	111.747
2H	28951	113.876
3H	11281	117.209
6H	88	108.046
3He	9255	101.388
4He	84298	114.778
6He	600	116.21
8He	47	108.734
10He	4	97.9272
6Li	3398	96.4124
7Li	1921	102.749
8Li	363	103.358
9Li	166	103.693
11Li	16	96.8301
6B	220	59.7965
7B	1228	69.5975
9B	944	90.3252
10B	674	93.4744
11B	84	101.112
12B	76	109.533
8Be	23	50.3714
10Be	1210	61.7608
11Be	1989	72.1771
12Be	479	80.6961
13Be	364	93.1359
14Be	15	80.8716
8C	1	22.0272
9C	1	14.8173
10C	10	33.5974
11C	181	34.589
12C	4012	40.5607
13C	1859	51.8213
14C	1302	65.2871
15C	18	65.1988
12N	13	33.1183
13N	5	50.7216
14N	21	18.8862
15N	797	23.7312
16N	14	39.2449

Table C. 3. Particle fluences through torus 3.11 cm² areas centered on an ion beam passing through different depths (cm) in a water phantom. Initial fluence equal to 500,000 ¹²C ions accelerated to 219 MeV/u.

Depth 0.001			Depth 1			Depth 2			Depth 3		
Particle	Quantity	Avg. E	Particle	Quantity	Avg. E	Particle	Quantity	Avg. E	Particle	Quantity	Avg. E
γ	30	1.85488	π-	23	66.1392	π-	28	59.8681	π-	26	60.1301
neutron	35	47.5604	(ν_e) □	4	30.3649	μ+	1	5.96461	(ν_e) □	4	32.5921
1H	30	71.9199	β+	1	38.8232	(ν_e) □	6	42.1979	β+	2	34.1181
2H	2	3.81804	β-	1	15.1082	β+	1	47.7233	β-	2	40.4982
3H	1	1.187	(ν_μ)	5	36.1998	β-	1	44.2596	(ν_μ)	6	32.5253
8He	1	2.71191	γ	15760	3.61308	(ν_μ)	8	33.9003	γ	34668	2.81477
12C	22	218.873	π+	18	84.1576	γ	26546	3.22736	π+	25	62.8238
			neutron	46120	104.41	π+	30	71.4554	neutron	110378	120.782
			1H	41628	125.782	neutron	84799	116.797	1H	100879	136.51
			2H	4634	115.868	1H	77583	135.246	2H	15976	134.602
			3H	868	137.863	2H	10492	130.568	3H	4229	153.881
			6H	4	153.661	3H	2413	151.114	6H	24	164.109
			3He	790	153.703	6H	8	187.28	3He	4248	155.114
			4He	3639	195.112	3He	2419	157.811	4He	24714	181.89
			6He	26	193.466	4He	12785	189.531	6He	158	178.755
			8He	1	203.569	6He	82	188.653	8He	19	174.674
			6Li	102	198.424	8He	7	193.673	6Li	763	179.075
			7Li	86	200.291	6Li	393	188.448	7Li	587	181.22
			8Li	21	198.94	7Li	319	190.912	8Li	132	180.395
			9Li	7	199.714	8Li	68	189.098	9Li	118	183.976
			6B	57	180.13	9Li	53	192.799	6B	398	158.218
			7B	87	196.887	6B	207	168.977	7B	555	171.893
			9B	38	200.529	7B	271	183.984	9B	282	178.54
			10B	45	201.758	9B	140	188.642	10B	385	183.26
			11B	2	207.457	10B	194	192.529	11B	15	180.454
			6Be	4	174.05	11B	3	197.587	6Be	23	128.274
			8Be	25	186.166	6Be	14	154.843	8Be	104	159.763
			10Be	145	199.914	8Be	71	174.729	10Be	1156	174.776
			11Be	263	204.034	10Be	559	188.28	11Be	2044	180.597
			12Be	2	203.591	11Be	1000	192.569	12Be	24	180.192
			8C	9	185.671	12Be	13	192.749	8C	34	138.861
			9C	15	189.855	8C	16	159.819	9C	121	155.253
			10C	61	197.624	9C	62	173.479	10C	422	164.901
			11C	251	201.265	10C	202	181.761	11C	2094	170.88
			12C	3340	205.688	11C	1014	186.11	12C	20571	177.62
			12N	26	200.394	12C	10735	191.983	12N	161	164.935
						12N	78	183.472			

Depth 4			Depth 5			Depth 6			Depth 7		
Particle	Quantity	Avg. E	Particle	Quantity	Avg. E	Particle	Quantity	Avg. E	Particle	Quantity	Avg. E
π^-	28	57.8752	π^-	μ^-	65.9927	π^-	8	57.497	π^-	6	58.6127
μ^+	1	6.19227	β^+	1	46.882	(ν_e) \square	1	25.7086	(ν_e) \square	1	25.7086
(ν_e) \square	2	26.4151	μ^-	1	4.36413	β^+	1	46.882	(ν_μ)	2	38.0617
β^+	5	20.5199	(ν_μ)	3	36.7551	(ν_μ)	1	33.3548	γ	66646	1.56934
β^-	1	27.6868	γ	50440	2.04069	γ	58546	1.78702	π^+	5	64.8502
(ν_μ)	6	37.2356	π^+	12	58.0104	π^+	8	56.8031	neutron	157374	105.687
γ	42760	2.36372	neutron	141521	117.492	neutron	150937	112.493	1H	138452	111.636
π^+	19	64.2665	1H	128144	127.775	1H	135104	120.593	2H	31266	117.781
neutron	128086	120.529	2H	24954	131.204	2H	28547	125.078	3H	10932	129.917
1H	116950	133.473	3H	7709	146.48	3H	9397	138.422	6H	54	133.651
2H	20681	135.059	6H	38	152.846	6H	48	142.302	3He	11160	116.839
3H	5969	151.644	3He	7889	139.125	3He	9590	128.768	4He	78174	140.67
6H	24	160.973	4He	51195	163.244	4He	64860	152.56	6He	496	140.965
3He	6025	148.369	6He	318	162.111	6He	418	151.737	8He	53	147.295
4He	37840	172.948	8He	34	160.997	8He	45	155.476	6Li	2503	129.514
6He	238	171.564	6Li	1581	156.976	6Li	2060	143.628	7Li	1938	135.281
8He	26	171.75	7Li	1245	160.017	7Li	1594	148.16	8Li	409	136.179
6Li	1165	168.726	8Li	273	160.203	8Li	339	148.616	9Li	357	145.467
7Li	923	171.071	9Li	246	166.176	9Li	297	156.659	6B	1140	91.6619
8Li	209	168.52	6B	796	126.961	6B	966	110.3	7B	1826	112.108
9Li	184	175.511	7B	1184	144.511	7B	1534	129.079	9B	990	128.19
6B	625	142.859	9B	654	154.91	9B	841	141.927	10B	1425	136.57
7B	875	158.701	10B	871	161.384	10B	1157	149.477	11B	30	134.606
9B	463	166.678	11B	25	158.489	11B	29	145.865	6Be	22	48.6508
10B	626	172.432	6Be	33	88.3132	6Be	28	71.6817	8Be	345	84.1946
11B	21	168.911	8Be	228	127.122	8Be	283	106.726	10Be	4007	113.865
6Be	31	110.962	10Be	2574	146.614	10Be	3286	131.098	11Be	7280	124.236
8Be	162	144.485	11Be	4605	154.254	11Be	5892	139.973	12Be	91	124.393
10Be	1809	161.333	12Be	61	154.016	12Be	77	139.703	8C	48	51.4801
11Be	3320	167.741	8C	72	93.5195	8C	71	67.0589	9C	324	61.0784
12Be	42	167.339	9C	265	113.711	9C	312	88.0752	10C	1566	81.1187
8C	47	115.815	10C	967	128.164	10C	1250	106.421	11C	7452	96.5486
9C	191	135.849	11C	4634	137.418	11C	6049	118.359	12C	66895	109.417
10C	686	147.297	12C	43103	146.324	12C	55222	128.823	12N	709	70.2251
11C	3287	154.752	12N	392	124.647	12N	545	100.616	16N	1	0.51874
12C	31532	162.482	12O	1	90.4787	12O	1	32.8595	12O	2	79.4668
14C	1	0.08695	16O	2	0.07058	16O	1	0.28777	16O	1	0.19813
12N	279	145.837							17F	1	1.17544
12O	1	127.622									

Depth 8			Depth 9			Depth 9.97995			Depth 9.98005		
Particle	Quantity	Avg. E	Particle	Quantity	Avg. E	Particle	Quantity	Avg. E	Particle	Quantity	Avg. E
π^-	5	46.9909	π^-	5	43.2278	π^-	3	61.4546	π^-	3	61.4544
(ν_μ)	4	39.3324	(ν_μ)	2	40.6031	(ν_e)	1	28.2192	(ν_e)	1	28.2192
γ	74460	1.39743	γ	81630	1.2997	β^+	1	11.8382	β^+	1	11.8382
π^+	3	72.3762	π^+	4	65.8786	γ	86360	1.14111	γ	86368	1.14093
neutron	160900	97.6371	neutron	163710	87.617	π^+	3	50.0584	π^+	3	50.0581
1H	137127	101.667	1H	132032	90.1458	neutron	160422	76.9758	neutron	160419	76.9741
2H	33515	108.146	2H	34853	96.5023	1H	113478	81.2683	1H	113475	81.2664
3H	12202	118.678	3H	13552	104.568	2H	33270	86.3509	2H	33268	86.354
6H	59	125.793	6H	73	106.045	3H	13771	92.6788	3H	13770	92.685
3He	12462	103.569	3He	13353	88.2372	6H	74	94.9258	6H	74	94.9256
4He	90764	127.08	4He	102478	111.235	3He	12145	76.7579	3He	12145	76.756
6He	553	129.346	6He	627	113.962	4He	107580	95.6543	4He	107582	95.652
8He	72	133.898	8He	76	125.533	6He	691	97.2206	6He	690	97.3608
6Li	2915	113.908	6Li	3390	93.8186	8He	86	115.386	8He	86	115.386
7Li	2296	120.921	7Li	2627	103.613	6Li	3447	75.725	6Li	3446	75.7328
8Li	487	122.343	8Li	535	106.53	7Li	2722	86.7229	7Li	2722	86.7214
9Li	430	131.491	9Li	487	118.096	8Li	550	89.6373	8Li	550	89.6361
6B	1237	70.8069	6B	1091	48.9228	9Li	492	104.888	9Li	492	104.887
7B	2206	92.4672	7B	2500	69.6234	11Li	1	35.9974	11Li	1	35.9963
9B	1159	112.451	9B	1316	94.3904	6B	385	38.2349	6B	385	38.2293
10B	1715	122.389	10B	1958	106.674	7B	2053	49.3776	7B	2053	49.3734
11B	40	116.089	11B	52	95.5377	9B	1342	76.163	9B	1342	76.1609
6Be	8	44.8955	6Be	5	35.9935	10B	2142	89.9474	10B	2142	89.9459
8Be	361	60.1122	8Be	257	35.7816	11B	54	73.9111	11B	54	73.9093
10Be	4700	94.4861	10Be	5295	71.0896	12B	1	27.2022	12B	1	27.1996
11Be	8710	106.76	11Be	10127	86.218	8Be	22	18.5759	8Be	22	18.56
12Be	98	107.601	12Be	109	87.4628	10Be	4791	45.8666	10Be	4791	45.8622
8C	20	41.1607	13Be	1	48.4333	11Be	11030	62.0941	11Be	11031	62.0907
9C	212	44.4152	8C	4	30.0811	12Be	116	61.1678	12Be	116	61.1641
10C	1644	52.6674	9C	68	26.2484	13Be	1	11.9657	13Be	1	11.9592
11C	8891	70.1951	10C	746	31.7313	9C	1	73.9586	9C	1	73.9563
12C	78786	87.0489	11C	8430	37.45	10C	11	33.5466	10C	11	33.5385
13C	1	66.7334	12C	90238	59.006	11C	114	15.2976	11C	114	15.2748
12N	526	50.4006	13C	2	16.2348	12C	78383	8.61996	12C	78305	8.61174
14N	1	0.74282	12N	297	37.388	14C	1	1.77759	14C	1	1.73993
16N	1	0.32752	14N	1	6.22188	12N	20	5.95161	12N	20	5.91537
12O	1	35.8155				19F	1	2.37074	16O	1	0.02036
						22Ne	2	0.55992	19F	1	2.3227
									22Ne	2	0.49076

Depth 10			Depth 11			Depth 12		
Particle	Quantity	Avg. E	Particle	Quantity	Avg. E	Particle	Quantity	Avg. E
π^-	3	61.3784	π^-	2	43.9519	π^-	1	74.0983
(ν_e) \square	1	28.2192	(ν_e) \square	2	36.4045	(ν_e) \square	1	16.9866
β^+	1	11.8382	β^+	1	23.3274	β^+	1	23.3274
γ	86338	1.1321	γ	78872	0.70929	(ν_μ)	1	42.4872
π^+	3	49.995	π^+	2	44.4639	γ	77102	0.49409
neutron	160062	76.8528	neutron	117928	81.3467	π^+	2	40.1063
1H	112475	81.4099	1H	73007	86.3146	neutron	85710	86.681
2H	33058	86.445	2H	24259	90.3738	1H	49963	89.0575
3H	13719	92.7158	3H	10839	95.1441	2H	17685	94.0777
6H	74	94.8781	6H	63	94.705	3H	8112	99.0461
3He	12053	76.8924	3He	8205	77.4725	6H	50	98.0928
4He	107241	95.5789	4He	88695	93.2365	3He	5784	77.1787
6He	689	97.1193	6He	568	96.7474	4He	69429	92.0245
8He	86	115.304	8He	80	113.387	6He	436	97.3921
6Li	3429	75.6866	6Li	2470	72.6565	8He	66	113.931
7Li	2711	86.5205	7Li	2158	81.9615	6Li	1672	69.2596
8Li	549	89.2475	8Li	445	87.045	7Li	1624	78.099
9Li	492	104.961	9Li	453	99.3028	8Li	330	82.5598
11Li	1	35.7359	11Li	1	18.8012	9Li	399	96.3469
6B	375	38.0092	6B	69	39.0981	6B	13	41.0091
7B	2017	49.2962	7B	859	41.6724	7B	270	35.0554
9B	1331	76.2142	9B	1050	67.8833	9B	741	60.197
10B	2139	89.7304	10B	1979	79.1038	10B	1622	71.6264
11B	55	72.5114	11B	40	73.0245	11B	26	73.9115
12B	1	26.6636	8Be	4	43.5599	10Be	248	26.4588
8Be	17	20.8885	10Be	1650	34.5114	11Be	3538	35.2501
10Be	4730	45.5641	11Be	7479	48.7405	12Be	40	44.2516
11Be	10996	61.6602	12Be	72	55.2594	10C	1	23.1023
12Be	113	62.1436	9C	2	37.4762	11C	6	19.2319
13Be	1	10.3533	10C	2	43.562			
9C	1	73.2166	11C	19	31.4849			
10C	11	31.805	15N	1	0.79691			
11C	64	21.4312						
12C	58229	6.9151						
12N	12	6.20419						
14N	1	3.18998						
15N	1	5.15327						
16O	1	0.82593						
22Ne	1	0.41076						

Table C. 4. Particle fluences through torus 3.11 cm^2 areas centered on an ion beam passing through different depths (cm) in a water phantom. Initial fluence equal to $500,000 \text{ } ^7\text{Li}$ ions accelerated to 134.5 MeV/u .

Depth 0.001			Depth 1			Depth 2			Depth 3		
Particle	Quantity	Avg. E	Particle	Quantity	Avg. E	Particle	Quantity	Avg. E	Particle	Quantity	Avg. E
γ	24	2.44503	β^+	1	39.7968	β^+	1	39.7968	μ^+	1	2.08184
neutron	34	26.0014	(ν_μ)	2	19.3259	(ν_μ)	1	30.8432	(ν_μ)	1	30.8432
1H	18	37.9121	γ	18017	3.07954	γ	28846	2.76958	γ	38086	2.38855
2H	3	19.9982	π^+	2	22.5332	π^+	2	16.0531	neutron	117768	75.7796
3H	2	13.3842	neutron	49528	64.4606	neutron	89986	72.943	1H	65635	78.1945
7Li	31	134.426	1H	30109	74.9537	1H	52906	78.8819	2H	19776	90.2533
			2H	5654	83.2014	2H	13227	89.5188	3H	11670	106.397
			3H	2567	107.536	3H	7201	109.294	6H	22	100.648
			6H	5	94.9454	6H	17	95.0414	3He	4029	87.8901
			3He	908	96.6326	3He	2462	94.4232	4He	23548	103.877
			4He	4620	118.005	4He	13888	111.403	6He	1566	112.633
			6He	251	124.279	6He	865	118.416	6Li	1858	102.328
			6Li	357	121.005	6Li	1082	112.101	7Li	25370	109.682
			7Li	4374	126.481	7Li	13653	118.282	6B	195	78.2567
			6B	24	109.226	8Li	1	0.83973	7B	121	93.4839
			7B	9	117.722	6B	97	94.2966	11Be	1	0.27784
						7B	56	106.101	16O	1	0.01013
						13C	1	0.1365			
Depth 4			Depth 5			Depth 6			Depth 7		
Particle	Quantity	Avg. E	Particle	Quantity	Avg. E	Particle	Quantity	Avg. E	Particle	Quantity	Avg. E
(ν_μ)	2	23.6775	β^+	1	40.4044	π^-	1	4.35552	(ν_μ)	1	43.5081
γ	46818	1.98699	(ν_μ)	2	25.75	(ν_μ)	1	43.5081	γ	72101	1.27746
neutron	135819	75.8262	γ	55385	1.68359	γ	63724	1.42077	neutron	151462	65.7132
1H	72860	75.0928	neutron	145965	73.993	neutron	150678	70.4193	1H	68249	58.6273
2H	25368	88.1368	1H	74349	70.6273	1H	72942	65.0586	2H	32270	71.3499
3H	15710	101.72	2H	29149	83.8691	2H	31489	78.1353	3H	21154	81.8838
6H	33	102.607	3H	18890	96.5808	3H	20639	89.8582	6H	51	78.2894
3He	5486	79.1553	6H	48	92.0016	6H	57	83.6422	3He	7151	49.5832
4He	33026	95.8266	3He	6659	69.7851	3He	7221	59.9925	4He	49297	66.7788
6He	2315	106.711	4He	41030	87.1512	4He	46720	77.5458	6He	4573	84.8501
6Li	2660	91.9094	6He	3148	99.9218	6He	3915	92.7657	6Li	4577	53.1068
7Li	38308	100.565	6Li	3395	80.4364	6Li	4106	67.771	7Li	79778	68.2772
6B	272	59.4469	7Li	52184	90.7877	7Li	66094	80.132	9Li	1	18.9368
7B	199	77.5854	6B	267	48.2397	6B	207	40.8709	6B	144	35.0815
15C	1	0.31439	7B	267	59.6246	7B	260	44.4646	7B	173	36.8706
15N	1	0.01123	9B	1	1.15955	11B	1	4.79955	11Be	1	1.93408
15O	1	0.53768	8Be	1	2.31857	12B	1	0.02595	11C	1	2.33423
			11C	1	4.95674	11Be	2	0.34644	12C	1	0.08506
			14N	1	0.0259	12C	1	0.14745	13C	1	0.00354
						14C	2	0.302	15C	1	0.06477
						14N	1	0.02966	14N	3	1.48368

Depth 8			Depth 9			Depth 9.97995			Depth 9.98005		
Particle	Quantity	Avg. E	Particle	Quantity	Avg. E	Particle	Quantity	Avg. E	Particle	Quantity	Avg. E
(v_μ)	1	43.5081	(v_μ)	1	43.5081	(v_μ)	1	43.5081	(v_μ)	1	43.50813
γ	78896	1.116	γ	85279	0.96693	γ	88768	0.78359	γ	88765	0.783503
neutron	148219	60.0989	neutron	140582	53.5559	neutron	120383	48.5108	neutron	120380	48.51143
1H	59949	51.8309	1H	47020	45.0297	1H	26508	42.9565	1H	26506	42.95119
2H	31841	63.0962	2H	29148	55.1338	2H	21770	51.4616	2H	21768	51.46039
3H	20641	72.5003	3H	19063	62.5662	3H	15220	55.0654	3H	15220	55.06479
6H	55	66.5654	6H	53	48.7673	6H	39	36.4588	6H	39	36.45829
3He	6233	39.567	3He	4083	30.1169	3He	1433	25.7234	3He	1433	25.71881
4He	48943	54.5837	4He	43645	41.1823	4He	26137	32.1239	4He	26133	32.12505
6He	5014	76.3065	6He	5397	66.2319	6He	5561	56.0252	6He	5561	56.02425
8He	1	1.40571	6Li	2280	21.2475	6Li	28	4.40193	6Li	28	4.385996
6Li	4433	36.2064	7Li	105061	37.2257	7Li	93505	6.38118	7Li	93401	6.377981
7Li	92924	54.5392	8Li	1	6.62743	7B	7	3.46625	7B	7	3.429341
6B	81	27.9518	6B	38	19.0508	16O	1	0.00404			
7B	98	31.9655	7B	68	24.5614						
9B	1	3.56171	10B	1	1.70908						
10B	1	2.81231	10Be	2	0.21768						
10Be	1	1.88046	11Be	1	1.75094						
11Be	2	3.64231	13Be	1	0.0438						
12C	1	2.70672	11C	1	0.33641						
14N	1	0.00564	12C	1	0.64507						
			13N	1	0.04701						
			15O	1	0.02782						
			16O	2	0.55226						

Depth 10			Depth 11			Depth 12		
Particle	Quantity	Avg. E	Particle	Quantity	Avg. E	Particle	Quantity	Avg. E
(v_μ)	1	43.5081	γ	83422	0.45126	(v_μ)	1	43.5081
γ	88579	0.77716	neutron	75892	53.6205	γ	81872	0.2983
neutron	119501	48.544	1H	11437	48.3473	neutron	52488	57.7035
1H	25954	43.1424	2H	13183	54.8252	1H	6154	50.2
2H	21562	51.5188	3H	9318	57.6786	2H	8987	55.9738
3H	15099	55.0562	6H	15	39.2768	3H	6506	59.4177
6H	39	36.3561	3He	313	29.4127	6H	4	66.2527
3He	1374	25.9485	4He	9948	30.1821	3He	107	29.8146
4He	25681	32.0333	6He	4756	51.6393	4He	3696	27.0609
6He	5554	55.8433	6Li	1	26.0543	6He	4014	48.0956
6Li	12	4.39528	16O	1	0.04034			
7Li	75470	5.45066						
7B	4	4.35311						
18F	1	0.64336						

Depth 10			Depth 11			Depth 12		
Particle	Quantity	Avg. E	Particle	Quantity	Avg. E	Particle	Quantity	Avg. E
γ	34773	1.04335	γ	31153	0.52889	γ	30117	0.3232
neutron	25405	31.3235	neutron	14814	36.4776	neutron	10086	39.4957
1H	6927	31.6098	1H	2254	36.9168	1H	978	38.7336
2H	3580	35.1084	2H	1899	37.3119	2H	1149	37.3523
3H	2575	42.1693	3H	1672	45.0705	3H	1224	45.2984
3He	202	12.8805	3He	10	29.506	3He	5	14.5134
4He	115493	5.41897	4He	29	12.9276	4He	1	2.54864
			16N	1	0.02576			

Table C. 6. Particle fluences through torus 3.11 cm^2 areas centered on an ion beam passing through different depths (cm) in a water phantom. Initial fluence equal to $500,000 \text{ }^1\text{H}$ ions accelerated to 116.5 MeV/u .

Depth 0.001			Depth 1			Depth 2			Depth 3		
Particle	Quantity	Avg. E	Particle	Quantity	Avg. E	Particle	Quantity	Avg. E	Particle	Quantity	Avg. E
γ	3	3.93814	γ	902	2.55531	γ	1517	2.2252	γ	2175	1.79951
neutron	4	21.3275	neutron	1943	42.6011	neutron	2978	46.3863	neutron	3603	46.803
1H	85	113.04	1H	17834	97.4589	1H	49314	97.0106	1H	89319	92.0707
									2H	1	3.36754

Depth 4			Depth 5			Depth 6			Depth 7		
Particle	Quantity	Avg. E	Particle	Quantity	Avg. E	Particle	Quantity	Avg. E	Particle	Quantity	Avg. E
γ	2801	1.52673	γ	3264	1.25384	γ	4102	1.14015	γ	4771	1.04176
neutron	3760	44.6513	neutron	3822	42.1029	neutron	4000	38.1825	neutron	4140	33.7742
1H	134325	85.3745	1H	181753	77.5862	1H	228434	68.7256	1H	269875	58.7126
4He	1	2.94406	2H	1	4.39005	2H	2	5.52936	4He	2	1.88457
			3He	1	1.21779	14N	1	0.02919	14C	1	0.00306
			12C	1	0.25051						

Depth 8			Depth 9			Depth 9.93995			Depth 9.94005		
Particle	Quantity	Avg. E	Particle	Quantity	Avg. E	Particle	Quantity	Avg. E	Particle	Quantity	Avg. E
γ	5443	1.0043	γ	6212	1.01381	γ	6926	1.06292	γ	6927	1.06342
neutron	4166	29.7602	neutron	4234	24.6438	neutron	3750	19.9592	neutron	3750	19.9592
1H	302248	46.9826	1H	323517	32.0637	1H	238815	9.08946	1H	238708	9.08721
4He	1	0.30472	4He	2	1.38993	16O	1	0.00458			
			14N	1	0.02625						
			15O	1	0.1042						
			16O	1	0.01005						

Depth 10			Depth 11			Depth 12		
Particle	Quantity	Avg. E	Particle	Quantity	Avg. E	Particle	Quantity	Avg. E
γ	6866	1.04791	γ	5831	0.51909	γ	5605	0.27174
neutron	3656	19.7926	neutron	1942	21.5963	neutron	1089	22.3733
1H	172788	7.69684	1H	3	23.3044	1H	2	9.76235

APPENDIX D

Particle Fluences through cylindrical surface with radius of 0.1 cm centered on an ion beam passing through a water phantom.

Table D. 1. Particle fluences cylindrical surface with radius of 0.1 cm centered on an ion beam passing through different depths in a water phantom. Initial fluence equal to 500,000 ^{20}Ne ions accelerated to 296 MeV/u. Surface area equal to $0.628 \cdot h \text{ cm}^2$, h given as range of depths.

Depth 0-0.001			Depth 0.001-1			Depth 0.001-1		
Particle	Quantity	Avg. E	Particle	Quantity	Avg. E	Particle	Quantity	Avg. E
γ	233	4.19811	π^-	482	72.4855	18N	1	280.383
π^+	4	43.8718	μ^+	4	5.41248	13O	1	279.472
neutron	127	38.2011	(ν_e)	12	31.1999	14O	17	271.84
			\square			15O	75	255.706
1H	86	54.439	β^+	4	32.2015	16O	263	274.928
2H	12	10.4729	β^-	2	48.5367	17O	24	279.43
3H	2	120.364	μ^-	4	4.50322	18O	18	280.71
3He	2	5.43156	(ν_μ)	18	29.4719	17F	21	278.362
4He	10	29.186	γ	54468	4.89707	18F	83	279.029
20Ne	22	295.912	π^+	458	83.744	19F	111	283.366
			neutron	102110	129.36	20F	2	282.084
			1H	100326	148.1	17Ne	6	275.488
			2H	10399	119.83	18Ne	24	279.625
			3H	1945	115.355	19Ne	115	281.884
			6H	6	180.633	20Ne	2582	284.802
			3He	1487	150.277	20Na	14	282.988
			4He	5047	196.986			
			6He	27	210.667			
			8He	3	176.426			
			6Li	194	226.352			
			7Li	82	227.295			
			8Li	23	211.265			
			9Li	6	206.158			
			6B	58	206.64			
			7B	76	220.577			
			9B	44	240.143			
			10B	33	241.308			
			11B	2	137.485			
			12B	1	1.3736			
			6Be	1	263.628			
			8Be	12	246.904			
			10Be	76	255.762			
			11Be	52	257.611			
			12Be	11	216.767			
			13Be	2	286.166			
			14Be	2	265.822			
			15Be	2	272.652			
			8C	5	212.974			
			9C	1	247.226			
			10C	13	248.018			
			11C	63	266.77			
			12C	240	245.617			
			13C	92	263.735			
			14C	23	237.452			
			16C	1	279.83			
			12N	5	217.7			
			13N	45	268.544			
			14N	167	262.534			
			15N	97	263.294			
			16N	9	272.761			
			17N	3	275.833			

Depth 1-2			Depth 1-2			Depth 2-3			Depth 2-3		
Particle	Quantity	Avg. E				Particle	Quantity	Avg. E			
π^-	396	63.5657	16N	19	250.526	π^-	247	61.6177	16N	24	243.845
μ^+	2	4.45297	17N	18	261.571	μ^+	1	2.98522	17N	19	248.923
(ν_e)	6	40.4571	18N	3	266.495	(ν_e)	7	33.3097	18N	1	256.644
\square						\square					
β^+	4	35.7488	12O	2	249.144	β^+	3	30.0155	12O	3	217.236
β^-	3	36.1809	13O	3	249.549	β^-	3	48.1324	13O	9	234.185
μ^-	2	5.44009	14O	43	256.685	μ^-	2	3.16295	14O	74	238.782
(ν_μ)	24	32.2069	15O	210	261.729	(ν_μ)	21	28.8732	15O	312	241.147
γ	60381	4.42438	16O	750	264.67	γ	60662	3.75901	16O	1182	246.706
π^+	364	78.3379	17O	109	264.495	π^+	285	78.2043	17O	180	248.074
neutron	129571	140.3	18O	80	266.563	neutron	127373	134.318	18O	97	251.646
1H	127936	157.856	19O	2	266.45	1H	125304	151.093	19O	5	247.462
2H	15217	144.759	17F	47	264.612	2H	16065	143.654	17F	65	243.258
3H	3115	149.538	18F	292	264.998	3H	3518	152.473	18F	467	246.074
6H	15	103.984	19F	353	267.11	6H	19	160.909	19F	554	250.358
3He	2768	182.713	20F	5	268.843	3He	3252	177.391	20F	5	249.938
4He	11685	230.229	16Ne	4	265.972	4He	15688	224.994	16Ne	10	234.109
6He	68	217.99	17Ne	24	257.039	6He	85	219.305	17Ne	28	236.09
8He	8	185.375	18Ne	83	260.913	8He	8	199.501	18Ne	114	242.349
6Li	581	235.065	19Ne	295	264.946	6Li	753	229.767	19Ne	484	245.242
7Li	260	236.045	20Ne	5639	268.021	7Li	308	228.039	20Ne	7766	248.979
8Li	30	250.638	20Na	32	264.001	8Li	66	217.724	20Na	45	243.578
9Li	16	204.851				9Li	16	209.307			
6B	116	221.578				6B	141	208.192			
7B	222	236.245				7B	287	233.072			
9B	110	251.015				9B	170	240.412			
10B	68	251.928				10B	91	237.987			
11B	4	194.278				11B	6	239.416			
12B	4	256.683				12B	2	253.873			
6Be	5	199.044				14B	1	268.782			
8Be	30	247.701				6Be	9	205.325			
10Be	193	252.357				8Be	30	229.245			
11Be	149	258.075				10Be	282	238.096			
12Be	24	260.762				11Be	282	239.739			
13Be	10	267.599				12Be	33	246.63			
14Be	1	262.367				13Be	16	236.286			
15Be	2	267.73				14Be	2	237.432			
8C	6	253.609				15Be	5	258.975			
9C	8	214.961				8C	6	168.12			
10C	57	250.595				9C	8	205.235			
11C	136	242.119				10C	55	221.987			
12C	704	253.798				11C	212	234.98			
13C	246	258.211				12C	1026	244.069			
14C	74	264.231				13C	398	244.516			
15C	4	260.279				14C	118	249.422			
16C	1	270.837				15C	8	243.819			
17C	1	276.343				16C	5	262.99			
12N	15	218.739				12N	25	234.086			
13N	96	250.911				13N	152	241.912			
14N	459	259.975				14N	715	244.041			
15N	285	260.872				15N	462	245.88			

Depth 3-4			Depth 3-4			Depth 4-5			Depth 4-5		
Particle	Quantity	Avg. E				Particle	Quantity	Avg. E			
π^-	162	62.6846	15N	548	230.848	π^-	77	53.8728	15N	668	212.895
μ^+	3	6.79617	16N	54	230.941	(ν_e)	5	36.4889	16N	54	207.62
(ν_e)	6	29.8902	17N	37	237.108	\square			17N	48	217.128
β^+	3	36.2784	18N	2	242.412	β^-	1	35.5064	18N	2	207.763
β^-	5	33.7518	12O	3	211.827	(ν_μ)	14	34.7398	12O	1	218.311
μ^-	2	3.46409	13O	15	216.029	γ	60336	2.84035	13O	15	183.251
(ν_μ)	16	35.0861	14O	92	215.963	π^+	86	65.1872	14O	85	196.896
γ	60415	3.20672	15O	412	224.478	neutron	113498	115.012	15O	453	205.515
π^+	137	68.0589	16O	1493	229.741	1H	109920	130.006	16O	1774	210.383
neutron	121503	124.949	17O	235	230.886	2H	15475	124.405	17O	278	211.178
1H	118715	141.041	18O	149	232.931	3H	3531	134.905	18O	179	215.544
2H	15902	136.746	19O	6	230.438	6H	13	118.304	19O	7	216.299
3H	3614	145.712	17F	111	223.301	3He	3251	153.667	17F	105	204.563
6H	14	124.046	18F	593	226.846	4He	17342	197.659	18F	685	207.1
3He	3247	165.49	19F	662	231.589	6He	102	195.729	19F	743	211.557
4He	16790	214.111	20F	7	229.22	8He	4	194.918	20F	12	209.688
6He	86	216.503	16Ne	4	202.28	10He	1	157.176	16Ne	5	187.311
8He	7	217.984	17Ne	35	215.931	6Li	792	196.375	17Ne	57	190.991
10He	2	203.793	18Ne	165	221.508	7Li	381	201.877	18Ne	206	198.62
6Li	722	214.217	19Ne	624	225.133	8Li	65	182.625	19Ne	753	202.671
7Li	367	217.018	20Ne	9165	228.804	9Li	22	206.876	20Ne	9818	207.235
8Li	59	213.802	20Na	56	219.398	11Li	2	244.73	20Na	75	194.916
9Li	19	208.211				6B	174	180.18			
6B	176	192.071				7B	345	199.134			
7B	318	214.32				9B	199	207.801			
9B	167	227.586				10B	116	203.366			
10B	99	229.576				11B	5	205.907			
11B	8	236.905				12B	7	178.976			
12B	5	221.385				14B	2	214.227			
6Be	5	213.055				6Be	10	170.447			
8Be	42	221.57				8Be	44	201.038			
10Be	351	227.01				10Be	386	204.598			
11Be	309	225.02				11Be	317	208.002			
12Be	37	222.164				12Be	59	210.226			
13Be	12	228.991				13Be	21	214.209			
14Be	5	235.067				14Be	2	226.177			
15Be	4	222.788				15Be	3	221.818			
8C	11	192.919				8C	14	167.807			
9C	8	210.677				9C	17	197.02			
10C	66	218.086				10C	78	194.955			
11C	266	219.026				11C	283	201.088			
12C	1266	225.441				12C	1456	208.659			
13C	444	229.137				13C	551	213.002			
14C	140	230.548				14C	134	213.205			
15C	6	238.553				15C	7	204.091			
16C	9	238.439				16C	4	226.197			
18C	1	237.614				17C	1	229.118			
12N	24	218.839				12N	28	191.052			
13N	176	225.488				13N	205	201.983			
14N	1031	227.385				14N	1132	208.048			

Depth 5-6			Depth 5-6			Depth 6-7			Depth 6-7		
Particle	Quantity	Avg. E				Particle	Quantity	Avg. E			
π^-	39	51.9575	15N	686	194.201	π^-	21	35.7857	15N	730	172.539
μ^+	1	4.78471	16N	57	197.013	(ν_e)	4	36.7967	16N	44	168.291
(ν_e)	6	38.1215	17N	38	198.175	\square			17N	46	179.946
\square			18N	1	171.066	β^+	1	47.1911	18N	1	169.542
β^+	4	25.7249	12O	3	171.559	β^-	1	16.3437	12O	5	127.203
β^-	1	42.8265	13O	17	174.68	μ^-	1	6.36086	13O	18	140.439
μ^-	1	6.38427	14O	100	178.541	(ν_μ)	4	28.3235	14O	93	154.953
(ν_μ)	9	33.2766	15O	477	184.78	γ	60689	2.4086	15O	549	159.432
γ	61055	2.58945	16O	1761	189.551	π^+	26	47.9407	16O	1808	166.106
π^+	42	52.6372	17O	289	191.137	neutron	98865	90.7828	17O	312	168.901
neutron	107196	102.715	18O	198	196.236	1H	94066	103.755	18O	165	175.248
1H	102898	117.465	19O	8	194.66	2H	14948	97.8419	19O	3	172.703
2H	15346	111.123	17F	112	181.379	3H	3702	100.099	17F	155	155.709
3H	3725	115.641	18F	741	185.315	6H	15	64.4381	18F	796	161.254
6H	19	158.68	19F	831	190.625	3He	3296	117.925	19F	894	167.625
3He	3422	135.015	20F	7	191.032	4He	17887	155.432	20F	8	164.926
4He	17756	177.329	16Ne	22	157.727	6He	100	137.951	16Ne	8	129.525
6He	101	166.091	17Ne	54	164.063	8He	10	147.208	17Ne	59	138.26
8He	10	154.496	18Ne	218	173.829	10He	1	186.263	18Ne	225	147.187
10He	1	202.615	19Ne	875	179.336	6Li	797	154.208	19Ne	927	153.615
6Li	762	175.174	20Ne	10861	184.522	7Li	390	153.116	20Ne	11573	159.345
7Li	370	178.147	20Na	80	171.405	8Li	62	158.337	20Na	89	141.16
8Li	43	187.1				9Li	24	134.811	20Mg	1	92.5518
9Li	19	177.523				11Li	1	186.886			
11Li	1	177.381				6B	177	126.525			
6B	192	160.193				7B	335	154.471			
7B	342	178.673				9B	200	167.306			
9B	198	185.902				10B	103	163.403			
10B	123	188.884				11B	9	164.277			
11B	13	193.647				12B	4	172.202			
12B	8	183.152				14B	1	147.084			
6Be	12	140.714				6Be	7	112.013			
8Be	42	170.99				8Be	39	149.913			
10Be	392	186.879				10Be	374	162.464			
11Be	300	187.625				11Be	330	164.476			
12Be	57	194.411				12Be	54	168.004			
13Be	14	195.339				13Be	16	161.243			
14Be	2	178.812				14Be	1	152.602			
15Be	5	196.769				15Be	6	155.316			
8C	11	126.864				8C	10	141.658			
9C	14	165.663				9C	7	133.86			
10C	76	171.672				10C	63	154.973			
11C	271	178.635				11C	311	152.122			
12C	1534	189.069				12C	1613	165.203			
13C	554	190.14				13C	541	168.194			
14C	139	196.262				14C	175	176.114			
15C	13	206.14				15C	15	169.858			
16C	7	198.412				16C	5	189.428			
12N	21	170.371				12N	35	154.141			
13N	247	182.002				13N	216	160.326			
14N	1120	187.915				14N	1229	165.524			

Depth 7-8			Depth 7-8			Depth 8-9			Depth 8-9		
Particle	Quantity	Avg. E				Particle	Quantity	Avg. E			
π^-	2	45.4568	16N	52	147.287	π^-	1	27.9402	18N	8	124.948
μ^+	1	4.70322	17N	40	156.527	(ν_e)	2	40.6486	12O	4	51.0809
(ν_e)	3	29.6008	18N	3	139.803	\square			13O	14	72.6827
\square						β^+	2	45.2773			
μ^-	1	1.92946	12O	1	91.4588	(ν_μ)	1	26.9021	14O	132	90.2708
(ν_μ)	4	28.2124	13O	14	118.719	γ	61526	2.24109	15O	542	100.261
γ	61033	2.33034	14O	115	127.99	π^+	3	108.081	16O	1738	107.169
π^+	9	62.9924	15O	526	132.985	neutron	83490	61.0772	17O	308	112.561
neutron	91083	76.9996	16O	1807	139.191	1H	77167	70.5427	18O	199	118.093
1H	85350	88.1736	17O	321	141.723	2H	13987	64.8042	19O	5	109.51
2H	14458	82.4659	18O	212	150.69	3H	4093	63.9504	17F	159	94.53
3H	3820	83.4246	19O	5	144.812	6H	28	62.6777	18F	918	101.711
6H	22	71.8658	17F	143	128.65	3He	3605	73.0233	19F	1019	111.328
3He	3398	95.7139	18F	861	133.229	4He	19430	98.2918	20F	13	109.242
4He	17989	128.86	19F	951	140.453	6He	126	83.1031	16Ne	6	41.6465
6He	106	119.096	20F	15	142.106	8He	6	80.24	17Ne	70	67.971
8He	9	68.2731	16Ne	10	99.1437	6Li	941	96.5641	18Ne	259	77.4082
10He	1	105.397	17Ne	60	102.963	7Li	431	94.1978	19Ne	1031	88.1477
6Li	788	128.913	18Ne	250	116.022	8Li	81	100.352	20Ne	12179	97.6672
7Li	348	130.871	19Ne	986	124.606	9Li	25	101.464	20Na	124	72.7067
8Li	68	127.438	20Ne	11649	131.245	11Li	2	176.019			
9Li	24	119.409	20Na	104	112.529	6B	201	77.7656			
11Li	1	150.767				7B	368	93.1714			
6B	153	99.4745				9B	243	99.7654			
7B	372	126.313				10B	124	103.673			
9B	212	135.838				11B	10	106.92			
10B	114	142.478				12B	7	99.9659			
11B	14	131.821				6Be	8	67.7423			
12B	2	164.912				8Be	53	83.5141			
6Be	12	81.8118				10Be	459	102.388			
8Be	41	118.915				11Be	352	106.352			
10Be	399	133.422				12Be	53	110.317			
11Be	320	138.64				13Be	17	113.188			
12Be	58	141.482				14Be	6	141.653			
13Be	26	146.615				15Be	4	103.508			
14Be	1	218.177				8C	10	66.1094			
15Be	3	187.267				9C	12	84.563			
8C	6	99.9648				10C	70	89.3762			
9C	9	121.87				11C	333	99.5509			
10C	74	123.843				12C	1714	107.758			
11C	308	130.12				13C	642	111.871			
12C	1623	139.158				14C	163	121.496			
13C	559	143.569				15C	13	86.4943			
14C	162	151.123				16C	7	138.936			
15C	3	141.765				17C	1	192.743			
16C	15	159.73				12N	39	92.1143			
17C	1	170.457				13N	237	99.7672			
12N	36	134.298				14N	1380	107.007			
13N	257	131.016				15N	794	115.926			
14N	1287	138.895				16N	50	114.972			
15N	724	146.521				17N	49	133.275			

Depth 10-11			Depth 10-11			Depth 11-12		
Particle	Quantity	Avg. E				Particle	Quantity	Avg. E
π^-	1	46.2915	15O	95	41.7265	(ν_e)	1	19.723
(ν_e)	1	44.5827	16O	464	49.7298	β^-	1	40.7152
β^+	1	36.8516	17O	111	58.1525	(ν_μ)	2	43.6921
γ	21840	0.86623	18O	123	75.1603	γ	17846	0.44177
π^+	2	21.7086	19O	2	52.8851	neutron	6283	54.9565
neutron	18654	45.9514	17F	15	31.283	1H	3814	71.5326
1H	12900	54.7474	18F	161	37.5817	2H	855	72.7296
2H	3068	51.5726	19F	408	48.6142	3H	299	73.5167
3H	1015	53.0621	19Ne	1	36.5248	6H	1	21.6198
6H	5	29.0511	20Ne	59	3.74278	3He	224	73.1206
3He	676	62.1631				4He	2105	89.1446
4He	7082	65.0745				6He	12	79.6335
6He	41	67.0888				8He	1	34.6559
8He	7	50.5129				6Li	67	71.5634
6Li	244	55.9899				7Li	45	83.0069
7Li	130	56.3083				8Li	6	64.3521
8Li	25	66.4913				9Li	5	81.7497
9Li	7	38.5898				11Li	1	4.37341
11Li	1	14.4858				6B	12	49.3897
6B	31	56.6316				7B	24	71.8095
7B	84	67.9659				9B	18	77.7678
9B	62	57.8387				10B	19	69.4777
10B	50	62.3222				11B	4	91.8497
11B	4	88.0843				12B	1	16.1768
12B	2	119.684				8Be	2	85.3605
14B	1	145.53				10Be	28	79.6599
8Be	6	54.0174				11Be	33	73.6996
10Be	119	67.1748				12Be	9	78.8577
11Be	113	67.3957				13Be	2	104.087
12Be	20	76.6042				10C	3	70.2065
13Be	8	89.2215				11C	17	79.6427
14Be	2	54.8046				12C	157	69.3761
15Be	2	99.5651				13C	75	75.118
9C	1	119.342				14C	27	88.2227
10C	19	60.5984				15C	1	164.652
11C	52	57.7788				16C	7	104.708
12C	488	58.5851				12N	1	42.312
13C	212	64.1225				13N	11	52.1468
14C	83	83.2512				14N	102	55.5664
15C	4	145.501				15N	130	74.4502
16C	6	77.6386				16N	17	81.1112
12N	6	46.0213				17N	18	71.7049
13N	47	58.8062				14O	3	37.5561
14N	391	58.3365				15O	10	30.7127
15N	332	66.6262				16O	62	40.488
16N	16	86.9255				17O	36	51.7855
17N	30	94.4788				18O	60	67.0212
18N	3	91.6155				18F	5	15.066
13O	3	25.1731				19F	72	31.5124
14O	12	46.8639				19Ne	1	26.4289

Table D. 2. Particle fluences cylindrical surface with radius of 0.1 cm centered on an ion beam passing through different depths in a water phantom. Initial fluence equal to 500,000 ^{16}O ions accelerated to 259 MeV/u. Surface area equal to $0.628 \cdot h \text{ cm}^2$, h given as range of depths.

Depth 0-0.001			Depth 0.001-1			Depth 1-2			Depth 2-3		
Particle	Quantity	Avg. E	Particle	Quantity	Avg. E	Particle	Quantity	Avg. E	Particle	Quantity	Avg. E
μ^-	1	8.10415	π^-	158	56.6465	π^-	153	58.1742	π^-	89	49.6942
γ	207	3.15046	(ν_e)	4	40.5111	μ^+	1	6.11639	μ^+	2	4.81323
neutron	132	33.6781	β^+	2	29.189	(ν_e)	4	42.2946	(ν_e)	6	29.2267
1H	87	41.9725	β^-	1	42.5758	β^+	1	32.5107	β^+	4	46.5349
2H	7	7.31166	μ^-	2	5.63702	β^-	1	39.5535	μ^-	1	6.73288
4He	14	2.44299	(ν_μ)	9	33.475	(ν_μ)	8	30.192	(ν_μ)	11	28.7011
16O	23	258.929	γ	45960	3.75865	γ	51413	3.56963	γ	51840	3.13092
			π^+	178	67.3653	π^+	142	63.0576	π^+	85	70.4082
			neutron	81167	107.692	neutron	100939	115.796	neutron	99720	111.834
			1H	78057	125.465	1H	98267	133.722	1H	96393	127.199
			2H	8334	101.291	2H	12092	122.266	2H	12851	119.317
			3H	1637	97.1575	3H	2646	128.448	3H	3061	132.135
			6H	6	40.3141	6H	9	141.725	6H	11	124.986
			3He	1318	131.06	3He	2279	157.063	3He	2674	154.656
			4He	4602	167.004	4He	10034	195.894	4He	12902	193.286
			6He	30	141.39	6He	77	172.355	6He	108	193.214
			8He	2	230.077	8He	2	121.399	8He	8	181.06
			10He	2	115.669	6Li	467	210.238	6Li	635	202.175
			6Li	179	195.739	7Li	235	205.42	7Li	299	205.362
			7Li	90	200.567	8Li	37	217.509	8Li	52	197.314
			8Li	17	139.246	9Li	13	207.601	9Li	22	185.104
			9Li	5	179.362	6B	132	183.109	6B	179	180.867
			11Li	2	220.506	7B	219	212.846	7B	345	202.713
			6B	42	174.439	9B	94	220.771	9B	140	205.519
			7B	91	203.39	10B	66	211.23	10B	73	208.056
			9B	30	229.555	11B	3	239.404	11B	8	210.562
			10B	20	224.823	12B	6	228.484	12B	3	205.944
			11B	4	239.342	14B	1	225.535	6Be	5	152.844
			12B	2	237.836	6Be	5	174.792	8Be	24	195.557
			6Be	1	200.468	8Be	26	205.515	10Be	249	207.705
			8Be	3	243.546	10Be	195	220.094	11Be	328	213.289
			10Be	62	220.142	11Be	210	224.226	12Be	55	214.253
			11Be	66	225.385	12Be	37	225.535	13Be	41	216.037
			12Be	10	188.71	13Be	16	234.675	14Be	3	216.197
			13Be	12	221.088	8C	10	211.618	8C	13	179.505
			14Be	1	236.055	9C	16	208.513	9C	20	188.621
			8C	1	243.946	10C	45	217.344	10C	82	202.976
			9C	7	205.138	11C	164	219.102	11C	242	206.35
			10C	24	216.237	12C	1022	228.596	12C	1562	214.35
			11C	63	227.703	13C	247	230.108	13C	378	216.204
			12C	367	231.005	14C	97	234.014	14C	171	215.329
			13C	108	230.453	15C	3	220.6	15C	2	213.073
			14C	32	221.067	12N	29	223.078	12N	45	206.372
			15C	1	241.476	13N	126	221.321	13N	193	211.539
			12N	10	238.335	14N	543	230.314	14N	872	214.104
			13N	38	234.626	15N	490	231.338	15N	697	218.342
			14N	176	232.464	16N	5	226.643	16N	11	217.35
			15N	171	239.881	12O	4	221.98	12O	4	203.436
			16N	2	245.108	13O	25	222.486	13O	70	202.98
			12O	5	225.89	14O	92	228.204	14O	155	210.446
			13O	4	235.207	15O	433	228.785	15O	731	212.843
			14O	30	243.212	16O	6712	234.502	16O	9442	218.1

15O	156	244.297
16O	2932	248.55

Depth 3-4			Depth 4-5			Depth 5-6			Depth 6-7		
Particle	Quantity	Avg. E	Particle	Quantity	Avg. E	Particle	Quantity	Avg. E	Particle	Quantity	Avg. E
π^-	52	43.4901	π^-	31	55.4045	π^-	15	43.237	π^-	5	34.4755
(v_e)	2	25.5272	(v_e)	1	13.5151	μ^+	1	5.4746	(v_e)	1	20.5555
\square			\square						\square		
β^+	3	37.608	β^+	1	51.5002	β^+	1	14.3167	β^+	2	45.9589
(v_μ)	3	28.8045	(v_μ)	1	30.2215	β^-	1	34.1799	γ	53050	2.41559
γ	52070	2.84083	γ	52574	2.67238	(v_μ)	5	27.4378	π^+	6	79.9954
π^+	52	54.8046	π^+	28	58.643	γ	52581	2.52269	neutron	77764	75.1567
neutron	93965	103.317	neutron	88398	95.2036	π^+	12	53.909	1H	72836	87.6712
1H	90033	119.015	1H	84780	109.177	neutron	83789	84.8984	2H	12021	80.3455
2H	12545	111.613	2H	12526	103.286	1H	79166	99.1261	3H	3227	86.5822
3H	3128	118.573	3H	3119	110.119	2H	12288	92.4247	6H	21	95.1503
6H	14	86.8021	6H	14	125.225	3H	3157	98.6098	3He	2822	98.231
3He	2675	143.971	3He	2737	128.359	6H	19	94.7912	4He	14576	129.114
4He	13951	180.887	4He	13916	166.861	3He	2861	113.933	6He	95	122.722
6He	79	166.823	6He	98	151.347	4He	14216	148.737	8He	5	158.815
8He	7	169.444	8He	6	198.813	6He	99	140.39	6Li	735	135.278
10He	1	201.85	6Li	657	175.775	8He	3	137.42	7Li	375	131.199
6Li	643	188.011	7Li	389	173.183	10He	1	114.283	8Li	70	139.518
7Li	360	188.318	8Li	42	168.794	6Li	770	153.02	9Li	31	127.072
8Li	54	183.6	9Li	16	179.901	7Li	393	154.822	11Li	4	68.0485
9Li	22	199.096	6B	162	154.018	8Li	61	150.811	6B	183	113.222
6B	175	171.781	7B	354	175.211	9Li	22	148.638	7B	350	128.875
7B	287	188.769	9B	169	178.057	6B	157	124.171	9B	166	138.767
9B	168	197.008	10B	98	177.997	7B	354	154.266	10B	98	144.682
10B	100	195.304	11B	11	181.924	9B	173	163.123	11B	8	146.256
11B	8	201.936	12B	11	176.398	10B	99	162.197	12B	8	158.981
12B	6	205.14	6Be	7	135.811	11B	14	175.903	6Be	3	136.599
6Be	12	161.626	8Be	40	173.437	12B	8	170.918	8Be	46	128.199
8Be	31	188.59	10Be	274	176.657	6Be	8	121.197	10Be	298	138.523
10Be	318	194.493	11Be	349	179.032	8Be	36	147.005	11Be	386	143.941
11Be	333	199.728	12Be	71	184.949	10Be	335	159.733	12Be	81	145.553
12Be	69	201.66	13Be	47	189.615	11Be	335	160.658	13Be	62	155.848
13Be	33	201.308	14Be	2	172.867	12Be	73	154.626	14Be	3	141.369
14Be	2	208.982	8C	5	140.35	13Be	57	176.677	8C	15	97.2328
8C	7	176.476	9C	20	166.425	14Be	4	166.237	9C	13	122.32
9C	9	157.523	10C	70	169.62	8C	10	127.155	10C	87	129.95
10C	83	185.548	11C	320	172.408	9C	11	144.92	11C	340	132.951
11C	305	192.768	12C	2021	182.839	10C	78	152.366	12C	2100	142.389
12C	1921	199.397	13C	525	182.412	11C	320	155.188	13C	592	143.748
13C	509	201.434	14C	220	185.005	12C	2101	164.293	14C	239	153.506
14C	214	203.65	15C	3	188.672	13C	532	165.93	15C	4	139.99
15C	9	183.71	12N	52	172.662	14C	258	169.233	12N	47	131.689
12N	55	189.279	13N	267	175.678	15C	3	165.171	13N	316	133.402
13N	223	191.036	14N	1179	179.953	12N	66	148.423	14N	1293	139.661
14N	1124	196.661	15N	1137	185.778	13N	292	154.543	15N	1225	146.116
15N	933	202.284	16N	14	181.122	14N	1263	161.628	16N	11	138.582
16N	7	201.441	12O	12	154.252	15N	1140	167.073	12O	10	109.768
12O	15	178.399	13O	76	163.784	16N	13	165.241	13O	76	114.96
13O	53	184.37	14O	242	171.591	12O	13	126.079	14O	257	125.238
14O	202	190.315	15O	1032	176.878	13O	81	140.149	15O	1197	132.827
15O	947	194.795	16O	11856	181.907	14O	240	148.91	16O	13402	140.297
16O	10602	200.641				15O	1142	156.339			
						16O	12896	162.093			

Depth 7-8			Depth 8-9			Depth 9-9.94995			Depth 9.94995-9.95005		
Particle	Quantity	Avg. E	Particle	Quantity	Avg. E	Particle	Quantity	Avg. E	Particle	Quantity	Avg. E
π^-	1	40.1806	π^-	1	45.0556	γ	48999	2.21217	γ	3	5.39901
(ν_μ)	3	28.0381	γ	53862	2.30548	neutron	56256	34.4026	neutron	3	15.8828
γ	52909	2.35086	neutron	65955	50.2741	1H	48090	40.3383	1H	2	20.9477
π^+	2	62.984	1H	59527	59.431	2H	9961	35.9216	6Li	1	14.0818
neutron	72058	63.5898	2H	11158	54.5106	3H	3279	34.6845	16O	6	4.92267
1H	66163	74.9822	3H	3518	54.7748	6H	25	46.8948			
2H	11482	68.3429	6H	29	59.9038	3He	2552	37.4912			
3H	3392	70.5901	3He	2961	60.8183	4He	18567	47.0591			
6H	26	57.401	4He	16858	79.7136	6He	130	36.101			
3He	2862	81.3417	6He	123	82.4087	8He	16	30.0695			
4He	15034	106.483	8He	16	54.4549	6Li	957	44.7017			
6He	121	99.6824	6Li	885	80.4405	7Li	515	47.0581			
8He	6	76.9981	7Li	454	81.1906	8Li	88	43.9421			
6Li	739	108.423	8Li	83	87.3218	9Li	38	45.8853			
7Li	384	109.408	9Li	34	64.8028	11Li	1	121.495			
8Li	64	105.813	11Li	2	32.0443	6B	136	33.7615			
9Li	19	87.8592	6B	185	62.3408	7B	415	44.0285			
11Li	2	184.43	7B	394	77.7791	9B	254	48.3457			
6B	186	87.7396	9B	218	85.1683	10B	146	47.0489			
7B	390	107.121	10B	144	88.8978	11B	9	42.7451			
9B	177	115.277	11B	7	92.0358	12B	11	61.0392			
10B	114	120.698	12B	20	109.692	14B	1	25.2352			
11B	12	127.334	6Be	6	42.4076	6Be	3	33.7278			
12B	10	125.203	8Be	43	72.6163	8Be	46	32.3111			
6Be	9	74.3035	10Be	436	83.0491	10Be	441	46.3106			
8Be	57	99.4856	11Be	420	90.4879	11Be	496	50.0202			
10Be	376	115.64	12Be	85	98.5497	12Be	78	51.2676			
11Be	395	118.784	13Be	57	116.399	13Be	58	83.7697			
12Be	66	120.683	14Be	2	103.479	14Be	3	38.3592			
13Be	48	138.05	8C	8	34.9963	15Be	2	31.6535			
14Be	3	113.391	9C	15	66.2238	8C	2	25.0437			
8C	9	80.1117	10C	94	73.1666	9C	14	25.9368			
9C	18	89.9044	11C	361	77.4004	10C	88	37.2414			
10C	93	102.47	12C	2116	89.8043	11C	402	41.7372			
11C	312	110.164	13C	601	94.8392	12C	1883	51.6189			
12C	2189	118.362	14C	256	108.974	13C	580	57.3233			
13C	574	121.402	15C	11	88.4788	14C	244	74.6351			
14C	242	136.245	12N	62	67.3349	15C	13	36.2631			
15C	4	119.213	13N	340	79.2885	12N	43	34.4667			
12N	64	101.51	14N	1311	87.3752	13N	222	43.1582			
13N	285	111.203	15N	1230	98.1922	14N	1181	50.2715			
14N	1316	115.719	16N	17	90.4221	15N	1190	64.8499			
15N	1251	125.415	12O	4	59.9629	16N	14	44.0963			
16N	8	114.276	13O	59	53.5176	13O	19	27.72			
12O	8	83.8839	14O	315	65.1236	14O	131	36.357			
13O	52	89.5355	15O	1344	75.4111	15O	956	36.9401			
14O	254	98.483	16O	14371	86.2584	16O	14272	44.6303			
15O	1277	108.057	17F	1	53.0448	17O	5	11.7096			
16O	13814	115.468				18O	1	14.4004			
						17F	2	13.9883			
						18F	6	11.8342			
						19F	2	10.2689			
						20Ne	3	2.33327			
						21Ne	1	3.47052			
						22Ne	1	3.60928			
						23Na	1	2.11698			
						24Mg	2	0.98584			

Depth 9.95005-10			Depth 10-11			Depth 11-12		
Particle	Quantity	Avg. E	Particle	Quantity	Avg. E	Particle	Quantity	Avg. E
γ	1468	1.67947	π^-	3	21.4704	γ	14885	0.31879
neutron	2094	26.3858	γ	17790	0.71427	neutron	4084	46.1492
1H	1583	32.5498	neutron	12158	38.0098	1H	2199	62.6419
2H	355	29.521	1H	7842	47.6098	2H	482	62.9688
3H	98	33.9256	2H	1867	47.2444	3H	183	65.1326
6H	2	16.6993	3H	655	42.5337	6H	1	83.3165
3He	79	34.1697	6H	7	44.7845	3He	127	71.0068
4He	589	40.226	3He	397	52.8386	4He	1062	74.4415
6He	2	9.25935	4He	3946	57.2434	6He	9	75.2187
6Li	27	38.2034	6He	19	45.695	8He	1	59.8552
7Li	19	34.9149	8He	4	34.957	6Li	37	63.7876
8Li	6	22.9754	6Li	149	58.0461	7Li	41	75.783
6B	4	46.8779	7Li	78	56.412	8Li	8	55.3597
7B	8	22.4082	8Li	14	26.5979	9Li	2	59.5447
9B	3	39.0084	9Li	12	61.4593	6B	4	43.766
10B	3	20.4647	11Li	1	48.1783	7B	12	67.9766
8Be	1	18.679	6B	15	46.4419	9B	16	75.8128
10Be	12	40.8588	7B	38	49.1758	10B	14	74.3112
11Be	7	51.7829	9B	38	77.7756	11B	3	30.9861
12Be	2	54.9129	10B	27	58.6878	8Be	1	31.4403
13Be	3	74.8794	11B	5	72.9956	10Be	14	47.9495
10C	4	26.1238	12B	3	130.538	11Be	47	68.6276
11C	8	30.3852	8Be	4	57.0567	12Be	9	80.9854
12C	58	39.7331	10Be	65	54.9335	13Be	15	96.8192
13C	15	69.9368	11Be	113	61.8358	11C	6	52.8871
14C	14	70.5312	12Be	16	87.251	12C	93	43.014
15C	1	132.376	13Be	18	82.6265	13C	68	54.5486
16C	1	4.63159	8C	1	25.9818	14C	78	66.7064
13N	4	45.267	9C	2	64.9544	14N	18	27.4522
14N	34	44.7837	10C	5	37.8165	15N	158	35.0514
15N	62	49.9324	11C	38	39.5974			
15O	3	3.27835	12C	381	45.9699			
16O	1173	6.54663	13C	146	54.5844			
			14C	141	68.4774			
			15C	1	113.767			
			12N	5	19.955			
			13N	26	31.2878			
			14N	216	39.3511			
			15N	600	48.5647			
			16N	2	16.8344			
			15O	1	77.5707			
			16O	97	4.0188			

Table D. 3. Particle fluences cylindrical surface with radius of 0.1 cm centered on an ion beam passing through different depths in a water phantom. Initial fluence equal to 500,000 ^{12}C ions accelerated to 219 MeV/u. Surface area equal to $0.628 \cdot h \text{ cm}^2$, h given as range of depths.

Depth 0-0.001			Depth 0.001-1			Depth 1-2			Depth 2-3		
Particle	Quantity	Avg. E	Particle	Quantity	Avg. E	Particle	Quantity	Avg. E	Particle	Quantity	Avg. E
γ	187	2.55402	π^-	50	47.2908	π^-	37	51.5323	π^-	γ	53.5906
neutron	108	25.8071	μ^+	1	2.43873	(ν_e)	2	29.9021	μ^+	1	5.59691
1H	66	44.1193	(ν_e)	3	19.3705	β^+	1	46.2186	(ν_e)	3	40.859
2H	5	9.20318	β^+	2	33.0635	β^-	1	39.4222	(ν_μ)	1	26.5136
3H	3	5.02513	β^-	1	33.3434	(ν_μ)	3	37.3205	γ	42095	2.86251
3He	3	3.14927	μ^-	1	7.54966	γ	41501	3.03917	π^+	18	51.8687
4He	3	4.26437	(ν_μ)	8	32.6316	π^+	39	50.0405	neutron	73957	87.3576
6He	1	1.45276	γ	37199	3.18466	neutron	75772	91.7546	1H	69513	102.672
8He	1	3.01657	π^+	37	61.9209	1H	71875	107.501	2H	10212	97.1158
12C	23	218.95	neutron	62301	84.5341	2H	9536	100.089	3H	2622	113.542
			1H	58252	101.778	3H	2315	111.121	6H	16	136.454
			2H	6788	84.4002	6H	9	120.975	3He	2315	131.338
			3H	1426	87.6031	3He	2039	135.003	4He	13010	165.521
			6H	4	154.171	4He	10243	170.432	6He	81	160.183
			3He	1115	113.064	6He	66	161.629	8He	10	168.678
			4He	4679	153.283	8He	6	193.663	10He	1	0.22359
			6He	34	149.662	6Li	329	172.67	6Li	409	168.601
			8He	1	204.481	7Li	250	185.262	7Li	302	171.298
			6Li	140	148.27	8Li	46	181.2	8Li	69	172.059
			7Li	97	181.756	9Li	43	186.067	9Li	64	180.347
			8Li	27	164.067	11Li	1	2.11683	11Li	1	0.63107
			9Li	8	176.866	6B	154	170.768	6B	196	164.545
			6B	65	166.993	7B	190	181.177	7B	308	168.61
			7B	92	187.466	9B	102	185.77	9B	148	179.651
			9B	39	192.551	10B	153	194.301	10B	191	184.514
			10B	46	199.721	11B	1	192.815	11B	12	181.262
			11B	3	140.031	6Be	12	155.856	6Be	8	134.308
			6Be	5	143.079	8Be	47	178.97	8Be	38	166.54
			8Be	26	184.25	10Be	414	192.982	10Be	593	178.937
			10Be	146	200.98	11Be	741	195.325	11Be	1045	184.594
			11Be	269	202.841	12Be	13	167.814	12Be	11	181.625
			12Be	4	103.301	8C	10	172.835	8C	17	154.261
			13Be	1	0.70628	9C	49	183.241	9C	55	165.598
			8C	9	192.375	10C	137	189.827	10C	216	173.993
			9C	15	193.657	11C	746	192.512	11C	1082	178.793
			10C	62	199.257	12C	8106	198.348	12C	11030	184.626
			11C	254	204.333	13C	4	0.54896	13C	5	0.89823
			12C	3574	210.002	14C	1	0.58462	12N	79	175.182
			13C	2	0.0535	12N	55	189.468	13N	1	2.23855
			14C	1	0.17477	14N	3	0.65319	14N	4	0.37332
			12N	27	198.85	15N	3	0.11083	15N	7	0.48454
			13N	2	0.25268	14O	1	0.00336	15O	5	0.33705
			14N	5	0.44191	16O	12	0.30446	16O	8	0.39117
			15N	3	0.62775						
			15O	6	0.35132						
			16O	7	0.16364						

Depth 3-4			Depth 4-5			Depth 5-6			Depth 6-7		
Particle	Quantity	Avg. E	Particle	Quantity	Avg. E	Particle	Quantity	Avg. E	Particle	Quantity	Avg. E
π^-	18	49.0892	π^-	6	33.3412	π^-	3	31.7113	γ	43617	2.35782
(ν_e)	2	24.7223	(ν_e)	1	47.6821	(ν_μ)	1	23.921	neutron	57400	58.2088
β^+	1	8.06126	β^-	1	17.0186	γ	42858	2.46986	1H	51782	69.871
(ν_μ)	3	30.3014	(ν_μ)	3	43.0445	π^+	2	42.4504	2H	9027	67.738
γ	42356	2.68434	γ	43072	2.53807	neutron	61499	67.1824	3H	2830	75.7397
π^+	7	42.3574	π^+	7	39.5481	1H	56732	79.5805	6H	12	64.5124
neutron	69391	81.3784	neutron	66229	74.286	2H	9461	76.8229	3He	2407	84.3285
1H	64897	95.5215	1H	60894	87.8289	3H	2723	85.4023	4He	14616	111.372
2H	9917	93.0191	2H	9836	84.1053	6H	16	65.6191	6He	94	101.86
3H	2665	105.446	3H	2658	95.9004	3He	2365	96.1458	8He	7	142.385
6H	3	48.31	6H	16	90.563	4He	14581	127.437	10He	1	1.72578
3He	2319	120.765	3He	2426	109.307	6He	112	118.295	6Li	509	109.961
4He	13900	155.588	4He	14275	142.554	8He	12	97.613	7Li	374	115.993
6He	89	148.515	6He	90	128.956	6Li	527	127.926	8Li	61	109.164
8He	5	179.658	8He	8	130.657	7Li	389	134.094	9Li	68	128.155
6Li	450	159.213	10He	1	141.049	8Li	77	126.592	6B	208	97.192
7Li	356	163.366	6Li	480	142.432	9Li	54	143.631	7B	324	108.877
8Li	80	153.423	7Li	359	148.351	6B	195	115.059	9B	159	118.581
9Li	67	163.51	8Li	67	151.498	7B	363	129.195	10B	281	130.588
6B	233	144.897	9Li	65	153.07	9B	196	131.19	11B	6	53.1632
7B	322	157.783	6B	187	127.221	10B	290	146.939	6Be	5	88.9692
9B	175	164.554	7B	335	143.789	11B	7	137.69	8Be	62	97.6554
10B	239	171.337	9B	196	154.488	6Be	6	85.1599	10Be	730	117.198
11B	7	164.488	10B	229	160.499	8Be	53	118.482	11Be	1423	125.556
6Be	10	143.866	11B	5	150.773	10Be	739	134.642	12Be	17	118.985
8Be	54	154.809	6Be	7	136.619	11Be	1341	142.378	8C	13	72.8004
10Be	651	165.741	8Be	71	138.046	12Be	17	141.09	9C	69	94.6392
11Be	1261	171.147	10Be	755	150.288	8C	12	98.8634	10C	325	102.42
12Be	22	162.957	11Be	1290	156.661	9C	58	113.988	11C	1434	111.491
8C	14	127.825	12Be	21	148.004	10C	287	121.765	12C	15744	119.605
9C	69	151.39	8C	23	129.099	11C	1427	130.689	13C	4	0.74695
10C	261	158.261	9C	71	133.246	12C	15245	138.016	14C	4	1.00911
11C	1232	164.276	10C	267	141.717	13C	4	0.9452	12N	158	98.9902
12C	12845	170.211	11C	1346	147.937	14C	2	0.55379	13N	2	1.34396
13C	4	1.10443	12C	14087	154.66	12N	153	120.681	14N	6	0.78855
14C	3	0.53817	13C	5	0.59547	14N	8	1.41492	15N	3	0.73432
12N	115	159.748	12N	112	140.791	15N	5	0.63552	12O	2	61.146
13N	2	1.42622	13N	2	0.93382	14O	1	0.53199	15O	3	0.41115
14N	3	0.40457	14N	6	0.65318	15O	1	1.03791	16O	8	0.64015
15N	1	0.49571	15N	2	0.53489	16O	6	0.64471			
15O	2	0.42807	14O	1	0.1886						
16O	3	0.48058	15O	5	0.43747						
			16O	8	0.32243						

Depth 7-8			Depth 8-9			Depth 9-9.97995			Depth 9.97995-9.98005		
Particle	Quantity	Avg. E	Particle	Quantity	Avg. E	Particle	Quantity	Avg. E	Particle	Quantity	Avg. E
γ	43555	2.29368	π^-	1	17.352	γ	41004	2.17545	γ	3	0.4509
neutron	52917	49.3676	γ	44038	2.32986	neutron	43460	26.3106	neutron	4	10.398
1H	46458	60.0417	neutron	49427	39.075	1H	33668	31.9076	1H	2	11.2115
2H	8840	57.1657	1H	42185	47.0199	2H	7698	28.8715	4He	1	28.4809
3H	2751	60.0536	2H	8738	44.7716	3H	2698	30.0558	11Be	1	57.8559
6H	16	54.1616	3H	3028	46.614	6H	10	25.6873	12C	14	8.36322
3He	2500	68.8796	6H	19	44.0423	3He	2150	32.3601			
4He	14910	91.328	3He	2506	52.9093	4He	16082	39.8815			
6He	93	81.4403	4He	15950	67.6844	6He	135	37.3307			
8He	17	109.371	6He	102	55.6659	8He	10	57.3153			
6Li	519	88.3396	8He	12	83.058	10He	1	6.08699			
7Li	383	95.8108	6Li	596	62.4736	6Li	619	36.4668			
8Li	82	96.7743	7Li	431	70.2764	7Li	443	38.6732			
9Li	68	109.247	8Li	69	63.613	8Li	78	36.1687			
6B	204	72.5456	9Li	62	90.459	9Li	47	55.0785			
7B	398	90.3163	11Li	1	18.1329	11Li	1	38.5689			
9B	188	101.947	6B	201	48.867	6B	147	28.6757			
10B	314	113.47	7B	411	63.7261	7B	366	34.5734			
11B	7	97.8554	9B	166	77.8415	9B	183	45.2509			
6Be	3	50.3363	10B	263	91.667	10B	287	64.3229			
8Be	52	81.8935	11B	12	69.6563	11B	10	34.8157			
10Be	725	97.9575	12B	1	3.7719	12B	4	8.63049			
11Be	1471	107.33	6Be	7	38.8716	6Be	2	34.2912			
12Be	14	98.7636	8Be	71	52.3613	8Be	55	24.4548			
13Be	1	0.34238	10Be	717	72.7691	10Be	586	43.229			
8C	11	67.778	11Be	1503	84.8862	11Be	1393	60.0982			
9C	65	71.3391	12Be	16	59.9105	12Be	27	35.1617			
10C	326	79.3513	13Be	2	31.9036	13Be	4	4.77479			
11C	1549	89.6068	15Be	1	1.39005	14Be	1	1.59094			
12C	16788	99.0092	8C	3	36.5071	8C	8	21.7161			
13C	13	6.84271	9C	57	46.383	9C	22	23.3336			
14C	1	0.44544	10C	279	54.5182	10C	130	28.9075			
12N	175	68.9931	11C	1432	62.137	11C	924	32.2069			
13N	2	1.37168	12C	17569	74.399	12C	18221	38.9895			
14N	10	0.98369	13C	8	2.64546	13C	11	4.52167			
15N	2	1.68812	15C	1	3.00854	14C	5	3.28791			
14O	2	0.77357	12N	156	52.3449	15C	1	1.52142			
15O	4	0.29989	14N	11	1.15651	12N	95	28.6589			
16O	2	0.70807	15N	4	1.70598	13N	8	4.48818			
			13O	1	0.09833	14N	16	3.02457			
			14O	2	0.80376	15N	12	3.13249			
			15O	4	1.44646	16N	2	3.84689			
			16O	4	1.14911	14O	1	0.0584			
			16Ne	1	1.62584	15O	7	2.39336			
						16O	12	2.91633			
						17O	1	1.47007			
						18O	1	5.50327			
						19F	1	3.2292			
						20Ne	1	1.93574			
						21Ne	1	0.71324			
						22Na	1	1.67659			

Depth 9.98005-10			Depth 10-11			Depth 11-12		
Particle	Quantity	Avg. E	Particle	Quantity	Avg. E	Particle	Quantity	Avg. E
γ	472	1.60641	γ	14410	0.61542	(ν_{-e})	1	28.188
neutron	628	19.5566	neutron	8113	28.4982	γ	12310	0.25191
1H	363	24.6719	1H	4167	37.2523	neutron	2521	33.7745
2H	78	18.1303	2H	1077	37.676	1H	1034	51.4826
3H	30	23.1298	3H	392	39.6707	2H	275	57.7887
3He	9	34.9818	6H	1	73.2211	3H	119	63.6631
4He	135	36.8395	3He	211	43.5799	3He	84	50.1842
6Li	5	35.2236	4He	2865	47.1778	4He	883	60.779
7Li	2	12.0736	6He	17	72.7377	6He	8	85.8778
8Li	1	26.677	8He	3	71.1974	6Li	21	51.0721
9Li	1	35.0095	6Li	82	49.172	7Li	27	60.7424
7B	1	9.36298	7Li	67	54.1686	8Li	10	73.2259
9B	1	39.9382	8Li	17	65.5451	9Li	13	87.1789
10B	3	84.3825	9Li	17	86.4604	7B	5	41.2266
11B	1	17.0994	6B	4	49.4082	9B	26	59.2128
10Be	7	25.4938	7B	34	30.4973	10B	63	63.4026
11Be	14	54.4871	9B	43	55.5204	10Be	26	37.2483
12C	810	6.77239	10B	144	63.627	11Be	262	43.1787
12N	1	4.01707	8Be	2	44.1509	11C	2	10.3056
			10Be	148	37.6143	12C	1	1.16178
			11Be	717	48.3614	13C	1	1.72599
			10C	1	74.4786	15N	1	2.31258
			11C	3	24.7088			
			12C	790	5.33041			
			14N	2	0.1993			

Table D. 4. Particle fluences cylindrical surface with radius of 0.1 cm centered on an ion beam passing through different depths in a water phantom. Initial fluence equal to 500,000 ${}^7\text{Li}$ ions accelerated to 134.5 MeV/u. Surface area equal to $0.628 \cdot h \text{ cm}^2$, h given as range of depths.

Depth 0-0.001			Depth 0.001-1			Depth 1-2			Depth 2-3		
Particle	Quantity	Avg. E	Particle	Quantity	Avg. E	Particle	Quantity	Avg. E	Particle	Quantity	Avg. E
γ	219	2.2983	μ^+	1	3.70913	γ	48905	2.80508	(v_e)	1	46.5746
neutron	112	16.869	(v_μ)	1	30.8432	neutron	80431	56.5187	\square	1	46.5746
1H	56	24.3166	γ	45920	2.8749	1H	54302	61.443	γ	48428	2.70663
2H	7	13.6873	π^+	2	24.3287	2H	11477	71.8134	neutron	76889	54.0457
3H	4	8.766	neutron	68330	51.6556	3H	5544	96.4401	1H	50736	58.117
4He	4	1.34929	1H	47464	58.4878	6H	20	59.8464	2H	11318	69.1
7Li	36	134.462	2H	8128	62.5385	3He	2002	82.1128	3H	5482	90.1564
12C	1	0.38087	3H	3262	86.6668	4He	10594	101.026	6H	15	52.5486
			6H	8	60.8808	6He	626	117.404	3He	2011	79.4118
			3He	1243	75.6001	6Li	779	110.751	4He	10982	94.9089
			4He	5989	93.6984	7Li	10275	122.128	6He	705	112.68
			6He	261	120.535	8Li	3	0.33778	8He	1	9.18089
			8He	2	5.06204	6B	84	93.0125	6Li	845	104.061
			10He	1	8.27527	7B	55	95.6306	7Li	13430	114.028
			6Li	393	114.506	9B	4	0.93778	8Li	4	7.28228
			7Li	4699	129.035	10B	2	1.2644	9Li	3	1.7288
			9Li	1	0.26733	6Be	1	2.52233	6B	110	87.3782
			6B	28	102.621	8Be	1	1.52599	7B	70	94.3018
			7B	19	58.8848	10Be	4	1.47696	9B	6	2.6439
			9B	7	0.90298	11Be	4	0.45063	10B	1	2.80879
			10B	9	1.00101	12Be	2	0.29539	10Be	8	1.45777
			11B	1	0.47553	11C	4	2.27155	11Be	6	1.10423
			8Be	1	2.65912	12C	15	0.55901	12Be	1	1.75802
			10Be	7	1.31708	13C	3	0.71844	8C	1	1.09684
			11Be	4	0.60535	14C	1	1.38504	10C	1	1.41407
			14Be	1	0.14981	13N	3	0.51818	11C	5	0.59495
			11C	1	0.00132	14N	10	0.78584	12C	13	0.64203
			12C	16	0.82903	15N	4	0.36285	13C	6	0.59292
			13C	8	1.29896	14O	4	0.60865	13N	1	0.84001
			12N	1	0.30001	15O	4	0.46074	14N	11	0.52764
			13N	2	0.19029	16O	8	0.23587	15N	3	0.14629
			14N	6	0.38263				15O	5	0.4205
			15N	5	0.37177				16O	14	0.41708
			14O	1	0.34344						
			15O	5	0.24459						
			16O	16	0.19309						

Depth 3-4			Depth 4-5			Depth 5-6			Depth 6-7		
Particle	Quantity	Avg. E	Particle	Quantity	Avg. E	Particle	Quantity	Avg. E	Particle	Quantity	Avg. E
γ	47767	2.60758	γ	46749	2.44507	γ	45890	2.32933	γ	44455	2.29059
neutron	71231	50.4954	π^+	1	6.17308	neutron	60001	41.9863	neutron	54715	37.0322
1H	46632	54.5535	neutron	65235	46.6263	1H	37140	45.7692	1H	32842	40.4984
2H	10899	64.8424	1H	41330	50.1726	2H	9733	54.069	2H	9077	47.1292
3H	5246	82.22	2H	10059	59.4585	3H	4517	66.1301	3H	4285	57.0408
6H	18	68.7148	3H	4949	76.4479	6H	17	56.3511	6H	7	54.5173
3He	1984	71.7558	6H	18	77.2695	3He	1872	58.3668	3He	1832	50.7127
4He	10771	88.028	3He	2019	65.1419	4He	9754	70.1407	4He	9018	59.4931
6He	775	105.681	4He	10144	79.4612	6He	841	88.926	6He	887	80.117
6Li	923	95.8981	6He	882	97.2064	6Li	884	75.4336	10He	1	3.53422
7Li	15551	105.291	8He	2	2.40584	7Li	18401	85.7205	6Li	843	64.6327
8Li	1	0.72703	10He	1	2.25776	8Li	4	3.49874	7Li	19403	74.5413
6B	93	80.2848	6Li	865	85.9815	9Li	2	1.68756	8Li	3	3.34267
7B	83	84.48	7Li	17302	95.947	6B	97	57.1573	6B	97	47.3052
9B	5	1.4726	8Li	3	1.37143	7B	81	57.4501	7B	73	47.1866
10B	3	1.92589	6B	113	70.3175	9B	2	1.34637	9B	3	2.56526
11B	1	4.08258	7B	86	67.0615	10B	2	3.58836	10B	2	0.76213
12B	1	3.05562	9B	2	0.12562	10Be	5	0.91885	11B	1	2.6907
10Be	6	1.63919	10B	1	2.6726	11Be	9	1.60232	10Be	8	1.78273
11Be	10	1.42696	12B	1	3.85223	12Be	1	2.42831	11Be	5	1.04142
13Be	1	0.41327	10Be	4	1.909	13Be	1	0.93034	13Be	1	1.22665
10C	1	1.66618	11Be	9	1.1335	11C	7	1.50164	11C	5	1.22656
11C	2	0.68219	12Be	1	0.06248	12C	12	1.15437	12C	23	1.21231
12C	14	0.62923	13Be	1	0.01483	13C	4	0.5862	13C	9	0.99112
13C	7	0.45517	11C	2	0.89917	14C	2	0.69664	14C	1	0.44203
14C	2	0.40406	12C	12	0.65854	13N	3	0.56818	12N	1	0.82462
12N	1	1.04165	13C	8	0.70439	14N	12	0.65915	13N	1	0.95355
13N	2	0.85407	14C	3	0.78803	15N	9	0.50841	14N	9	0.81003
14N	6	0.50763	12N	1	1.03447	15O	6	0.69386	15N	3	0.808
15N	7	0.5049	13N	4	0.46138	16O	8	0.30974	15O	5	0.55103
15O	7	0.41176	14N	7	0.55215				16O	8	0.70259
16O	4	0.4753	15N	8	0.34013						
			16N	1	0.03033						
			14O	1	1.06226						
			15O	8	0.6493						
			16O	7	0.18265						

Depth 7-8			Depth 8-9			Depth 9-9.97995			Depth 9.97995-9.98005		
Particle	Quantity	Avg. E	Particle	Quantity	Avg. E	Particle	Quantity	Avg. E	Particle	Quantity	Avg. E
γ	42790	2.17505	γ	40531	2.09901	γ	33510	1.75866	γ	2	0.00208
neutron	48839	31.3876	neutron	43623	24.675	neutron	32605	16.6068	neutron	2	21.0988
1H	27789	34.8173	1H	22761	27.8835	1H	14145	19.8792	1H	1	6.76473
2H	8230	39.7659	2H	7346	30.5292	2H	4722	20.8803	7Li	1	10.5483
3H	4063	46.4296	3H	3587	34.5482	3H	2655	23.3996			
6H	9	43.6246	6H	13	24.1133	6H	7	15.0046			
3He	1760	40.2947	3He	1611	29.3688	3He	1006	18.5693			
4He	8259	48.3881	4He	7696	34.0586	4He	5064	20.3134			
6He	747	69.7317	6He	741	58.1206	6He	668	45.2933			
6Li	779	50.6534	6Li	648	34.649	8He	1	12.8001			
7Li	20251	61.9025	7Li	20772	46.6943	6Li	315	17.763			
8Li	1	1.24065	8Li	3	4.33384	7Li	20747	24.9001			
9Li	2	2.77063	9Li	1	0.74025	8Li	9	9.47194			
6B	77	36.9036	6B	69	25.4695	9Li	1	0.85127			
7B	60	40.0123	7B	56	28.4154	6B	22	11.5607			
9B	5	2.23609	9B	12	2.5632	7B	33	17.6895			
10B	8	2.33733	10B	3	1.64409	9B	3	2.32355			
11B	1	2.32918	8Be	2	5.04125	10B	2	3.82599			
10Be	8	1.4826	10Be	6	2.07813	10Be	5	2.34252			
11Be	1	1.78458	11Be	13	1.45412	11Be	4	1.09789			
12Be	3	1.99641	12Be	3	3.22772	14Be	1	1.15929			
14Be	1	2.12532	13Be	1	0.25712	11C	1	2.89744			
9C	1	14.7072	11C	7	2.72165	12C	20	1.3422			
11C	4	0.63652	12C	23	1.42478	13C	13	1.32879			
12C	23	1.50403	13C	9	1.1682	14C	3	2.23183			
13C	11	0.74058	14C	2	0.22269	15C	2	2.41533			
14C	2	1.77429	13N	4	0.97182	13N	2	1.89802			
12N	1	1.10624	14N	12	1.27043	14N	14	1.38549			
13N	1	0.29731	15N	6	0.66949	15N	10	1.36841			
14N	7	0.92782	16N	2	0.2424	16N	3	1.4969			
15N	8	0.74235	15O	7	1.1209	17N	1	0.13253			
16N	2	0.176	16O	7	0.65511	15O	1	0.65848			
13O	1	3.49574				16O	4	1.11581			
15O	4	0.68148				17O	1	0.33848			
16O	4	0.66148				18F	1	1.00092			
						21F	1	0.63157			

Depth 9.98005-10			Depth 10-11			Depth 11-12		
Particle	Quantity	Avg. E	Particle	Quantity	Avg. E	Particle	Quantity	Avg. E
γ	353	0.88708	γ	14306	0.25885	(v _{μ})	1	43.5081
neutron	274	15.9594	neutron	3773	19.8409	γ	12718	0.09044
1H	73	17.2386	1H	657	27.3467	neutron	1302	23.8401
2H	30	20.5051	2H	429	30.6576	1H	157	32.6858
3H	35	23.2354	3H	621	24.3079	2H	105	37.2875
3He	6	14.7893	3He	42	15.8235	3H	125	37.6648
4He	52	15.6468	4He	561	21.2006	3He	10	24.2115
6He	11	35.7856	6He	416	38.0767	4He	70	27.6789
7Li	851	5.37365	7Li	1166	4.27886	6He	218	41.8475

Table D. 5. Particle fluences cylindrical surface with radius of 0.1 cm centered on an ion beam passing through different depths in a water phantom. Initial fluence equal to 500,000 ^4He ions accelerated to 116.5 MeV/u. Surface area equal to $0.628 \cdot h \text{ cm}^2$, h given as range of depths.

Depth 0-0.001			Depth 0.001-1			Depth 1-2			Depth 2-3		
Particle	Quantity	Avg. E	Particle	Quantity	Avg. E	Particle	Quantity	Avg. E	Particle	Quantity	Avg. E
γ	57	2.84448	π^-	1	14.9959	π^-	1	8.13889	γ	14698	2.69688
neutron	30	12.289	γ	12640	2.83492	(ν_μ)	1	31.4841	π^+	1	47.9676
1H	19	27.8082	π^+	1	6.84968	γ	14283	2.77385	neutron	18621	38.866
2H	2	17.7022	neutron	16237	39.415	π^+	1	13.7725	1H	16279	50.7284
4He	50	114.172	1H	13954	51.0092	neutron	18963	41.1283	2H	3058	59.3356
			2H	2140	57.9754	1H	16876	53.5452	3H	1173	79.175
			3H	736	79.423	2H	3018	63.1941	6H	1	1.22691
			3He	906	90.9004	3H	1132	82.7003	3He	1909	84.1282
			4He	7494	107.309	3He	1861	89.9465	4He	21052	97.135
			6He	1	0.72123	4He	15876	103.582	6He	1	0.94882
			6Li	2	1.89237	6He	1	2.3569	6Li	11	1.84919
			7Li	3	2.55246	6Li	8	1.43479	7Li	1	0.53323
			7B	2	2.06032	7Li	4	1.77844	8Li	1	1.72353
			9B	2	1.5803	8Li	1	1.71646	7B	3	2.19243
			10B	1	0.3443	11Li	1	0.4594	9B	3	1.53675
			11C	1	5.64523	7B	1	4.15534	11B	1	0.7533
			12C	4	0.27374	9B	5	0.6139	10Be	2	0.1543
			13N	1	0.77103	10Be	2	1.06256	11Be	2	0.32439
			14N	2	0.02966	11Be	2	0.20782	12C	9	0.45493
			15N	2	0.21156	11C	3	0.48026	13C	1	0.27974
			16O	2	0.10223	12C	2	0.44867	13N	2	0.0119
						13C	1	0.10481	14N	3	0.22624
						14C	1	0.00258	15N	1	0.02463
						14N	2	0.87081	15O	1	0.14397
						16O	5	0.18664	16O	1	0.248

Depth 3-4			Depth 4-5			Depth 5-6			Depth 6-7		
Particle	Quantity	Avg. E	Particle	Quantity	Avg. E	Particle	Quantity	Avg. E	Particle	Quantity	Avg. E
γ	15142	2.51809	γ	15413	2.46513	γ	15871	2.3985	γ	16458	2.37083
neutron	17500	35.5357	neutron	16714	32.2692	π^+	1	24.9526	neutron	14743	24.7397
1H	15185	47.4118	1H	14188	43.2887	neutron	15628	28.6206	1H	11727	34.1043
2H	3044	54.1078	2H	2888	49.7065	1H	12868	38.7816	2H	2706	37.6288
3H	1176	72.1753	3H	1212	65.5202	2H	2845	43.871	3H	1185	49.0828
3He	1948	75.8601	6H	1	16.5713	3H	1211	58.0207	6H	1	5.08121
4He	24915	90.0232	3He	1928	68.6114	3He	1985	59.6769	3He	2048	49.4826
6He	2	2.28111	4He	28340	82.1811	4He	30640	73.533	4He	33074	63.9222
6Li	2	1.86348	6Li	8	2.54832	6He	1	0.32166	6He	1	2.23982
7Li	4	2.4305	7Li	2	0.54008	6Li	6	2.15811	6Li	14	3.03981
8Li	1	1.78291	9Li	1	2.31173	7Li	2	2.22175	7Li	2	2.22264
7B	2	0.55343	7B	3	2.97403	8Li	1	0.96466	7B	1	1.11862
10B	1	1.05557	10Be	1	1.72967	9Li	1	0.01576	10B	1	4.45989
10Be	1	0.21559	11C	2	0.4571	9B	3	1.14455	10Be	4	1.34215
11Be	2	0.52033	12C	8	0.609	10B	1	1.5818	11Be	3	1.56213
11C	1	1.98588	13C	1	0.92646	10Be	1	0.58309	13Be	1	0.92971
12C	7	0.34636	13N	1	0.05397	11Be	2	0.46187	11C	1	0.01234
13N	1	0.2139	14N	2	0.25998	12C	4	0.51999	12C	6	0.39702
14N	3	0.79853	15N	1	0.00328	13C	1	1.0465	13C	1	0.03377
15N	1	1.08359	15O	1	0.34038	13N	1	0.20749	14C	1	0.75588
15O	2	0.3823	16O	1	0.2981	14N	1	0.41988	12N	1	0.44214
16O	8	0.09511				15N	3	0.47742	13N	1	0.20914
						14O	1	0.55128	14N	6	0.33792
									15N	2	0.33926
									15O	5	0.43427
									16O	2	0.29946

Depth 7-8			Depth 8-9			Depth 9-9.95995			Depth 9.995995-9.96005		
Particle	Quantity	Avg. E	Particle	Quantity	Avg. E	Particle	Quantity	Avg. E	Particle	Quantity	Avg. E
γ	16459	2.41722	γ	17171	2.58903	γ	15134	2.48884	neutron	2	21.6245
neutron	13454	20.7367	neutron	12264	15.7691	neutron	9685	11.0161	4He	8	4.3813
1H	10240	28.8984	1H	8474	22.9357	1H	5869	16.8774			
2H	2489	30.0481	2H	2230	21.4396	2H	1258	13.0836			
3H	1141	39.2022	3H	1157	27.2708	3H	659	17.0833			
3He	1962	37.704	3He	1789	25.9587	3He	876	14.6992			
4He	34670	52.9811	4He	35657	39.7418	4He	33613	21.6522			
6Li	7	2.12849	6Li	8	4.36784	6Li	2	1.44744			
7Li	2	2.97251	8Li	1	2.29356	9B	1	0.11034			
7B	2	1.45996	7B	2	3.29931	10Be	1	0.84431			
10B	3	1.8952	9B	2	0.94116	11Be	1	1.18827			
11B	1	0.41615	10B	1	0.65821	12C	4	0.65009			
11Be	2	1.11009	10Be	2	0.87969	13N	1	0.26486			
11C	1	0.703	11Be	3	0.15028	14N	2	0.06053			
12C	10	0.85455	12Be	1	1.32728	15O	1	0.06903			
13C	3	1.00444	11C	2	1.22788	16O	2	0.47019			
14C	1	0.17639	12C	16	0.74398	17O	1	0.15405			
12N	1	0.53444	13C	3	0.44006	17F	1	0.48317			
13N	2	0.19701	13N	1	0.44581						
14N	2	0.75268	14N	4	0.55899						
15N	1	0.46007	15N	2	0.46274						
15O	2	0.2708	15O	2	0.25923						
16O	4	0.11622	16O	2	0.47263						

Depth 9.96005-10			Depth 10-11			Depth 11-12		
Particle	Quantity	Avg. E	Particle	Quantity	Avg. E	Particle	Quantity	Avg. E
γ	331	1.12736	γ	5157	0.29776	γ	4589	0.04337
neutron	123	8.67838	neutron	804	13.8603	neutron	302	14.0197
1H	76	14.7608	1H	280	18.1712	1H	18	26.8722
2H	4	19.4536	2H	30	24.0858	2H	8	30.0474
3H	4	28.2232	3H	67	26.5964	3H	13	31.8179
3He	4	14.6961	3He	7	4.69304			
4He	2243	5.50709	4He	1766	4.28932			

Table D. 6. Particle fluences cylindrical surface with radius of 0.1 cm centered on an ion beam passing through different depths in a water phantom. Initial fluence equal to 500,000 ¹H ions accelerated to 116.5 MeV/u. Surface area equal to 0.628*h cm², h given as range of depths.

Depth 0-0.001			Depth 0.001-1			Depth 1-2			Depth 2-3		
Particle	Quantity	Avg. E	Particle	Quantity	Avg. E	Particle	Quantity	Avg. E	Particle	Quantity	Avg. E
γ	13	2.78788	γ	2918	2.64854	γ	3282	2.616	γ	3432	2.48568
neutron	9	14.299	neutron	3044	33.0962	neutron	3234	33.8896	neutron	3183	32.2945
1H	102	108.591	1H	21005	91.9299	1H	38222	94.9108	1H	48948	91.28
			2H	13	3.33631	2H	12	2.87858	2H	15	3.24678
			4He	16	1.55031	3H	1	2.08776	3H	2	1.67609
			12C	1	0.0272	3He	1	2.18418	3He	1	2.09184
			16O	1	0.08938	4He	7	0.91668	4He	9	1.94701
						13C	1	0.10622	15N	1	0.00648
						13N	1	0.04525	15O	1	0.05418
						14N	1	0.0062	16O	4	0.00833
						16O	4	0.01984			
Depth 3-4			Depth 4-5			Depth 5-6			Depth 6-7		
Particle	Quantity	Avg. E	Particle	Quantity	Avg. E	Particle	Quantity	Avg. E	Particle	Quantity	Avg. E
γ	3294	2.50492	γ	3025	2.39095	γ	3094	2.2875	γ	3008	2.27467
neutron	2925	29.2745	neutron	2540	26.3696	neutron	2285	24.6364	neutron	1968	21.5264
1H	55529	85.6875	1H	59536	79.0286	1H	60237	71.2561	1H	57024	62.269
2H	9	3.54908	2H	8	2.76896	2H	5	7.05119	2H	3	2.5703
3H	1	2.40295	3H	1	0.92874	3H	1	2.66744	3H	1	1.23007
3He	2	0.86613	4He	10	1.07606	3He	2	4.47089	4He	9	1.72206
4He	10	1.04295	7B	1	0.70901	4He	9	1.17246	14N	2	0.21551
6Li	1	1.10112	11C	1	0.15101	14N	1	0.05574	15O	1	0.03856
10C	1	0.18684	12C	2	0.22892	15N	1	0.00115	16O	2	0.02035
12C	1	0.16134	15N	1	0.11762	15O	1	0.00159			
			14O	1	0.06233	16O	2	0.00109			
			16O	1	0.04485						
Depth 7-8			Depth 8-9			Depth 9-9.93995			Depth 9.93995-9.94005		
Particle	Quantity	Avg. E	Particle	Quantity	Avg. E	Particle	Quantity	Avg. E	Particle	Quantity	Avg. E
γ	2831	2.13053	γ	2818	2.121	γ	2703	2.20331	γ	1	4.58694
neutron	1625	19.1238	neutron	1368	15.6734	neutron	850	10.4702	1H	5	7.23864
1H	49711	51.9534	1H	42309	39.222	1H	31958	22.2756			
2H	1	2.76167	2H	5	2.59309	2H	1	5.10778			
3He	1	0.06118	4He	7	1.45647	4He	10	0.63451			
4He	10	1.27264	12C	1	0.1512	15O	1	0.01513			
12C	2	0.09394	16O	3	0.00357						
15N	1	0.07793									
15O	1	0.0463									
16O	3	0.01005									
Depth 9.94005-10			Depth 10-11			Depth 11-12					
Particle	Quantity	Avg. E	Particle	Quantity	Avg. E	Particle	Quantity	Avg. E			
γ	94	1.65614	γ	926	0.37362	γ	834	0.04738			
neutron	37	9.0238	neutron	140	7.67881	neutron	40	3.39362			
1H	2419	7.91613	1H	2363	6.40652						

APPENDIX E

Particle Fluences through cylindrical surface with radius of 1 cm centered on an ion beam passing through a water phantom.

Table E. 1. Particle fluences cylindrical surface with radius of 1 cm centered on an ion beam passing through different depths in a water phantom. Initial fluence equal to 500,000 ^{20}Ne ions accelerated to 296 MeV/u. Surface area equal to $6.28 \cdot h \text{ cm}^2$, h given as range of depths.

Depth 0-0.001			Depth 0.001-1			Depth 1-2			Depth 2-3		
Particle	Quantity	Avg. E	Particle	Quantity	Avg. E	Particle	Quantity	Avg. E	Particle	Quantity	Avg. E
γ	104	1.58137	π^-	153	56.4312	π^-	312	66.9777	π^-	270	71.0254
neutron	20	13.5977	($\bar{\nu}_e$)	35	34.4023	μ^+	2	25.0247	μ^+	5	4.74059
1H	3	79.7862	\square			($\bar{\nu}_e$)	42	39.8843	($\bar{\nu}_e$)	58	35.5298
			β^+	30	38.5621	\square			\square		
			β^-	11	30.4525	β^+	29	38.0912	β^+	39	33.7321
			($\bar{\nu}_\mu$)	77	31.5538	β^-	12	34.9635	β^-	23	31.8682
			γ	77021	1.6334	μ^-	5	21.8762	μ^-	1	3.58174
			π^+	170	66.6114	($\bar{\nu}_\mu$)	109	32.5377	($\bar{\nu}_\mu$)	95	31.5312
			neutron	24814	36.0011	γ	114726	1.87644	γ	141270	1.66541
			1H	10314	73.3057	π^+	289	74.8692	π^+	265	83.8245
			2H	408	42.372	neutron	61529	68.3841	neutron	85611	87.9115
			3H	14	29.6421	1H	38862	108.757	1H	59499	129.77
			3He	8	30.4036	2H	1992	73.7821	2H	3616	93.1491
						3H	142	49.8938	3H	271	77.2139
						3He	64	62.9346	3He	164	90.651
						4He	9	51.7651	4He	45	85.6483
									15O	1	0.09246
Depth 3-4			Depth 4-5			Depth 5-6			Depth 6-7		
Particle	Quantity	Avg. E	Particle	Quantity	Avg. E	Particle	Quantity	Avg. E	Particle	Quantity	Avg. E
π^-	210	69.3843	π^-	136	72.7356	π^-	82	67.0496	π^-	52	63.1293
μ^+	4	3.83498	μ^+	1	2.72402	μ^+	2	1.48908	μ^+	1	4.08729
($\bar{\nu}_e$)	39	38.5871	($\bar{\nu}_e$)	28	35.3444	($\bar{\nu}_e$)	24	40.5213	($\bar{\nu}_e$)	19	34.1844
\square			\square			\square			\square		
β^+	28	32.956	β^+	22	33.276	β^+	18	32.1917	β^+	10	31.2406
β^-	13	37.1127	β^-	9	36.271	β^-	7	34.7787	β^-	4	35.345
μ^-	1	7.60048	($\bar{\nu}_\mu$)	76	32.7915	μ^-	1	46.6811	μ^-	1	5.04081
($\bar{\nu}_\mu$)	90	32.7572	γ	184874	1.19744	($\bar{\nu}_\mu$)	47	32.5602	($\bar{\nu}_\mu$)	40	33.001
γ	164141	1.38417	π^+	130	84.1812	γ	202068	1.04095	γ	217756	0.95869
π^+	223	78.7168	neutron	105990	97.164	π^+	92	74.5479	π^+	52	77.1866
neutron	98969	95.1462	1H	74943	137.924	neutron	110147	96.2765	neutron	113746	94.1445
1H	69967	136.781	2H	5406	110.969	1H	77617	136.173	1H	78711	132.446
2H	4500	103.224	3H	539	98.3573	2H	6258	117.778	2H	7062	122.425
3H	383	83.6393	6H	1	234.979	3H	714	114.226	3H	892	126.743
6H	2	25.1584	3He	384	114.867	6H	2	95.3397	6H	1	190.049
3He	297	102.012	4He	96	114.136	3He	511	127.844	3He	774	141.642
4He	65	106.132	6Li	1	161.939	4He	254	160.027	4He	622	186.388
			14O	1	0.29441	6He	1	256.877	6He	4	250.015
						6Li	2	171.238	6Li	11	207.197
						7Li	1	237.758	7Li	1	236.328
						6B	4	155.034	6B	8	142.448
						7B	1	150.414	7B	3	160.389
						16O	1	0.11762	8Be	1	116.666
									13C	1	199.165
									16O	1	0.05146

Depth 7-8			Depth 8-9			Depth 9-9.95995			Depth 9.95995-9.96005		
Particle	Quantity	Avg. E	Particle	Quantity	Avg. E	Particle	Quantity	Avg. E	Particle	Quantity	Avg. E
π^-	28	59.1231	π^-	17	57.6466	π^-	12	42.4564	γ	20	1.1123
μ^+	1	2.70049	(ν_e)	7	31.4861	(ν_e)	12	38.834	neutron	12	69.7529
(ν_e)	18	38.1782	\square			\square			1H	5	107.699
β^+	8	28.7243	β^+	11	43.5066	β^+	4	38.8568	2H	1	17.4112
β^-	6	34.4966	β^-	6	37.4672	β^-	1	36.6032			
μ^-	1	72.497	(ν_μ)	25	29.8894	(ν_μ)	14	36.0527			
(ν_μ)	22	34.1261	γ	236633	0.89563	γ	223948	0.83749			
γ	230024	0.91534	π^+	24	83.8647	π^+	24	74.8338			
π^+	34	74.3705	neutron	116852	86.2205	neutron	109746	81.2446			
neutron	115826	90.6366	1H	76112	122.456	1H	68368	116.895			
1H	78421	128.687	2H	8614	127.17	2H	8601	125.008			
2H	7749	126.165	3H	1489	141.756	3H	1835	139.791			
3H	1226	135.833	3He	1345	146.865	6H	6	167.102			
6H	1	183.984	4He	2503	193.573	3He	1606	143.2			
3He	992	147.715	6He	11	201.103	4He	3892	182.712			
4He	1400	199.137	8He	1	190.574	6He	21	202.823			
6He	5	226.516	6Li	78	191.386	8He	2	223.527			
6Li	17	205.991	7Li	17	189.984	10He	1	173.292			
7Li	9	207.723	8Li	3	220.129	6Li	120	175.366			
8Li	1	215.601	6B	39	133.284	7Li	45	190.531			
9Li	1	243.199	7B	21	171.413	8Li	9	195.932			
6B	21	129.809	9B	3	168.608	9Li	1	147.407			
7B	7	188.316	10B	3	176.635	6B	49	118.226			
9B	2	205.081	6Be	1	101.916	7B	56	147.321			
6Be	1	146.885	8Be	3	124.92	9B	11	183.883			
11Be	1	192.529	10Be	10	168.476	10B	10	183.454			
12Be	1	196.263	11Be	3	164.495	6Be	1	78.6971			
10C	3	134.121	10C	1	156.548	8Be	5	120.361			
			11C	3	126.71	10Be	19	150.611			
			12C	8	148.053	11Be	12	148.706			
			13C	2	152.924	14Be	1	214.749			
			13N	1	162.322	8C	2	83.1573			
			14N	2	132.047	9C	1	101.966			
			15N	3	55.4538	10C	1	79.179			
						11C	3	137.561			
						12C	14	131.012			
						13C	1	148.763			
						12N	1	124.607			
						13N	1	97.6546			
						14N	1	81.0281			
						15N	2	126.912			
						15O	1	51.63			

Depth 9.96005-10			Depth 10-11			Depth 11-12		
Particle	Quantity	Avg. E	Particle	Quantity	Avg. E	Particle	Quantity	Avg. E
(v_μ)	1	29.7839	π-	7	51.5095	π-	8	73.6395
γ	8923	0.7516	(v_e)	9	41.7569	(v_e)	8	40.2256
			□			□		
π+	1	87.1269	β+	7	34.837	β+	5	21.0008
neutron	4490	76.9301	β-	2	29.2863	β-	2	45.62
1H	2707	113.871	(v_μ)	14	32.6174	(v_μ)	17	39.5427
2H	389	121.929	γ	209993	0.62161	γ	189437	0.42393
3H	74	148.871	π+	13	78.497	π+	13	64.0079
3He	66	139.449	neutron	105127	78.7072	neutron	85819	81.4124
4He	205	176.97	1H	62434	112.62	1H	50479	110.563
6He	1	227.484	2H	9319	121.323	2H	9346	115.978
6Li	7	154.167	3H	2191	131.939	3H	2605	121.32
7Li	2	200.548	6H	8	146.668	6H	8	143.801
8Li	1	224.528	3He	1939	130.031	3He	2217	118.327
9Li	1	215.814	4He	6531	164.547	4He	9684	141.299
6B	2	90.0168	6He	28	170.553	6He	64	134.455
7B	2	138.838	8He	1	183.427	8He	3	188.184
10B	1	131.548	6Li	212	159.45	6Li	335	132.772
12Be	1	132.175	7Li	75	163.805	7Li	139	145.44
12C	2	114.185	8Li	17	188.682	8Li	20	125.806
13C	1	101.611	9Li	3	163.441	9Li	7	134.49
14N	1	108.48	6B	64	95.1354	6B	65	98.9662
			7B	96	121.809	7B	139	96.2617
			9B	34	158.448	9B	34	124.151
			10B	20	186.658	10B	28	144.079
			11B	2	116.502	11B	1	171.924
			8Be	7	84.5696	8Be	10	63.9308
			10Be	34	129.219	10Be	63	105.674
			11Be	22	138.022	11Be	58	122.505
			12Be	4	154.003	12Be	10	139.434
			9C	1	37.2243	13Be	2	149.114
			10C	6	79.5556	9C	1	22.4576
			11C	25	80.6019	10C	6	62.3629
			12C	45	115.055	11C	35	71.7353
			13C	8	104.739	12C	81	85.069
			14C	2	131.579	13C	23	100.662
			12N	1	31.917	14C	4	120.936
			13N	2	60.9953	12N	1	46.5947
			14N	9	78.1585	13N	6	57.5363
			15N	3	72.4941	14N	25	62.5447
			15O	1	24.5282	15N	13	79.8409
			16O	3	77.5371	15O	1	16.2412
			18O	1	72.8869	16O	1	51.7126

Table E. 2. Particle fluences cylindrical surface with radius of 1 cm centered on an ion beam passing through different depths in a water phantom. Initial fluence equal to 500,000 ^{16}O ions accelerated to 259 MeV/u. Surface area equal to $6.28 \cdot h \text{ cm}^2$, h given as range of depths.

Depth 0-0.001			Depth 0.001-1			Depth 1-2			Depth 2-3		
Particle	Quantity	Avg. E	Particle	Quantity	Avg. E	Particle	Quantity	Avg. E	Particle	Quantity	Avg. E
γ	108	1.19735	π^-	49	48.509	π^-	106	55.4921	π^-	83	53.6054
neutron	16	16.3037	μ^+	1	5.68343	μ^+	2	4.87379	μ^+	1	6.06166
1H	4	32.5285	(ν_e)	17	27.6805	(ν_e)	30	34.5551	(ν_e)	24	29.0591
			\square			\square			\square		
			β^+	10	28.7495	β^+	26	35.0155	β^+	17	39.0441
			β^-	6	39.8839	β^-	8	32.7448	β^-	7	31.5223
			(ν_μ)	41	35.8795	(ν_μ)	54	35.3935	(ν_μ)	38	34.8887
			γ	67517	1.28481	γ	99630	1.48081	γ	123285	1.34423
			π^+	66	54.3744	π^+	107	65.4181	π^+	98	61.8141
			neutron	21168	31.884	neutron	51213	58.9309	neutron	69585	73.744
			1H	7908	64.5705	1H	29884	95.6785	1H	45279	113.48
			2H	323	39.7023	2H	1542	63.5811	2H	2820	82.1287
			3H	12	36.3359	3H	127	46.6356	3H	255	58.4778
			3He	6	32.3018	3He	72	64.6463	3He	129	81.7944
			4He	1	19.1304	4He	13	48.3962	4He	26	62.6735
									7Li	1	0.74906
									6B	1	29.6926
Depth 3-4			Depth 4-5			Depth 5-6			Depth 6-7		
Particle	Quantity	Avg. E	Particle	Quantity	Avg. E	Particle	Quantity	Avg. E	Particle	Quantity	Avg. E
π^-	69	52.397	π^-	43	68.9457	π^-	25	56.6459	π^-	γ	65.812
μ^+	1	2.46941	μ^+	1	3.16301	(ν_e)	6	28.754	(ν_e)	3	47.0796
(ν_e)	25	31.9166	(ν_e)	17	36.5887	\square			\square		
\square			β^+	10	38.7667	β^+	9	31.26	β^+	5	28.8402
β^+	14	40.3369	β^+	2	52.1069	β^-	5	38.5755	β^-	4	29.0104
β^-	5	36.6859	β^-	1	6.02088	(ν_μ)	21	34.1194	(ν_μ)	14	35.8697
μ^-	1	4.65948	(ν_μ)	26	33.3096	γ	176245	0.97886	γ	189095	0.92839
(ν_μ)	51	31.164	γ	159252	1.05668	π^+	24	76.4002	π^+	18	77.6555
γ	143390	1.1962	π^+	52	74.3052	neutron	88708	81.2946	neutron	90568	78.8486
π^+	62	79.2974	neutron	84628	81.6336	1H	58116	117.603	1H	58236	114.441
neutron	79000	79.6867	1H	56036	119.564	2H	5100	103.677	2H	5702	106.177
1H	52603	118.736	2H	4341	100.004	3H	618	97.529	3H	789	117.398
2H	3587	90.4235	3H	448	83.7401	3He	410	113.698	6H	2	123.275
3H	324	68.9096	6H	1	14.4285	4He	342	156.769	3He	657	125.667
3He	191	88.2798	3He	285	103.596	6B	3	115.348	4He	859	172.547
4He	57	75.7271	4He	125	126.863				6He	2	188.944
6He	1	114.416	6B	2	63.0384				6Li	9	179.692
6B	1	80.0948							7Li	2	178.049
									8Li	2	171.91
									6B	7	127.797
									7B	4	134.982
									9B	1	115.847
									15O	1	0.01283

Depth 7-8			Depth 8-9			Depth 9-9.4995			Depth 9.4995-9.95005		
Particle	Quantity	Avg. E	Particle	Quantity	Avg. E	Particle	Quantity	Avg. E	Particle	Quantity	Avg. E
π^-	6	58.5308	π^-	3	70.1724	π^-	3	84.9712	γ	23	0.31689
(v_e)	β^-	34.4702	(v_e)	4	40.1009	(v_e)	3	12.5895	neutron	3	111.682
\square			\square			\square					
β^+	2	38.2351	β^+	3	38.7969	β^+	2	46.7817	1H	5	93.2212
β^-	1	24.7003	(v_μ)	4	28.8269	β^-	1	27.0764	2H	1	7.73612
(v_μ)	12	32.9399	γ	205235	0.89297	(v_μ)	6	33.9323			
γ	198767	0.88713	π^+	4	62.0055	γ	192738	0.82683			
π^+	12	56.8645	neutron	92588	71.2791	π^+	5	55.2417			
neutron	92923	75.3409	1H	55304	104.745	neutron	87227	66.9843			
1H	57692	110.542	2H	7001	109.894	1H	48582	99.2628			
2H	6497	111.258	3H	1353	121.607	2H	6903	107.353			
3H	1135	127.388	6H	3	100.755	3H	1590	122.498			
6H	3	123.077	3He	1190	124.704	6H	3	88.5523			
3He	905	129.75	4He	3197	164.459	3He	1395	117.515			
4He	1799	170.346	6He	26	188.599	4He	4659	150.766			
6He	9	176.785	8He	1	171.416	6He	29	168.02			
6Li	41	168.595	6Li	89	158.243	6Li	144	140.421			
7Li	18	186.427	7Li	45	158.496	7Li	79	149.584			
8Li	2	184.696	8Li	3	194.647	8Li	6	140.781			
9Li	1	201.36	9Li	1	193.434	9Li	3	129.143			
6B	21	110.61	6B	40	104.103	6B	48	80.3199			
7B	13	142.143	7B	36	123.712	7B	54	105.969			
10B	1	177.566	9B	9	145.974	9B	20	137.394			
11B	1	186.643	10B	5	166.382	10B	6	141.464			
8Be	1	136.608	6Be	1	39.6313	8Be	4	64.935			
10Be	4	153.722	8Be	3	88.5185	10Be	18	105.766			
9C	2	60.1366	10Be	11	125.734	11Be	12	115.419			
10C	1	101.902	11Be	5	147.424	12Be	3	141.136			
11C	2	81.7174	13Be	1	171.671	13Be	1	139.739			
12C	1	135.609	9C	2	67.6291	10C	2	33.802			
12N	1	106.371	10C	7	71.4426	11C	8	71.6988			
			11C	7	80.4886	12C	24	85.8117			
			12C	7	108.935	13C	3	104.747			
			13C	1	131.598	14C	1	127.638			
			13N	2	75.725						
			14N	1	89.4237						

Depth 9.95005-10			Depth 10-11			Depth 11-12		
Particle	Quantity	Avg. E	Particle	Quantity	Avg. E	Particle	Quantity	Avg. E
γ	9625	0.69568	π^-	4	26.8264	π^-	3	44.7754
π^+	2	13.779	β^+	3	29.237	(ν_e)	3	25.582
neutron	4542	65.2298	(ν_μ)	5	36.649	β^+	2	23.5244
1H	2393	96.3206	γ	181262	0.57692	β^-	1	41.2687
2H	369	106.038	π^+	2	214.09	(ν_μ)	4	27.7093
3H	105	122.553	neutron	84388	64.5167	γ	162529	0.36767
3He	81	118.683	1H	44120	94.7652	π^+	2	76.3804
4He	298	141.031	2H	7824	102.154	neutron	64829	67.7648
6He	1	199.791	3H	2143	112.357	1H	33001	93.762
6Li	13	125.609	6H	2	93.8561	2H	7452	97.1125
7Li	6	118.941	3He	1764	102.877	3H	2546	101.167
6B	2	108.692	4He	7613	130.218	6H	13	94.4474
9B	2	145.995	6He	48	137.342	3He	1831	93.5412
10B	1	169.647	8He	1	129.547	4He	10116	110.642
8Be	1	117.028	6Li	247	115.558	6He	68	121.018
10Be	2	106.893	7Li	121	126.658	8He	1	159.056
11Be	2	120.776	8Li	13	130.198	10He	1	99.0517
12Be	1	97.5599	9Li	7	139.881	6Li	361	98.8693
11C	2	65.481	11Li	1	165.851	7Li	198	106.883
12C	1	98.7189	6B	59	63.1211	8Li	35	103.277
13C	2	94.6315	7B	110	88.6809	9Li	15	109.51
14N	1	19.7127	9B	30	109.646	6B	40	60.3721
16O	1	0.00368	10B	19	130.575	7B	118	73.9601
			11B	2	161.539	9B	44	91.9959
			8Be	4	41.3274	10B	37	112.244
			10Be	54	80.1452	11B	4	123.843
			11Be	49	93.6881	12B	1	118.432
			12Be	3	128.589	8Be	4	38.787
			13Be	1	94.8054	10Be	62	67.8829
			10C	2	44.6055	11Be	79	74.3067
			11C	19	41.5366	12Be	11	85.3887
			12C	62	64.5763	13Be	8	93.6397
			13C	12	67.9236	11C	11	35.6803
			14C	5	75.3558	12C	48	43.873
			15C	1	107.276	13C	27	61.5366
			13N	1	20.6684	14C	6	58.8269
			14N	5	33.3796	14N	2	23.7329
			15N	1	58.2412	15N	3	22.9334
			16O	2	0.02364			

Table E. 3. Particle fluences cylindrical surface with radius of 1 cm centered on an ion beam passing through different depths in a water phantom. Initial fluence equal to 500,000 ^{12}C ions accelerated to 219 MeV/u. Surface area equal to $6.28 \cdot h \text{ cm}^2$, h given as range of depths.

Depth 0-0.001			Depth 0.001-1			Depth 1-2			Depth 2-3				
Particle	Quantity	Avg. E	Particle	Quantity	Avg. E	Particle	Quantity	Avg. E	Particle	Quantity	Avg. E		
γ	104	0.53721	π^-	μ^-	38.5457	π^-	25	60.2554	π^-	γ	48.8861		
neutron	15	12.7942	(ν_e)	\square	4	23.7985	μ^+	1	6.42099	(ν_e)	\square	9	39.5104
			β^+	2	33.725	(ν_e)	\square	9	27.9621	β^+	2	49.0937	
			β^-	3	35.5557	β^+	4	41.7012	β^-	2	30.0036		
			(ν_μ)	17	34.5534	β^-	2	25.6869	μ^-	1	6.87538		
			γ	57487	1.13915	(ν_μ)	16	32.9641	(ν_μ)	14	35.5371		
			π^+	15	31.0565	γ	83655	1.26643	γ	102870	1.18249		
			neutron	17601	26.3197	π^+	23	49.8897	π^+	19	75.6021		
			1H	5521	57.5235	neutron	40672	47.9109	neutron	54685	59.6278		
			2H	263	34.3702	1H	21623	82.3132	1H	32550	95.743		
			3H	13	27.6509	2H	1196	53.7219	2H	2110	67.1721		
			3He	5	41.2476	3H	99	33.9165	3H	186	50.6178		
						3He	36	56.7246	3He	92	65.3337		
						4He	7	38.3824	4He	17	53.2197		
Depth 3-4			Depth 4-5			Depth 5-6			Depth 6-7				
Particle	Quantity	Avg. E	Particle	Quantity	Avg. E	Particle	Quantity	Avg. E	Particle	Quantity	Avg. E		
π^-	14	49.8185	π^-	13	63.3433	π^-	7	62.811	π^-	2	40.401		
(ν_e)	\square	5	μ^+	1	2.51043	(ν_e)	\square	2	β^+	2	41.3759		
β^-	2	40.4982	(ν_e)	\square	4	37.1733	β^+	1	43.9444	(ν_μ)	2	30.3843	
(ν_μ)	12	33.7664	β^+	6	18.3585	(ν_μ)	5	35.8782	γ	158400	0.88152		
γ	119687	1.07158	β^-	3	30.6103	γ	146639	0.91323	π^+	2	52.635		
π^+	15	45.5338	(ν_μ)	11	35.342	π^+	7	46.5989	neutron	70132	63.2388		
neutron	61311	64.0102	γ	134056	0.97757	neutron	67903	65.0804	1H	40404	94.9341		
1H	36949	99.6003	π^+	10	67.0786	1H	40416	98.1678	2H	4544	95.198		
2H	2810	76.5233	neutron	65440	65.3814	2H	3889	93.5408	3H	764	110.672		
3H	278	65.0411	1H	39599	100.186	3H	524	100.655	6H	1	107.919		
3He	168	78.4688	2H	3332	86.2455	6H	1	7.1065	3He	646	111.843		
4He	32	78.142	3H	365	80.1503	3He	349	105.396	4He	1244	148.236		
6He	1	30.2471	3He	239	95.4658	4He	459	146.722	6He	7	166.174		
15N	1	0.00337	4He	134	129.893	6Li	3	115.862	8He	1	184.82		
			6Li	1	0.34695	7Li	1	143.808	6Li	17	140.788		
			6B	3	72.2811	6B	7	114.22	7Li	4	150.247		
			16O	1	0.02893				9Li	1	172.666		
									6B	18	88.1555		
									7B	8	124.985		
									11Be	1	135.719		

Depth 7-8			Depth 8-9			Depth 9- 9.97995			Depth 9.997995-9.98005		
Particle	Quantity	Avg. E	Particle	Quantity	Avg. E	Particle	Quantity	Avg. E	Particle	Quantity	Avg. E
π^-	1	93.7765	(ν_e) $\bar{\nu}$	2	39.2731	π^-	1	11.3433	γ	13	1.09241
μ^+	1	6.82241	(ν_μ)	4	33.223	(ν_e) $\bar{\nu}$	1	11.3997	neutron	8	71.7195
(ν_e) $\bar{\nu}$	3	22.0462	γ	171973	0.83724	β^-	1	40.339	1H	4	84.9765
γ	167574	0.85113	neutron	70716	56.4175	(ν_μ)	4	42.4548	2H	1	43.9068
π^+	2	47.1174	1H	36580	85.8708	γ	165689	0.7763			
neutron	70888	60.4181	2H	5601	96.0886	π^+	2	53.0441			
1H	39436	90.9843	3H	1358	114.983	neutron	69069	52.2416			
2H	4986	97.3204	6H	2	154.511	1H	32015	79.8785			
3H	1071	118.468	3He	1194	103.227	2H	5856	90.721			
6H	2	123.387	4He	4131	132.198	3H	1740	106.058			
3He	882	110.324	6He	26	142.891	6H	6	156.658			
4He	2459	142.897	8He	2	143.039	3He	1509	89.9776			
6He	16	147.266	6Li	80	117.115	4He	6236	117.769			
6Li	39	132.322	7Li	60	128.328	6He	47	122.756			
7Li	22	135.323	8Li	13	141.219	8He	2	128.974			
8Li	4	147.786	9Li	4	133.123	6Li	153	102.728			
6B	30	71.2717	6B	57	57.7896	7Li	92	115.306			
7B	29	102.785	7B	46	79.8817	8Li	21	118.788			
9B	7	132.217	9B	18	114.448	9Li	11	129.953			
10B	3	137.667	10B	4	132.992	6B	42	48.0286			
8Be	3	39.1109	8Be	5	38.6798	7B	65	65.341			
10Be	8	95.9783	10Be	22	77.1785	9B	27	99.0211			
11Be	4	112.373	11Be	15	96.3317	10B	24	112.559			
11C	1	64.6505	11C	9	37.0117	11B	2	125.885			
12C	2	0.19706	12C	10	58.4775	8Be	2	26.008			
			16O	1	0.00171	10Be	40	55.1806			
						11Be	39	72.6778			
						12Be	2	106.056			
						11C	1	0.55316			
						12C	6	27.3526			

Depth 9.98005-10			Depth 10-11			Depth 11-12		
Particle	Quantity	Avg. E	Particle	Quantity	Avg. E	Particle	Quantity	Avg. E
γ	3195	0.63396	π^-	1	86.1358	(ν_e)		
neutron	1319	51.0708	β^+	1	11.8382	\square	4	28.1094
1H	596	76.9205	(ν_μ)	2	35.2923	β^+	2	48.1846
2H	133	87.8579	γ	149864	0.51324	β^-	1	35.5138
3H	37	100.721	π^+	1	51.9339	(ν_μ)	4	38.4528
3He	34	79.4898	neutron	63225	50.4492	γ	134788	0.30693
4He	165	106.597	1H	26969	75.7766	neutron	45883	53.5552
6He	1	156.016	2H	6457	81.6592	1H	18459	75.2475
6Li	3	80.3054	3H	2212	91.5091	2H	5469	78.4205
7Li	3	94.488	6H	8	126.412	3H	2421	81.7362
8Li	1	130.19	3He	1795	77.6191	6H	11	69.1272
6B	2	40.1967	4He	9497	98.5452	3He	1365	70.7566
7B	5	51.5574	6He	67	113.36	4He	11551	84.561
10B	1	124.172	8He	4	122.003	6He	91	91.5715
10Be	5	54.436	6Li	216	84.9698	8He	12	81.4718
11Be	2	67.8104	7Li	160	94.5963	6Li	252	67.4714
			8Li	32	96.1472	7Li	201	77.1373
			9Li	20	109.828	8Li	69	85.4973
			6B	11	42.8379	9Li	30	83.8962
			7B	78	51.2905	6B	4	40.2103
			9B	43	79.4816	7B	34	31.7398
			10B	47	92.1288	9B	72	62.7086
			10Be	74	40.6737	10B	74	70.3103
			11Be	98	57.669	11B	5	69.3135
			12Be	2	83.801	10Be	27	24.354
			12C	1	0.78642	11Be	137	39.8975
						12Be	3	49.9945

Table E. 4. Particle fluences cylindrical surface with radius of 1 cm centered on an ion beam passing through different depths in a water phantom. Initial fluence equal to 500,000 ^7Li ions accelerated to 134.5 MeV/u. Surface area equal to $6.28 \cdot h \text{ cm}^2$, h given as range of depths.

Depth 0-0.001			Depth 0.001-1			Depth 1-2			Depth 2-3		
Particle	Quantity	Avg. E	Particle	Quantity	Avg. E	Particle	Quantity	Avg. E	Particle	Quantity	Avg. E
γ	97	0.85541	($\bar{\nu}_e$)	1	45.1277	($\bar{\nu}_\mu$)	1	7.80865	($\bar{\nu}_e$)	1	46.5746
neutron	16	7.07217	γ	69458	1.14169	γ	100628	1.22306	β^+	1	39.7968
1H	1	11.6345	neutron	20105	16.6796	neutron	43821	27.8368	($\bar{\nu}_\mu$)	1	29.3301
			1H	3263	39.8128	1H	13059	52.7856	γ	122533	1.08851
			2H	166	28.1571	2H	880	37.9833	π^+	1	13.797
			3H	15	16.7836	3H	66	26.1143	neutron	56037	34.4335
			3He	3	25.4416	3He	16	33.6958	1H	19502	59.0732
			4He	1	10.8319	4He	4	17.4368	2H	1694	45.9883
						15O	1	0.00294	3H	184	39.1019
									6H	1	6.39712
									3He	39	42.4487
									4He	9	62.0564
Depth 3-4			Depth 4-5			Depth 5-6			Depth 6-7		
Particle	Quantity	Avg. E	Particle	Quantity	Avg. E	Particle	Quantity	Avg. E	Particle	Quantity	Avg. E
β^+	1	43.1026	($\bar{\nu}_\mu$)	2	24.7535	β^+	1	40.4044	γ	176519	0.76672
γ	140251	1.01502	γ	154834	0.89587	($\bar{\nu}_\mu$)	2	25.75	neutron	72136	42.6003
neutron	63113	38.9223	neutron	67678	41.8631	γ	167145	0.8295	1H	21661	56.1095
1H	21861	61.4258	1H	23061	61.2627	neutron	70831	43.1489	2H	5970	70.7878
2H	2487	57.9153	2H	3734	69.364	1H	22782	59.5399	3H	3243	90.6743
3H	389	69.2952	3H	1046	89.9108	2H	4998	72.8638	6H	8	94.2648
3He	164	62.0854	6H	2	112.715	3H	2190	93.683	3He	1081	50.3107
4He	179	86.9643	3He	437	63.1198	6H	2	95.1902	4He	5591	71.8067
			4He	1137	85.1951	3He	781	57.6592	6He	197	93.6193
			6He	10	101.247	4He	3159	80.3459	6Li	204	51.7003
			6Li	17	70.658	6He	69	98.1104	7Li	209	66.8709
			7Li	2	78.6253	6Li	75	63.5255	6B	1	40.4792
			10Be	1	0.20731	7Li	44	77.6534			
						6B	1	28.3871			
						12C	1	0.01062			

Depth 7-8			Depth 8-9			Depth 9-9.97995			Depth 9.97995-9.98005		
Particle	Quantity	Avg. E	Particle	Quantity	Avg. E	Particle	Quantity	Avg. E	Particle	Quantity	Avg. E
γ	182656	0.74733	γ	182303	0.68405	γ	170978	0.54076	γ	17	0.58322
neutron	72184	40.9102	neutron	71309	38.328	neutron	68431	34.5874	neutron	5	22.69
1H	19031	52.1254	1H	15918	47.7048	1H	11595	42.9451	1H	1	163.174
2H	6570	67.0206	2H	6986	58.2368	2H	6790	50.2812	2H	2	53.8804
3H	4142	83.8859	3H	4639	73.0742	3H	5182	60.2837	4He	1	25.8276
6H	7	86.6335	6H	16	80.2228	6H	16	61.7407			
3He	1033	40.8412	3He	831	33.3183	3He	390	25.9323			
4He	7490	61.3904	4He	8828	48.475	4He	7888	35.7875			
6He	278	84.1367	6He	405	73.5725	6He	388	57.1672			
8He	1	0.36047	6Li	272	20.7621	6Li	17	15.2988			
6Li	366	36.0313	7Li	694	37.6895	7Li	427	17.5633			
7Li	480	54.7769	7B	1	39.3724	17N	1	0.57149			
6B	3	32.4743	12C	1	0.15289						
7B	1	23.9589	13C	1	0.10528						
			16O	1	0.00031						

Depth 9.98005-10			Depth 10-11			Depth 11-12		
Particle	Quantity	Avg. E	Particle	Quantity	Avg. E	Particle	Quantity	Avg. E
γ	3274	0.38884	γ	155505	0.30219	γ	141131	0.1585
neutron	1264	34.1399	neutron	53855	33.9126	neutron	29936	36.3945
1H	207	39.576	1H	6445	40.8293	1H	2809	43.8917
2H	127	45.7807	2H	5298	44.2723	2H	2584	48.3092
3H	103	47.8501	3H	4479	49.0023	3H	1970	52.681
3He	4	23.1212	6H	19	37.2036	6H	9	31.7265
4He	126	31.5636	3He	102	25.0595	3He	24	25.8948
6He	9	40.8737	4He	3366	28.8841	4He	815	27.413
			6He	347	40.5424	6He	116	39.0059
			6B	1	8.2286			
			16O	1	0.0023			

Table E. 5. Particle fluences cylindrical surface with radius of 1 cm centered on an ion beam passing through different depths in a water phantom. Initial fluence equal to 500,000 ^4He ions accelerated to 116.5 MeV/u. Surface area equal to $6.28 \cdot h \text{ cm}^2$, h given as range of depths.

Depth 0-0.001			Depth 0.001-1			Depth 1-2			Depth 2-3		
Particle	Quantity	Avg. E	Particle	Quantity	Avg. E	Particle	Quantity	Avg. E	Particle	Quantity	Avg. E
γ	33	1.14151	(v_e) \square	1	47.3231	(v_μ)	2	41.3774	(v_e) \square	1	36.106
neutron	4	6.6061	β^+	1	38.0834	γ	33973	1.05051	γ	41692	0.98992
1H	1	34.4466	γ	23279	1.0117	π^+	1	3.6637	neutron	15323	28.2916
			neutron	5506	13.744	neutron	11773	23.2303	1H	5111	50.6675
			1H	851	36.6215	1H	3226	46.4113	2H	402	42.4227
			2H	28	23.1629	2H	211	34.2822	3H	27	37.3058
			3H	1	37.4106	3H	14	29.5965	3He	16	50.5539
						3He	3	30.4136	4He	2	40.2798
						4He	1	2.27421			

Depth 3-4			Depth 4-5			Depth 5-6			Depth 6-7		
Particle	Quantity	Avg. E	Particle	Quantity	Avg. E	Particle	Quantity	Avg. E	Particle	Quantity	Avg. E
(v_μ)	1	31.4841	γ	55271	0.82664	γ	60879	0.7821	γ	64910	0.81211
γ	48461	0.89283	neutron	18897	30.3678	π^+	1	39.9035	neutron	20009	28.1038
neutron	17240	30.0587	1H	6376	50.6219	neutron	19638	29.39	1H	5846	43.9922
1H	6036	51.7582	2H	1369	61.6576	1H	6504	47.8292	2H	1934	54.6039
2H	798	57.609	3H	510	83.5595	2H	1750	59.8903	3H	1015	71.7828
3H	160	82.2054	3He	481	52.1087	3H	825	79.5704	3He	845	33.2605
3He	144	56.724	4He	801	74.2051	6H	1	6.49979	4He	2170	54.8923
4He	84	76.7363				3He	795	43.0594	16O	1	0.0031
						4He	1763	66.0827			

Depth 7-8			Depth 8-9			Depth 9-9.95995			Depth 9.95995-9.96005		
Particle	Quantity	Avg. E	Particle	Quantity	Avg. E	Particle	Quantity	Avg. E	Particle	Quantity	Avg. E
γ	68350	0.82683	(v_e) \square	1	52.2138	γ	64946	0.77478	γ	9	1.10306
π^+	1	10.7701	γ	70010	0.85578	neutron	19340	20.0682	neutron	2	7.73508
neutron	20695	25.5657	neutron	20462	22.7728	1H	2216	33.6258	3H	1	19.3497
1H	4968	40.5117	1H	3764	36.8857	2H	1752	29.7458			
2H	2145	48.4035	2H	2211	38.4588	3H	1518	32.9178			
3H	1195	61.2661	3H	1447	47.0541	3He	23	21.6571			
3He	649	23.0823	3He	203	17.4681	4He	641	12.7379			
4He	2304	41.8754	4He	2330	26.6227						

Depth 9.96005-10			Depth 10-11			Depth 11-12		
Particle	Quantity	Avg. E	Particle	Quantity	Avg. E	Particle	Quantity	Avg. E
γ	2459	0.53043	γ	57231	0.40969	γ	50567	0.16536
neutron	676	19.0678	neutron	12958	20.2985	neutron	6398	22.5908
1H	49	29.8953	1H	1013	33.53	1H	387	36.2161
2H	49	25.2089	2H	659	31.7906	2H	282	34.7353
3H	41	27.8087	3H	512	34.5422	3H	208	43.051
4He	1	30.9477	3He	3	23.435			
			4He	10	18.994			

Table E. 6. Particle fluences cylindrical surface with radius of 1 cm centered on an ion beam passing through different depths in a water phantom. Initial fluence equal to 500,000 ^1H ions accelerated to 116.5 MeV/u. Surface area equal to $6.28 \cdot h \text{ cm}^2$, h given as range of depths.

Depth 0-0.001			Depth 0.001-1			Depth 1-2			Depth 2-3		
Particle	Quantity	Avg. E	Particle	Quantity	Avg. E	Particle	Quantity	Avg. E	Particle	Quantity	Avg. E
γ	3	0.41714	γ	4768	1.24292	γ	6776	1.24557	γ	8163	1.11516
1H	1	46.3896	neutron	1176	15.1031	neutron	2430	23.3381	neutron	3069	26.8266
			1H	459	30.664	1H	2435	41.1597	1H	3708	48.5005
Depth 3-4			Depth 4-5			Depth 5-6			Depth 6-7		
Particle	Quantity	Avg. E	Particle	Quantity	Avg. E	Particle	Quantity	Avg. E	Particle	Quantity	Avg. E
γ	9504	1.05666	γ	10489	0.98425	γ	11514	0.94549	γ	12479	0.94321
neutron	3503	28.3184	neutron	3419	27.1958	neutron	3428	25.4357	neutron	3380	23.9669
1H	4696	52.5327	1H	5442	53.8904	1H	5960	52.6043	1H	6560	48.7203
Depth 7-8			Depth 8-9			Depth 9-9.93995			Depth 9.93995-9.94005		
Particle	Quantity	Avg. E	Particle	Quantity	Avg. E	Particle	Quantity	Avg. E	Particle	Quantity	Avg. E
γ	13210	0.91895	γ	13792	0.95999	γ	12731	0.87861	1H	1	7.17312
neutron	3344	21.5291	neutron	3232	19.4254	neutron	2780	17.2561			
1H	6692	42.4195	1H	6803	33.3017	1H	5750	18.1908			
						4He	1	0.69725			
Depth 9.94005-10			Depth 10-11			Depth 11-12					
Particle	Quantity	Avg. E	Particle	Quantity	Avg. E	Particle	Quantity	Avg. E			
γ	736	0.65275	γ	10695	0.44602	γ	9270	0.18867			
neutron	161	17.2671	neutron	2054	14.9308	neutron	1123	15.4582			
1H	83	6.29535	1H	37	6.26156	1H	3	38.6236			

VITA

Name: Michael Patrick Butkus

Address: Department of Nuclear Engineering
Texas A&M University
3133 TAMU
College Station, TX 77843

Email Address: mpbutkus@yahoo.com

Education: B.Eng., Chemical Engineering, New Mexico Tech University, 2008
M.S., Health Physics, Texas A&M University, 2011